Dissertation

submitted to the

Combined Faculties for the Natural Sciences and Mathematics

of the Ruperto-Carola University of Heidelberg, Germany

for the degree of

Doctor of Natural Sciences

presented by

Ioana Goganau

born in Craiova, Romania

Oral examination: 19th of September, 2016

Electrical stimulation and activity for axonal regeneration

Referees:

Prof. Dr. Hilmar Bading

Prof. Dr. Armin Blesch

Table of content

List of figures

List of tables

Abbreviations and acronyms

AAV	adeno-associated virus	MAG	myelin-associated glycoprotein
AC	alternative current	MAP	microtubule-associated protein
Akt	protein kinase B (PKB)	MAP1B	microtubule-associated protein 1B
ANOVA	analysis of variance	Map3K2	mitogen activated protein kinase kinase kinase 2
ATF3	activating transcription factor 3	MAPK	mitogen-activated protein kinase
BDNF	brain-derived neurotrophic factor	MCV	mean conduction velocity
BMSC	bone marrow stromal cells	MEK	mitogen-activated protein kinase kinase
CaM	calmodulin	MPSS	methylprednisolone sodium succinate
CAM	cell adhesion molecule	Ms	mouse
CaMBP4	CaM binding protein 4	mTOR	mammalian target of Rapamycine
CaMK	CaM dependent protein kinase	mTORC1	mammalian target of rapamycin complex 1
CaMKK	CaM dependent protein kinase kinase	NCS1	neuronal calcium sensor-1
cAMP	cyclic adenosine monophosphate	NFATs	nuclear factors of activated T-cells
CDF	calcium dependent facilitation	NFH	neurofilament heavy
CL	conditioning lesion	NF-κB	nuclear factor kappa-light-chain-enhancer of activated B cells
CMV	cytomegalovirus	NGF	nerve growth factor
CNS	central nervous system	NKCC1	Na(+)-K(+)-2Cl(-) cotransporter
CREB	cAMP response element binding protein	Nogo-A	neurite outgrowth inhibitor A
CSPG	chondroitin sulfate proteoglycans	NRCAM	neuronal cell adhesion molecule
CST	corticospinal tract	NT	neurotrophic factors
CTB	cholera toxin B	PB	phosphate buffer
DAB	3,3'-diaminobenzidine	PBS	phosphate buffer saline
DC	direct current	PDE4	phosphodiesterase 4
DCL	dorsal column lesion	PDL	Poly-D-lysine
Dk	donkey	PFA	paraformaldehyde
DMEM	Dulbecco's modified eagle medium	PI-3	phosphatidylinositol-3’ kinase
DMSO	dimethyl sulfoxide	PKA	protein kinase A
DPBS	Dulbecco's phosphate-buffered saline	PKC	protein kinase C
DREADDs	designer receptors exclusively activated by designer drugs	PNS	peripheral nervus system
DRG	dorsal root ganglia	PTEN	phosphatase and tensin homolog

DYHC1	dynein heavy chain
EDTA	Ethylenediaminetetraacetic acid
eGFP	enhanced green flourescent protein
ERK	extracellular signal–regulated kinases
ES	electrical stimulation
FBS	fetal bovine serum
GABA	gamma-aminobutyric acid
GAP-43	Growth Associated Protein 43
GDNF	glial cell line-derived neurotrophic factor
GFAP	Glial fibrillary acidic protein
GFP	green flourescent protein
Gt	goat
HBSS	Hank's Balanced Salt Solution
HDAC5	histone deacetylase 5
Hs	horse
IGF-I	insulin-like growth factor
JNK	c-Jun N-terminal kinases
KLF	Kruppel-like transcription factors
KSPG	keratan sulfate proteoglycans
L1CAM	L1 Cell Adhesion Molecule
LB	Luria-Bertani medium
LIF	leukemia inhibitory factor
LIS1	Platelet-activating factor acetylhydrolase IB subunit alpha
RAF	rapidly accelerated fibrosarcoma kinase
RAG	regeneration associated genes
RARβ	retinoic acid beta
RAS	rat sarcoma protein/p21
Rb	rabbit
RGB	Red-Green-Blue
RNA	Ribonucleic acid
ROK	Rho-associated kinase
SCI	spinal cord injury
SEM	standard error of mean
SERCA	Sarco-endoplasmic reticulum Ca^{2+} ATPase
SFI	sciatic function index
STAT3	signal transducer and activator of transcription 3
SYN	synapsin I (promoter)
TBS	Tris-buffered saline
TF	transcription factor
TR	treadmill running
TrkB	Tyrosine/Tropomyosin receptor kinase B
TTX	tetrodotoxin

Dedication

To my parents for giving me love, support and wings to fly.

Acknowledgements

My supervisor, Prof. Dr. Armin Blesch: I would like to thank you for the confidence that I can succeed in such an endeavor. It has been a privilege to work under your supervision, to start and bring this project to a conclusion and I couldn't have done it without your incredible guidance throughout my PhD. My experience showed me that every experiment is a bet with nature and I have to work hard and learn a lot to improve my chances against such almighty opponent. Thus, I have learned a bit of your strategy to design experiments, a bit of your wisdom to interpret results, a healthy dose of skepticism and the motivation to carry on no matter what. Thank you for all of that.

Prof. Dr. med. Norbert Weidner: many thanks for great scientific and personal advice, within my thesis advisory committee meetings and in general. Though I haven't been dealing with patients in the past years, it has been an opportunity to be so close to the clinic, through seminars and discussions, always keeping in mind the bigger picture.

To Prof. Dr. Hilmar Bading: thank you very much for the advice and critical contributions during my thesis advisory meetings, as well as the supplies to expand my experiments in new directions and your scientific insight.

My colleagues, past and present, Dr. Beatrice Sandners, Melanie Motsch, Dr. Manuel Gunther, Dr. Julianne McCall, Ina Simeonova, Ming Deng, Christopher Sliwinski, Thomas Schackel, Shengwen Liu: it has been wonderful to meet you and share nice moments in conferences, retreats and seminars, as well as everyday work. I have learned many things from each of you, surgeries, techniques, ideas. Thank you all.

Hartmut Hoffmann-Berling International Graduate School of Molecular and Cellular Biology (HBIGS) board of directors, founders and staff: without which I wouldn't have discovered Heidelberg, the lab and my project. Thank you for that and the chance to attend great courses, meet other students, and get integrated into an inspiring PhD community. It has also been motivating and a great experience to serve for two years as Student Speaker and I thank all the staff, especially Dr. Rolf Lutz for the support, as well as my co-speakers: Kathrin Tegeler and Sebastian Unger.

To Interdisciplinary Center for Neurosciences (IZN): thank you for the opportunity to be in contact with the neuroscience community in Heidelberg, to expand my knowledge and

meet amazing scientists. It was a pleasure to also represent IZN students together with Ina Simeonova, and I would like to give special thanks to Ina, for taking so much in her hands within the second year as co-speakers, allowing me to focus more on my research.

To my family, my parents, Monica and Ion Goganau, my brother, Alexandru Marian Goganau, my aunt, Anca Patrascu and uncle, Eugen Pop, my grandmother, Marilena Patrascu: you have always encouraged me in whatever I set my mind on, though I know you would prefer that I was closer to home and you wondered, at least a little bit, why I chose to pursue yet another study. To my mother, aunt and grandmother, thank you for all the lovely small things, reminding me to eat, stay healthy, not work too much, meet friends, take holidays, enjoy life and come home once in a while. To my brother, the real doctor of the family, I am grateful you are there closer to the everyone, so that I can be the black sheep without a guilty conscience and follow my passions. To all, thank you for your love, support and always being there for me.

Abstract of the dissertation

To date, there are no specific treatments available that efficiently target the loss of neural connectivity after a spinal cord injury (SCI). Thus patients usually suffer from life-long motor, sensory and autonomic dysfunction. Neuron-intrinsic growth programs are activated after a lesion in the peripheral nervous system (PNS) and can contribute to enhanced regeneration in a subsequent central lesion. Yet this so-called conditioning lesion (CL) holds little translational potential for SCI. Electrical stimulation (ES) can influence various cellular functions, including neuronal growth and could provide a practical approach to enhance regeneration after SCI. However, the mechanisms and a practical means for applying ES as a therapy after SCI are insufficiently understood.

I hypothesized that evoked neuronal activity by direct ES of the peripheral nerve can enhance the growth potential of dorsal root ganglia (DRG) neurons in a similar way to CL, supporting the regeneration of the injured central branch ascending in the dorsal column.

ES (20Hz, 2*MT, 0.2ms, 1h) was applied in vivo to the sciatic nerve of adult Fischer 344 rats, followed by ex-vivo assessment of the growth potential, showing about 2-fold enhanced neurite growth compared to sham animals. ES increased the percentage of neurons with neurites >100um, but there was no change in the percentage of neurite bearing neurons, indicating that the effect on growth is due to enhanced elongation and not initiation. Longer duration stimulation (7h) also enhances growth by 67 ± 25%, as well as repeated stimulation for 7 days (55 ± 24%). The pattern of growth and timeline is similar to a CL, suggesting a similar or a partial overlap in the mechanism.

Growth effects of 1h ES were also assessed in vivo in a model of spinal cord injury, together with cell transplantation of BMSCs (bone marrow stromal cells) at 4 weeks post-injury. Stimulated fibers were labeled by sciatic nerve injection of the transganglionic tracer Cholera toxin B (CTB). Animals with ES for 1h showed significantly increased axonal regeneration into the spinal cell graft within the lesion compared to sham animals. Repeated stimulation with chronic electrodes showed a similar effect, but also a slight influence from chronic electrode implantation in chronic sham animals. Dieback of axons was not modified in any of the conditions. To evaluate possible side effects that may interfere with clinical applicability, I also tested pain-like behavior, showing a lack of allodynia or thermal hyperalgesia after ES. This further highlights the translational potential of this strategy in combinatorial approaches such as cell transplantation.

In parallel, I investigated the mechanisms underlying the observed neuronal activity-mediated increases in neurite growth. Using in vitro depolarization of DRG neurons as a model, my data show that neurite growth is influenced depending on the duration of the depolarization and the delay between stimulation and measurement. Since depolarization induces calcium influx, I examined in a separate set of experiments calcium signaling, showing that blocking nuclear calcium signaling with recombinant calmodulin-binding proteins reduces growth in DRG cultures at 72h by 50 ± 10%. However, a cytoplasmic block enhances growth by 35 ± 11%, and has similar effects in vivo after adeno-associated virus gene transfer into lumbar DRGs. This differential effect of nuclear and cytoplasmic calcium signaling provides an explanation for previous reports, which have shown stimulation or reduction of growth following neuronal activity. Furthermore, I investigated HDAC5 (histone deacetylase 5), showing export from the nucleus in DRGs (92 ± 5% nuclear before and 14 ± 1% after depolarization). These in vitro experiments suggest that neuronal activity-mediated effects on axon growth could involve epigenetic mechanisms, dependent on calcium/calmodulin signaling.

To follow up on these experiments, RNA sequencing was performed to investigate differential gene expression at 1 day and 7 days after ES, compared to sham animals, naive animals and animals that underwent a peripheral lesion, collecting 30M SE reads/sample on a HiSeq2000. As expected CL induces and represses an extensive number of genes compared to naïve animals. ES induced/reduced expression of a much lower number of genes relative to sham animals with smaller changes in gene expression. Several genes and pathways could be identified that are known to play a role in regeneration, suggesting that ES-mediated effects on axon regeneration are likely a summation of several activated pathways that overlap only partially with CL.

Taken together, my results reveal the capacity of neurons to modulate their growth response depending on their activity in vivo. Electrical stimulation is shown to be an effective means to increase axonal regeneration in a central lesion, and could provide a feasible therapeutic approach either alone or in combination with other strategies such as cell transplantation.

Zusammenfassung der Dissertation

Noch immer stehen keine speziellen Behandlungen zur Verfügung, die effizient auf den Verlust neuronaler Konnektivität nach einer Verletzung des Rückenmarks (SCI) abzielen. Daher leiden Patienten unter erheblichen lebenslanger motorischer, sensorischer und autonomer Dysfunktion. Neuron-intrinsische Wachstumsprogramme werden nach einer Läsion im peripheren Nervensystem (PNS) aktiviert und können in einer subsequenten zentralen Läsion zu einer verbesserten Regeneration beitragen. Jedoch hat diese sogenannte Konditionierungs-Läsion (CL) wenig translationelles Potential für Rückenmarksverletzungen. Elektrische Stimulation (ES) kann verschiedene Zellfunktionen beeinflussen, einschliesslich neuronalem Wachstum, und könnte einen praktischen Ansatz bieten, um die Regeneration nach Rückenmarksverletzungen zu verbessern. Jedoch sind die Mechanismen und ein praktisches Mittel für die Anwendung von ES als Therapie in Rückenmarksverletzungen unzureichend aufgeklärt.

Ich stellte die Hypothese auf, dass neuronale Aktivität durch direkte ES des peripheren Nervens das Wachstumspotential von Neuronen der Dorsalwurzelganglien (DRGs) in ähnlicher Weise wie CL verbessern kann, und somit die Regeneration des verletzten zentralen aufsteigenden Astes in der dorsalen Hintersträngen unterstützen kann.

ES (20Hz, 2 * MT, 0,2 ms, 1 h) wurde in vivo am Nervus ischiadicus von erwachsenen Fischer 344 Ratten appliziert, gefolgt von der ex-vivo-Bewertung des Wachstumspotenzials. Im Vergleich zu Kontroll-Tieren (sham), konnte das Neuritenwachstum verdoppelt werden. ES erhöhte den Prozentsatz an Neuronen mit Neuriten >100um, jedoch änderte sich der Prozent an Neuronen mit Neuriten nicht, was darauf hinweist, dass die Wirkung auf das Wachstum von Neuriten und nicht auf die Bildung neuer Neuriten zurückzuführen ist. Eine Längere Stimulation (7 Stunden) verbesserte auch das Wachstum um 67 ± 25%, sowie wiederholte Stimulation für 7 Tage (55 ± 24%). Das Muster des Wachstums und der zeitliche Ablauf sind ähnlich wie bei einer CL, was auf einen ähnlichen oder teilweisen überlappenden Mechanismus hindeutet.

Wachstumseffekte von 1h ES wurden auch in vivo in einem Verletzungsmodell des Rückenmarks zusammen mit Zelltransplantation von Stromazellen des Knochenmarks (BMSCs) 4 Wochen nach der Verletzung untersucht. Angeregte Fasern wurden durch Injektion des transganglionischen Tracers Choleratoxin B (CTB) markiert.

Axonale Regeneration in das Zelltransplantat zeigte deutlich verstärktes Wachstum bei Tiere, die ES für 1 h erhielten zeigten signifikant bessere axonale Regeneration in das zelluläre Transplantat innerhalb der Läsion im Vergleich zu Kontroll-Tieren. Wiederholte

Stimulation mit chronischen Elektroden zeigten eine ähnliche Wirkung, jedoch auch einen leichten Einfluss der chronischen Elektrodenimplantation bei chronischen Kontroll-Tieren zeigt. Das Absterben von Axonen war unter keiner der Bedingungen modifiziert. Um mögliche Nebenwirkungen zu bewerten, die die klinische Anwendbarkeit beeinträchtigen, habe ich auch Schmerz-ähnliches Verhalten getestet. Dabei waren Anzeichen von Allodynie oder thermischer Hyperalgesie nach ES nicht sichtbar. Diese Daten heben das hohe translationelle Potential dieser Therapiestrategie in kombinatorischen Ansätzen, wie z.B. Zelltransplantation hervor.

Parallel dazu untersuchte ich die Mechanismen, die dem durch neuronale Aktivität hervor gerufenen, erhöhten Neuriten-Wachstum zugrunde liegen. Unter Verwendung von in vitro Depolarisation von DRG Neuronen als Modell, zeigen meine Daten, dass Neuritenwachstum in Abhängigkeit von der Dauer der Depolarisation und der Verzögerung zwischen Anregung und Messung beeinflusst wird. Da Depolarisation Kalziumeinstrom induziert, untersuchte ich in einem separaten Set von Experimenten Kalzium-induzierte Signale. Dabei zeigte sich, dass die Blockierung von Kalzium-Signalen im Zellkern mit rekombinanten Calmodulin-bindenden Proteinen das Wachstum von DRG-Kulturen nach 72h um 50 ± 10% reduziert. Jedoch führte ein zytoplasmatischer Block das Wachstum um 35 ± 11%, und hat ähnliche Wirkungen in vivo nach adeno-assoziierten Virus Gentransfer in lumbale DRGs. Diese unterschiedliche Wirkung von nukleärem und zytoplasmatischen Kalzium-Signal liefert eine Erklärung für frühere Berichte, die Stimulation oder Reduktion des Wachstums nach neuronaler Aktivität gezeigt haben. Darüber hinaus untersuchte ich HDAC5 (Histon-Deacetylase 5), und konnte den Export aus dem Zellkern in DRGs zeigen (92 ± 5% Kern vor und 14 ± 1% nach Depolarisation). Diese in-vitro-Experimente deuten darauf hin, dass die durch neuronale Aktivität vermittelten Effekte auf Axonwachstum durch epigenetische Mechanismen beeinflusst werden könnten, abhängig von Kalzium/ Calmodulin-Signalen.

Auf diesen Versuchen aufbauend wurde eine RNA-Sequenzierung durchgeführt, um die differentielle Genexpression 1 und 7 Tage nach der ES im Vergleich zu Kontroll-Tieren, naiven Tiere und Tiere, die eine periphere Läsion untergingen, zu untersuchen (30M SE Reads / Probe auf einem HiSeq2000). Wie erwartet induzierte und unterdrückte eine CL eine umfangreiche Anzahl von Genen im Vergleich zu unbehandelten Tieren. ES induzierte / verminderte die Expression einer viel geringeren Anzahl von Genen relativ zu Kontroll-Tieren mit kleineren Änderungen in der Genexpression. Mehrer Gene und Signalwege konnten identifiziert werden, von den bekannt ist, dass sie eine Rolle in der Regeneration spielen. Das deutet darauf hin, dass ES-vermittelte Effekte auf axonale

Regeneration wahrscheinlich eine Summierung von mehreren aktivierten Signalwege ist, die nur teilweise mit CL überlappen.

Zusammengenommen zeigen meine Ergebnisse die Fähigkeit von Neuronen, ihre Wachstumsreaktion in Abhängigkeit von ihrer Aktivität in vivo zu modulieren. Die elektrische Stimulation zeigt sich als ein wirksames Mittel, um die Regeneration von Axonen in einer zentralen Läsion zu erhöhen, und könnte einen umsetzbaren therapeutischen Ansatz liefern, entweder allein oder in Kombination mit anderen Strategien, wie Zelltransplantation.

1. Introduction

1.1. Spinal cord injury

1.1.1. Incidence and outcomes of spinal cord injury

The spinal cord is an essential part of the central nervous system (CNS) connecting the brain to the peripheral nervous system (PNS) through long axonal pathways, taking part in motor and sensory functions, as well as containing the neural circuits for various somatic and autonomic reflexes. Around the world there are every year an estimated 250 000 - 500 000 new cases of spinal cord injury (SCI) (Biering-Sorensen et al., 2011), accompanied typically by loss of motor, sensory and autonomic function that can vary depending on the level of the lesion, severity, etiology and individual factors, resulting in some degree of life-long disability. SCI requires long term medical care and fundamentally alters the life expectation and quality of life of the affected individuals.

The disability weight factor, developed by the World Health Organization, to reflect the severity of diseases on a scale from 0 (perfect health) to 1 (equivalent to death), shows that spinal cord injury causes the most severe disability of all non-fatal injury types and one the highest across all disease spectrum, with some variations depending on the level: below the level of the neck 0.623 [0.434, 0.777] and at cervical level 0.732 [0.544, 0.871)] in the absence of treatment (Salomon et al., 2015).

Although currently there is no available specific treatment for SCI, survival can be achieved through prompt intervention and appropriate clinical measures. Life-threatening acute complications result from the lost functions and can be specifically compensated, while other chronic complications can be prevented and/or treated. Thus appropriate emergency medical care and spinal cord specialized centers, particularly in high-income countries, have increased survival after SCI (Biering-Sorensen et al., 2011).

Never the less all available strategies are symptomatic. The underlying functional deficit is not changed by these treatments, and as result, even in the most performant medical systems, after treating complications such as infections, pressure sores and spasticity, and using rehabilitation or substitution strategies, patients are still left with a substantial level of disability (for SCI below the level of the neck 0.296 [0.198, 0.414], and 0.589 [0.415, 0.748] for cervical level (Salomon et al., 2015)), putting a considerable burden on the health systems, as well as on the life of the individuals affected (Ackery et al., 2004). To further improve the condition of SCI patients, additional treatment strategies are

necessary that would have in sight restoration of lost functions by targeting the primary cause of the neurological deficits: loss of neural connectivity at the level of the spinal cord.

1.1.2. Pathophysiology of spinal cord injury

Mechanical trauma in the context of an acute compression event causes direct interruption of axons as well as general tissue loss, followed by secondary damage from the disruption of blood flow, inflammation, and other phenomena as summarized in **Fig.1.1.** As a consequence of axon destruction, glutamate is released which can induce excitotoxicity in uninjured neurons, as well as oligodendrocyte death and demyelination of initially spared fibers (Park et al., 2004), while the directly lesioned neurons can undergo cellular atrophy or even death after a spinal cord lesion through anterograde (Wallerian) or retrograde axonal degeneration (Tuszynski et al., 1999, Kwon et al., 2002, Fleming et al., 2006, Luo and O'Leary, 2005). In particular in some spinal cord populations such as corticospinal tract (CST), retrograde cell death has been reported to affect about 20% of total neurons (Hains et al., 2003), while other studies to do not report such neuronal death (Nielson et al., 2011), but rather that cortical neurons undergo atrophy (Wannier et al., 2005) and lose sensibility to neurotrophic factors through receptor downregulation (Hollis et al., 2009a). The rubrospinal tract is also known to become atrophic, but remains sensitive to factors such as brain-derived neurotrophic factor (BDNF) or neurotrophic factors (NT) -4/5 (Kobayashi et al., 1997), even at 1 year after the lesion (Kwon et al., 2002). Though degeneration can be interpreted as a negative event following SCI, there is also increasing evidence that it is in some cases necessary to allow compensatory mechanisms to take place. For example, axonal Wallerian degeneration of injured fibers has been shown to be a prerequisite for sprouting of spared fibers (Collyer et al., 2014).

Different neuronal populations reveal various levels of intrinsic growth capacity after a central injury, affecting both the natural evolution of the disease as well as raising issues for potential therapeutic strategies. Both CST and rubrospinal tracts can respond to externally supplied growth factors, but extend few neurites revealing a low intrinsic growth capacity even when externally stimulated. In contrast, the primary sensory/dorsal root ganglia (DRG) neurons survive well and are capable of extensive sprouting in response to several neurotrophic factors both in acute (Bradbury et al., 1999, Tuszynski et al., 1996) and chronic conditions (Romero et al., 2001). However, to grow for long distances over a lesion gap to eventually reinnervate their neuronal targets, additional strategies need to be employed such as gradients of growth factors (Taylor et al., 2006). Nevertheless, in virtually all tracts, central injury alone fails to activate the genetic programs for axonal regeneration, though the existence of such programs is well known. In contrast, a

peripheral lesion can efficiently induce the intrinsic growth capacity of primary sensory neurons increasing regrowth in a subsequent central lesion, thus acting as a conditioning lesion (Neumann and Woolf, 1999). Regrettably this is not the spontaneous response to a central lesion, where it seems circuit complexity has developed at the expense of regenerative ability (Popovich and Longbrake, 2008).

Additionally, the local milieu undergoes changes due to loss of glia and trophic support, presenting areas of necrosis, cavities and invasion of immune cells, such as reactive astrocytes, microglia, macrophages, and oligodendrocyte progenitors (Fleming et al., 2006, McKeon et al., 1991), which produce repulsive molecules such as keratan sulfate proteoglycans (KSPGs) (Jones and Tuszynski, 2002), several chondroitin sulfate proteoglycans (CSPGs) including neurocan, brevican, and versican (Jones et al., 2003), as well as Nogo-A, myelin-associated glycoprotein (MAG) and other myelin-based inhibitors (Schwab, 2004, Fitch and Silver, 2008, Silver and Miller, 2004), creating an overall inhibitory environment for growth. Rats and mice demonstrate similar inflammatory and astroglial activity resulting in glial scar formation and secondary tissue damage around the lesion site, with a similar timing for these cellular reorganization events (Tang et al., 2003, Silver and Miller, 2004).

Due to the damage and disconnection of ascending sensory, descending motor and modulatory projections and changes in the local circuitry, the specific pathology of SCI develops: loss of conscious motor or bladder and bowel control are due to damaged somatic or autonomic descending tracts, fine touch, thermal or pain perception are lost due to the interrupted ascending tracts, reflexes are initially absent due to loss of tonic facilitator influences **(Fig.1.1).** If the primary functional loss is not compensated, then the specific pathology is followed by complications, such that lack of muscle activity and movement leads to atrophy, deep vein thrombosis, osteoporosis or pressure ulcers, further aggravated by lack of sensory input from the skin, respiratory or bladder dysfunctions can lead to infections, while other symptoms can later result from maladaptive plasticity in the injured spinal cord (Chen et al., 1999, Dietz and Colombo, 2004). These complications can be prevented or managed symptomatically, however these treatments do not constitute specific SCI therapies.

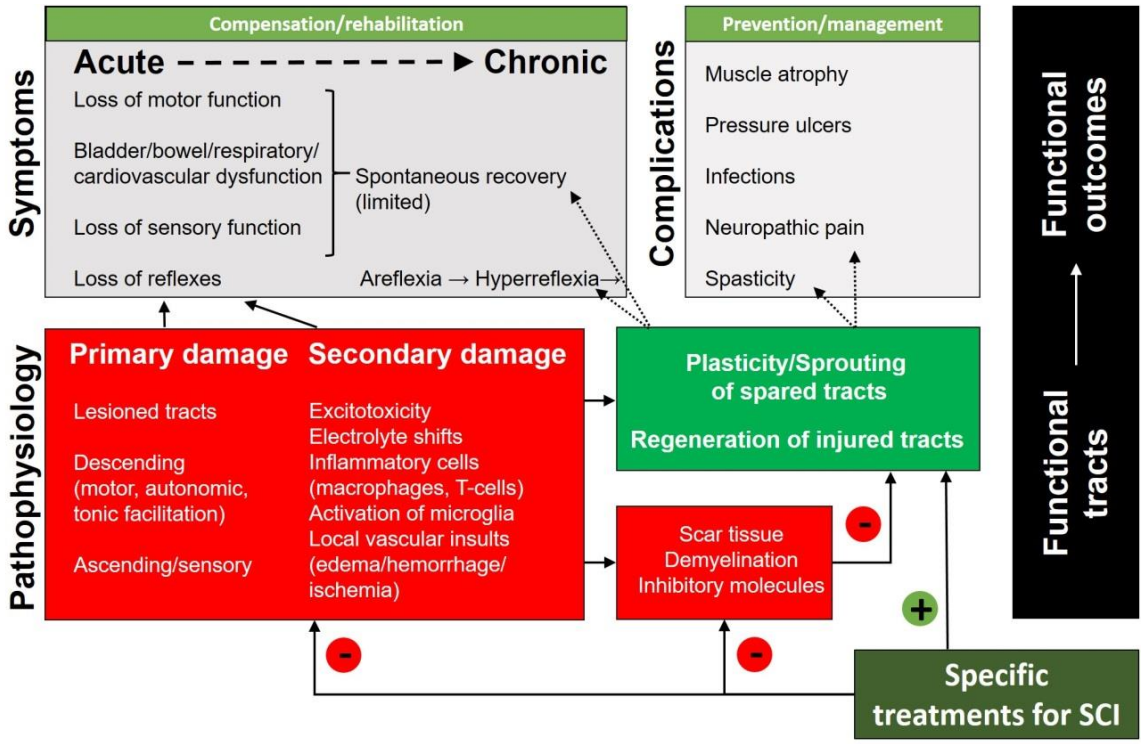

Fig.1.1. Symptoms, complications and underlying pathophysiology of spinal cord injury. Mechanical trauma causes the primary interruption of axons after SCI, followed by secondary damage. Both contribute to the specific SCI symptoms, as well as complications given by the functional deficit. Specific treatments for SCI need to limit damage or positively influence regeneration and plasticity, leading to an increased number of functional tracts.

In complete SCI patients, there is generally absence of functions below the level of the injury, with limited spontaneous recovery over time (Zariffa et al., 2011), however in patients with incomplete SCI, there can be various levels of function preservation below the level of injury, and spontaneous improvement can occur in the first year after injury, both in motor (Zariffa et al., 2012) and in sensory functions (Wirz et al., 2015). This is possible, even if the damage has been extensive, and the initial neurological tests reveal only minimal sparing such as muscle flicker or unilateral sacral sensory sparing (Folman and el Masri, 1989). Spontaneous locomotor recovery has also been reported in animal models of incomplete SCI through compensation by remaining tracts, even if more than 95% of CST fibers are originally disrupted (Weidner et al., 2001), with several factors being credited, such as reticulospinal tract sprouting (Ballermann and Fouad, 2006), CST tract sprouting, as well as propriospinal circuits (Bareyre et al., 2004). However, both in humans and in animals, this spontaneous CNS remodeling does not always result in improved function. The inefficient recovery can also be partially attributed to the chronic changes in the local environment, as previously described, including inhibitory molecules that result

in a long-lasting molecular barrier and the scar tissue in the lesion site, which constitute a physical and chemical barrier, impeding axonal growth and synaptogenesis.

Further symptoms can arise from the very tendency to recover some of the lost functions. An illustrative example of the spontaneous evolution of SCI symptoms in the context of plasticity is given by spinal reflexes, which are reduced or completely absent in the acute phase of a SCI, due to lack of tonic facilitator influence, constituting the “spinal shock”. Reflexes can recover through increase of sensitivity to stimulation and new afferents from interneurons or spared descending tracts (Ditunno et al., 2004). Return of reflexes can be considered to some extent a positive adaptive response, since patients can partially use them for physical rehabilitation, and operant conditioning of spinal reflexes can contribute to walking in incomplete SCI patients (Thompson and Wolpaw, 2015). However, when reaching an extreme, detrimental symptoms can develop such as spasticity. Similarly, aberrant sprouting and poor recovery of the circuitry in the somatosensory tracts can lead to paresthesia and neuropathic pain (Romero et al., 2000).

1.1.3. Therapeutic and experimental approaches to SCI

The final functional outcomes of SCI are strongly influenced by the final functional myelinated spared or regenerated tracts. Thus specific treatment strategies for SCI, aiming to decrease the neurological deficit need to address the complex pathophysiology of SCI. Potential directions therefore include limiting secondary damage, or enhancing regeneration and plasticity, either directly or indirectly by limiting adverse event such as scar tissue, inhibitory molecules or demyelination, as summarized in **Fig1.1.**

A first therapeutic strategy has been to limit secondary damage and this has resulted in one of the classic, acute treatments for SCI: administration of a high dose of the glucocorticoid steroid methylprednisolone sodium succinate (MPSS) in the first hours after a SCI for its anti-inflammatory and supposedly neuroprotective effects (Bracken et al., 1985, Bracken et al., 1990). However, other clinical trials and data reanalysis show the improvement to be influenced by statistical modeling and the considerable heterogeneity of the SCI population (Bracken and Holford, 2002, Ito et al., 2009, Sayer et al., 2006, Coleman et al., 2000). Thus MPSS effects on neurological functions have since been reinterpreted as a statistical artifact, and currently there is insufficient proof for MPSS’s use in SCI patients. Additionally, there are significant concerns about side effects in MPSS treated patients, high-dose steroids being identified as a predictor for major complications (Ito et al., 2009, Dimar et al., 2010). In animal studies the results have been similar,

showing inhibition of inflammation after MPSS (Bartholdi and Schwab, 1995), but variable results on functional improvement (Koyanagi and Tator, 1997, Yoon et al., 1999) and even inhibition of sprouting (Guizar-Sahagun et al., 2004). Neuroprotection remains never the less a feasible direction and many other studies have tried to limit secondary damage (reviewed in (Hall and Springer, 2004)), but the global inhibition of inflammation is likely to be inadequate, since there is evidence that certain components of the inflammatory response are useful and necessary (Cafferty et al., 2004, Cao et al., 2006, Chen et al., 2008, Zhong et al., 1999). Other modifications of the local environment such as digestion of the scar tissue with chondroitinase ABC (Bradbury et al., 2002, Silver, 2004 #232) or removal of inhibitory cues can also contribute to recovery.

Many of the recent experimental approaches to promote functional recovery after SCI have focused on plasticity or regeneration. Growth requirements and responses to external factors are specific for different neuronal population (Tuszynski et al., 1996) and reconstituting the exact original tract structure after a SCI is a challenging and almost impossible endeavor. However, even partial restoration of damaged spinal tracts can result in significant improvement of limb, respiratory, bowel, bladder or sexual function, as demonstrated by spontaneous recovery in some patients, largely independent on age, type or location of the injury (Aarabi et al., 2008, Dietz and Colombo, 2004, Folman and el Masri, 1989, Little and Halar, 1985, Wirz et al., 2015, Zariffa et al., 2011). This proves that enhancing plasticity or regeneration can bring a substantial benefit for patients, even if perfect tissue restoration cannot realistically be achieved.

Regeneration and plasticity strategies are summarized in **Fig.1.2**, ordered by their scientific feasibility based on animal, as well as human studies (modified from (McDonald and Sadowsky, 2002)). There is a significant overlap of methodologies for both strategies: glial or general cell replacement, growth factors or enhanced gene expression can support both injured and uninjured fibers, while use of neuronal precursors to create relays could create circuits either with spared or regenerating fibers **(Fig.1.2.)**. Nevertheless, we can consider that even with extensive intervention, regeneration will be harder to achieve, because unlike plasticity, spontaneous regeneration of injured fibers in the mammalian spinal cord has not been described. The challenges are also similar: necessity to enhance intrinsic growth potential, to limit aberrant connectivity by directing growth towards the appropriate target, achieving long-tract axonal regrowth, appropriate synaptogenesis and functional connectivity.

Cell transplantation to the spinal cord has been shown to be beneficial in various models, either using grafts that have a constitutive effect such as peripheral nerve grafts

(Richardson et al., 1980), glial (Ramon-Cueto and Nieto-Sampedro, 1994), fetal (Stokes and Reier, 1992), bone marrow stromal cells (BMSCs) (Hofstetter et al., 2002) or neural precursors (Lu et al., 2003) or grafts modified to express certain factors, constituting also a method for gene transfer. Transplantation of modified cells has also been shown to be effective and has practical advantages over other local delivery methods such as infusion and virus injection, due to local release and immediate availability of gene products.

A lot of interest has been given to delivery of neurotrophins, known from development and peripheral regeneration to have multiple role in regenerative pathways, growth and neuronal survival (Boyd and Gordon, 2003, Cui, 2006). The neurotrophin family of growth factors includes such members as nerve growth factor (NGF), brain-derived neurotrophic factor (BDNF), neurotrophic factor (NT)-3, NT-4/5, insulin-like growth factor (IGF-I), glial cell line-derived neurotrophic factor (GDNF). They have been used in SCI because of their multiple roles on host tissue, such as preventing cell death (Giehl and Tetzlaff, 1996, Hollis et al., 2009b), preventing or reversing atrophy (Kobayashi et al., 1997), enhancing growth and overcoming extrinsic inhibitory influences (Gao et al., 2003, Grill et al., 1997), increasing expression of regeneration associated genes (RAG) (Geremia et al., 2010, Kobayashi et al., 1997). Factors such as BDNF and NT-4 that potently act on several neuronal populations, both in acute and chronic conditions appear to be particularly advantageous (Kobayashi et al., 1997, Kwon et al., 2002, Ruitenberg et al., 2004). The effects of these factors are influenced by the cell type and are slightly different in intensity depending on the receptor activated and cellular location or distance from the cell body. BDNF for example requires additional interventions such as overexpression of the cognate receptor, trkB, to induce corticospinal neurons growth, due to downregulation after lesion (Hollis et al., 2009a) and has different effects on the same population when applied next to the same populations cell body, as opposed to application in the spinal cord. Neurotrophic factors delivery does not come without risks, and systemic long term administration has been reported to have various side effects such as pain, weight loss or Schwann cell hypertrophy. Never the less, it has been proven that transient administration is sufficient to induce sprouting and the regenerated fibers are maintained for a long time, even if the expression of neurotrophins, such as BDNF, is withdrawn (Blesch and Tuszynski, 2007). However, this is not valid for all regenerating fibers and neurotrophins. Continuous delivery of NT-3 is necessary to maintain regenerated sensory when axons are located in areas devoid of dendritic processes such as in dorsal column white matter or within cellular grafts, suggesting neurothrophins need to be continuously delivered until the fibers form functional connections (Hou et al., 2012).

In the same time, to reach the appropriate target, regenerating fibers need to be guided, a task which has also been approached using neurotrophins as attractive guidance molecules, which stimulate directional growth especially when delivered at tip of an axon (Zhou and Snider, 2006). Transected ascending neurons extensively grow in response to NT-3 (Bradbury et al., 1999), but long distance growth can only be achieved if it is continuously delivered in a gradient beyond the lesion site (Alto et al., 2009). Thus, to achieve reinnervation, sequential expression at different locations would be likely needed, either through inducible release or other strategies, while to prevent sprouting in undesired targets concomitant expression of negative cues such as semaphorins could be used (Alto et al., 2009, Bolsover et al., 2008, Giger et al., 2010, Ziemba et al., 2008).

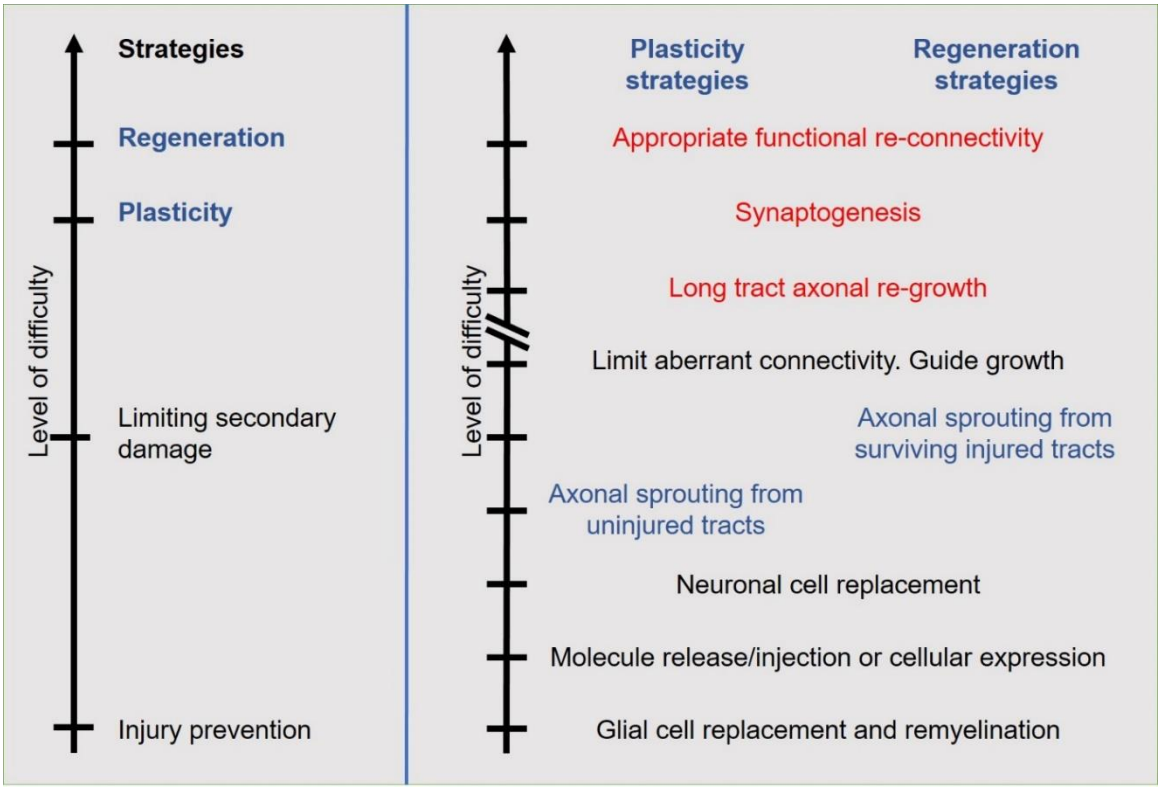

Fig.1.2. Hierarchy of scientific feasibility of specific treatment strategies for SCI. Modified from (McDonald and Sadowsky, 2002).

Enhancing expression of genes necessary for growth, missing either because of developmental down-regulation or altered response to injury, is a promising approach both for plasticity and regeneration purposes. The gene expression changes required for efficient neuronal growth are extensive, comprising of an array of neuropeptides and cytokines that partially reflects the original development. Examples of such molecules shown to enhance axonal sprouting through intrinsic mechanisms, include cyclic adenosine monophosphate (cAMP) (Cai et al., 2001), cAMP response element binding protein (CREB) (Gao et al., 2003), activating transcription factor 3 (ATF3) (Seijffers et al.,

2006), signal transducer and activator of transcription 3 (STAT3) (Qiu et al., 2005), as well as expression of developmentally down-regulated molecules such as leukemia inhibitory factor (LIF) (Blesch et al., 1999), retinoic acid beta (RARβ) (Wong et al., 2006), neuronal calcium sensor-1 (NCS1) (Yip et al., 2010) or Kruppel-like transcription factors (KLF) (Moore et al., 2009). Also, deletions of negative regulators for growth or cytoskeleton and motility, such as PTEN (phosphatase and tensin homolog) (Park et al., 2008) or inactivation of Rho and its downstream target Rho-associated kinase (ROK) (Dergham et al., 2002) have been shown to have positive effects. Simultaneous activation of mTOR and another major stimulus in central neurons regeneration, such as STAT3 pathways via ciliary neurotrophic factor/leukemia inhibitory factor (CNTF/LIF), leads to greatly enhanced and sustained regeneration in the optic nerve (Sun et al., 2011), proving that general principles in the activation of intrinsic regenerative programs exist, and suggesting that such strategies could be further developed to support regeneration. Indeed also in SCI, combining several neurotrophic factors (Xu et al., 1995), several proteins involved in growth (Bomze et al., 2001), or growth factors with enhanced intrinsic growth capacity further enhance axonal regeneration, as supported by several studies (Lu et al., 2004, Alto et al., 2009, Kadoya et al., 2009, Blesch et al., 2006). However, the application of gene therapy in patients still faces challenges in design for efficiency, as well as safety and remains far from clinical translation.

Other strategies such as electrical stimulation or magnetic stimulation have had a different association to SCI, being used initially as early as 1950 for direct functional purposes such as management of spasticity after SCI (Lee et al., 1950), treatment of urinary incontinence after SCI (Caldwell et al., 1965), management of pain (Nashold and Friedman, 1972) or as assessment measure for integrity of tracts through evoked potentials (Giblin, 1964, Levy, 1987). Electrical stimulation has since been regularly used in clinical settings for indications such as muscle training, pain management or rehabilitation of motor functions (McDonald and Sadowsky, 2002), demonstrating the availability of the technique and possible versatility. In the treatment of disuse-induced muscle atrophy (Asensio-Pinilla et al., 2009) or other functional stimulations such as vagal nerve stimulation (Schilero et al., 2009) the effects can be explained by straight-forward mechanisms: ES is the trigger for activating a neural circuit which has a defective central component due to the SCI. In the same time ES, training or transcranial magnetic stimulation have been shown to actually influence the structure of the stimulated neural components, such that stimulation enhances compensatory sprouting, can enhance survival of oligodendrocytes, influence progenitors in the spinal cord in animal models, as well as motor functional recovery in patients (Carmel and Martin, 2014, Gary et al., 2012, Gibson et al., 2014, Becker et al.,

2010, Benito et al., 2012). Electrically-induced cortical activity as well as rehabilitative training in a reaching task was associated with enhanced growth associated proteins and second messengers (i.e., BDNF, GAP-43 and cAMP) and induced plasticity and sprouting of unlesioned, spared CST axons, validating this clinically applicable strategy to enhance axonal growth in descending fiber tracts (Brus-Ramer et al., 2007). It has also been shown that activity can promote remyelination of regenerated structures, by recruiting oligodendrocyte progenitor cells, further supporting functional improvement (Gautier et al., 2015). At the same time, pharmacological treatments promoting plasticity following CNS injury have been shown to only stimulate successful functional recovery when applied with training (Garcia-Alias et al., 2009). Training has potentially the benefit of selecting functionally relevant connections (Girgis et al., 2007). Thus, it is likely that activity is essential to translate axonal regeneration into functional recovery in adults as well as in development (Raff et al., 2002, Luo and O'Leary, 2005). Electrical stimulation may have similar benefits as training and may enhance the effects of pharmacological approach, as alternative or even in combination with training.

1.1.4. Clinical translation of SCI experimental approaches

Various strategies have been shown to have beneficial functional effects in animal studies, yet have failed to be successful in clinical trials. While challenges such as intrinsic and extrinsic factors are similar both in humans as well as in experimental animals, there are certain differences that need to be considered for choosing an appropriate model and decreasing boundaries for translation of animal studies.

Most obvious differences between SCI lesions in experimental animals such as rats or mice and humans are relative size and functional neuroanatomy of spinal projections and spinal cord and thus distance requirements for axonal growth, in order to improve functional outcomes. Additionally, spontaneous recovery in rats and mice, formation of new afferents and plasticity appears to be more efficient and faster than in humans, reflected by faster return of reflexes after spinal lesion (days or hours) (Bennett et al., 1999), compared to the long duration of the spinal shock in humans (weeks to months) (Ditunno et al., 2004), as well as a much better overall functional recovery compared to humans. This implies that there might be higher intrinsic growth capacity and together with reduced physical distances in small experimental animals, it suggests that small effects in animal models are unlikely to have any impact in patients, unless the strategy can be scaled up directly. Physical differences also influence certain strategies such as cell transplantation due to graft volume, while speed of revascularization and diffusion capacity have similar limitations. Guidance strategies, virus injections and other similar

manipulations would also have to be considerably scaled up to achieve similar effects in humans as in animal models, and would need an extensive spatial and temporal control for release and distribution of gene products.

Besides physical differences there are also pathophysiological differences between species, partially due to size but also to tissue reactivity. It is known that the lesion site in human SCI can present areas of necrosis, focal cystic atrophy of the cord and myelomalacia (Tuszynski et al., 1999), making it pathologically more similar to a rat model which also shows large cystic cavities, with more rostral/caudal elongation than in mice, while mice show mostly scar tissue and a proportionally much smaller area of cavitation (Byrnes et al., 2010). Thus rats are more appropriate for cyst filling and therapies targeting regeneration strategies across a lesion.

Strategies such as training or electrical stimulation could potentially be easier to scale up to different organism sizes, because they use physiological proprieties of the neural structures. Though the mechanisms are not entirely understood, and there is no clear consensus for the most beneficial way of applying activity as therapy, the neural activity itself appears to be driving force for the effects of electrical stimulation or training, and the all-or-nothing behavior of action potential assures efficient transmission over long distances, providing an advantage for clinical translation, together with the availability of the techniques and long history of use for various purposes in patients, including in spinal cord injury.

This is reflected by present active clinical studies, such that from 269 interventional studies for spinal cord injury on "ClinicalTrials.Gov" website as Phase 1 or 2 studies (retrieved 31 May 2016), 76 (28.2%) are related to training, while 67 (24.9%) use various stimulation procedures including electrical stimulation to peripheral nerves or to the spinal cord or trans cranial magnetic stimulation as therapeutic intervention, for functional electrical stimulation, rehabilitation or management of complications such as pain and spasticity. Comparatively, 22 (7.4%) use cell or scaffolds transplantation approaches.

1.2. Somatosensory primary neurons, regeneration and spinal cord injury

1.2.1. Gross anatomy of primary sensory neurons

From each segment of the spinal cord, there are 2 series of rootlets emerging on each side, a dorsal series and a ventral series. The dorsal rootlets come together to form a single dorsal root on which a swelling formed of primary sensory neurons cell bodies is located, the dorsal root ganglion (DRG). The primary sensory neurons are pseudo unipolar, transmitting afferent sensory information such as touch, pain, temperature and proprioception, from their peripheral branch located in the peripheral nerve, to the cell body located in the dorsal root ganglia, then forming synapses with the second order neurons in different laminae of the spinal cord or continuing directly through the ascending central branch in the dorsal column. The dorsal root ganglia develop from the neural crest and are often associated more with the peripheral nervous system (Catala and Kubis, 2013), but they also belong for the CNS through their central branch.

The second order neurons give rise to various ascending spinal tracts such as spino-cerebelar, -thalamic, -hypotalamic, -reticular, -tectal, and -olivary tracts, while the directly ascending fibers form the medial lemniscus/dorsal column and terminate either in the cuneate (cuneatus) or in the gracile (Gracillis) nucleus, for upper body, respectively lower body. The dorsal column fibers are particularly important for the conscious fine touch, discriminative touch, pressure, vibration and conscious proprioception, while pain is generally associated with spinothalamic or spinoreticular tracts (Schneider et al., 1977, Dennis and Melzack, 1977, Iggo et al., 1985, Willis, 1985).

Thus DRG neurons belong both to the peripheral nervous system through their distal branch as well as to the CNS and show different reactions to injury in the two branches. This confers them special proprieties and an important place in the field of neuroregeneration.

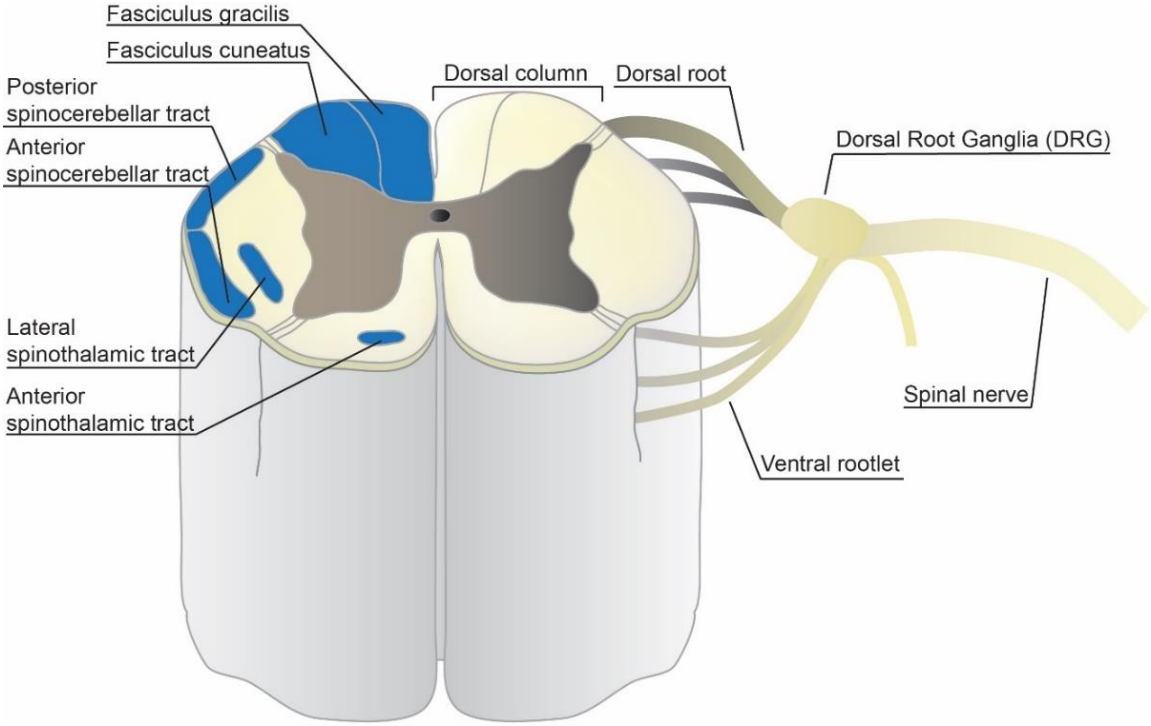

Fig.1.3. Anatomy of the sensory tracts and primary sensory neurons. The cell body of the primary sensory neurons is located in the dorsal root ganglia (DRG), while the peripheral branch is located in the spinal nerve and brings sensory information from receptors on the skin or in the tissues. The central branch ascends through the ipsilateral dorsal columns or forms synapses with the second order neurons in the grey matter of the spinal cord and continues through ascending tracts in the lateral or anterior columns.

1.2.2. Regeneration and axotomy response after peripheral lesion in DRGs

If the peripheral branch is injured, DRG neurons show efficient and many times complete regeneration and functional recovery, while if the central branch located in the dorsal column is injured in a spinal cord lesion, the same cells show little to no recovery after injury and the connections are permanently lost. This different response to axotomy in the peripheral and central nervous system have been extensively investigated, in particular in DRG neurons and has been shown to be due to complex transcriptional modifications which happen exclusively after a peripheral axotomy (Smith and Skene, 1997). An even more striking propriety of these neurons is that if the peripheral injury is inflicted before a central lesion, there is enhanced regeneration also in the dorsal column, thus in the central nervous system (McQuarrie and Grafstein, 1973, Richardson and Issa, 1984). In this context the peripheral lesion acts as a conditioning lesion (CL), and the complex transcriptional changes triggered by the peripheral axotomy contribute to the intrinsic ability of primary sensory neurons to regenerate their axons also in the central lesion (Smith and Skene, 1997, Hoffman, 2010, Hoffman, 1989), showing the intrinsic growth ability is not limited to peripheral regeneration, but if activated, it is generally beneficial for

axonal growth. Moreover, such a lesion is effective also if done briefly after a central lesion or even in a chronic injury (Kadoya et al., 2009, Blesch et al., 2012), and typically induces extension of long sparsely branched neuron (Smith and Skene, 1997), that can effectively grow into a spinal cord lesion or into a peripheral nerve graft (Neumann and Woolf, 1999).

The failure of DRG neurons to activate such regenerative programs after a central lesion alone, appears to be one important factor limiting central regeneration, making conditioning lesions of great interest for spinal cord injury research. Why the growth potential is activated in one but not the other type of lesion, thus exact mechanistic rationale for this difference of intrinsic growth potential activation is still unclear. However, it demonstrates that an appropriate molecular apparatus can induce regeneration in adult neurons, thus many studies have focused on understanding the gene expression changes and pathways involved, in an attempt to stimulate the intrinsic growth program by modifying gene expression or targeting relevant pathways.

Mechanisms involved in peripheral lesion include various transcription factors (TF), which are upregulated shortly after injury together with trophic factors and cytokines, while genes involved in neurotransmission are downregulated (Hoffman, 2010) (for review see (Bareyre and Schwab, 2003)). Some pathways and gene expression profiles partially recapitulate development (Cai et al., 2001, Smith and Skene, 1997)}. However, evidence is emerging that developmental versus regenerative axon growth may have distinct signaling pathways, both at the level of gene transcription and at the level of local axon assembly (Zhou and Snider, 2006).

Many of the identified pathways have been tested independently for their potency to induce enhanced growth capacity in dorsal root ganglia with various levels of success. One of the most investigated pathways is cAMP and CREB, a TF activated by cAMP, both being shown to enhance axonal growth, yet no long distance regeneration has been achieved (Cai et al., 2001, Gao et al., 2004). Other important transcription factors are ATF3 (Seijffers et al., 2006, Seijffers et al., 2007) and STAT3 (Qiu et al., 2005) have also been shown to enhance axonal growth, but with similarly limited effects on elongation in vivo. Other factors involved in the conditioning injury-induced spinal axons regeneration are neuropoietic cytokines, such as interleukin-6 (IL-6) and LIF (Cafferty et al., 2004, Cao et al., 2006) as well as various trophic factors such as CNTF, NGF-like neurotrophins, or NT-3 (Wu et al., 2006, Gao et al., 2003). cAMP is also involved in the neurotrophin signaling, since activation of extracellular signal-regulated kinase (Erk) inhibits phosphodiesterase 4 (PDE4), leading to increased cAMP production. Thus some growth factors do not have additive effects with CL, for example CNTF (Gao et al., 2003). Neurotrophic factors can

however replace CL in a clinical relevant strategy and have also been proposed as guidance cues for axonal growth in and beyond the lesion, in particular in combinatorial approaches (for review see (McCall et al., 2012)). Primary sensory neurons have been shown to be highly responsive to several neurotrophic factors such as NGF (Tuszynski et al., 1994), BDNF, NT-3 (Xu et al., 1995), NT-4/5 (Blesch et al., 2004), and GDNF (Blesch and Tuszynski, 2003), which have been used in various experimental approaches. Nevertheless, some neurotrophic factors such as NT-3 have an additional effect on top of a conditioning lesion, especially when applied in a gradient beyond a lesion and can induce long distance growth and bridge the lesion (Hou et al., 2012).

Since a conditioning lesion itself has little translational potential, an alternative activation of the pathways involved could provide a therapeutically relevant approach of increasing intrinsic growth potential. Never the less, cAMP as well as many other tested pathways have inferior effects compared to CL (Blesch et al., 2012) indicating that multiple mechanisms are likely involved and synchronous initiation of several transcriptional programs is required to fully activate signaling cascades for axonal regeneration. Nevertheless, available data suggests that if CL effect could be fully translated to a clinically relevant methodology, it would be beneficial in SCI. Conditioning lesion has a similar effect on gene expression even when applied after the SCI, suggesting that the timeline for activating an intrinsic growth program would not be a barrier for translation (Blesch et al., 2012). In addition, combining a CL with other interventions such as bone marrow stromal cells grafted in a dorsal column lesion site and lentiviral NT-3 gene transfer rostral to the lesion site, is effective and results in increased number and distance of sensory axons bridging across the graft (Alto et al., 2009) proving that enhanced intrinsic growth is relevant for combinatorial approaches in spinal cord injury. Thus, methods of enhancing intrinsic growth potential in a similar or equivalent way to CL, that could be easily translated to the clinic, while maintaining efficiency, would be a feasible therapeutic approach, that could bring a great benefit to spinal cord injury patients.

1.2.3. Sensory function and regeneration after SCI

Many studies in SCI have focused on understanding and restoring motor function or descending control since the motor deficit is a more visible and prominent symptom. Meanwhile, in the sensory system, the focus has been more on its unique growth capacity in the context of peripheral preconditioning lesion and understanding the intrinsic growth capacity. However, recent studies have also brought to attention the importance of the

sensory input and function loss after spinal cord injury, revealing complex roles in plasticity after injury in the spinal cord, as well as in the brain.

The remodeling of CST axons after spinal cord injury contributes to spontaneous spinal motor circuit repair and partial motor recovery, and has been shown to be dynamically regulated in maturity by the competitive, activity-dependent actions of sensory fibers (Jiang et al., 2016)}. Thus sensory activity could potentially be harnessed to promote motor systems repair. Similarly, feedback from the muscle spindles through proprioceptive neurons has been shown to support reorganization of the circuits in the spinal cord and to be necessary for the recovery of motor skills (Takeoka et al., 2014). Sensory information can also modulate internal circuits responsible for semi-automatic movement, such as walking, and can contribute to better outcomes, even without the fine tuning via supraspinal control (Thompson and Wolpaw, 2015), while if descending pathways could be efficiently regenerated after SCI, their fine function would be significantly impaired, if the sensory pathways are not also restored.

The sensory-motor cortex has been reported to undergo modifications after SCI due to lack of sensory input either in complete or unilateral spinal cord injury, both in humans and in animal models (Ghosh et al., 2009, Henderson et al., 2011). In SCI patients, functional reorganization results from changes in brain anatomy, modifying the representation of body parts. This may result in some recovery of function and contribute to behavioral adaptations by new representations in the cortex (Ghosh et al., 2009), but may be an impediment if regeneration is to be achieved. If the therapeutic goal is to induce axons to grow to their targets and reintegrate into the original circuit, it would be desirable that the network maintains its structure until reinnervation has occurred. Somatosensory input has been shown to be important for neuroprotection and maintaining original circuitry in irreversible peripheral lesions (Herrera-Rincon et al., 2012), thus artificial sensory stimulation may be necessary to preserve the cortical structures in SCI while neuroregenerative strategies are applied.

Additional challenges to effective restoration of sensory function after SCI are directing the regenerating fibers to their appropriate target and avoiding maladaptive plasticity, which can lead to neuropathic pain or paresthesia **(Fig.1.4.)**.

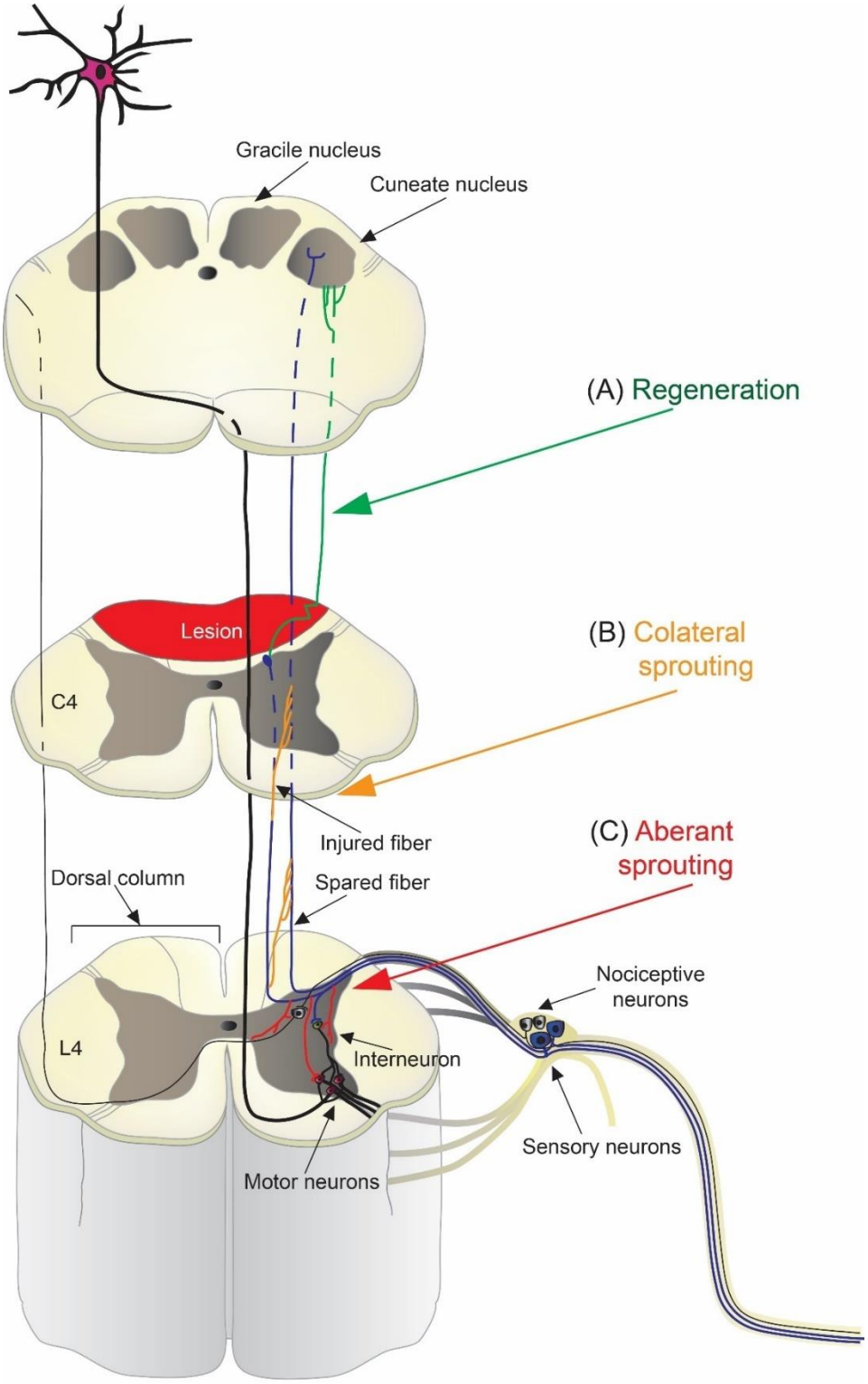

Fig.1.4. Regeneration and sprouting of sensory tracts after a spinal cord injury. Primary sensory neurons severed after a spinal cord lesion involving the dorsal column can form retraction bulbs at the limit of healthy tissue and the lesion. **(A)** Ideally the sensory fibers would undertake efficient regeneration and reach their original target. **(B)** The neurons can sprout to uninjured fibers and converge towards their original target in a process called collateral sprouting, or in a similar way **(C)** can form aberrant circuits in the spinal cord resulting in spasticity, neuropathic pain or paresthesia.

1.3. Activity and neuronal regeneration

1.3.1. Activity plays multiple roles in developing and adult neurons

Neuronal activity is an essential component of the normal function of neural structures and has multiple roles in cell migration, formation of circuits and survival in the developing nervous system (Hanson et al., 2008, Spitzer, 2006, Zhang and Poo, 2001). Neuronal firing has been shown to promote growth, in a parameter specific manner, such that increased frequency alters the pathfinding of developing axons (Hanson and Landmesser, 2006), while complete inhibition of activity leads to cell death (Wright, 1981, Lipton, 1986, Furber et al., 1987, Rubel et al., 1990, Galli-Resta and Resta, 1992).

In the developing nervous system, as well as in the adult under certain circumstances such as injury, regeneration or sprouting, relevant neurons and their connections are positively selected, while unnecessary cells undergo apoptosis and inactive projections are pruned (Raff et al., 2002, Luo and O'Leary, 2005). The reduced survival and growth in developing and axotomized adult neurons, have been shown to be caused by similar mechanisms, such as injury-induced loss of trophic stimuli and loss of neural activity (reviewed in (Goldberg and Barres, 2000)). Trophic support via tyrosine kinase receptors normally activates the RAS-RAF-MEK-ERK cascade (reviewed in (Grewal et al., 1999)) and the phosphatidylinositol-3' kinase (PI-3)/Akt/mTOR pathway, necessary and sufficient for survival by phosphorylating and activating transcription factors such as CREB, Forkhead and NF-κB, which sequentially regulate gene expression, or anti-apoptotic factors thereby blocking caspase-mediated cell death (reviewed in (Datta et al., 1999)). In the absence of growth factors, initiation of these pathways by activity becomes essential for survival, neural growth or differentiation as shown in various experimental models. Embryonic sympathetic and primary sensory neurons survive in the absence of growth factors when cAMP levels are increased, or when neurons are depolarized through calcium-dependent mechanisms (Rydel and Greene, 1988, Franklin et al., 1995). In a similar way, depolarization increases survival of other embryonic or early postnatal neurons such as granular neurons (Gallo et al., 1987), chick nodose neurons (Larmet et al., 1992) or cortical neurons (Baker et al., 1991). In embryonic DRGs, depolarizing stimuli can also induce neurite growth (Wood and Willits, 2006), as well as in PC12, when acting together with subthreshold activation of NGF receptors (Solem et al., 1995). In cortical neurons, activity induces retardation of neurite growth and/or synapse formation, however it can prevent deafferentiation or silencing induced cell death (Baker et al., 1991).

Developing neurons lack some of the receptors and ion channels, which are expressed at later stages as part of their final functional differentiation, while expressing other features. Thus neurons go through sequential stages that can display differential responses to external signals including activity. A major difference from adult neurons is the response to gamma-aminobutyric acid (GABA), the main adult inhibitory neurotransmitter, which is excitatory in developing neurons due to the genetically controlled high expression of the Na^+-K^+-$2Cl^-$ cotransporter (NKCC1) and chloride exporter KCC2 (Chabrol et al., 2012). The activity induced in young neurons by this mechanism, has a long term impact in the development of normal excitatory synaptic transmission and gating (Wang and Kriegstein, 2011), as well as in the maintenance of newly formed dendritic branches of developing neurons (Chabrol et al., 2012). Later in maturation, when neurons become dependent on neurotrophic factors, depolarization and activity play a less important role in survival (Larmet et al., 1992), with the exception of some populations. However, activity continues to play important roles in many other functions.

In mature neurons, spontaneous and evoked activity has also been shown to modulate function by potentiating or depressing circuits, as well as influence structure by influencing plasticity and growth and guiding axons, both in the peripheral and the central nervous system (Amir and Devor, 2000, Brushart et al., 2005, Gordon et al., 2008, Hanson and Landmesser, 2004, Udina et al., 2008). Similar effects have also been described for in vitro models emphasizing the impact at the single cell level, or even at the subcellular level, as demonstrated by the growth cone turning effect of an electrical field (Rajnicek et al., 2006). Like in developing neurons, adult neuronal populations have specific responses to different types of activity, for example high K+ has been shown to produce retraction of growth cones from phasic axons, while growth cones of tonic axon continue to advance, showing that the normal physiological pattern of activity in different populations contributes to different reactions to activity, likely due to differences in Ca2+ regulation and/or sensitivity to intracellular Ca2+ (Arcaro and Lnenicka, 1997).

Release and expression of neurotrophic factors, as well as their receptors and cellular localization has also been shown to be dependent on neuronal activity (Lu et al., 1991, Cohen-Cory et al., 1993, Tongiorgi, 1997 #573). Thus activity can modulate multiple responses and have additional impact on neighboring cells, either through molecular or even direct electrical influence (Amir and Devor, 2000, Lnenicka and Hong, 1997, Amir and Devor, 1996, Belhage et al., 1993). At the same time, neurotrophic factors can modify electrical proprieties of mouse adult sensory neurons within a few days, such that addition of NGF shortens action potentials (AP), while withdrawal results in longer AP durations,

suggesting such feedback loops may be important in regulating neuronal physiological properties and/or their response to injury (Chalazonitis et al., 1987).

1.3.2. Calcium/calmodulin signaling is involved in activity-dependent effects on survival and growth

The variations of response in different cell types and developmental stages, can be generally accounted for by the expression of various signal transducers and ion channels, as well as the presence or absence of additional factors. The main secondary messengers present in virtually all activity models is calcium (Arcaro and Lnenicka, 1997, Cohan, 1992, Du et al., 2000, Franklin and Johnson, 1994, Hansen et al., 2003, Isomura and Kato, 1999, Khoutorsky and Spira, 2009) and to a lesser extent cAMP, which also appears to play a role in activity induced effects (Ahn et al., 1998, Udina et al., 2008).

The calcium entry in response to activity, as well as the effects, appear to be compartmentalized and change with development. Before becoming neurotrophic factor-dependent, neurons generally depend on elevated intracellular Ca2+ and die, unless rescued by depolarization induced Ca2+ release from intracellular stores (Koike et al., 1989), or extracellular Ca2+ entry (Gallo et al., 1987). In the presence of growth factors such as BDNF, intracellular calcium is no longer essential, but depolarization can further enhance survival (Larmet et al., 1992). Release of Ca2+ from internal stores and propagation to the nucleus, has been shown to activate Ca2+ responsive transcription factors, bind Ca2+ responsive promoter elements and modify gene expression leading to long-term cellular effects (Hardingham et al., 2001), while some activity dependent effects, such as influencing the growth cone, only require local Ca2+ elevation. Depolarization of the growth cone induces dose dependent slowing of growth, up to retraction of growth cones at high doses, including in isolated growth cones (Cohan, 1992). Similarly, an electrical field can turn a growth cone (Rajnicek et al., 2006), confirming that the mechanisms in this case are local. In axons of differentiated cells, calcium entry and activity effects are more dependent on N-type channels, while in the cell body either in differentiated or undifferentiated cells, depolarization induces calcium influx dependent on L-type channels (Reber et al., 1990). Nevertheless, even if activity effects can vary depending on the cell type, location and developmental stage, calcium is generally involved, and the differences in response appear to be due largely to the way the signal is transduced.

There are several molecules that bind and regulate cellular functions in response to calcium, one of the most important ones being calmodulin (CaM). CaM plays an important

role in Ca2+ activity signal transduction, regulating several enzymes after calcium increase either from extracellular or intracellular sources. It can activate CaM dependent protein kinases (CaMKs), protein phosphatases and adenylate cyclases, influencing processes such as development, growth, gene expression, cytoskeletal organization, ion-channel regulation and protein phosphorylation (Egea et al., 1998, Elziere et al., 2014, Hansen et al., 2003, Nagendran and Hardy, 2011, Polak et al., 1991, Solem et al., 1995, Soler et al., 1998, Vaillant et al., 1999, Wu et al., 2001). An even finer control is provided by calcium/calmodulin-dependent protein kinase (CaMKs) that can decode frequency-modulated responses. CaMKII has been reported to be activated and acquire autonomous function in response to brief bursts of action potentials correlated with the frequency of Ca2+ transients, and not with the total concentration of intracellular Ca2+ (Eshete and Fields, 2001). Additionally, either CaMKII or CaMKIV activation are sufficient to support neuronal survival in spinal ganglia neurons in the absence of growth factors, however CaMKII inhibits axon outgrowth while CaMKIV does not (Hansen et al., 2003). In development, CaMKIV has been reported to have high expression concomitant with extensive growth and dendrite elaboration in the cerebral cortex and contribute to basal and activity-induced dendrite complexity, mediating branching and elongation, but not primary dendrite formation (Redmond et al., 2002, Nagendran and Hardy, 2011). CaMKIV has also been reported to be necessary for neurotrophin-induced transcriptional changes, while CREB can act as a convergence point for Ca2+ signaling, cAMP and MAPK and induce CREB-dependent transcription (Spencer et al., 2008, Wu et al., 2001). Both CaMKIV and MAPK pathways appear to be relevant for gene expression induced by physiologic synaptic stimulation. CaMKIV induces fast CREB phosphorylation dominant between 0 and 10 minutes of stimulation, and acts concomitantly with later induced MAPK pathway at 30 mins, while at 60 minutes the MAPK activation becomes dominant, both contributing to overcome myelin-mediated inhibition of axonal growth (Wu et al., 2001). Calmodulin and CaMKIV have been reported to activate several MAPK such as JNK-1, p38 and ERK2 (Egea et al., 1998, Enslen et al., 1996) suggesting a considerable overlap in signal transduction and nuclear CaMKs as a convergence point.

In contrast, CaMKI has been reported to be present mostly in the cytoplasm, including in the growth cone, activating ERK and JNK, and mediating depolarization-induced promotion of growth cone motility and axon outgrowth by local mechanisms (Schmitt et al., 2004, Wayman et al., 2004). CaMKII is also responsible for cytoplasmic effects, such as movement of TrkB from intracellular storage to the cell surface in response to extracellular Ca2+ entry by high frequency neuronal activity (Du et al., 2000) or inhibition of axon outgrowth (Hansen et al., 2003). Interestingly, CaMKII has several C-terminal

variants, which have different localizations and possibly functions, for example delta CaMKII shows increased developmental expression and co-localizes together with GAP-43, known to be involved in axonal growth, while alpha CaMKII associates with the dendritic microtubule-associated protein MAP-2 (Faison et al., 2002).

CaMKII has also been reported to be involved in synaptic plasticity and modulating the activity of Ca_V channels. Direct binding to the C-terminal domain of P/Q type of calcium channel such as $Ca_V2.1$, leads to persistent inactivation due to CaMKII becoming Ca2+ independent through autophosphorylation (Magupalli et al., 2013), while interaction with a L-type, $Ca_V1.2$, induces facilitation, and remains Ca^{2+}/CaM dependent, possibly acting as a calcium spike frequency detector (Hudmon et al., 2005). L-type channels result in Ca2+ raises that preferentially signal ~10 times more efficient to the nucleus than P/Q-type and have a different pattern of CREB mediated gene expression (Wheeler et al., 2012), while N-type channels induced gene expression is dependent on PKA and PKC (Brosenitsch and Katz, 2001) illustrating possible complex spatial-temporal interactions between cytoplasmic and nuclear calcium signaling. Thus, all these mechanisms, without being exhaustive, act at different levels at which calcium signaling can be modulated to finely tune responses to activity, depending on type, developmental and pathophysiological state of a neuron.

1.3.3. Acute electrophysiological response to axotomy and calcium signaling are involved in initiation of regeneration

To date, there is no consensus or unified theory on the effects of activity or electrical stimulation on regeneration in adult neurons or the mechanisms underlying various experimental findings. However, it has been shown in several models that electrical activity of injured neurons plays a crucial role in activating signaling pathways and genes in the context of peripheral axotomy and may be one of the triggers for enhanced growth capacity. The acute response to axonal transection involves direct influx of Ca2+ and Na+ at the lesion site, due to the transient loss of membrane integrity, which induce vigorous spiking activity at the lesion site and generate even more calcium influx, by action potentials back-propagated to the cell soma, and opening of voltage dependent calcium channels, both in invertebrate and vertebrate neurons (Mandolesi et al., 2004, Rehder et al., 1992). Furthermore, loading of the cell with Na+ causes inversion of the Na+-Ca2+ exchanger, leading to additional entry of calcium (Mandolesi et al., 2004).

The first necessary step after an axotomy is the resealing of the neurite stump and formation of the growth cone. Transected Heliosoma neurons show filopodia as early as

2-5 min after transection, followed by development of the veil in a few more minutes, thus 50% of growth cones are formed within 10 minutes and reach 100% within 30-45 minutes (Rehder et al., 1992). Similarly, transected vertebrate neurons gradually seal their membranes, in about 15 to 60 min, a process shown to be dependent on calpain, a Ca2+ activated cysteine protease and synaptotagmin, a Ca2+ regulated protein, as well as other membrane fusion proteins such as syntaxin and synaptobrevin (Detrait et al., 2000, Yoo et al., 2003). Increased extracellular calcium inhibits growth cone formation in a dose dependent way which would suggest detrimental effects of calcium. However, growth cone formation is also completely impaired in low extracellular calcium leading to chronically leaky membranes and cell death, showing that calcium signaling is necessary for resealing (Rehder et al., 1992).

Axotomy of peripheral nerves is well known for its capacity to induce complex gene expression changes in the cell soma of sensory neurons, an effect known as conditioning lesion, or in motor neurons, most often called axotomy reaction (McQuarrie and Grafstein, 1973, Smith and Skene, 1997, Mader et al., 2004). These responses contribute to successful regeneration in particular after peripheral lesions and also contribute to central regeneration after a subsequent dorsal column lesion (Richardson and Issa, 1984). The initiation of these processes has been explained either by the deprivation of target derived trophic factors (Hendry, 1975, Purves et al., 1988) such as NGF, BDNF, NT-3, GDNF (Obata et al., 2003, Groves et al., 1999, Yan et al., 1999, Henderson et al., 1994, Liuzzi and Tedeschi, 1991), or by electrophysiological initial disturbances that involve the entire neuron and play a role in the increased regeneration (Titmus and Faber, 1990, Borgens, 1988), while other studies suggest a dual mode of signaling: an early phase induced by injury-induced activity, and a late phase, including regeneration, sprouting or neuronal death, by deprivation of trophic factors (Mader et al., 2004).

In an in vitro model of axotomy, reducing extracellular Ca2+, or disrupting this activity either at the level of sodium channels or through specific calcium blockers reduces neurite regeneration (Mandolesi et al., 2004) signifying that the electrical activity and particularly the calcium influx contributes to a pro-regenerative response, and has a long term impact on regeneration. The electrical hypothesis is supported also by other studies showing that besides roles in growth cone formation and fusion of axonal fragments, calcium as well as cAMP support branching after a lesion in adult Caenorhabditis elegans neurons, while calcium blockage inhibits the normal robust regenerative growth of these neurons (Ghosh-Roy et al., 2010). More recently it has been shown that peripheral lesion of the sciatic nerve in mice is associated with back-propagating Ca2+ waves to the nucleus and this activity contributes to enhanced regeneration through PKCmu activation and histone

deacetylase 5 (HDAC5) export from the nucleus, allowing acetylation of histones and opening of DNA for expression of several genes involved in the regenerative response of these neurons (Cho et al., 2013). In a study comparing effects of short term ES with transport block and axotomy of the hypoglossal nerve it has been shown that ES induces an axotomy like reaction, in motor neurons, astroglia and microglia, however much faster and shorter lived, while transport block induces more slowly and longer lasting effects than primary axotomy (Mader et al., 2004).

1.3.4. Peripheral but not central axotomy induces long term changes in electrical proprieties of the neurons

Electrical activity plays multiple roles in immediate and delayed events after injury of neurons. Additionally, the expression of various CaMKs and calcium channels can be altered in pathological chronic conditions, such as axotomy, possibly contributing differently to responses such as growth or plasticity.

Lesion of the peripheral branch acutely reduces input through sensory fibers to the DRGs, while a dorsal column lesion, preserves input, suggesting that following injury potentials, silencing is necessary for increased intrinsic growth (Enes et al., 2010). Nevertheless, such silencing is very short-lived, since several other studies have reported a long-lasting increase of excitability in DRG neurons after peripheral axotomy, appearing within a few days after and lasting for weeks after an axotomy, through modification of Na+, K+, Cl+ and/or Ca2+ conductance (Abdulla and Smith, 2001a, Abdulla and Smith, 2001b, Djouhri et al., 2012, Sleeper et al., 2000, Zhang et al., 1997, Andre et al., 2003, Boudes and Scamps, 2012). Such alterations of electrical proprieties of neurons affect both branches after a lesion, but appear exclusively after section of the peripheral process, and not after central axotomy (Czeh et al., 1977, Gallego et al., 1987, Belmonte et al., 1988). In contrast to peripheral lesions of DRGs, chronic central branch lesion by sectioning the dorsal root, produces no significant changes, or even opposite effects (Czeh et al., 1977). Modifications appear in both branches about 3 weeks after a peripheral injury (Czeh et al., 1977), as well as at earlier time points such as 8 days (Gallego et al., 1987) or even 2 days (Belmonte et al., 1988). In vitro recordings of sensory neurons from the petrosal ganglion emphasize common changes as early as 2 days after axotomy, including increased maximum rate of depolarization and spike duration, a decrease after polarization amplitude of time-dependent inward rectification and in the amplitude and duration of the after-hyperpolarization (AHP) and conduction velocity (Belmonte et al., 1988).

Many of these changes have been investigated in the context of neuropathic pain, and the correlation with regeneration is not well understood. However, based on the signaling of activity-induced effects, such modifications may also be linked to regenerative proprieties. Some of the effects of axotomy persist for different durations up to months after cutting the nerve, but revert to normal upon successful reinnervation of individual fibers (Belmonte et al., 1988) suggesting the changes are not time dependent, but regeneration or target contact dependent. In DRGs innervating triceps surae and plantaris muscle, such changes can be created also without injuring the sensory fibers, by creating a disuse condition through sectioning of ventral roots plus Achilles tendon severance, but the changes in electrophysiological proprieties are much smaller (Czeh et al., 1977). The reduction of conduction speed and reduction/absence of time-dependent hyperpolarization, appearing in disuse conditions, suggests that the changes could be caused by lack of target signaling, as well as lack of activity in the sensory fibers themselves. Electrical changes are controlled by gene expression of different channels such as axotomy-induced expression of calcium-activated chloride current in mouse dorsal root ganglion neurons (Andre et al., 2003, Boudes and Scamps, 2012) or sympathetic neuros (Sanchez-Vives and Gallego, 1994), or decreased expression of tetrodotoxin-resistant (TTX) sodium channels in rat DRGs after peripheral lesion (Sleeper et al., 2000).

The initiation of the changes is not well understood and cannot be explained by structural differences between the two branches of DRG neurons since there are no major structural or electrophysiological differences in uninjured neurons, but the mechanism likely involves gene expression. The electrical changes, appear fast and last for a long period of time, but return to basal values upon successful reinnervation, thus overall they appear parallel successful regeneration after injury, though causality is not clear. It is possible that such changes are part of the increased intrinsic growth potential battery of changes and are linked not only to adverse effects such as neuropathic pain, but could be necessary and responsible for axonal growth and regeneration.

1.3.5. Calcium signaling and regeneration of DRG neurons

In DRGs, activity has been reported to have various effects, ranging from inhibition caused by high K^+ induced depolarization in adult DRG cultures (Enes et al., 2010), to stimulation by electrical fields in embryonic DRGs (Wood and Willits, 2006). In vivo electrical stimulation has been reported to have positive effects on peripheral and central growth, showing neuronal activity could support growth also in adult DGRs (Geremia et al., 2007, Udina et al., 2008). Some studies back the idea that an electrical gradient may be necessary for axonal development and regeneration applied locally at the level of the

dorsal column (Borgens et al., 1986), while a different approach is to stimulate the peripheral branch to activate the intrinsic growth potential (Geremia et al., 2007, Udina et al., 2008) possibly in a way similar to a conditioning lesion. Synaptic activity, as well as injury to the nerve, elicits transient influxes of Ca2+ in DRGs, and have been demonstrated to be linked to pro-regenerative gene expression (Cho et al., 2013) suggesting the influx of calcium back-propagating to the cell nucleus may be responsible for the conditioning lesion or axotomy effect. The immediate back-propagating calcium wave after axotomy, invades the soma and nucleus, and through various early mechanisms including export of HDAC5 from the nucleus in a PKCμ-dependent manner, has been shown to ultimately cause increased growth (Cho et al., 2013). In hippocampal neurons, export of HDAC5 and other class IIa HDACs is induced by activity and nuclear calcium signaling and calmodulin dependent (Schlumm et al., 2013) thus linking the nuclear events with calcium influx. In ontrast, after a peripheral lesion, electrical activity strongly inhibited axon outgrowth in cultured naive adult sensory neurons, while in conditioned neurons the L-type current through $Ca_V1.2$ channels is downregulated and genetic ablation of $Ca_V1.2$ caused an increase in axon outgrowth from dissociated DRG neurons and enhanced peripheral nerve regeneration in vivo (Enes et al., 2010), showing negative effects of calcium entry on growth. Thus it appears that the early calcium influx is beneficial and leads to positive gene expression changes, while sustained late influx is detrimental, but the different effects may also be linked to different cellular compartments. Nuclear propagation and Ca2+ induced gene expression have been shown to be dependent on intracellular storages of calcium to induce axon regeneration (Cho et al., 2013, Hardingham et al., 2001). Mild depolarization signals generally recruit Ca_V1 channels, which are 10-fold more effective in signaling to the nucleus than are Ca_V2 channels and have a distinct pattern of gene expression, whereas stronger depolarization recruits Ca_V2 channels (Wheeler et al., 2012)**.** Sarco-endoplasmic reticulum Ca^{2+} ATPase (SERCA) activity has been shown to be also decreased after injury and to be inhibited directly by activity (Duncan et al., 2013). Spinal nerve ligation leads to diminished CaMKII activity, without actual changes in expression, and hyperexcitability by elimination of calcium dependent facilitation (CDF) of L-type channels, which leads to slowed depolarization to above the I_{Ca} reversal potential and slowed rate of recovery of Ca2+ concentrations after an AP, compared to control neurons (Tang et al., 2012). Thus according to these studies, the electrical changes induced by injury are at least partially induced by activity and can influence further electrical activity responses in a complex manner: can limit or reveal different Ca2+ effects, shift the compartment dynamics of the influx and modify signal transduction. Some of these changes may actually be a prerequisite for growth. At the moment there is no unified theory about the effects of activity upon regeneration of adult DGRs, however there is sufficient

evidence to support that at least some activity patterns can have positive effects on growth in these neurons, thus modulating their activity is a promising strategy to enhance regeneration after spinal cord injury. In the same time, the mechanisms involved in such effects require further investigations.

1.4. Electrical stimulation for axonal regeneration

1.4.1. Means of modulating neuronal activity

Since activity can lead to specific effects, contributing to a finely adjusted interdependence between function and structure in the nervous system, modulation of activity is a very interesting strategy for treatment spinal cord injury. Particular promising directions are effects such as survival of certain neuronal populations, preferential maintenance of functionally relevant projections, growth and regeneration in injured structures or compensatory sprouting in the uninjured tracts.

Neuronal activity can be induced or enhanced by electrical stimulation (ES), transcranial magnetic pulses or through training, as well can be blocked by special ES patterns, or through chemical and genetic approaches. ES, training or transcranial magnetic stimulation have been shown to induce efficient activation and various effects both in animal models and in patients (Carmel and Martin, 2014, Gary et al., 2012, Gibson et al., 2014, Becker et al., 2010, Benito et al., 2012). Several studies have used peripheral nerve stimulation to investigate the effects on peripheral or central axonal regeneration from the stimulated structures (Al-Majed et al., 2000b, Gordon et al., 2007, Udina et al., 2008), while another stimulation approach is to apply an electrical field locally at the level of the spinal cord (Borgens et al., 1986) or to stimulate the remaining intact structures such as corticospinal axons to induce plasticity and sprouting (Brus-Ramer et al., 2007, Carmel et al., 2010). Treadmill training has been shown to be as efficient as ES for neuromodulation, and partially prevents the development of hyperreflexia in a rat model of spinal cord injury (Asensio-Pinilla et al., 2009), and contributes to plasticity and recovery (Girgis et al., 2007), and expression of neurotrophic factors and their receptors (Skup et al., 2002).

More recently, optogenetic approaches (Gibson et al., 2014, Park et al., 2015) or designer receptors exclusively activated by designer drugs (DREADDs) have been used to induce or block activity in vivo in specific subpopulations, opening several research directions for the role of activity, as well as possible therapeutics (Chen et al., 2015, Urban and Roth, 2015, Wess et al., 2013, Zhu and Roth, 2014). However, though the function can be finely controlled offering a great scientific research tool, the translational limitations remain the same as with all gene transfer strategies.

ES as well as training offer more feasible ways of modifying activity in neural structures. ES is able to recruit any nervous fibers or structure, while training involves mostly motor fibers and proprioceptive fibers only. Additionally, ES can be easier to control than training

(Fouad et al., 2000) and can be applied independently of lesion severity, including in complete lesions and immediately after an injury.

1.4.2. Electrical stimulation for peripheral regeneration

The first reported effects of ES in mammal neural growth have been established in intact rat saphenous nerve. Alternative current (AC) stimulation (20 Hz, 0.1 ms pulse, 1000 μA, suprathreshold, 10 minutes in 3 sessions) was shown to enhance sprouting of nerve endings in the skin of the hind paw; also direct field stimulation (DC) enhanced similar sprouting when cathode was placed distally to the growth tip, while anode stimulation had no effects (Pomeranz et al., 1984). Similarly, applying a brief conditioning burst of impulses in intact A delta axons, was shown to influence compensatory sprouting and accelerate innervation and restoring of sensitivity in experimentally denervated skin (Nixon et al., 1984). The mechanisms of DC appear to be local, acting at the growth cone, while the effects of AC impulses were shown to be dependent on generating action potentials (Pomeranz et al., 1984, Nixon et al., 1984).

Other studies have focused on stimulating injured peripheral fibers, which despite generally good regeneration, could further improve function and be beneficial for patients by enhancing speed and precision of regrowth (reviewed in (Gordon et al., 2007)). For this purpose, peripheral nerves are typically stimulated by applying electrodes to the nerve trunk, at the level of the injury and suture. One hour of 20 Hz ES of the femoral nerve has been shown to enhance regeneration of motor neurons to their appropriate target and considerably shorten the time of reinnervation (Al-Majed et al., 2000b). The same kind of stimulation was found to greatly increase expression of BDNF and trkB earlier than lesion only, at 8h compared to 7 days respectively, however the increase was shortly lived and returned to lesion only levels by 7 days (Al-Majed et al., 2000a) suggesting ES is not sufficient to maintain long term expression. The growth speed of fibers was not modified by ES, rather the effects are due to increasing the number of fibers with efficient growth and decreasing the delay in crossing the suture to the distal stump (Brushart et al., 2002). No additive effects were found on motor reinnervation when combining ES and scar digestion by chondroitinase ABC injection in the lesion (Beaumont et al., 2009), further supporting that they both act by facilitating the fibers to overcome the stump.

Sensory fiber regeneration in the periphery has been approached in a similar way, showing by sequential double labeling from the muscles an increased percentage of sensory fibers, returning to the muscles, and normal proportion of DRGs reinnervating the skin, though the mechanisms of such specificity are not entirely clear (Brushart et al., 2005). Further

studies showed involvement of the intrinsic growth potential and regeneration associated genes such as GAP-43 as well as neurothrophins such as BDNF, in ES enhanced growth of sensory fibers (Geremia et al., 2007). Similar effects have been reported also after only 30 min of ES (Alrashdan et al., 2010).

ES for 1h in the acute phase of sciatic nerve injury, can be also combined with treadmill running (TR) (4 weeks, 2h/day) in rats, resulting in higher levels of muscle reinnervation and more regenerated myelinated fibers (Asensio-Pinilla et al., 2009). Such a combination was shown to also have beneficial effects on neuropathic pain reduction, while supporting reinnervation, possibly by modulation of growth factors since the ES and TR induced intermediate levels of BDNF and GDNF in DRG, and of BDNF and NT3 in the ventral horn, compared to ES alone (Cobianchi et al., 2013). Such levels may be sufficient for growth without inducing adverse effects on pain. In the same time ES and recombinant adenoviral vector-mediated BDNF have no additive effects supporting the idea that effects of ES are indeed mediated through such expression (Alrashdan et al., 2011). Furthermore, ES induced BDNF expression seems to require activity-induced intracellular Ca2+ increase and Erk activation (Wenjin et al., 2011).

1.4.3. Electrical stimulation to enhance central regeneration of primary sensory neurons

Peripheral nerve regeneration studies strongly support beneficial effects of electrical stimulation on regeneration both of sensory and motor fibers (reviewed in (Gordon et al., 2008)). In At the same time, the mechanisms evoked also suggest ES could act in a similar way on central regeneration, since ES has being associated with increased expression of growth-associated genes such as GAP-43, neuronal plasticity/growth (Al-Majed et al., 2000a, Al-Majed et al., 2000b), and neurotrophic factors such as BDNF and GDNF in DRG (Cobianchi et al., 2013). A comparison of peripheral nerve injury and ES, suggests they could be acting through similar mechanisms (Fig.1.5).

Though evidence for activity induced growth exist also in the CNS, the number or publications is more restricted. ES-induced plasticity and sprouting of spared fibers has been shown in corticospinal axons after unilateral spinal cord injury in rodents (Brus-Ramer et al., 2007, Carmel et al., 2010) validating this strategy to enhance axonal growth in the CNS. However, the mechanisms remain poorly understood and the optimal way to apply such a stimulation after SCI is unknown.

ES of sensory fibers in the periphery for 1h increases BDNF expression and intracellular cAMP and can promote sensory fiber growth in vitro and in vivo following SCI (Udina et al., 2008). There are similarities between the ES and the conditioning lesion effects, since both require a delay for enhancing growth and induce cAMP at comparable levels (Udina et al., 2008). ES effects on peripheral regeneration have also been associated with cAMP, as well as the release of various neurotrophic factors (BDNF) and increased expression of trkB receptor, tubulin and actin (Al-Majed et al., 2000a). However in peripheral regeneration of motor neurons, no conditioning-like effect was found from ES applied to intact nerve 7 days previous prior to injury (Brushart et al., 2002). This suggests reactions to stimulation may differ in an injured versus intact nerve, but does not exclude a conditioning like effect in primary sensory neurons.

The effect of ES on growth in culture 7 days after stimulation were considerable (Udina et al., 2008), however there is no clear information about the magnitude relative to the CL effect. Though cAMP was induced at comparable levels to CL, ELISA measures of cAMP are rather unreliable and the in vivo effects of ES were limited to sprouting into towards the lesion and little growth within, compared to long distance sprouting induced by CL (Udina et al., 2008). Whether appropriate sham controls were included in these studies is also not clearly specified. Thus cAMP elevation is not necessarily the only mechanism involved and a poor predictor of in vivo growth after a DCL. Nevertheless, some overlap with CL is suggested, yet it is not clear if, and what are the mechanisms through which ES enhances intrinsic growth potential.

Based on the literature, one hypothesis is that ES induces calcium signaling which is known to be upstream of several pathways including cAMP, MAPK, transcription factors and various genes. The direct effect of electrical stimulation on a neural structure are influenced by several parameters: such as frequency, duration of stimulation protocol, pattern, intensity, type of impulse or baseline voltage. For example, a protocol delivering the same number of pulses, but at 200 Hz in a patterned stimulation lasting 1h, did not increase growth compared to sham surgery (Udina et al., 2008) showing there is some specificity linking effects and parameters of ES. Changing the stimulation, could possibly further increase the effects to achieve more growth in vivo, to the extent induced by CL. Since ES-induced expression of BDNF and trkB was found to be shortly lived compared to lesion induced levels (Al-Majed et al., 2000a), repeated or prolonged stimulation might be necessary in vivo to achieve growth comparable to CL after a DCL. Also considering the complexity of the local changes after SCI, other combinatorial treatments such as cell injection into the lesion might be needed.

Taken together, the current literature suggests that some pro-regenerative effects of ES after lesions in the spinal cord might exist, yet mechanisms underlying these changes and the parameters influencing these effects remain unknown.

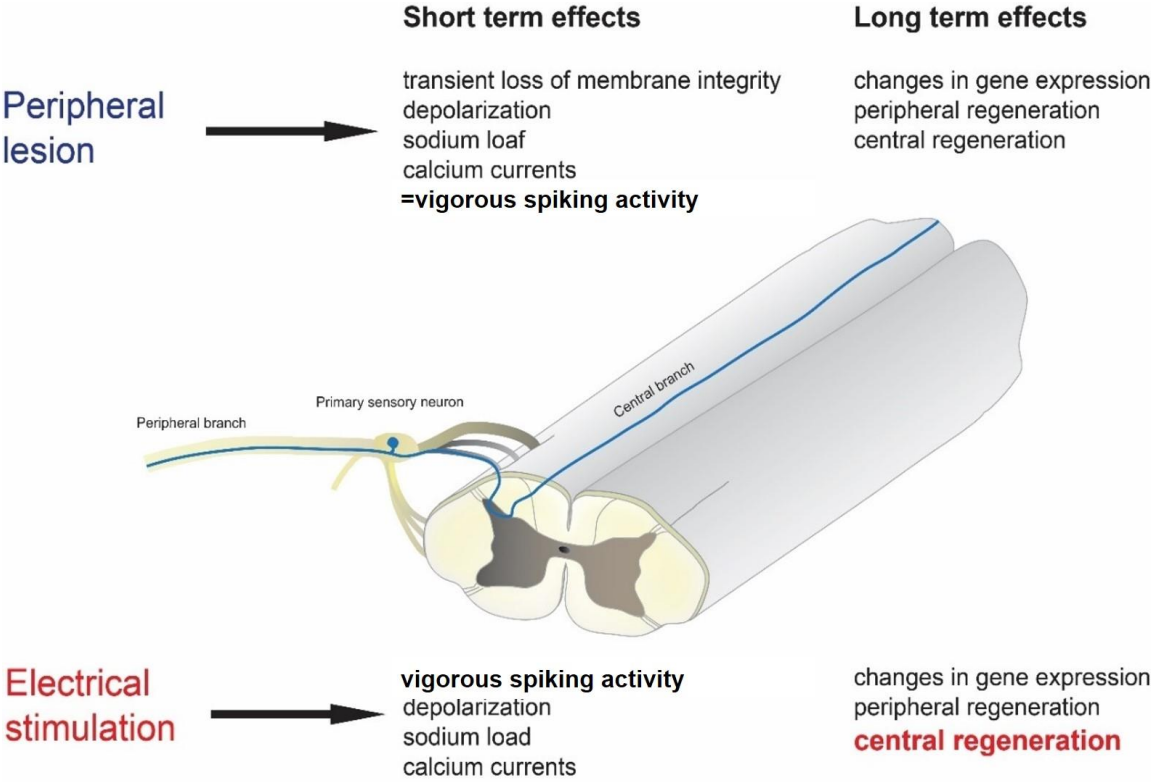

Fig.1.5. Peripheral lesion versus peripheral electrical stimulation. In primary sensory neurons, axotomy of the peripheral branch induces complex changes in gene expression of dorsal root ganglion (DRG) neurons contributing to successful regeneration after PNS lesions. Injury-induced back propagating calcium influx has been shown to contribute to the enhanced growth potential observed in peripheral injury. Additional neuronal activity via electrical stimulation (ES) can further enhance growth and specificity in peripheral reinnervation. However little is known about the effects of ES on central regeneration.

References

1. Aarabi, B., Koltz, M. & Ibrahimi, D. 2008. Hyperextension cervical spine injuries and traumatic central cord syndrome. *Neurosurg Focus,* 25**,** E9.
2. Abdulla, F. A. & Smith, P. A. 2001a. Axotomy- and autotomy-induced changes in Ca2+ and K+ channel currents of rat dorsal root ganglion neurons. *J Neurophysiol,* 85**,** 644-58.
3. Abdulla, F. A. & Smith, P. A. 2001b. Axotomy- and autotomy-induced changes in the excitability of rat dorsal root ganglion neurons. *J Neurophysiol,* 85**,** 630-43.
4. Ackery, A., Tator, C. & Krassioukov, A. 2004. A global perspective on spinal cord injury epidemiology. *J Neurotrauma,* 21**,** 1355-70.
5. Ahn, S., Olive, M., Aggarwal, S., Krylov, D., Ginty, D. D. & Vinson, C. 1998. A dominant-negative inhibitor of CREB reveals that it is a general mediator of stimulus-dependent transcription of c-fos. *Mol Cell Biol,* 18**,** 967-77.
6. Al-Majed, A. A., Brushart, T. M. & Gordon, T. 2000a. Electrical stimulation accelerates and increases expression of BDNF and trkB mRNA in regenerating rat femoral motoneurons. *Eur J Neurosci,* 12**,** 4381-90.
7. Al-Majed, A. A., Neumann, C. M., Brushart, T. M. & Gordon, T. 2000b. Brief electrical stimulation promotes the speed and accuracy of motor axonal regeneration. *J Neurosci,* 20**,** 2602-8.
8. Alrashdan, M. S., Park, J. C., Sung, M. A., Yoo, S. B., Jahng, J. W., Lee, T. H., Kim, S. J. & Lee, J. H. 2010. Thirty minutes of low intensity electrical stimulation promotes nerve regeneration after sciatic nerve crush injury in a rat model. *Acta Neurol Belg,* 110**,** 168-79.
9. Alrashdan, M. S., Sung, M. A., Kwon, Y. K., Chung, H. J., Kim, S. J. & Lee, J. H. 2011. Effects of combining electrical stimulation with BDNF gene transfer on the regeneration of crushed rat sciatic nerve. *Acta Neurochir (Wien),* 153**,** 2021-9.
10. Alto, L. T., Havton, L. A., Conner, J. M., Hollis Ii, E. R., Blesch, A. & Tuszynski, M. H. 2009. Chemotropic guidance facilitates axonal regeneration and synapse formation after spinal cord injury. *Nat Neurosci,* 12**,** 1106-13.
11. Amir, R. & Devor, M. 1996. Chemically mediated cross-excitation in rat dorsal root ganglia. *J Neurosci,* 16**,** 4733-41.
12. Amir, R. & Devor, M. 2000. Functional cross-excitation between afferent A- and C-neurons in dorsal root ganglia. *Neuroscience,* 95**,** 189-95.
13. Andre, S., Boukhaddaoui, H., Campo, B., Al-Jumaily, M., Mayeux, V., Greuet, D., Valmier, J. & Scamps, F. 2003. Axotomy-induced expression of calcium-activated chloride current in subpopulations of mouse dorsal root ganglion neurons. *J Neurophysiol,* 90**,** 3764-73.
14. Arcaro, K. F. & Lnenicka, G. A. 1997. Differential effects of depolarization on the growth of crayfish tonic and phasic motor axons in culture. *J Neurobiol,* 33**,** 85-97.
15. Asensio-Pinilla, E., Udina, E., Jaramillo, J. & Navarro, X. 2009. Electrical stimulation combined with exercise increase axonal regeneration after peripheral nerve injury. *Exp Neurol,* 219**,** 258-65.
16. Baker, R. E., Ruijter, J. M. & Bingmann, D. 1991. Elevated potassium prevents neuronal death but inhibits network formation in neocortical cultures. *Int J Dev Neurosci,* 9**,** 339-45.
17. Ballermann, M. & Fouad, K. 2006. Spontaneous locomotor recovery in spinal cord injured rats is accompanied by anatomical plasticity of reticulospinal fibers. *Eur J Neurosci,* 23**,** 1988-96.
18. Bareyre, F. M., Kerschensteiner, M., Raineteau, O., Mettenleiter, T. C., Weinmann, O. & Schwab, M. E. 2004. The injured spinal cord spontaneously forms a new intraspinal circuit in adult rats. *Nat Neurosci,* 7**,** 269-77.
19. Bareyre, F. M. & Schwab, M. E. 2003. Inflammation, degeneration and regeneration in the injured spinal cord: insights from DNA microarrays. *Trends Neurosci,* 26**,** 555-

63.
20. Bartholdi, D. & Schwab, M. E. 1995. Methylprednisolone inhibits early inflammatory processes but not ischemic cell death after experimental spinal cord lesion in the rat. *Brain Res,* 672**,** 177-86.
21. Beaumont, E., Cloutier, F. C., Atlan, M., Rouleau, D. M. & Beaumont, P. H. 2009. Chondroitinase ABC and acute electrical stimulation are beneficial for muscle reinnervation after sciatic nerve transection in rats. *Restor Neurol Neurosci,* 27**,** 297-305.
22. Becker, D., Gary, D. S., Rosenzweig, E. S., Grill, W. M. & Mcdonald, J. W. 2010. Functional electrical stimulation helps replenish progenitor cells in the injured spinal cord of adult rats. *Exp Neurol,* 222**,** 211-8.
23. Belhage, B., Hansen, G. H. & Schousboe, A. 1993. Depolarization by K+ and glutamate activates different neurotransmitter release mechanisms in GABAergic neurons: vesicular versus non-vesicular release of GABA. *Neuroscience,* 54**,** 1019-34.
24. Belmonte, C., Gallego, R. & Morales, A. 1988. Membrane properties of primary sensory neurones of the cat after peripheral reinnervation. *J Physiol,* 405**,** 219-32.
25. Benito, J., Kumru, H., Murillo, N., Costa, U., Medina, J., Tormos, J. M., Pascual-Leone, A. & Vidal, J. 2012. Motor and gait improvement in patients with incomplete spinal cord injury induced by high-frequency repetitive transcranial magnetic stimulation. *Top Spinal Cord Inj Rehabil,* 18**,** 106-12.
26. Bennett, D. J., Gorassini, M., Fouad, K., Sanelli, L., Han, Y. & Cheng, J. 1999. Spasticity in rats with sacral spinal cord injury. *J Neurotrauma,* 16**,** 69-84.
27. Biering-Sorensen, F., Bickenbach, J. E., El Masry, W. S., Officer, A. & Von Groote, P. M. 2011. ISCoS-WHO collaboration. International Perspectives of Spinal Cord Injury (IPSCI) report. *Spinal Cord,* 49**,** 679-83.
28. Blesch, A., Lu, P., Roet, K., Loew, K. I. & Tuszynski, M. H. 2006. Phosphodiesterase-IV inhibitors and conditioning lesions in combination with lentiviral NT-3 gene transfer promote sensory axonal bridging across C3 spinal cord lesions. *2006 Abstract Viewer/Itinerary Planner. Atlanta, GA: Society for Neuroscience, 2006. Online.***,** Program No. 522.10.
29. Blesch, A., Lu, P., Tsukada, S., Taylor, L., Roet, K., Coppola, G., Geschwind, D. & Tuszynski, M. H. 2012. Conditioning lesions before or after spinal cord injury recruit broad genetic mechanisms that sustain axonal regeneration: superiority to cAMP-mediated effects. . *Exp Neurol,* in press.
30. Blesch, A. & Tuszynski, M. H. 2003. Cellular GDNF delivery promotes growth of motor and dorsal column sensory axons after partial and complete spinal cord transection, and induces remyelination. *J Comp Neurol,* 467**,** 403-17.
31. Blesch, A. & Tuszynski, M. H. 2007. Transient growth factor delivery sustains regenerated axons after spinal cord injury. *J Neurosci,* 27**,** 10535-45.
32. Blesch, A., Uy, H. S., Grill, R. J., Cheng, J. G., Patterson, P. H. & Tuszynski, M. H. 1999. Leukemia inhibitory factor augments neurotrophin expression and corticospinal axon growth after adult CNS injury. *J Neurosci,* 19**,** 3556-66.
33. Blesch, A., Yang, H., Weidner, N., Hoang, A. & Otero, D. 2004. Axonal responses to cellularly delivered NT-4/5 after spinal cord injury. *Mol Cell Neurosci,* 27**,** 190-201.
34. Bolsover, S., Fabes, J. & Anderson, P. N. 2008. Axonal guidance molecules and the failure of axonal regeneration in the adult mammalian spinal cord. *Restor Neurol Neurosci,* 26**,** 117-30.
35. Bomze, H. M., Bulsara, K. R., Iskandar, B. J., Caroni, P. & Skene, J. H. 2001. Spinal axon regeneration evoked by replacing two growth cone proteins in adult neurons. *Nat Neurosci,* 4**,** 38-43.
36. Borgens, R. B. 1988. Voltage gradients and ionic currents in injured and regenerating axons. *Adv Neurol,* 47**,** 51-66.
37. Borgens, R. B., Blight, A. R., Murphy, D. J. & Stewart, L. 1986. Transected dorsal column axons within the guinea pig spinal cord regenerate in the presence of an applied electric field. *J Comp Neurol,* 250**,** 168-80.

38. Boudes, M. & Scamps, F. 2012. Calcium-activated chloride current expression in axotomized sensory neurons: what for? *Front Mol Neurosci,* 5**,** 35.
39. Boyd, J. G. & Gordon, T. 2003. Neurotrophic factors and their receptors in axonal regeneration and functional recovery after peripheral nerve injury. *Mol Neurobiol,* 27**,** 277-324.
40. Bracken, M. B. & Holford, T. R. 2002. Neurological and functional status 1 year after acute spinal cord injury: estimates of functional recovery in National Acute Spinal Cord Injury Study II from results modeled in National Acute Spinal Cord Injury Study III. *J Neurosurg,* 96**,** 259-66.
41. Bracken, M. B., Shepard, M. J., Collins, W. F., Holford, T. R., Young, W., Baskin, D. S., Eisenberg, H. M., Flamm, E., Leo-Summers, L., Maroon, J. & Et Al. 1990. A randomized, controlled trial of methylprednisolone or naloxone in the treatment of acute spinal-cord injury. Results of the Second National Acute Spinal Cord Injury Study. *N Engl J Med,* 322**,** 1405-11.
42. Bracken, M. B., Shepard, M. J., Hellenbrand, K. G., Collins, W. F., Leo, L. S., Freeman, D. F., Wagner, F. C., Flamm, E. S., Eisenberg, H. M., Goodman, J. H. & Et Al. 1985. Methylprednisolone and neurological function 1 year after spinal cord injury. Results of the National Acute Spinal Cord Injury Study. *J Neurosurg,* 63**,** 704-13.
43. Bradbury, E. J., Khemani, S., Von, R., King, Priestley, J. V. & Mcmahon, S. B. 1999. NT-3 promotes growth of lesioned adult rat sensory axons ascending in the dorsal columns of the spinal cord. *Eur J Neurosci,* 11**,** 3873-83.
44. Bradbury, E. J., Moon, L. D., Popat, R. J., King, V. R., Bennett, G. S., Patel, P. N., Fawcett, J. W. & Mcmahon, S. B. 2002. Chondroitinase ABC promotes functional recovery after spinal cord injury. *Nature,* 416**,** 636-40.
45. Brosenitsch, T. A. & Katz, D. M. 2001. Physiological patterns of electrical stimulation can induce neuronal gene expression by activating N-type calcium channels. *J Neurosci,* 21**,** 2571-9.
46. Brus-Ramer, M., Carmel, J. B., Chakrabarty, S. & Martin, J. H. 2007. Electrical stimulation of spared corticospinal axons augments connections with ipsilateral spinal motor circuits after injury. *J Neurosci,* 27**,** 13793-801.
47. Brushart, T. M., Hoffman, P. N., Royall, R. M., Murinson, B. B., Witzel, C. & Gordon, T. 2002. Electrical stimulation promotes motoneuron regeneration without increasing its speed or conditioning the neuron. *J Neurosci,* 22**,** 6631-8.
48. Brushart, T. M., Jari, R., Verge, V., Rohde, C. & Gordon, T. 2005. Electrical stimulation restores the specificity of sensory axon regeneration. *Exp Neurol,* 194**,** 221-9.
49. Byrnes, K. R., Fricke, S. T. & Faden, A. I. 2010. Neuropathological differences between rats and mice after spinal cord injury. *J Magn Reson Imaging,* 32**,** 836-46.
50. Cafferty, W. B., Gardiner, N. J., Das, P., Qiu, J., Mcmahon, S. B. & Thompson, S. W. 2004. Conditioning injury-induced spinal axon regeneration fails in interleukin-6 knock-out mice. *J Neurosci,* 24**,** 4432-43.
51. Cai, D., Qiu, J., Cao, Z., Mcatee, M., Bregman, B. S. & Filbin, M. T. 2001. Neuronal cyclic AMP controls the developmental loss in ability of axons to regenerate. *J Neurosci,* 21**,** 4731-9.
52. Caldwell, K. P., Flack, F. C. & Broad, A. F. 1965. Urinary Incontinence Following Spinal Injury Treated by Electronic Implant. *Lancet,* 1**,** 846-7.
53. Cao, Z., Gao, Y., Bryson, J. B., Hou, J., Chaudhry, N., Siddiq, M., Martinez, J., Spencer, T., Carmel, J., Hart, R. B. & Filbin, M. T. 2006. The cytokine interleukin-6 is sufficient but not necessary to mimic the peripheral conditioning lesion effect on axonal growth. *J Neurosci,* 26**,** 5565-73.
54. Carmel, J. B., Berrol, L. J., Brus-Ramer, M. & Martin, J. H. 2010. Chronic electrical stimulation of the intact corticospinal system after unilateral injury restores skilled locomotor control and promotes spinal axon outgrowth. *J Neurosci,* 30**,** 10918-26.
55. Carmel, J. B. & Martin, J. H. 2014. Motor cortex electrical stimulation augments sprouting of the corticospinal tract and promotes recovery of motor function. *Front Integr Neurosci,* 8**,** 51.

56. Catala, M. & Kubis, N. 2013. Gross anatomy and development of the peripheral nervous system. *Handb Clin Neurol,* 115**,** 29-41.
57. Chabrol, F. P., Eglen, S. J. & Sernagor, E. 2012. GABAergic control of retinal ganglion cell dendritic development. *Neuroscience,* 227**,** 30-43.
58. Chalazonitis, A., Peterson, E. R. & Crain, S. M. 1987. Nerve growth factor regulates the action potential duration of mature sensory neurons. *Proc Natl Acad Sci U S A,* 84**,** 289-93.
59. Chen, D., Apple, D. F., Jr., Hudson, L. M. & Bode, R. 1999. Medical complications during acute rehabilitation following spinal cord injury--current experience of the Model Systems. *Arch Phys Med Rehabil,* 80**,** 1397-401.
60. Chen, Q., Smith, G. M. & Shine, H. D. 2008. Immune activation is required for NT-3-induced axonal plasticity in chronic spinal cord injury. *Exp Neurol,* 209**,** 497-509.
61. Chen, X., Choo, H., Huang, X. P., Yang, X., Stone, O., Roth, B. L. & Jin, J. 2015. The first structure-activity relationship studies for designer receptors exclusively activated by designer drugs. *ACS Chem Neurosci,* 6**,** 476-84.
62. Cho, Y., Sloutsky, R., Naegle, K. M. & Cavalli, V. 2013. Injury-induced HDAC5 nuclear export is essential for axon regeneration. *Cell,* 155**,** 894-908.
63. Cobianchi, S., Casals-Diaz, L., Jaramillo, J. & Navarro, X. 2013. Differential effects of activity dependent treatments on axonal regeneration and neuropathic pain after peripheral nerve injury. *Exp Neurol,* 240**,** 157-67.
64. Cohan, C. S. 1992. Depolarization-induced changes in neurite elongation and intracellular Ca2+ in isolated Helisoma neurons. *J Neurobiol,* 23**,** 983-96.
65. Cohen-Cory, S., Elliott, R. C., Dreyfus, C. F. & Black, I. B. 1993. Depolarizing influences increase low-affinity NGF receptor gene expression in cultured Purkinje neurons. *Exp Neurol,* 119**,** 165-75.
66. Coleman, W. P., Benzel, D., Cahill, D. W., Ducker, T., Geisler, F., Green, B., Gropper, M. R., Goffin, J., Madsen, P. W., 3rd, Maiman, D. J., Ondra, S. L., Rosner, M., Sasso, R. C., Trost, G. R. & Zeidman, S. 2000. A critical appraisal of the reporting of the National Acute Spinal Cord Injury Studies (II and III) of methylprednisolone in acute spinal cord injury. *J Spinal Disord,* 13**,** 185-99.
67. Collyer, E., Catenaccio, A., Lemaitre, D., Diaz, P., Valenzuela, V., Bronfman, F. & Court, F. A. 2014. Sprouting of axonal collaterals after spinal cord injury is prevented by delayed axonal degeneration. *Exp Neurol,* 261**,** 451-61.
68. Cui, Q. 2006. Actions of neurotrophic factors and their signaling pathways in neuronal survival and axonal regeneration. *Mol Neurobiol,* 33**,** 155-79.
69. Czeh, G., Kudo, N. & Kuno, M. 1977. Membrane properties and conduction velocity in sensory neurones following central or peripheral axotomy. *J Physiol,* 270**,** 165-80.
70. Datta, S. R., Brunet, A. & Greenberg, M. E. 1999. Cellular survival: a play in three Akts. *Genes Dev,* 13**,** 2905-27.
71. Dennis, S. G. & Melzack, R. 1977. Pain-signalling systems in the dorsal and ventral spinal cord. *Pain,* 4**,** 97-132.
72. Dergham, P., Ellezam, B., Essagian, C., Avedissian, H., Lubell, W. D. & Mckerracher, L. 2002. Rho signaling pathway targeted to promote spinal cord repair. *J Neurosci,* 22**,** 6570-7.
73. Detrait, E. R., Yoo, S., Eddleman, C. S., Fukuda, M., Bittner, G. D. & Fishman, H. M. 2000. Plasmalemmal repair of severed neurites of PC12 cells requires Ca(2+) and synaptotagmin. *J Neurosci Res,* 62**,** 566-73.
74. Dietz, V. & Colombo, G. 2004. Recovery from spinal cord injury--underlying mechanisms and efficacy of rehabilitation. *Acta Neurochir Suppl,* 89**,** 95-100.
75. Dimar, J. R., Fisher, C., Vaccaro, A. R., Okonkwo, D. O., Dvorak, M., Fehlings, M., Rampersaud, R. & Carreon, L. Y. 2010. Predictors of complications after spinal stabilization of thoracolumbar spine injuries. *J Trauma,* 69**,** 1497-500.
76. Ditunno, J. F., Little, J. W., Tessler, A. & Burns, A. S. 2004. Spinal shock revisited: a four-phase model. *Spinal Cord,* 42**,** 383-95.
77. Djouhri, L., Fang, X., Koutsikou, S. & Lawson, S. N. 2012. Partial nerve injury induces

electrophysiological changes in conducting (uninjured) nociceptive and nonnociceptive DRG neurons: Possible relationships to aspects of peripheral neuropathic pain and paresthesias. *Pain,* 153**,** 1824-36.
78. Du, J., Feng, L., Yang, F. & Lu, B. 2000. Activity- and Ca(2+)-dependent modulation of surface expression of brain-derived neurotrophic factor receptors in hippocampal neurons. *J Cell Biol,* 150**,** 1423-34.
79. Duncan, C., Mueller, S., Simon, E., Renger, J. J., Uebele, V. N., Hogan, Q. H. & Wu, H. E. 2013. Painful nerve injury decreases sarco-endoplasmic reticulum Ca(2)(+)-ATPase activity in axotomized sensory neurons. *Neuroscience,* 231**,** 247-57.
80. Egea, J., Espinet, C. & Comella, J. X. 1998. Calmodulin modulates mitogen-activated protein kinase activation in response to membrane depolarization in PC12 cells. *J Neurochem,* 70**,** 2554-64.
81. Elziere, L., Sar, C., Venteo, S., Bourane, S., Puech, S., Sonrier, C., Boukhadaoui, H., Fichard, A., Pattyn, A., Valmier, J., Carroll, P. & Mechaly, I. 2014. CaMKK-CaMK1a, a new post-traumatic signalling pathway induced in mouse somatosensory neurons. *PLoS One,* 9**,** e97736.
82. Enes, J., Langwieser, N., Ruschel, J., Carballosa-Gonzalez, M. M., Klug, A., Traut, M. H., Ylera, B., Tahirovic, S., Hofmann, F., Stein, V., Moosmang, S., Hentall, I. D. & Bradke, F. 2010. Electrical activity suppresses axon growth through Ca(v)1.2 channels in adult primary sensory neurons. *Curr Biol,* 20**,** 1154-64.
83. Enslen, H., Tokumitsu, H., Stork, P. J., Davis, R. J. & Soderling, T. R. 1996. Regulation of mitogen-activated protein kinases by a calcium/calmodulin-dependent protein kinase cascade. *Proc Natl Acad Sci U S A,* 93**,** 10803-8.
84. Eshete, F. & Fields, R. D. 2001. Spike frequency decoding and autonomous activation of Ca2+-calmodulin-dependent protein kinase II in dorsal root ganglion neurons. *J Neurosci,* 21**,** 6694-705.
85. Faison, M. O., Perozzi, E. F., Caran, N., Stewart, J. K. & Tombes, R. M. 2002. Axonal localization of delta Ca2+/calmodulin-dependent protein kinase II in developing P19 neurons. *Int J Dev Neurosci,* 20**,** 585-92.
86. Fitch, M. T. & Silver, J. 2008. CNS injury, glial scars, and inflammation: Inhibitory extracellular matrices and regeneration failure. *Exp Neurol,* 209**,** 294-301.
87. Fleming, J. C., Norenberg, M. D., Ramsay, D. A., Dekaban, G. A., Marcillo, A. E., Saenz, A. D., Pasquale-Styles, M., Dietrich, W. D. & Weaver, L. C. 2006. The cellular inflammatory response in human spinal cords after injury. *Brain,* 129**,** 3249-69.
88. Folman, Y. & El Masri, W. 1989. Spinal cord injury: prognostic indicators. *Injury,* 20**,** 92-3.
89. Fouad, K., Metz, G. A., Merkler, D., Dietz, V. & Schwab, M. E. 2000. Treadmill training in incomplete spinal cord injured rats. *Behav Brain Res,* 115**,** 107-13.
90. Franklin, J. L. & Johnson, E. M., Jr. 1994. Block of neuronal apoptosis by a sustained increase of steady-state free Ca2+ concentration. *Philos Trans R Soc Lond B Biol Sci,* 345**,** 251-6.
91. Franklin, J. L., Sanz-Rodriguez, C., Juhasz, A., Deckwerth, T. L. & Johnson, E. M., Jr. 1995. Chronic depolarization prevents programmed death of sympathetic neurons in vitro but does not support growth: requirement for Ca2+ influx but not Trk activation. *J Neurosci,* 15**,** 643-64.
92. Furber, S., Oppenheim, R. W. & Prevette, D. 1987. Naturally-occurring neuron death in the ciliary ganglion of the chick embryo following removal of preganglionic input: evidence for the role of afferents in ganglion cell survival. *J Neurosci,* 7**,** 1816-32.
93. Gallego, R., Ivorra, I. & Morales, A. 1987. Effects of central or peripheral axotomy on membrane properties of sensory neurones in the petrosal ganglion of the cat. *J Physiol,* 391**,** 39-56.
94. Galli-Resta, L. & Resta, G. 1992. A quantitative model for the regulation of naturally occurring cell death in the developing vertebrate nervous system. *J Neurosci,* 12**,** 4586-94.

95. Gallo, V., Kingsbury, A., Balazs, R. & Jorgensen, O. S. 1987. The role of depolarization in the survival and differentiation of cerebellar granule cells in culture. *J Neurosci,* 7**,** 2203-13.
96. Gao, Y., Deng, K., Hou, J., Bryson, J. B., Barco, A., Nikulina, E., Spencer, T., Mellado, W., Kandel, E. R. & Filbin, M. T. 2004. Activated CREB is sufficient to overcome inhibitors in myelin and promote spinal axon regeneration in vivo. *Neuron,* 44**,** 609-21.
97. Gao, Y., Nikulina, E., Mellado, W. & Filbin, M. T. 2003. Neurotrophins elevate cAMP to reach a threshold required to overcome inhibition by MAG through extracellular signal-regulated kinase-dependent inhibition of phosphodiesterase. *J Neurosci,* 23**,** 11770-7.
98. Garcia-Alias, G., Barkhuysen, S., Buckle, M. & Fawcett, J. W. 2009. Chondroitinase ABC treatment opens a window of opportunity for task-specific rehabilitation. *Nat Neurosci,* 12**,** 1145-51.
99. Gary, D. S., Malone, M., Capestany, P., Houdayer, T. & Mcdonald, J. W. 2012. Electrical stimulation promotes the survival of oligodendrocytes in mixed cortical cultures. *J Neurosci Res,* 90**,** 72-83.
100. Gautier, H. O., Evans, K. A., Volbracht, K., James, R., Sitnikov, S., Lundgaard, I., James, F., Lao-Peregrin, C., Reynolds, R., Franklin, R. J. & Karadottir, R. T. 2015. Neuronal activity regulates remyelination via glutamate signalling to oligodendrocyte progenitors. *Nat Commun,* 6**,** 8518.
101. Geremia, N. M., Gordon, T., Brushart, T. M., Al-Majed, A. A. & Verge, V. M. 2007. Electrical stimulation promotes sensory neuron regeneration and growth-associated gene expression. *Exp Neurol,* 205**,** 347-59.
102. Geremia, N. M., Pettersson, L. M., Hasmatali, J. C., Hryciw, T., Danielsen, N., Schreyer, D. J. & Verge, V. M. 2010. Endogenous BDNF regulates induction of intrinsic neuronal growth programs in injured sensory neurons. *Exp Neurol,* 223**,** 128-42.
103. Ghosh-Roy, A., Wu, Z., Goncharov, A., Jin, Y. & Chisholm, A. D. 2010. Calcium and cyclic AMP promote axonal regeneration in Caenorhabditis elegans and require DLK-1 kinase. *J Neurosci,* 30**,** 3175-83.
104. Ghosh, A., Sydekum, E., Haiss, F., Peduzzi, S., Zorner, B., Schneider, R., Baltes, C., Rudin, M., Weber, B. & Schwab, M. E. 2009. Functional and anatomical reorganization of the sensory-motor cortex after incomplete spinal cord injury in adult rats. *J Neurosci,* 29**,** 12210-9.
105. Giblin, D. R. 1964. Somatosensory Evoked Potentials in Healthy Subjects and in Patients with Lesions of the Nervous System. *Ann N Y Acad Sci,* 112**,** 93-142.
106. Gibson, E. M., Purger, D., Mount, C. W., Goldstein, A. K., Lin, G. L., Wood, L. S., Inema, I., Miller, S. E., Bieri, G., Zuchero, J. B., Barres, B. A., Woo, P. J., Vogel, H. & Monje, M. 2014. Neuronal activity promotes oligodendrogenesis and adaptive myelination in the mammalian brain. *Science,* 344**,** 1252304.
107. Giehl, K. M. & Tetzlaff, W. 1996. BDNF and NT-3, but not NGF, prevent axotomy-induced death of rat corticospinal neurons in vivo. *Eur J Neurosci,* 8**,** 1167-75.
108. Giger, R. J., Hollis, E. R., 2nd & Tuszynski, M. H. 2010. Guidance molecules in axon regeneration. *Cold Spring Harb Perspect Biol,* 2**,** a001867.
109. Girgis, J., Merrett, D., Kirkland, S., Metz, G. A., Verge, V. & Fouad, K. 2007. Reaching training in rats with spinal cord injury promotes plasticity and task specific recovery. *Brain,* 130**,** 2993-3003.
110. Goldberg, J. L. & Barres, B. A. 2000. The relationship between neuronal survival and regeneration. *Annu Rev Neurosci,* 23**,** 579-612.
111. Gordon, T., Brushart, T. M., Amirjani, N. & Chan, K. M. 2007. The potential of electrical stimulation to promote functional recovery after peripheral nerve injury--comparisons between rats and humans. *Acta Neurochir Suppl,* 100**,** 3-11.
112. Gordon, T., Brushart, T. M. & Chan, K. M. 2008. Augmenting nerve regeneration with electrical stimulation. *Neurol Res,* 30**,** 1012-22.

113. Grewal, S. S., York, R. D. & Stork, P. J. 1999. Extracellular-signal-regulated kinase signalling in neurons. *Curr Opin Neurobiol,* 9**,** 544-53.
114. Grill, R., Murai, K., Blesch, A., Gage, F. H. & Tuszynski, M. H. 1997. Cellular delivery of neurotrophin-3 promotes corticospinal axonal growth and partial functional recovery after spinal cord injury. *J Neurosci,* 17**,** 5560-72.
115. Groves, M. J., An, S. F., Giometto, B. & Scaravilli, F. 1999. Inhibition of sensory neuron apoptosis and prevention of loss by NT-3 administration following axotomy. *Exp Neurol,* 155**,** 284-94.
116. Guizar-Sahagun, G., Grijalva, I., Salgado-Ceballos, H., Espitia, A., Orozco, S., Ibarra, A., Martinez, A., Franco-Bourland, R. E. & Madrazo, I. 2004. Spontaneous and induced aberrant sprouting at the site of injury is irrelevant to motor function outcome in rats with spinal cord injury. *Brain Res,* 1013**,** 143-51.
117. Hains, B. C., Black, J. A. & Waxman, S. G. 2003. Primary cortical motor neurons undergo apoptosis after axotomizing spinal cord injury. *J Comp Neurol,* 462**,** 328-41.
118. Hall, E. D. & Springer, J. E. 2004. Neuroprotection and acute spinal cord injury: a reappraisal. *NeuroRx,* 1**,** 80-100.
119. Hansen, M. R., Bok, J., Devaiah, A. K., Zha, X. M. & Green, S. H. 2003. Ca2+/calmodulin-dependent protein kinases II and IV both promote survival but differ in their effects on axon growth in spiral ganglion neurons. *J Neurosci Res,* 72**,** 169-84.
120. Hanson, M. G. & Landmesser, L. T. 2004. Normal patterns of spontaneous activity are required for correct motor axon guidance and the expression of specific guidance molecules. *Neuron,* 43**,** 687-701.
121. Hanson, M. G. & Landmesser, L. T. 2006. Increasing the frequency of spontaneous rhythmic activity disrupts pool-specific axon fasciculation and pathfinding of embryonic spinal motoneurons. *J Neurosci,* 26**,** 12769-80.
122. Hanson, M. G., Milner, L. D. & Landmesser, L. T. 2008. Spontaneous rhythmic activity in early chick spinal cord influences distinct motor axon pathfinding decisions. *Brain Res Rev,* 57**,** 77-85.
123. Hardingham, G. E., Arnold, F. J. & Bading, H. 2001. Nuclear calcium signaling controls CREB-mediated gene expression triggered by synaptic activity. *Nat Neurosci,* 4**,** 261-7.
124. Henderson, C. E., Phillips, H. S., Pollock, R. A., Davies, A. M., Lemeulle, C., Armanini, M., Simmons, L., Moffet, B., Vandlen, R. A., Simpson, L. C. C. T. S. L., Koliatsos, V. E., Rosenthal, A. & Et Al. 1994. GDNF: a potent survival factor for motoneurons present in peripheral nerve and muscle. *Science,* 266**,** 1062-4.
125. Henderson, L. A., Gustin, S. M., Macey, P. M., Wrigley, P. J. & Siddall, P. J. 2011. Functional reorganization of the brain in humans following spinal cord injury: evidence for underlying changes in cortical anatomy. *J Neurosci,* 31**,** 2630-7.
126. Hendry, I. A. 1975. The response of adrenergic neurones to axotomy and nerve growth factor. *Brain Res,* 94**,** 87-97.
127. Herrera-Rincon, C., Torets, C., Sanchez-Jimenez, A., Avendano, C. & Panetsos, F. 2012. Chronic electrical stimulation of transected peripheral nerves preserves anatomy and function in the primary somatosensory cortex. *Eur J Neurosci,* 36**,** 3679-90.
128. Hoffman, P. N. 1989. Expression of GAP-43, a rapidly transported growth-associated protein, and class II beta tubulin, a slowly transported cytoskeletal protein, are coordinated in regenerating neurons. *J Neurosci,* 9**,** 893-7.
129. Hoffman, P. N. 2010. A conditioning lesion induces changes in gene expression and axonal transport that enhance regeneration by increasing the intrinsic growth state of axons. *Exp Neurol,* 223**,** 11-8.
130. Hofstetter, C. P., Schwarz, E. J., Hess, D., Widenfalk, J., El Manira, A., Prockop, D. J. & Olson, L. 2002. Marrow stromal cells form guiding strands in the injured spinal cord and promote recovery. *Proc Natl Acad Sci U S A,* 99**,** 2199-204.

131. Hollis, E. R., 2nd, Jamshidi, P., Low, K., Blesch, A. & Tuszynski, M. H. 2009a. Induction of corticospinal regeneration by lentiviral trkB-induced Erk activation. *Proc Natl Acad Sci U S A,* 106**,** 7215-20.
132. Hollis, E. R., 2nd, Lu, P., Blesch, A. & Tuszynski, M. H. 2009b. IGF-I gene delivery promotes corticospinal neuronal survival but not regeneration after adult CNS injury. *Exp Neurol,* 215**,** 53-9.
133. Hou, S., Nicholson, L., Van Niekerk, E., Motsch, M. & Blesch, A. 2012. Dependence of regenerated sensory axons on continuous neurotrophin-3 delivery. *J Neurosci,* 32**,** 13206-20.
134. Hudmon, A., Schulman, H., Kim, J., Maltez, J. M., Tsien, R. W. & Pitt, G. S. 2005. CaMKII tethers to L-type Ca2+ channels, establishing a local and dedicated integrator of Ca2+ signals for facilitation. *J Cell Biol,* 171**,** 537-47.
135. Iggo, A., Steedman, W. M. & Fleetwood-Walker, S. 1985. Spinal processing: anatomy and physiology of spinal nociceptive mechanisms. *Philos Trans R Soc Lond B Biol Sci,* 308**,** 235-52.
136. Isomura, Y. & Kato, N. 1999. Action potential-induced dendritic calcium dynamics correlated with synaptic plasticity in developing hippocampal pyramidal cells. *J Neurophysiol,* 82**,** 1993-9.
137. Ito, Y., Sugimoto, Y., Tomioka, M., Kai, N. & Tanaka, M. 2009. Does high dose methylprednisolone sodium succinate really improve neurological status in patient with acute cervical cord injury?: a prospective study about neurological recovery and early complications. *Spine (Phila Pa 1976),* 34**,** 2121-4.
138. Jiang, Y. Q., Zaaimi, B. & Martin, J. H. 2016. Competition with Primary Sensory Afferents Drives Remodeling of Corticospinal Axons in Mature Spinal Motor Circuits. *J Neurosci,* 36**,** 193-203.
139. Jones, L. L., Margolis, R. U. & Tuszynski, M. H. 2003. The chondroitin sulfate proteoglycans neurocan, brevican, phosphacan, and versican are differentially regulated following spinal cord injury. *Exp Neurol,* 182**,** 399-411.
140. Jones, L. L. & Tuszynski, M. H. 2002. Spinal cord injury elicits expression of keratan sulfate proteoglycans by macrophages, reactive microglia, and oligodendrocyte progenitors. *J Neurosci,* 22**,** 4611-24.
141. Kadoya, K., Tsukada, S., Lu, P., Coppola, G., Geschwind, D., Filbin, M., Blesch, A. & Tuszynski, M. H. 2009. Combined intrinsic and extrinsic neuronal mechanisms facilitate bridging axonal regeneration one year after spinal cord injury. *Neuron,* 64**,** 165-72.
142. Khoutorsky, A. & Spira, M. E. 2009. Activity-dependent calpain activation plays a critical role in synaptic facilitation and post-tetanic potentiation. *Learn Mem,* 16**,** 129-41.
143. Kobayashi, N. R., Fan, D. P., Giehl, K. M., Bedard, A. M., Wiegand, S. J. & Tetzlaff, W. 1997. BDNF and NT-4/5 prevent atrophy of rat rubrospinal neurons after cervical axotomy, stimulate GAP-43 and Talpha1-tubulin mRNA expression, and promote axonal regeneration. *J Neurosci,* 17**,** 9583-95.
144. Koike, T., Martin, D. P. & Johnson, E. M., Jr. 1989. Role of Ca2+ channels in the ability of membrane depolarization to prevent neuronal death induced by trophic-factor deprivation: evidence that levels of internal Ca2+ determine nerve growth factor dependence of sympathetic ganglion cells. *Proc Natl Acad Sci U S A,* 86**,** 6421-5.
145. Koyanagi, I. & Tator, C. H. 1997. Effect of a single huge dose of methylprednisolone on blood flow, evoked potentials, and histology after acute spinal cord injury in the rat. *Neurol Res,* 19**,** 289-99.
146. Kwon, B. K., Liu, J., Messerer, C., Kobayashi, N. R., Mcgraw, J., Oschipok, L. & Tetzlaff, W. 2002. Survival and regeneration of rubrospinal neurons 1 year after spinal cord injury. *Proc Natl Acad Sci U S A,* 99**,** 3246-51.
147. Larmet, Y., Dolphin, A. C. & Davies, A. M. 1992. Intracellular calcium regulates the survival of early sensory neurons before they become dependent on neurotrophic factors. *Neuron,* 9**,** 563-74.

148. Lee, W. J., Mc, G. J. & Duvall, E. N. 1950. Continuous tatanizing (low voltage) currents for relief of spasm. A clinical study of twenty-seven spinal cord injury patients. *Arch Phys Med Rehabil,* 31**,** 766-71.
149. Levy, W. J. 1987. Transcranial stimulation of the motor cortex to produce motor-evoked potentials. *Med Instrum,* 21**,** 248-54.
150. Lipton, S. A. 1986. Blockade of electrical activity promotes the death of mammalian retinal ganglion cells in culture. *Proc Natl Acad Sci U S A,* 83**,** 9774-8.
151. Little, J. W. & Halar, E. 1985. Temporal course of motor recovery after Brown-Sequard spinal cord injuries. *Paraplegia,* 23**,** 39-46.
152. Liuzzi, F. J. & Tedeschi, B. 1991. Peripheral nerve regeneration. *Neurosurg Clin N Am,* 2**,** 31-42.
153. Lnenicka, G. A. & Hong, S. J. 1997. Activity-dependent changes in voltage-dependent calcium currents and transmitter release. *Mol Neurobiol,* 14**,** 37-66.
154. Lu, B., Yokoyama, M., Dreyfus, C. F. & Black, I. B. 1991. Depolarizing stimuli regulate nerve growth factor gene expression in cultured hippocampal neurons. *Proc Natl Acad Sci U S A,* 88**,** 6289-92.
155. Lu, P., Jones, L. L., Snyder, E. Y. & Tuszynski, M. H. 2003. Neural stem cells constitutively secrete neurotrophic factors and promote extensive host axonal growth after spinal cord injury. *Exp Neurol,* 181**,** 115-29.
156. Lu, P., Yang, H., Jones, L. L., Filbin, M. T. & Tuszynski, M. H. 2004. Combinatorial therapy with neurotrophins and cAMP promotes axonal regeneration beyond sites of spinal cord injury. *J Neurosci,* 24**,** 6402-9.
157. Luo, L. & O'leary, D. D. 2005. Axon retraction and degeneration in development and disease. *Annu Rev Neurosci,* 28**,** 127-56.
158. Mader, K., Andermahr, J., Angelov, D. N. & Neiss, W. F. 2004. Dual mode of signalling of the axotomy reaction: retrograde electric stimulation or block of retrograde transport differently mimic the reaction of motoneurons to nerve transection in the rat brainstem. *J Neurotrauma,* 21**,** 956-68.
159. Magupalli, V. G., Mochida, S., Yan, J., Jiang, X., Westenbroek, R. E., Nairn, A. C., Scheuer, T. & Catterall, W. A. 2013. Ca2+-independent activation of Ca2+/calmodulin-dependent protein kinase II bound to the C-terminal domain of CaV2.1 calcium channels. *J Biol Chem,* 288**,** 4637-48.
160. Mandolesi, G., Madeddu, F., Bozzi, Y., Maffei, L. & Ratto, G. M. 2004. Acute physiological response of mammalian central neurons to axotomy: ionic regulation and electrical activity. *FASEB J,* 18**,** 1934-6.
161. Mccall, J., Weidner, N. & Blesch, A. 2012. Neurotrophic factors in combinatorial approaches for spinal cord regeneration. *Cell Tissue Res,* 349**,** 27-37.
162. Mcdonald, J. W. & Sadowsky, C. 2002. Spinal-cord injury. *Lancet,* 359**,** 417-25.
163. Mckeon, R. J., Schreiber, R. C., Rudge, J. S. & Silver, J. 1991. Reduction of neurite outgrowth in a model of glial scarring following CNS injury is correlated with the expression of inhibitory molecules on reactive astrocytes. *J Neurosci,* 11**,** 3398-411.
164. Mcquarrie, I. G. & Grafstein, B. 1973. Axon outgrowth enhanced by a previous nerve injury. *Arch Neurol,* 29**,** 53-5.
165. Moore, D. L., Blackmore, M. G., Hu, Y., Kaestner, K. H., Bixby, J. L., Lemmon, V. P. & Goldberg, J. L. 2009. KLF family members regulate intrinsic axon regeneration ability. *Science,* 326**,** 298-301.
166. Nagendran, T. & Hardy, L. R. 2011. Calcium/calmodulin-dependent protein kinase IV mediates distinct features of basal and activity-dependent dendrite complexity. *Neuroscience,* 199**,** 548-62.
167. Nashold, B. S., Jr. & Friedman, H. 1972. Dorsal column stimulation for control of pain. Preliminary report on 30 patients. *J Neurosurg,* 36**,** 590-7.
168. Neumann, S. & Woolf, C. J. 1999. Regeneration of dorsal column fibers into and beyond the lesion site following adult spinal cord injury. *Neuron,* 23**,** 83-91.
169. Nielson, J. L., Strong, M. K. & Steward, O. 2011. A reassessment of whether cortical

motor neurons die following spinal cord injury. *J Comp Neurol,* 519**,** 2852-69.
170. Nixon, B. J., Doucette, R., Jackson, P. C. & Diamond, J. 1984. Impulse activity evokes precocious sprouting of nociceptive nerves into denervated skin. *Somatosens Res,* 2**,** 97-126.
171. Obata, K., Yamanaka, H., Dai, Y., Tachibana, T., Fukuoka, T., Tokunaga, A., Yoshikawa, H. & Noguchi, K. 2003. Differential activation of extracellular signal-regulated protein kinase in primary afferent neurons regulates brain-derived neurotrophic factor expression after peripheral inflammation and nerve injury. *J Neurosci,* 23**,** 4117-26.
172. Park, E., Velumian, A. A. & Fehlings, M. G. 2004. The role of excitotoxicity in secondary mechanisms of spinal cord injury: a review with an emphasis on the implications for white matter degeneration. *J Neurotrauma,* 21**,** 754-74.
173. Park, K. K., Liu, K., Hu, Y., Smith, P. D., Wang, C., Cai, B., Xu, B., Connolly, L., Kramvis, I., Sahin, M. & He, Z. 2008. Promoting axon regeneration in the adult CNS by modulation of the PTEN/mTOR pathway. *Science,* 322**,** 963-6.
174. Park, S., Koppes, R. A., Froriep, U. P., Jia, X., Achyuta, A. K., Mclaughlin, B. L. & Anikeeva, P. 2015. Optogenetic control of nerve growth. *Sci Rep,* 5**,** 9669.
175. Polak, K. A., Edelman, A. M., Wasley, J. W. & Cohan, C. S. 1991. A novel calmodulin antagonist, CGS 9343B, modulates calcium-dependent changes in neurite outgrowth and growth cone movements. *J Neurosci,* 11**,** 534-42.
176. Pomeranz, B., Mullen, M. & Markus, H. 1984. Effect of applied electrical fields on sprouting of intact saphenous nerve in adult rat. *Brain Res,* 303**,** 331-6.
177. Purves, D., Snider, W. D. & Voyvodic, J. T. 1988. Trophic regulation of nerve cell morphology and innervation in the autonomic nervous system. *Nature,* 336**,** 123-8.
178. Qiu, J., Cafferty, W. B., Mcmahon, S. B. & Thompson, S. W. 2005. Conditioning injury-induced spinal axon regeneration requires signal transducer and activator of transcription 3 activation. *J Neurosci,* 25**,** 1645-53.
179. Raff, M. C., Whitmore, A. V. & Finn, J. T. 2002. Axonal self-destruction and neurodegeneration. *Science,* 296**,** 868-71.
180. Rajnicek, A. M., Foubister, L. E. & Mccaig, C. D. 2006. Growth cone steering by a physiological electric field requires dynamic microtubules, microfilaments and Rac-mediated filopodial asymmetry. *J Cell Sci,* 119**,** 1736-45.
181. Ramon-Cueto, A. & Nieto-Sampedro, M. 1994. Regeneration into the spinal cord of transected dorsal root axons is promoted by ensheathing glia transplants. *Exp Neurol,* 127**,** 232-44.
182. Reber, B. F., Porzig, H., Becker, C. & Reuter, H. 1990. Depolarization-induced changes of free intracellular Ca(2+) concentration and of [(3)H]dopamine release in undifferentiated and differentiated PC12 cells. *Neurochem Int,* 17**,** 197-203.
183. Redmond, L., Kashani, A. H. & Ghosh, A. 2002. Calcium regulation of dendritic growth via CaM kinase IV and CREB-mediated transcription. *Neuron,* 34**,** 999-1010.
184. Rehder, V., Jensen, J. R. & Kater, S. B. 1992. The initial stages of neural regeneration are dependent upon intracellular calcium levels. *Neuroscience,* 51**,** 565-74.
185. Richardson, P. M. & Issa, V. M. 1984. Peripheral injury enhances central regeneration of primary sensory neurones. *Nature,* 309**,** 791-793.
186. Richardson, P. M., Mcguinness, U. M. & Aguayo, A. J. 1980. Axons from CNS neurons regenerate into PNS grafts. *Nature,* 284**,** 264-5.
187. Romero, M. I., Rangappa, N., Garry, M. G. & Smith, G. M. 2001. Functional regeneration of chronically injured sensory afferents into adult spinal cord after neurotrophin gene therapy. *J Neurosci,* 21**,** 8408-16.
188. Romero, M. I., Rangappa, N., Li, L., Lightfoot, E., Garry, M. G. & Smith, G. M. 2000. Extensive sprouting of sensory afferents and hyperalgesia induced by conditional expression of nerve growth factor in the adult spinal cord. *J Neurosci,* 20**,** 4435-45.
189. Rubel, E. W., Hyson, R. L. & Durham, D. 1990. Afferent regulation of neurons in the brain stem auditory system. *J Neurobiol,* 21**,** 169-96.

190. Ruitenberg, M. J., Blits, B., Dijkhuizen, P. A., Te Beek, E. T., Bakker, A., Van Heerikhuize, J. J., Pool, C. W., Hermens, W. T., Boer, G. J. & Verhaagen, J. 2004. Adeno-associated viral vector-mediated gene transfer of brain-derived neurotrophic factor reverses atrophy of rubrospinal neurons following both acute and chronic spinal cord injury. *Neurobiol Dis,* 15**,** 394-406.
191. Rydel, R. E. & Greene, L. A. 1988. cAMP analogs promote survival and neurite outgrowth in cultures of rat sympathetic and sensory neurons independently of nerve growth factor. *Proc Natl Acad Sci U S A,* 85**,** 1257-61.
192. Salomon, J. A., Haagsma, J. A., Davis, A., De Noordhout, C. M., Polinder, S., Havelaar, A. H., Cassini, A., Devleesschauwer, B., Kretzschmar, M., Speybroeck, N., Murray, C. J. & Vos, T. 2015. Disability weights for the Global Burden of Disease 2013 study. *Lancet Glob Health,* 3**,** e712-23.
193. Sanchez-Vives, M. V. & Gallego, R. 1994. Calcium-dependent chloride current induced by axotomy in rat sympathetic neurons. *J Physiol,* 475**,** 391-400.
194. Sayer, F. T., Kronvall, E. & Nilsson, O. G. 2006. Methylprednisolone treatment in acute spinal cord injury: the myth challenged through a structured analysis of published literature. *Spine J,* 6**,** 335-43.
195. Schilero, G. J., Spungen, A. M., Bauman, W. A., Radulovic, M. & Lesser, M. 2009. Pulmonary function and spinal cord injury. *Respir Physiol Neurobiol,* 166**,** 129-41.
196. Schlumm, F., Mauceri, D., Freitag, H. E. & Bading, H. 2013. Nuclear calcium signaling regulates nuclear export of a subset of class IIa histone deacetylases following synaptic activity. *J Biol Chem,* 288**,** 8074-84.
197. Schmitt, J. M., Wayman, G. A., Nozaki, N. & Soderling, T. R. 2004. Calcium activation of ERK mediated by calmodulin kinase I. *J Biol Chem,* 279**,** 24064-72.
198. Schneider, R. J., Kulics, A. T. & Ducker, T. B. 1977. Proprioceptive pathways of the spinal cord. *J Neurol Neurosurg Psychiatry,* 40**,** 417-33.
199. Schwab, M. E. 2004. Nogo and axon regeneration. *Curr Opin Neurobiol,* 14**,** 118-24.
200. Seijffers, R., Allchorne, A. J. & Woolf, C. J. 2006. The transcription factor ATF-3 promotes neurite outgrowth. *Mol Cell Neurosci,* 32**,** 143-54.
201. Seijffers, R., Mills, C. D. & Woolf, C. J. 2007. ATF3 increases the intrinsic growth state of DRG neurons to enhance peripheral nerve regeneration. *J Neurosci,* 27**,** 7911-20.
202. Silver, J. & Miller, J. H. 2004. Regeneration beyond the glial scar. *Nat Rev Neurosci,* 5**,** 146-56.
203. Skup, M., Dwornik, A., Macias, M., Sulejczak, D., Wiater, M. & Czarkowska-Bauch, J. 2002. Long-term locomotor training up-regulates TrkB(FL) receptor-like proteins, brain-derived neurotrophic factor, and neurotrophin 4 with different topographies of expression in oligodendroglia and neurons in the spinal cord. *Exp Neurol,* 176**,** 289-307.
204. Sleeper, A. A., Cummins, T. R., Dib-Hajj, S. D., Hormuzdiar, W., Tyrrell, L., Waxman, S. G. & Black, J. A. 2000. Changes in expression of two tetrodotoxin-resistant sodium channels and their currents in dorsal root ganglion neurons after sciatic nerve injury but not rhizotomy. *J Neurosci,* 20**,** 7279-89.
205. Smith, D. S. & Skene, J. H. 1997. A transcription-dependent switch controls competence of adult neurons for distinct modes of axon growth. *J Neurosci,* 17**,** 646-58.
206. Solem, M., Mcmahon, T. & Messing, R. O. 1995. Depolarization-induced neurite outgrowth in PC12 cells requires permissive, low level NGF receptor stimulation and activation of calcium/calmodulin-dependent protein kinase. *J Neurosci,* 15**,** 5966-75.
207. Soler, R. M., Egea, J., Mintenig, G. M., Sanz-Rodriguez, C., Iglesias, M. & Comella, J. X. 1998. Calmodulin is involved in membrane depolarization-mediated survival of motoneurons by phosphatidylinositol-3 kinase- and MAPK-independent pathways. *J Neurosci,* 18**,** 1230-9.
208. Spencer, T. K., Mellado, W. & Filbin, M. T. 2008. BDNF activates CaMKIV and PKA

in parallel to block MAG-mediated inhibition of neurite outgrowth. *Mol Cell Neurosci,* 38**,** 110-6.
209. Spitzer, N. C. 2006. Electrical activity in early neuronal development. *Nature,* 444**,** 707-12.
210. Stokes, B. T. & Reier, P. J. 1992. Fetal grafts alter chronic behavioral outcome after contusion damage to the adult rat spinal cord. *Exp Neurol,* 116**,** 1-12.
211. Sun, F., Park, K. K., Belin, S., Wang, D., Lu, T., Chen, G., Zhang, K., Yeung, C., Feng, G., Yankner, B. A. & He, Z. 2011. Sustained axon regeneration induced by co-deletion of PTEN and SOCS3. *Nature***,** in press.
212. Takeoka, A., Vollenweider, I., Courtine, G. & Arber, S. 2014. Muscle spindle feedback directs locomotor recovery and circuit reorganization after spinal cord injury. *Cell,* 159**,** 1626-39.
213. Tang, Q., Bangaru, M. L., Kostic, S., Pan, B., Wu, H. E., Koopmeiners, A. S., Yu, H., Fischer, G. J., Mccallum, J. B., Kwok, W. M., Hudmon, A. & Hogan, Q. H. 2012. Ca(2)(+)-dependent regulation of Ca(2)(+) currents in rat primary afferent neurons: role of CaMKII and the effect of injury. *J Neurosci,* 32**,** 11737-49.
214. Tang, X., Davies, J. E. & Davies, S. J. 2003. Changes in distribution, cell associations, and protein expression levels of NG2, neurocan, phosphacan, brevican, versican V2, and tenascin-C during acute to chronic maturation of spinal cord scar tissue. *J Neurosci Res,* 71**,** 427-44.
215. Taylor, L., Jones, L., Tuszynski, M. H. & Blesch, A. 2006. Neurotrophin-3 gradients established by lentiviral gene delivery promote short-distance axonal bridging beyond cellular grafts in the injured spinal cord. *J Neurosci,* 26**,** 9713-21.
216. Thompson, A. K. & Wolpaw, J. R. 2015. Restoring walking after spinal cord injury: operant conditioning of spinal reflexes can help. *Neuroscientist,* 21**,** 203-15.
217. Titmus, M. J. & Faber, D. S. 1990. Axotomy-induced alterations in the electrophysiological characteristics of neurons. *Prog Neurobiol,* 35**,** 1-51.
218. Tuszynski, M. H., Gabriel, K., Gage, F. H., Suhr, S., Meyer, S. & Rosetti, A. 1996. Nerve growth factor delivery by gene transfer induces differential outgrowth of sensory, motor, and noradrenergic neurites after adult spinal cord injury. *Exp Neurol,* 137**,** 157-73.
219. Tuszynski, M. H., Gabriel, K., Gerhardt, K. & Szollar, S. 1999. Human spinal cord retains substantial structural mass in chronic stages after injury. *J Neurotrauma,* 16**,** 523-31.
220. Tuszynski, M. H., Peterson, D. A., Ray, J., Baird, A., Nakahara, Y. & Gage, F. H. 1994. Fibroblasts genetically modified to produce nerve growth factor induce robust neuritic ingrowth after grafting to the spinal cord. *Exp Neurol,* 126**,** 1-14.
221. Udina, E., Furey, M., Busch, S., Silver, J., Gordon, T. & Fouad, K. 2008. Electrical stimulation of intact peripheral sensory axons in rats promotes outgrowth of their central projections. *Exp Neurol,* 210**,** 238-47.
222. Urban, D. J. & Roth, B. L. 2015. DREADDs (designer receptors exclusively activated by designer drugs): chemogenetic tools with therapeutic utility. *Annu Rev Pharmacol Toxicol,* 55**,** 399-417.
223. Vaillant, A. R., Mazzoni, I., Tudan, C., Boudreau, M., Kaplan, D. R. & Miller, F. D. 1999. Depolarization and neurotrophins converge on the phosphatidylinositol 3-kinase-Akt pathway to synergistically regulate neuronal survival. *J Cell Biol,* 146**,** 955-66.
224. Wang, D. D. & Kriegstein, A. R. 2011. Blocking early GABA depolarization with bumetanide results in permanent alterations in cortical circuits and sensorimotor gating deficits. *Cereb Cortex,* 21**,** 574-87.
225. Wannier, T., Schmidlin, E., Bloch, J. & Rouiller, E. M. 2005. A unilateral section of the corticospinal tract at cervical level in primate does not lead to measurable cell loss in motor cortex. *J Neurotrauma,* 22**,** 703-17.
226. Wayman, G. A., Kaech, S., Grant, W. F., Davare, M., Impey, S., Tokumitsu, H., Nozaki, N., Banker, G. & Soderling, T. R. 2004. Regulation of axonal extension and growth

cone motility by calmodulin-dependent protein kinase I. *J Neurosci,* 24**,** 3786-94.
227. Weidner, N., Ner, A., Salimi, N. & Tuszynski, M. H. 2001. Spontaneous corticospinal axonal plasticity and functional recovery after adult central nervous system injury. *Proc Natl Acad Sci U S A,* 98**,** 3513-3518.
228. Wenjin, W., Wenchao, L., Hao, Z., Feng, L., Yan, W., Wodong, S., Xianqun, F. & Wenlong, D. 2011. Electrical stimulation promotes BDNF expression in spinal cord neurons through Ca(2+)- and Erk-dependent signaling pathways. *Cell Mol Neurobiol,* 31**,** 459-67.
229. Wess, J., Nakajima, K. & Jain, S. 2013. Novel designer receptors to probe GPCR signaling and physiology. *Trends Pharmacol Sci,* 34**,** 385-92.
230. Wheeler, D. G., Groth, R. D., Ma, H., Barrett, C. F., Owen, S. F., Safa, P. & Tsien, R. W. 2012. Ca(V)1 and Ca(V)2 channels engage distinct modes of Ca(2+) signaling to control CREB-dependent gene expression. *Cell,* 149**,** 1112-24.
231. Willis, W. D. 1985. Nociceptive pathways: anatomy and physiology of nociceptive ascending pathways. *Philos Trans R Soc Lond B Biol Sci,* 308**,** 253-70.
232. Wirz, M., Dietz, V. & European Multicenter Study of Spinal Cord Injury, N. 2015. Recovery of sensorimotor function and activities of daily living after cervical spinal cord injury: the influence of age. *J Neurotrauma,* 32**,** 194-9.
233. Wong, L. F., Yip, P. K., Battaglia, A., Grist, J., Corcoran, J., Maden, M., Azzouz, M., Kingsman, S. M., Kingsman, A. J., Mazarakis, N. D. & Mcmahon, S. B. 2006. Retinoic acid receptor beta2 promotes functional regeneration of sensory axons in the spinal cord. *Nat Neurosci,* 9**,** 243-50.
234. Wood, M. & Willits, R. K. 2006. Short-duration, DC electrical stimulation increases chick embryo DRG neurite outgrowth. *Bioelectromagnetics,* 27**,** 328-31.
235. Wright, L. 1981. Cell survival in chick embryo ciliary ganglion is reduced by chronic ganglionic blockade. *Brain Res,* 227**,** 283-6.
236. Wu, D., Zhang, Y., Bo, X., Huang, W., Xiao, F., Zhang, X., Miao, T., Magoulas, C., Subang, M. C. & Richardson, P. M. 2006. Actions of neuropoietic cytokines and cyclic AMP in regenerative conditioning of rat primary sensory neurons. *Exp Neurol,* 204**,** 66-76.
237. Wu, G. Y., Deisseroth, K. & Tsien, R. W. 2001. Activity-dependent CREB phosphorylation: convergence of a fast, sensitive calmodulin kinase pathway and a slow, less sensitive mitogen-activated protein kinase pathway. *Proc Natl Acad Sci U S A,* 98**,** 2808-13.
238. Xu, X. M., Guenard, V., Kleitman, N., Aebischer, P. & Bunge, M. B. 1995. A combination of BDNF and NT-3 promotes supraspinal axonal regeneration into Schwann cell grafts in adult rat thoracic spinal cord. *Exp Neurol,* 134**,** 261-72.
239. Yan, Q., Wang, J., Matheson, C. R. & Urich, J. L. 1999. Glial cell line-derived neurotrophic factor (GDNF) promotes the survival of axotomized retinal ganglion cells in adult rats: comparison to and combination with brain-derived neurotrophic factor (BDNF). *J Neurobiol,* 38**,** 382-90.
240. Yip, P. K., Wong, L. F., Sears, T. A., Yanez-Munoz, R. J. & Mcmahon, S. B. 2010. Cortical overexpression of neuronal calcium sensor-1 induces functional plasticity in spinal cord following unilateral pyramidal tract injury in rat. *PLoS Biol,* 8**,** e1000399.
241. Yoo, S., Nguyen, M. P., Fukuda, M., Bittner, G. D. & Fishman, H. M. 2003. Plasmalemmal sealing of transected mammalian neurites is a gradual process mediated by Ca(2+)-regulated proteins. *J Neurosci Res,* 74**,** 541-51.
242. Yoon, D. H., Kim, Y. S. & Young, W. 1999. Therapeutic time window for methylprednisolone in spinal cord injured rat. *Yonsei Med J,* 40**,** 313-20.
243. Zariffa, J., Curt, A., Group, E. S. & Steeves, J. D. 2012. Functional motor preservation below the level of injury in subjects with American Spinal Injury Association Impairment Scale grade A spinal cord injuries. *Arch Phys Med Rehabil,* 93**,** 905-7.
244. Zariffa, J., Kramer, J. L., Fawcett, J. W., Lammertse, D. P., Blight, A. R., Guest, J., Jones, L., Burns, S., Schubert, M., Bolliger, M., Curt, A. & Steeves, J. D. 2011.

Characterization of neurological recovery following traumatic sensorimotor complete thoracic spinal cord injury. *Spinal Cord,* 49**,** 463-71.
245. Zhang, J. M., Donnelly, D. F., Song, X. J. & Lamotte, R. H. 1997. Axotomy increases the excitability of dorsal root ganglion cells with unmyelinated axons. *J Neurophysiol,* 78**,** 2790-4.
246. Zhang, L. I. & Poo, M. M. 2001. Electrical activity and development of neural circuits. *Nat Neurosci,* 4 Suppl**,** 1207-14.
247. Zhong, J., Dietzel, I. D., Wahle, P., Kopf, M. & Heumann, R. 1999. Sensory impairments and delayed regeneration of sensory axons in interleukin-6-deficient mice. *J Neurosci,* 19**,** 4305-13.
248. Zhou, F. Q. & Snider, W. D. 2006. Intracellular control of developmental and regenerative axon growth. *Philos Trans R Soc Lond B Biol Sci,* 361**,** 1575-92.
249. Zhu, H. & Roth, B. L. 2014. Silencing synapses with DREADDs. *Neuron,* 82**,** 723-5.
250. Ziemba, K. S., Chaudhry, N., Rabchevsky, A. G., Jin, Y. & Smith, G. M. 2008. Targeting axon growth from neuronal transplants along preformed guidance pathways in the adult CNS. *J Neurosci,* 28**,** 340-8.

2. Rationale and hypotheses

The main hypothesis of this doctoral thesis is that neuronal activity by electrical stimulation (ES) has growth promoting effects, in a similar way as conditioning lesions of the peripheral branch of DRG neurons. This proposal is based on findings, which suggest that the clinically relevant technique of neuronal electrical stimulation (ES) can augment the intrinsic regenerative capacity of injured neurons within the spinal cord. Thus, the overall goals of the doctoral thesis are to establish ES as a practical approach to induce regenerative programs in injured neurons that can be translated to larger animal models and humans, to use ES in combinatorial treatments for axon regeneration, and to explore the mechanisms of ES-induced regeneration of injured axons.

Aim 1: Determine whether repetitive, chronic ES of peripheral sensory fibers will activate regenerative programs in dorsal root ganglion neurons.

> **Objective 1.1.** Analyze the growth of sensory fibers in vitro (DRG cultures) following ES of the sciatic nerve with different parameters.
>
> **Objective 1.2.** Explore the impact of variables in the electrical stimulation paradigm on regenerative growth of injured neurons.
>
> **Objective 1.3.** Identify the most efficient stimulating approach to promote neurite growth of sensory fibers.

Aim 2: Determine whether single or repetitive stimulation of sensory axons promotes regeneration and axonal bridging across a spinal lesion site in vivo in a combinatorial approach with cellular grafts.

> **Objective 2.1.** Evaluate growth in a cervical dorsal column lesion after ES.
>
> **Objective 2.2.** Evaluate potential side effects relevant for clinical translation including altered pain processing using standard behavioral assays for nociception.

Aim 3: Analyze mechanisms involved in activity/electrical stimulation-mediated effects on neurite growth of dorsal root ganglion neurons.

> **Objective 3.1.** Evaluate the contribution of depolarization on growth in vitro

Objective 3.2. Evaluate contribution of nuclear calcium signaling and calmodulin (CaM) dependent signaling pathways on growth in vitro.

Aim 4: Analyze the transcriptional changes and the signaling pathways in sensory neurons following ES of the sciatic nerve.

3. Materials and methods

3.1. Surgical procedures

3.1.1. Animals

In all experiments adult (8-14weeks) female Fischer 344 rats (150-200g) were used, according to animal care guidelines. All experimental animal procedures were approved by the Regierungspräsidium Karlsruhe.

3.1.2. Anesthesia and analgesia

Surgeries were performed either under Isoflurane anesthesia (3-4% induction, up to 5 min and 1-1.5% maintenance) with an inhalator (FMI Gmbh) or under a ketamine-xylazine anesthesia mix (125 mg/kg ketamine, 6.35 mg/kg xylazine, 1.25 mg/kg acepromazine), administered intramuscularly (i.m.) as described. Generally, for minimally-invasive interventions and long anesthesia times, isoflurane anesthesia and for more invasive surgeries such as laminectomy with spinal injury, or in-vivo DRG injection, ketamine-xylazine anesthesia was used. Within the same experiment, all groups received the same anesthesia. Postoperative pain relief was administered by subcutaneous (s.c) buprenorphine (Temgesic) injection (0,03mg/kg/day) for 2 days after surgery followed by Carprofen (4-5mg/kg/day), as needed. Prophylactic antibiotics were delivered s.c. for 2 days post-surgery (ampicillin 25mg/150g rat, twice a day).

3.1.3. In vivo electrical stimulation

3.1.3.1. Experimental groups

An overview of the experimental groups is presented in **Fig.3.1**. Briefly, cuff electrodes were placed on the sciatic nerve in the mid-thigh area in anesthetized rats, after exposing the nerve and gently dissecting the connective tissue, and electrical stimulation (ES) was performed as described below. Control animals received either no manipulation (naïve) or sham electrodes implantation without stimulation (sham). As a positive control, one group of rats underwent conditioning lesions (CL) of the sciatic nerve (crush at mid-thigh level for 20s with a jeweler's forceps). The electrodes were removed immediately after ES, or remained in place for chronic/repeated stimulation, with a subcutaneous connector between the shoulder blades. Implants were left for up to 7 days for in vitro growth experiments and up to 28 days for in vivo growth experiments with no displacement or

obvious adverse effects. Within each experiment, sham electrodes were left in place for the same time as stimulating electrodes, to control for any nonspecific effects due to the cuff. In 2 pilot experiments, we performed stimulation, CL or sham unilaterally, to check for any influence on the contralateral side. We found no indication of any influence in neurite growth assay. Thus in subsequent experiments, the 2 sides of an animal were assessed independently. Isolation, plating and in vitro growth assessments are described under DRG cultures in Experimental Procedures. Additional experimental groups received similar treatment and were perfused after 1 or 7 days and the DRGs were collected for immunohistochemistry. For a complete description of groups see **Annex 1: Experimental groups.**

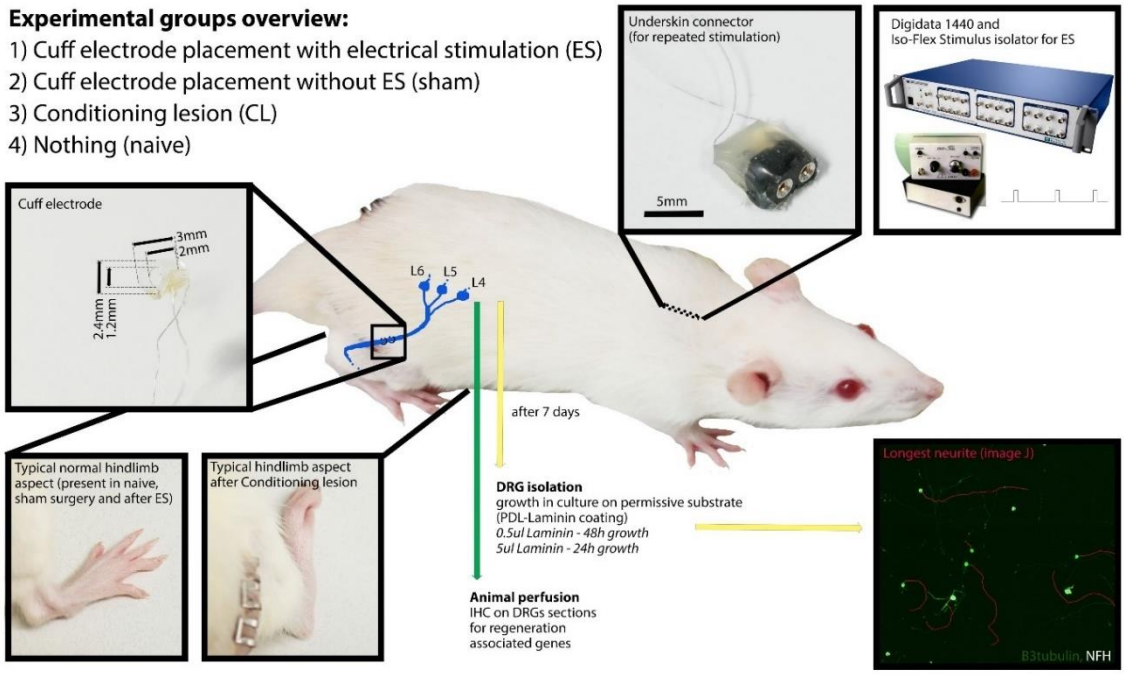

Fig.3.1. Methods and experimental groups overview. A cuff electrode is placed on the sciatic, with ES or without stimulation (sham). Additional control animals received no manipulation (naïve) or underwent conditioning lesions (CL). After 7 days DRGs were isolated for in vitro neurite growth or animals were perfused and DRGs dissected for IHC or RNA isolation.

3.1.3.2. Electrodes

For the stimulation of the sciatic nerve I manufactured silicone cuff electrodes **(Fig.4.1)**, from silicone tube (8079, Science-Products, 1.574mm inner diameter; 2.413mm outer diameter), Teflon coated steel wire single strand annealed (SS-2TA, Science-Products) and connectors embedded in silicone non-toxic glue, matching output connector manufactured for the Iso-Flex stimulus isolator (A.M.P.I.). The silicone tube was cut in

3mm cylinders with a longitudinal opening through which the nerve was inserted in the cuff. The wires were fixed on one side of the cuff with knots, the isolation was removed from the part of the wires inside the cuff and the wires shaped as circular electrodes on the inside surface of the cuff. While building the electrodes, silicone glue was used, if necessary, to better fix or to isolate the wires outside the cuff. Anode and cathode were at a distance of 2-2.5 mm in the silicone tube. Final inner diameter of the cuffs was 1.2-1.4mm, thus mildly lose around a rat sciatic nerve to minimize pressure to the nerve **(Fig.4.1.D)**.

3.1.3.3. Electrical stimulation set-up and parameters

ES was applied to the intact nerve using Iso-Flex Stimulus Isolators (A.M.P.I.) controlled by digitizer Digidata 1440 (Axon Instruments) **(Fig.3.1)**. The standard parameters used were: 20Hz, constant current stimulation, pulse duration 0.2 ms for 1h, because these have been shown to be most effective for promoting DRG peripheral axon outgrowth (Geremia et al., 2007) and also promote central regeneration (Udina et al., 2008). Stimulation intensity was set to 2 times motor threshold (MT) intensity, assessed by the first visible movement of the hind-paw, activating both afferent and efferent large myelinated Aß-fibers and motor fibers. If stimulation was done bilaterally, the MT was determined independently for every stimulated side, and intensity set as appropriate. When nerves were repeatedly stimulated, the threshold was reassessed at every stimulation session. Stimulation lasted generally for 1h unless indicated otherwise. In some experiments I stimulated continuously for 7h, with switch of electrode polarity after every hour, to make the stimulation as similar as possible to the 1h stimulation, while at the same time minimizing cumulative chemical changes. In some experiments, variations to frequency or stimulation intensity were examined as described. The setup used did not allow biphasic or alternating stimulation, however our long duration stimulations (7h) would emphasize any unbalanced electrolysis effects on neurite growth, if such effects were to exist.

3.1.4. In vivo growth after central lesion and cell injection

3.1.4.1. Experimental groups

Animals were anesthetized with a ketamine-xylazine mix as described and received a dorsal column lesion (DCL) and BMSCs cell injection to fill the lesion, followed by either ES (n=7), or cuff electrodes with no stimulation (n=6). Cuffs were removed after the stimulation and animals were allowed to recover. Additional animals received either no

manipulation of the sciatic (lesion only group) or CL (n=6 each). To test if repeated ES could further increases growth in an in vivo setup, two additional groups with chronic implants with or without stimulation were examined, and ES was repeated once for 1h at 7 days after the initial stimulation (n=6 each). Animals were sacrificed at four weeks post-lesion, perfused, spinal tissue extracted, and post fixed.

3.1.4.2. Dorsal column lesion wire-knife lesion

For the in vivo assessment of ES induced growth, animals underwent a standardized lesion of the dorsal columns (DCL). Anesthetized animals were placed in a stereotactic apparatus and a longitudinal incision at the cervical level was made. C7 was identified by the length of the posterior process and if necessary rats were additionally fixed with a surgical forceps on the C7 posterior process. The muscles were gently removed from the vertebra by pushing with a cotton tip to avoid tissue damage and the posterior arch of the vertebras was exposed. A posterior laminectomy was performed at the C4 level using a small Rongeur and the spinal cord exposed. The lesion was done with a wire-knife previously calibrated for depth of insertion and fixed into a stereotactic micromanipulator. After fixation, a hole was made in the dura-mater with a 30-gauge needle, 1.1mm lateral to the midline to insert the microwire knife. The wire-knife was lowered to a depth of 1.1 mm ventral to the dorsal cord surface and extruded to form a 2.25mm wide arc with the tip visible on the contralateral side of the posterior spinal cord just beneath the dura. The knife was slowly moved up with the micromanipulator, while pressing the dura with a blunt tip, to ensure complete transection. While moving up, the wire-knife was slowly retracted such that it did not penetrate the dura on the opposite side. This lesion interrupts all dorsal column sensory fibers, with minimal disruptions of blood-vessels and dura.

3.1.4.3. BMSCs injection

After the DCL, all animals received a cell injection of bone marrow stromal cells (BMSCs) to fill the lesion and provide a favorable environment for growth. BMSCs were isolated from GFP transgenic rats to be able to identify the graft by GFP fluorescence. Each animal from all experimental groups received 2µl BMSCs (60.000cells/µl in PBS with glucose), passage 2-4, with pulled glass micropipettes attached to a Picospritzer. The glass micropipettes were inserted at the midline into the lesion at a depth of 0.5 mm and the cells were injected using a Picospritzer at a rate or 1µl/min. Pipettes were left in place after the injection to prevent extrusion of cells and then slowly withdrawn. Overlying muscle layers were sutured and the skin was stapled.

BMSCs were expanded from frozen stocks, for 5 to 7 days before surgery and prepared for injection on the day of the surgery. Briefly they were digested with 0.25% trypsin, at 37°C for 5mins, then centrifuged at 800rpm for 5min at RT, counted, suspended in PBS-glucose and kept on ice until injections.

3.1.4.4. CTB tracing

To visualize regenerating dorsal column sensory fibers, animals received injections of the transganglionic tracer, cholera toxin B subunit (CTB, 1%; 2 µl) bilateral into the sciatic nerves, 3 days prior to perfusions. Rats were anesthetized with isoflurane, the sciatic nerve was exposed and the CTB was gently injected within the nerve with a Hamilton syringe, proximally to the crush or cuff location, as previously described (Oudega et al., 1994). After 3 days, the time needed for CTB to be transported, the rats were deeply anesthetized and transcardially perfused with ice cold saline followed by 4% paraformaldehyde (PFA) in 0.1 M PB. The brain and spinal cord were isolated and post-fixed in 4% PFA for 24h.

3.1.5. In vivo injection of AAV in lumbar DRGs and CL in virus injected animals

3.1.5.1. Experimental groups

To test if blocking cytoplasmic calcium signaling could enhance CL effect in vivo, we expressed CaMBP4 (n=10) in the L4-L5 DRG of adult female Fischer rats (150-200g). This was done by in vivo DRGs injection of AAV1/2 virus producing Syn-eGFP in order to identify the infected cells and Syn-CaMBP4. As control we used Syn-eGFP, Syn-MutCaMBP4 (inactive) (n=10). Four weeks later, animals received bilateral CL with jeweler's forceps for 20s or sham surgery, followed by DRGs isolation 7 days later. One group of CaMBP4 animals (n=2) did not receive a CL, to obtain a rough estimate, whether the injection already influences the growth capacity in the absence of a CL.

3.1.5.2. DRGs AAV1/2 injection

Animal were anesthetized with a ketamine-xylazine mix as described and underwent a dorsal laminectomy of the lumbar spinal cord, identifying L4 and L5 by anatomical position relative to the illium. The L4 and L5 from each side of the animals were injected with 1.3µl of virus ($1x10^9$/µl), producing either mutated (n=10) or active CaMBP4 (n=10), using glass micropipettes connected to a PicoSpritzer. Postoperative pain relief was supplied by buprenorphine. The location of the injection was confirmed later for all animals upon

dissection and isolation of DRGs, by the laminectomy and presence of scar tissue around the respective DRGs.

3.1.5.3. Recombinant adeno-associated viruses

To express CaMBP4 in vivo, we used an AAV1/2 virus injected in the DRGs producing CaMBP4 or MutCaMBP4 and enhanced green florescent protein (eGFP) under Syn promoter. Virus was kindly provided by Dr. H. Bading.

Table 3.1: Viruses

Name	Short description	Source
AAV1/2 Syn-CaMBP4_cyt	Active CaMBP4, enhanced green florescent protein (eGFP)	Dr. E. Freitag (Group Prof. Dr. H. Bading)
AAV1/2 Syn-MutCaMBP4	inactive CaMBP4 due to a point mutation, eGFP, used as control virus injection.	Dr. E. Freitag (Group Prof. Dr. H. Bading)

3.2. Assessment of regeneration in vivo

3.2.1. In vivo regeneration after DCL

3.2.1.1. Immunohistochemistry

Using a cryostat (CM 3000, Leica, Germany), 35 µm sagittal sections, of the spinal cord tissue with the DCL, were cut and 8 series were collected in TCS and stored at 4°C. CTB was visualized by light level immunohistochemistry, while the transplanted BMSCs and lesion border were visualized by immunofluorescent labeling for GFP and GFAP, respectively. Briefly, free-floating sections were washed 3 times with TBS, incubated with 0.6% H_2O_2 for 15 min, followed by 2 more TBS washes and blocked with 5% horse serum, 0.25% Triton (TX-100) for 1 h. They were then incubated with goat anti-CTB antibody (1:80.000 in TBS, 0.25% Triton, 1% serum) for 3 nights at 4 °C, on an orbital shaker (60rpm). After 3 more TBS-1% serum washes, the sections were incubated with anti-goat biotinylated secondary antibody in TBS-1% serum and incubated with an avidin–biotin–peroxidase complex (Vector Laboratories) in TBS. The sections were treated with DAB solution (Vector DAB kit, SK4100, Vector laboratories) for 3 min. After washing the sections 3 more times, the fluorescence labeling was started. Sections were blocked in 5% donkey serum for 1.5h and incubated overnight with antibodies against GFAP and GFP as described, in TBS, 0.25% Triton, 1% donkey serum. On the next day, the sections were washed 2 times and incubated with secondary antibody for 2.5h at room temperature

on an orbital shaker in the dark. After washing 3 more times the sections were mounted on Superfrost slides, dried for 30-60 min and coverslipped with Cytoseal.

Table 3.2: Primary antibodies for in vivo growth in SC sections

Primary antibody	Made in	Producer	Dilution used
Anti CTB	Gt	List Biological	1:80000
Anti-GFP	Rb	Life Technologies	1:750
Anti-GFAP	Ms	Milipore	1:1000

Table 3.3: Secondary antibodies for in vivo growth in SC sections

Secondary antibody	Made in	Producer	Dilution used
goat IgG (H+L) biotinylated	Hs	Vector	6ul/ml TBS
mouse IgG (H+L) Alexa Fluor 594	Dk	Invitrogen	1:300
rabbit IgG (H+L) Alexa Fluor 488	Dk	Molecular Probes	1:1000

3.2.1.2. Assessment of axonal growth into the graft

All sagittal spinal cord sections from one out of 8 series were screened to identify sections containing CTB positive axons. Each CTB positive section was directly visualized with a microscope (Olympus BX53) under epifluorescent illumination to identify the lesion border by GFAP (astrocytes) and GFP (transplanted cells/cell graft) immunolabeling. The border was approximated to a series of 250µm straight lines, proximal to any GFAP positive cell bodies, while GFAP protrusions across the line were allowed. The 250µm lines correspond to the side of the grid scale in the eye piece, that was used for measurements. All axon profiles crossing the lines for 0µm, 50µm, 100µm, 250µm and 500µm on the eye piece grid scale were counted directly under the microscope at 40x magnification, while zooming in and out to get the most accurate representation. All measurements from the same animal were summed for each category: 0µm, 50µm, 100µm, 250µm and 500um.

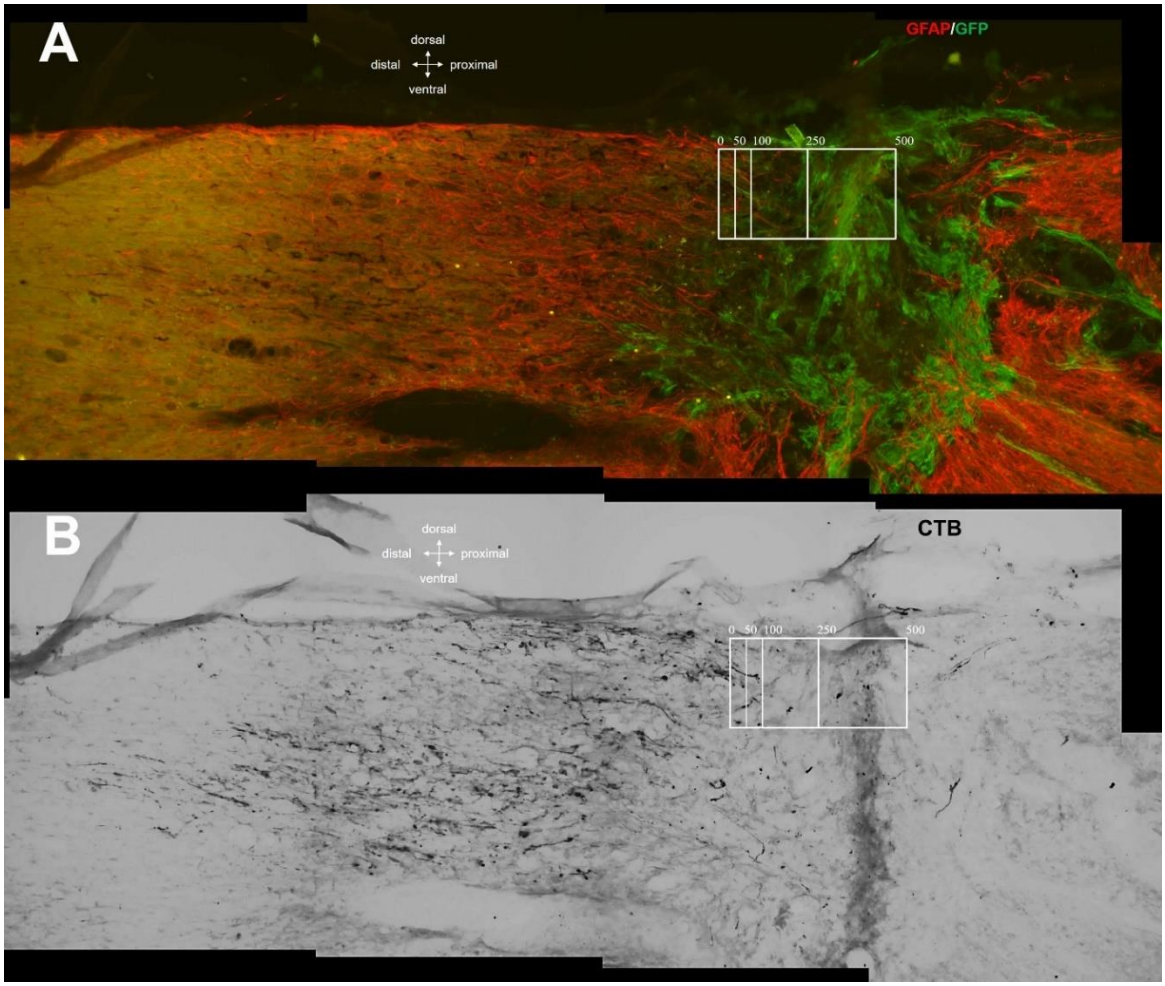

Fig.3.2. Assessment of growth into the graft with the eye-piece grid method. (A) The distal tissue-graft border was identified on sagittal spinal cord sections based on GFAP (astrocytes) and GFP (transplanted cells/cell graft) staining. The border was approximated to a series of 250µm straight lines, proximal to any GFAP positive cell bodies, while GFAP protrusions across the line were allowed. A grid scale in the eye piece, we used for measurements. Depicted to scale. **(B)** All CTB positive axon profiles crossing the lines for 0µm, 50µm, 100µm, 250µm and 500µm on the eye piece grid scale were counted directly under with the microscope at 40X magnification.

3.2.1.3. Imaging and quantification of growth cones and retraction bulbs

Sections were imaged on an upright microscope (Olympus BX53), both in light level for CTB and in immunofluorescence for GFAP (astrocytes) and GFP signal (transplanted cells/cell graft), at 20x magnification and image composites were assembled in CellO (Olympus), to cover the entire lesion area and caudally the CTB positive fibers with retraction bulbs.

The quantification was done using ImageJ, by first marking the border between GFAP and GFP positive signal and then tracing all axon endings caudally (retraction bulbs) and within

the graft (growth cones and bulbs). For determining the tissue-graft interface, we considered a line where there are no longer GFAP positive cell bodies, but only processes. Nerve endings were assessed by number and distance from the border, or stacked into cumulative intervals for analysis (cumulative sum of the number of regenerated axons in 25 or 50µm steps).

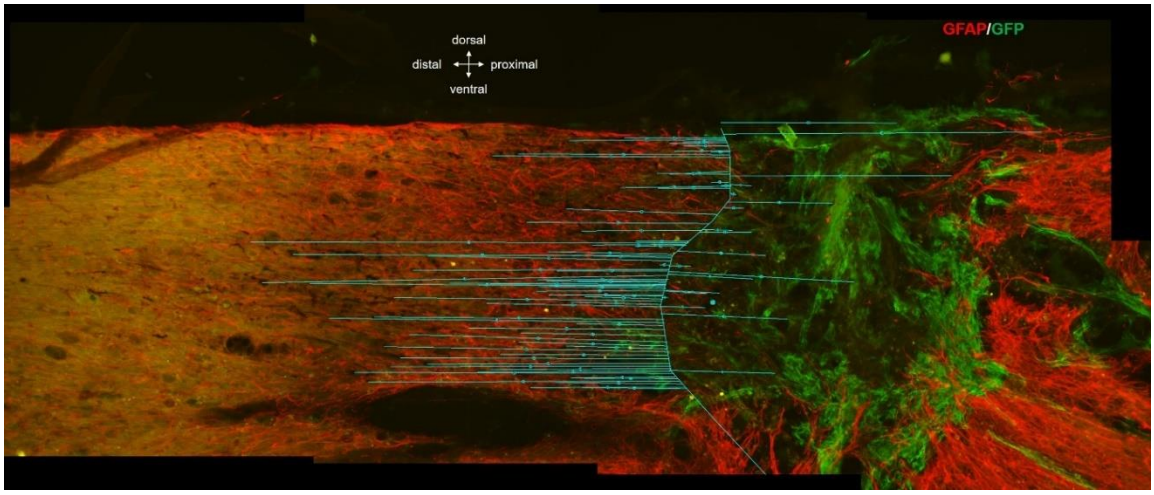

Fig.3.3. Assessment of die-back and growth into the graft with ImageJ. The distal tissue-graft border was identified on sagittal spinal cord sections based on GFAP (astrocytes) and GFP (transplanted cells/cell graft) staining, proximal to any GFAP positive cell bodies. The border was drawn and saved in ImageJ, then on the respective CTB image, each retraction bulb or growth cone distal or proximal to the border was marked and a distance to the border was measured. Tracings here overlaid on the respective GFAP/GFP image.

3.2.2. Assessment of in vivo peripheral regeneration after CL

The sciatic nerves from animals that received AAV injections were also dissected, post-fixed for 24h in 4%PFA, then moved to sucrose 30%. The sciatic nerves were transversally cut at 1 cm distally from the CL, in 16um slices and directly mounted on gelatin coated slides. The sections were labeled for GFP, ßIII-tubulin and stained with DAPI **(Fig.3.4)**. The outline of the nerves was traced based on the ßIII-tubulin labeling to determine the nerve area and GFP+ axonal profiles were counted on the sections in CellO (Olympus).

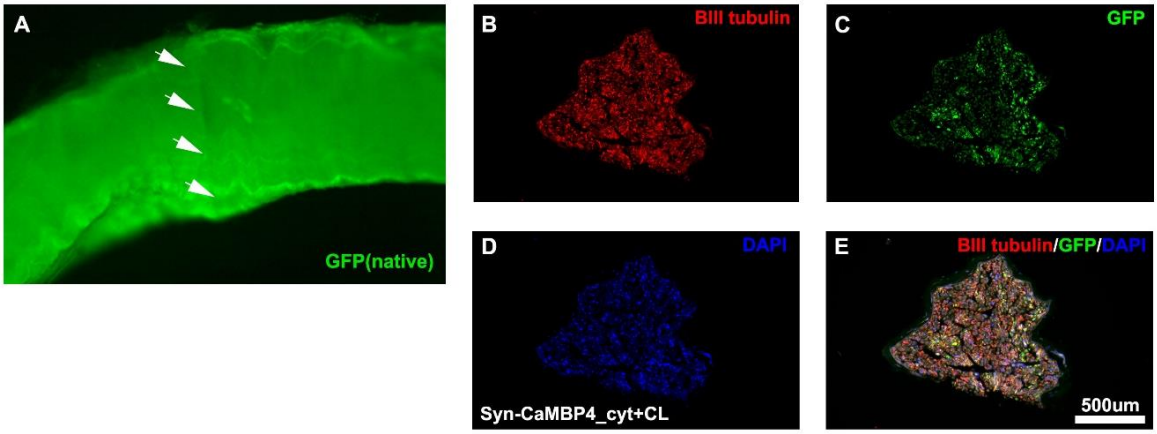

Fig.3.4. In vivo sciatic regeneration assessment. (A) Isolated sciatic nerve after virus injection in the DRGs and CL, direct native GFP fluorescence (no IHC). Arrows indicate the site of the CL. Sciatic nerves were transversally cut in 16µm thick slices at 1 cm distally from the CL and directly mounted. They were stained for **(B)** BIII-tubulin, **(C)** GFP and **(D)** DAPI. **(E)** Merge.

3.3. Sensory testing

3.3.1. Fine touch - von Frey filaments sensory test

Animals were habituated for 1h/day for 3 days prior to the first sensory testing and for 30 minutes immediately before each testing, on an elevated grid platform in individual cages. The sensory response in the hind limbs was assessed with von Frey filaments (Ugo Basile) by applying the filament to the palmar center of the hind paws. A positive response occurs when the paw is withdrawn from the filament. After testing of a paw, a brief rest period of 2-3 minutes was allowed before testing the other paw with the same filament. We used 5 filaments of different strengths with a rate of average response in normal animals around 10% for the thinnest filament and 90% for the thickest filament. Each was applied 5 times for each paw and the response rate was reported as % response of total valid applications in awake and freely moving animals. If a rat walked immediately after applying a filament instead of lifting the paw, it was not considered and the filament was later reapplied. The change in absolute number of withdrawals to a stimulus may indicate an increase in the spinal reflex and not necessarily the development of allodynia. For better distinction of allodynia, as opposed to spinal reflexes, only withdrawals accompanied by supraspinal behavior such as head turning to attend to the stimulus, biting of von Frey filament or licking the paw should be counted as response. This was additionally reported, if present, at 7 and 15 days post-surgery to specifically check for allodynia.

3.3.2. Thermal sensitivity – Plantar Heater test (Hargreaves)

Animals were habituated for 1h/day for 3 days prior to the first sensory testing and for 30 minutes immediately before every testing on an elevated Plexiglas platform in individual cages. Latency for hindlimb withdrawal in response to stimulation with a radiant heat source (Ugo Basile) was measured. The generator automatically stops upon paw withdrawal from the heat beam and the latency is reported on the electronic screen. We used an intensity of 60 units, corresponding to the upper mid emission range. If no paw withdrawal occurred after 30 seconds, the radiant source automatically stops to prevent tissue damage and the animal was assigned the maximal withdrawal latency of 30 seconds. Each paw was assessed 4 times and the values averaged. Testing was alternated left-right with a delay for an individual paw of 10-12 minutes, to prevent sensitization. If enclosing needed to be cleaned, the rat was allowed 5 more minutes of habitation before resuming measurements.

3.3.3. Data analysis

Statistical comparisons were performed using GraphPad 7.0.1 software. Comparisons were performed with one-way analysis of variance (ANOVA) and post-hoc tests/comparisons as indicated. Statistical significance was accepted at p values < 0.05, and indicated as follows: $p<0.05$=*, $p<0.01$=**, $p<0.001$=***, $p<0.0001$=****. Values are expressed as mean ± standard error of mean (SEM).

3.4. DRG culture experimental procedures

3.4.1. DRGs isolation

3.4.1.1. Whole DRGs isolation

For electroporation and in vitro depolarization, all DRGs from one naïve animal were isolated using the spinal cord flush method. Briefly, the rats were killed by an overdose of anesthesia mixture and decapitated. The spinal column was removed and paravertebral muscles trimmed. The caudal end was cut to expose an opening of the vertebral canal through which a 20ml syringe with an 18-gauge needle was inserted and ice cold Hank's Balanced Salt Solution (HBSS, Ca/Mg-free) was injected, such that the spinal cord was expulsed through the rostral opening under the pressure of the liquid. The column was cut longitudinally in half along the dorsal and ventral axes, exposing the DRGs. Each DRG was removed from the intervertebral foramina by gently grasping the dorsal root with a

micro forceps and cutting the distal nerve with micro scissors. Then the DRG was carefully trimmed of nerve roots and the larger ones (cervical and lumbar DRGs), were cut half way into the center of the ganglion to improve digestion. The DRGs were placed in Hibernate A medium on ice until all DRGs from each rat were collected. Subsequently they were washed with HBSS and incubated in Collagenase/Dispase solution in HBSS (Collagenase XI, 2.5mg/ml, 1200 units/mg and Dispase I, Worthington, 5mg/ml, 4 units/mg) at 37^{o}C for 30 min, shifting every 10 minutes to ensure equal digestion. The enzymatic digestion was stopped by washing once with 10% fetal bovine serum (FBS) in complete medium (1 ml) followed by a wash with serum-free complete medium (1ml). In new serum-free complete medium (1 ml), the DRG were then mechanically dissociated by trituration with fire-polished Pasteur pipettes, debris left to settle and cell suspension moved to a new tube. From here the DRGs underwent electroporation or were plated for other experiments as further described.

3.4.1.2. Lumbar DRGs isolation

From animals that underwent in vivo manipulation of the sciatic such as ES, sham, CL, naïve (control) or virus injection into the respective DRGs (see Surgical Procedures for details), only the L4-L6 DGRs were dissected for *in vitro* neurite outgrowth assays, using the posterior approach. The rats were killed by an overdose of anesthesia mixture and decapitated. The lumbar spinal column was removed, muscles trimmed and posterior processes and the vertebral posterior arch were carefully removed with a Rongeur. Lumbar DRGs L4-L6 were identified based on anatomical landmarks and size and shape criteria: L5 is located at the level of the ilium, L5 and L4 are approximately round and two times as large as L6, while L6 is elongated. The L4-L6 from each side were dissected and each side was collected independently, digested with Collagenase/Dispase in an appropriate volume (200-300µl) and dissociated as previously described. For these experiments we focused on changes at 7 days time point when maximum effects on neurite outgrowth and changes in gene expression are observed after CL.

3.4.2. DRGs cell culture - plates and growth medium

Plates and medium were always prepared on the day of the DRG isolation. Briefly six-well polystyrene plates (35mm wells) were first coated with 16.67µg/ml Poly-D-lysine (PDL) (Sigma; in autoclaved H_2Od) for 1h at room temperature (1.5ml/well). The plates were then washed with H_2Od and coated with laminin (Sigma; in DPBS) by incubating at room temperature for 3h. Laminin concentration was 0.5µg/ml or 5µg/ml depending on the experiment as specified. After laminin, the plates were gently washed with DPBS, filled

with 2ml of complete culture medium (DMEM/F12, 1×B27, 2mM L-glutamine, and Pen-Strep 10mg/ml) per well and placed at 37˚C until cell plating.

Twelve-well polystyrene plates (22.1 mm wells) were handled similarly, with 0.5ml used for coating and 1ml culture medium per well.

Glass covers slips were previously treated with acid (HCl 1M, overnight at 65°C) and maintained in 70% isopropanol. After drying under the hood, they were placed and coated in twelve-well plates. Due to lower surface adherence, coating was in higher concentration than for plastic surfaces, respectively: PDL (Sigma; 100µg/ml in sterile water) and laminin 25µg/ml.

3.4.3. In vitro electroporation

The cell pellet obtained after the isolation, digestion and trituration of DRGs from naïve animals, was centrifuged (5 minutes at 1000 rpm), washed with DPBS, centrifuged again and re-suspended in P3 buffer (Lonza) at a concentration of 3×10^5 cells/20µl of reaction volume. For each reaction, 20µl of cell suspension was transferred to a new tube and combined with 2.1µl plasmid DNA (see Plasmids section for dilution), composing up to 10% of the reaction mixture volume. The DNA/cell mixture was then transferred to the 20µl reaction strip. Electroporation was carried out using the Lonza 4D-Nucleofector X-unit system, code: DR 114. Reaction strips were allowed to sit at room temperature for 10 min, then warm serum-free complete medium was added, and the cells were gently distributed, with a cell density of 10^5cells/35 mm wells in 2 ml medium. Three hours after electroporation, the medium was replaced with warm serum-free complete medium.

3.4.4. Replating of DRGs neuron cultures

To allow sufficient time for expression of electroporated plasmids or to reinitiate growth after a certain time of in vitro growth, we used the DRGs replating technique as described (Saijilafu et al., 2013). Briefly, DRG neurons were cultured for different durations, from 1h up to 7 days, then media was removed and they were then digested with Trypsin 0.125% in EDTA for 5min at 37°C. The DRGs were then collected, centrifuged (5min at 800 rpm), resuspended in serum-free complete medium and replated in newly coated plates to reinitiate axon growth. Plates were fixed at 24h or 48h after replating. Cultures were also observed during the growth with the microscope at various times, and if the growth was too extensive potentially making assessment difficult, plates were fixed slightly earlier than planned (40h instead of 48h). As seen in **(Fig.3.5)** a longer interval from isolation to replating positively influences the maximum growth achieved.

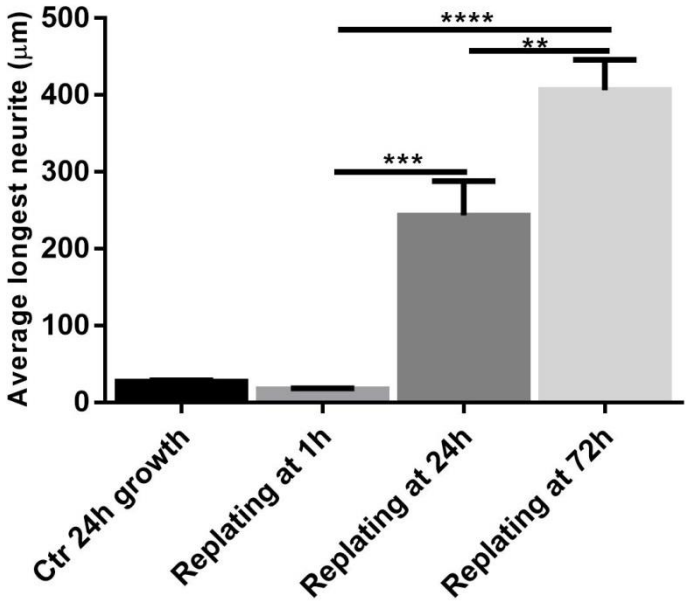

Fig.3.5. A longer delay before replating DRG cultures positively influences neurite growth. Naïve DRGs were isolated and were cultured on PDL/Laminin(0.5µg/µl). They were directly grown for 24h or replated at 1h, 24h or 72h and then grown for 24h. Plates were stained for ßIII-tubulin and longest neurite or each cell was assessed in ImageJ. n=4-12 wells/condition. Bars=mean+SEM, One-way Anova, Tukey's multiple comparisons test, ∗p<0.05, ∗∗p<0.01 ∗∗∗p<0.001 ∗∗∗∗p<0.0001.

3.4.5. In vitro depolarization

Freshly isolated DRGs were plated at a density of 25.000 cells/35mm^2 well in normal media with or without KCl (40mM). The concentration was chosen as it has been shown to have effects on growth without affecting cell viability (Enes et al., 2010). As a control for osmolarity, we used the same concentration of NaCl in additional control wells. Cells were incubated for the indicated time, then media replaced in all wells from an experiment, to account for any cell loss due to washing. In some cases, cultures were replated in normal media, and allowed to grow. They were then fixed and labeled.

3.4.6. DRGs culture immunohistochemistry

DRG cultures were fixed with ice-cold 4% paraformaldehyde (PFA) for 30 minutes and labeled with antibodies. An example of normal DRGs in culture can be seen in **Fig.3.6.**

Briefly DGRs cultures were blocked with TBS, 0.1%TritonX, 5% donkey serum for 1h at room temperature, then the primary antibody was added in TBS, 0.1%TritonX, 1% donkey serum at 4˚C overnight. The plates were washed 3 times with TBS, then the secondary antibodies were added in TBS, 0.1%TritonX, 1% donkey serum for 3h at room temperature

in the dark. DAPI was added for 10 minutes in the first washing step followed by 2 more washing steps with TBS. Plates were maintained at 4˚C in TBS, imaged and subsequently TBS was replaced with Fluoromount G (SouthernBiotech) and plates were stored at RT in the dark. Labeling of coverslips was performed in a similar way in 24-well plates, followed by direct mounting upside-down on glass slides with Fluoromount G (SouthernBiotech).

Antibodies against ßIII-tubulin were used to identify neurons and their neurites, and in some cases GFAP antibodies were used to visualize satellite cells, and DAPI for nuclear staining **(Fig.3.6)**. Neurofilament 200 or NFH was used to label large myelinated DRG neurons. For electroporated or virus injected cells, antibodies against GFP, FLAG or HA were used, depending on the experiment.

Table 3.4: Primary antibodies for DRG culture stainings

Primary antibodies	Made in	Producer	Dilution used
Anti BIII-tubulin	Ms	Promega	1:1000
Anti Neurofilament H (200k)	Rb	Milipore	1:1000
Anti-GFP	Rb	Life Technologies	1:1000
Anti-HA	Ms	Cell Signaling	1:1000
Anti-FLAG M2	Ms	Sigma	1:1000
Anti-GFAP	Rb	AbD Serotech	1:1000
Anti-GFAP	Ms	Milipore	1:1000

Table 3.5: Secondary antibodies for DRG culture stainings

Secondary antibodies	Made in	Producer	Dilution used
mouse IgG (H+L) Alexa Fluor 488	Dk	Invitrogen	1:1000
mouse IgG (H+L) Alexa Fluor 594	Dk	Life Technologies	1:1000
rabbit IgG (H+L) Alexa Fluor 488	Dk	Molecular Probes	1:1000
rabbit IgG (H+L) Alexa Fluor 594	Dk	Invitrogen	1:1000

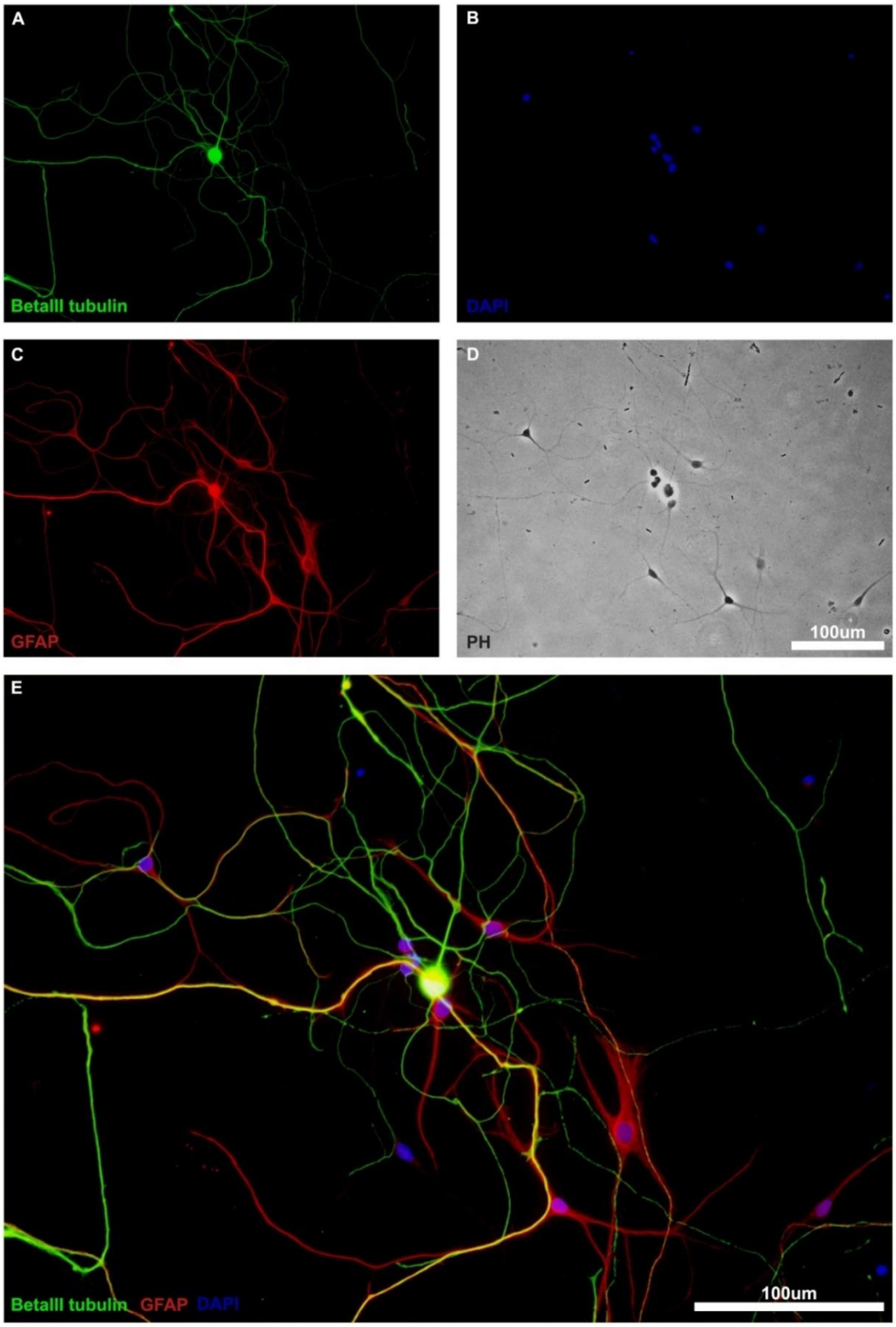

Fig.3.6. Naive DGRs cultures obtained with the standard isolation protocol. The cultures are mixed, containing **(A)** neurons (ßIII-tubulin) as well as **(B)** several other cell types as shown by DAPI nuclear staining, including **(C)** satellite cells (GFAP positive).The different size of cell body, nucleus and morphology between neurons and satellite cells is visible both in **(E)** immunofluorescence and in **(D)** phase contrast.

3.4.7. Neurite growth assessment

3.4.7.1. Imaging

Plates were automatically imaged using an Olympus IX81 inverted microscope equipped with a motorized stage and controlled by Olympus Cell-P Software. For 4x images, we captured twelve 4x5 images that were automatically stitched into non-overlapping composites per 35mm well surface (72 images per 6-well plate). In some cases, 10x images were captured, resulting in 4x5 automatically stitched non-overlapping composites 80% compressed for storage purposes (264 images per 6-well plate).

3.4.7.2. Longest neurite growth assessment

For analysis, image files were converted in NIH ImageJ to 8-bit RGB format. Image files were opened using the NeuronJ plug-in, and neurons were identified by ßIII-tubulin labeling. For transfected neurons, we measured ßIII-tubulin-GFP double labeled neurons. Longest neurite outgrowth assessments were done by semi automatically tracing the longest neurite of each neuron, starting with the base of the neurite at the edge of the cell soma. The lengths in pixels were averaged for each well and converted with the appropriate conversion scale to µm, taking into account image compression. The average longest neurite growth for each condition was then normalized to sham to exclude possible influences of plate coating and isolation conditions in separate experiments, as well as surgical related side-effects.

3.4.7.3. Cell classification by longest neurite length

To determine if the overall variations in average longest neurite values are due to elongation or initiation, neurons were classified by the length of the longest neurite into categories. The number of cells in each category was expressed as percentage of the total number of neurons. For replated cells, I used the following categories (<50, 50-250, 250-500 and >500µm), while for 24h growth immediately after isolation smaller categories (<20, 20-40, 40-100 and >100µm) were used due to differences in growth. Measurements shorter than the minimum diameter of a cell body (15-20µm) correspond to cells without neurites and were in some case separately analyzed.

3.4.7.4. Total neurite growth assessment

For some of the experiments, we performed total neurite tracing on DRG cell cultures, using CellP (Olympus), a proprietary software feature. Briefly the package needs to be

supplied with images and certain threshold options, and does the full tracing independently of the user. The number of neuronal cell bodies has to be counted independently, to get the average total neurite length per number of cells. Traced images were thoroughly checked for errors of detection, because automatic total neurite measurement from CellP depends crucially on image quality, making it sensitive to artifacts. Each detected unit is allocated with an unique identification number present both in the traced images and in the output file, thus artifacts can be excluded. CellP does not differentially detect double labeled neurons such as it is needed for transfected or virus injected DRGs, thus it can only be used for single labeling experiments.

3.4.7.5. Data analysis

All samples from the same experiment were done in parallel, if possible, labeled, imaged and assessed in the same way. Technical replicates were averaged. As no interdependence was observed between the 2 sides of an animal and to minimize the number of animals needed, both sides were considered independent values (1 animal, n=2). For the majority of animals, both sides had the same condition.

In case of sets of experiments with high variability due to technical conditions (surgical conditions, isolation, reactives, antibodies and imaging conditions), every experiment was normalized to their control values, and the normalized data was further analyzed.

For normalization we use the values for the shams or naïve (if present) on the day, expressing all growth relative to control data. Though naïve animals were not present in all experiments, at least 2 sham conditions were performed per group of animals/day.

3.4.8. Calcium imaging in DRG cultures

I performed qualitative/semi-quantitative calcium imaging to show that the DRG cultures are functional and respond as expected to KCl with a Ca^{2+} increase. For this, naïve DRGs were plated on PDL/laminin coated plates (0.5µg/ml) and cultured for 48h. After 2 washes with warm HBSS (37°C), cells were incubated with 1µM Fluo-4 calcium indicator (Life Technologies) in DMEM complete medium with no FBS for 30 minutes. The cells were then washed with warm HBSS, and left in normal medium for 10-15 minutes to settle. The culture plates were placed in the Olympus IX81 inverted microscope, and the appropriate volume of KCl stock was pipetted in, to achieve 50mM concentration. A programmed sequence of images was recoded at 20x magnification, starting before the KCl addition. Fluorescence intensity before and after the addition could be quantified from the image

sequence with ImageJ, and for each cell the increase of fluorescence was normalized to the baseline values, resulting in % increase in value.

3.4.9. Quantification of HDAC5-FLAG export

Total DRG neurons were isolated and electroporated as previously described. For information about the plasmid and dilution see the Plasmid section. Each reaction was split into 3 wells (35mm^2) on PDL/laminin coated plates (0.5µg/ml) and the neurons were allowed to grow for 72h in order to allow for appropriate gene expression. At this point KCl (40mM) was added to the medium. As a control for osmolarity, control wells were treated with NaCl (40mM), untreated. An hour later cells were fixed with 4% PFA and labeled with an anti-FLAG antibody and DAPI to identify the location of the HDAC5 construct. For each well a minimum of 60 neurons was assessed. The cultures were assessed by eye with 20x magnification, identifying neurons based on cellular size and morphology in Phase contrast (large and with multiple neurites) and nuclear aspect in DAPI channel (larger/less condensed nuclei than satellite cells and usually oval or kidney shaped) **(Fig.3.6)**. Only clear strong positive cells were assessed, each positive neuron being classified as nuclear only, nuclear and cytoplasmic or cytoplasmic only, depending on the HDAC5-FLAG fluorescence in relation to the DAPI staining. In case of 2 adjacent neurons with identical phenotype only one was assessed. Neurons that could not be clearly distinguished were not assessed. Neurons with irregular DAPI staining across the cytoplasm, fragmented or missing nuclei, were considered not viable prior to addition of KCl/NaCl and therefore not evaluated. Cell clusters with more than 2 cells, were also not assessed when the labeling could not be clearly associated.

3.5. Differential gene expression by RNA sequencing

3.5.1. Experimental groups

Animals received electrical stimulation for 1h (ES), sham cuffs (sham), conditioning lesion (CL) or just opening of the skin (naïve). Two times points were chosen for this experiment: 1-day time-point to see early gene expression and 7 days for longer term gene expression, when effects on growth were detected, having an n=4/condition/time-point (total 32). The cohorts for each time-point, were handled together for DRG and RNA isolation.

3.5.2. DRG isolation

The rats were heavily anesthetized with isoflurane at induction concentration (4%) for 5 minutes and decapitated. L4-L6 DRGs were dissected on ice in the same way as lumbar DGRs for neurite outgrowth assays. The DRGs from both sides of an animal were pooled in the same tube in RNA-Later (Ambion, Thermo Fischer Scientific). Samples were kept at 4°C for 24h, then RNA-Later was removed and DRGs were stored at -80°C until RNA isolation.

3.5.3. RNA isolation

RNA was isolated using the RNA-easy kit (quiagene)according to the manufacturer's instructions. Sample concentration and 280/260 ratios were checked on ND-1000 Spectrophotometer (Nanodrop) for purity, and RNA integrity (RIN) was further examined on a 2100 Bioanalyzer (Agilent) in the Deep Sequencing Core Facility of Heidelberg University. RIN values were between 9.4 and 10. In 3 samples there was an error of peak detection, but with a good aspect of the electropherograms, so the samples were included.

3.5.4. Libraries and data acquisition

Library preparation was made by the Deep Sequencing Core Facility of the Heidelberg University using Illumina Ribozero kit (llumina). Reading was performed on Illumina HiSeq 2000, at 50 bp length, single end (SE), with desired number reads per sample 30M.

3.5.5. Data analysis

Data analysis was made by the Bioinformatics department at Indiana University. Briefly, sequence reads were converted via FASTQ Parser and aligned with Tophat2 (Kim et al., 2013, Trapnell et al., 2009) to Rnor_5.0 (Ensembl release 79). All annotated genes with greater than one read per million mappable reads in at least four samples were included for differential gene expression with EdgeR (Bioconductor) (Robinson et al., 2010).

Table 3.6: Library size and Tophat2 mapping summary 1 day ES/sham/CL and naïve.

Cond.	total reads	mapped reads	reads mapped ambiguously	%mapped reads	%read mapped ambiguously (mapped-ambiguously/mapped)
CL	27,482,348	26,743,871	3,793,633	97.31	14.19
CL	13,938,369	13,558,134	1,861,883	97.27	13.73
CL	32,826,841	31,885,259	4,059,582	97.13	12.73

CL	14,327,811	14,000,562	1,697,139	97.72	12.12
ES	24,110,030	23,512,601	2,649,955	97.52	11.27
ES	65,155,458	63,812,482	8,963,352	97.94	14.05
ES	52,659,531	51,503,115	6,072,151	97.8	11.79
ES	63,777,062	62,089,466	7,814,451	97.35	12.59
naive	34,012,078	32,986,937	4,931,645	96.99	14.95
naive	45,791,301	44,443,472	6,748,422	97.06	15.18
naive	41,309,263	40,320,489	5,977,882	97.61	14.83
naïve	46,504,628	44,773,233	7,030,262	96.28	15.7
sham	59,736,152	58,490,811	6,539,643	97.92	11.18
sham	23,125,773	22,611,599	2,676,897	97.78	11.84
sham	20,538,274	19,909,528	2,739,969	96.94	13.76
sham	60,729,962	59,175,404	7,018,762	97.44	11.86

Table 3.7: Library size and Tophat2 mapping summary 7day ES/sham/CL and naïve.

Cond.	total reads	mapped reads	reads mapped ambiguously	%mapped reads	%read mapped ambiguously (mapped-ambiguously/mapped)
CL	26,581,023	25,959,458	3,220,510	97.66	12.41
CL	46,141,386	45,000,885	6,680,252	97.53	14.84
CL	30,850,051	30,124,670	4,572,833	97.65	15.18
CL	16,252,804	15,857,725	2,583,726	97.6	16.29
ES	46,677,310	45,389,491	5,774,058	97.24	12.72
ES	34,113,900	33,107,379	4,542,211	97.05	13.72
ES	40,826,664	39,725,323	4,976,158	97.3	12.53
ES	35,155,623	34,208,690	4,430,408	97.31	12.95
naive	72,246,468	70,637,464	7,439,552	97.77	10.53
naive	30,397,686	29,709,739	2,722,131	97.74	9.16
naive	16,901,836	16,510,362	1,754,444	97.68	10.63
naive	45,191,823	44,226,177	4,533,160	97.9	10.25
sham	57,720,927	56,327,560	5,705,033	97.59	10.13
sham	21,970,872	21,394,857	2,484,553	97.38	11.61
sham	13,106,158	12,760,312	1,638,670	97.36	12.84
sham	35,559,765	34,620,652	4,986,889	97.36	14.4

3.6. Plasmids

3.6.1. List of plasmids and brief description

The original DNA plasmids used for electroporation were kindly provided by Dr. H. Bading. See **Table 3.8.** for details about Vector, dilution and source.

Table 3.8: Plasmids

Name	Vector and short description	Dilution	Original source
CMV-CaMBP4	**pAAV_CMV_eGFP-T2A-CaMBP4-NLS-HA,** active CaMBP4, enhanced green florescent protein (eGFP), bicistronic with a T2A ribosome skip sequence	1µg/µl in TE Buffer	Dr. E. Freitag (Group Prof. Dr. H. Bading)
CMV-MutCaMBP4	**pAAV_CMV_eGFP-T2A-mutBP4(S2)-NLS_HA,** inactive CaMBP4 due to a point mutation, eGFP, bicistronic with a T2A ribosome skip sequence. Used as control electroporation.	1µg/µl in TE Buffer	Dr. E. Freitag (Group Prof. Dr. H. Bading)
Syn-CaMBP4	**hSyn-CaMBP4-HA_hSyn-eGFP** Active CaMBP4, eGFP.	1µg/µl in TE Buffer	Dr. E. Freitag (Group Prof. Dr. H. Bading)
Syn-MutCaMBP4	**hSyn-mut-CaMBP4(S2)-NLS-HA_hSyn-eGFP,** inactive CaMBP4 due to a point mutation, eGFP. Used as control electroporation.	1µg/µl in TE Buffer	Dr. E. Freitag (Group Prof. Dr. H. Bading)
HDAC5-FLAG	**HDAC5** (Gene Bank accession number AF 132608) with C-terminal FLAG construct fusion protein, inserted between NotI-XhoI sites on pBJ5 vector	3.2µg/µl in TE Buffer	Dr. D. Mauceri (Group Prof. Dr. H. Bading)

3.6.2. Growing and collecting bacterial cultures for a plasmid prep

From the culture plates, a single isolated colony was picked with a sterile pipette tip and added to 5mL LB media with Ampicillin (100µg/mL) in snap-cap tubes (starter culture), and was shaken at 37°C for 4-5h, until it became cloudy. Alternatively, to get a pre-culture from frozen stock, a small amount of the frozen glycerol stock was scooped out and pipetted up and down in a new starter culture.

Glycerol bacterial stocks were made from full grown cultures, by mixing 600µL bacterial solution with 400µL glycerol in one Eppendorf tube and saved in -80°C for long time use.

To obtain a bacterial culture for plasmid isolation, we added the pre-culture, after 4-5h of growth, to the appropriate culture bottle with LB-Ampicilin (100µg/mL), with a volume depending on the desired plasmid yield and shaken (220rpm) at 37°C, overnight (12-18h), until cloudy.

3.6.3. Plasmid isolation

Plasmid isolation was done with PureLink® HiPure Plasmid Filter Maxiprep Kit (Invitrogen) according to kit manufacture protocol. Columns were suspended on a rack and 30 mL Equilibration Buffer (EQ1) was directly added, into the filtration cartridge, and drained by gravity flow. The overnight culture was poured in centrifuge bottles, balanced within 0.01 grams and centrifuged at 6000rpm, for 15 mins (SLA-3000 rotor, SORVALL centrifuge). The supernatant was removed and the bacterial pellet was resuspended in 10mL of Resuspension Buffer (R3) containing provided RNaseA. When homogeneous, 10ml lysis buffer (L7) was added, mixed by inverting the tube and incubated at RT for 5 minutes. Afterwards, 10 mL Precipitation Buffer (N3) was added and mixed immediately by inverting the tube until homogenized, then loaded into the filter column and let drain under gravity flow until it stopped. The residual bacterial lysate was washed with 10ml wash buffer (W8) to increase yield. The inner cartridge was discarded and the maxi column was washed with 50 mL of Wash Buffer (W8). DNA was eluted in a 50ml centrifuge tube with 15ml Elution Buffer (E4) and precipitated with 10.5 mL Isopropanol, then centrifuged at >12,000 × g for 30 minutes at 4°C (SS-34 rotor, SORVALL centrifuge). Supernatant was removed and 5 ml 70% ethanol was added to the pellet and centrifuged for 5 more minutes. Supernatant was discarded, the pellet was air-dried for 10-15 min, then resuspended in TE Buffer. The concentration in ng/µL and the 260/280 ratio for each plasmid were determined with ND-1000 Spectrophotometer (Nanodrop).

3.6.4. Quality check of plasmids

To check the isolated plasmids, if the plasmids could not be differentiated due to very small differences between active/inactive construct, we sent plasmid samples for sequencing, otherwise cDNA digestion with restriction enzymes was performed. Enzymes for specific DNA sequences were selected with MaxVector to achieve desired experimental setting. Buffers for digestion, temperature and time used for incubation, were chosen as appropriate, according to the chart from New England Biolabs (NEB).

The base recipe per 10µL of a single enzyme digestion as followed: XµL cDNA, 8 – XµL deionized water, 1µL 10x Restriction enzyme buffer, 0.5µL restriction enzyme. For a double digest, 0.5µL of each enzyme were used. Digested DNA was run in a 1% agarose gel with a 1:100.000 dilution of Ethidium Bromide (EtBr, 10mg/mL stock solution) for 45 minutes at 140 volts, together with samples of undigested DNA and 2-log DNA ladder for reference. The DNA fragments in the gel were visualized using an Ultraviolet (UV) lamp and photos were taken to check sizes of obtained fragments.

3.6.5. Transforming bacteria

CaCl2 competent bacteria were used for transformation. The bacterial aliquot was taken from -80°C and thawed on ice, then 0.5uL DNA (1mg/mL; 0.05mg of DNA per transformation) was added in 100uL of bacterial solution, and incubated on ice for 30 min. The bacterial and DNA mixture was heat-shocked at 42°C for 60 seconds and placed on ice for 10 minutes to increase transformation efficiency. Then 400mL of LB medium was added and the mixture was incubated at 37°C for 1h. LB with Ampicillin culture plates were taken out from 4°C and incubated at 37°C for 15min, and 100µL of mixture was plated per dry LB plate with Ampicillin. Plates were incubated overnight at 37°C.

3.7. BMSCs isolation and culture for cell transplantation

BMSCs were isolated from GFP transgenic rats via centrifugation method as previously described (Dobson et al., 1999). Briefly, the rat was euthanized and tibia and femur dissected and collected in a tube with PBS. Dissection continued under the cell culture hood, muscles were trimmed and bones ends cut below the joint head using a bone cutter. The bones were placed and fixed in 2ml Eppendorf tubes and centrifuged at 3000g for 2 minutes. The bone marrow pellet was resuspended in PBS and centrifuged at 1000rpm for 10 minutes. The cells are seeded at 10*10E+6 cells (1ml) in T75 with 20ml culture medium (Alpha Medium, Biochrom AG) + 20%FBS (Biochrom AG) + 1%PenStrep (Gibco) + 1%L-Glutamine (Gibco)), and incubated at 37°C +5%CO_2.

The BMSC attach to the plate within 24h, while hematopoietic cells and other cells types remain floating, or are only mildly adherent. Thus after 3 days, all other cells can be dislodged by knocking the plates and washing two times with PBS. 10ml fresh culture media are added and was changed every 3-4 days. Splitting was done when cells were 80% confluent, usually 5-7 days after isolation, then as needed. Cell were detached with 0.25% trypsin, at 37°C for 5mins, then centrifuged 800rpm for 5min at RT and split in new flasks 1:3 to 1:5. For long term storage, cells were diluted 250.000-500.000cells/ml in freezing media (Culture media + 10% DMSO).

For cell injection after DCL, stored aliquots were unfrozen approximately a week before the planned surgery and expanded as needed, to achieve the needed cell number and passage, 120.000cells/animal (diluted 60.000cells/µl in PBS glucose), passage 2-4.

3.8. General statistics and data analysis

Statistical comparisons were performed using GraphPad 7.0.1 software. Comparisons between 2 groups were performed with Student's t-test, while for several groups one-way or two-way analysis of variance (ANOVA) was used and post-hoc tests/comparisons as indicated. Statistical significance was accepted at p values < 0.05, and indicated as follows: $p<0.05$=*, $p<0.01$=**, $p<0.001$=***, $p<0.0001$=****. Mean values were expressed as mean±standard error of mean (SEM), unless otherwise indicated.

References

1. Dobson, K. R., Reading, L., Haberey, M., Marine, X. & Scutt, A. 1999. Centrifugal isolation of bone marrow from bone: an improved method for the recovery and quantitation of bone marrow osteoprogenitor cells from rat tibiae and femurae. *Calcif Tissue Int,* 65**,** 411-3.
2. Enes, J., Langwieser, N., Ruschel, J., Carballosa-Gonzalez, M. M., Klug, A., Traut, M. H., Ylera, B., Tahirovic, S., Hofmann, F., Stein, V., Moosmang, S., Hentall, I. D. & Bradke, F. 2010. Electrical activity suppresses axon growth through Ca(v)1.2 channels in adult primary sensory neurons. *Curr Biol,* 20**,** 1154-64.
3. Geremia, N. M., Gordon, T., Brushart, T. M., Al-Majed, A. A. & Verge, V. M. 2007. Electrical stimulation promotes sensory neuron regeneration and growth-associated gene expression. *Exp Neurol,* 205**,** 347-59.
4. Kim, D., Pertea, G., Trapnell, C., Pimentel, H., Kelley, R. & Salzberg, S. L. 2013. TopHat2: accurate alignment of transcriptomes in the presence of insertions, deletions and gene fusions. *Genome Biol,* 14**,** R36.
5. Oudega, M., Varon, S. & Hagg, T. 1994. Regeneration of adult rat sensory axons into intraspinal nerve grafts: promoting effects of conditioning lesion and graft predegeneration. *Exp Neurol,* 129**,** 194-206.
6. Robinson, M. D., Mccarthy, D. J. & Smyth, G. K. 2010. edgeR: a Bioconductor package for differential expression analysis of digital gene expression data. *Bioinformatics,* 26**,** 139-40.
7. Saijilafu, Hur, E. M., Liu, C. M., Jiao, Z., Xu, W. L. & Zhou, F. Q. 2013. PI3K-GSK3 signalling regulates mammalian axon regeneration by inducing the expression of Smad1. *Nat Commun,* 4**,** 2690.
8. Trapnell, C., Pachter, L. & Salzberg, S. L. 2009. TopHat: discovering splice junctions with RNA-Seq. *Bioinformatics,* 25**,** 1105-11.
9. Udina, E., Furey, M., Busch, S., Silver, J., Gordon, T. & Fouad, K. 2008. Electrical stimulation of intact peripheral sensory axons in rats promotes outgrowth of their central projections. *Exp Neurol,* 210**,** 238-47.

4. Results

4.1. Ex-vivo effects of in vivo electrical stimulation

4.1.1. Electrical stimulation parameters and set-up – optimization of protocol

To apply ES chronically or repeatedly, I designed and manufactured cuff electrode implants **(Fig.4.1)** using a standardized geometry and implantation procedure. ES (0.2ms pulse length, frequency of 20Hz, 5V, intensity of two times the motor threshold (MT) for 1h) was performed by placing a cuff electrode on the sciatic nerve at mid-thigh level while sham animals in each experiment received cuff electrodes without stimulation for the same duration. One group of animals received conditioning lesions (CL) to compare the effects of ES with effects of CL on axonal growth. L4-L6 DRGs were isolated after 7 days, dissociated and seeded on 0.5µg/ml laminin coated plates for 48h growth **(Fig.4.1.A)**. In a first set of experiments, the cultures were labeled for BIII-tubulin as a general neuronal marker, as well as NF200 as a marker for large myelinated fibers, and the longest neurite for double labeled, as well as all ßIII-tubulin neurons were assessed in ImageJ. In an initial experiment, I evaluated the use of cuff electrodes for chronic or repeated stimulation, thus chronic implants were left in situ both in ES and in sham animals until isolation (7 days) and growth was expressed relative to naïve controls.

Both CL and ES show a tendency to enhance growth under these experimental conditions **(Fig.4.2.B,C)**, which is more pronounced when all neurons are assessed **(Fig.4.2.B)**, compared to only large NF200 positive neurons **(Fig.4.2.C)**, however the effect appears to be smaller than expected when compared to previously published data (Udina et al., 2008). Also in several other independent experiments **(Fig.4.2.E, F)**, ES had a tendency to enhance growth, however across all stimulated animals the effect was variable, making assessment difficult to interpret. In this context, a conclusion could be that there is indeed no consistent effect from ES on growth capacity and the nerve dissection or electrode implantation is a confounding factor. However, CL also failed to properly show the expected growth enhancing effects, thus the ex-vivo analysis in the previously described experiments, may not be sufficiently sensitive.

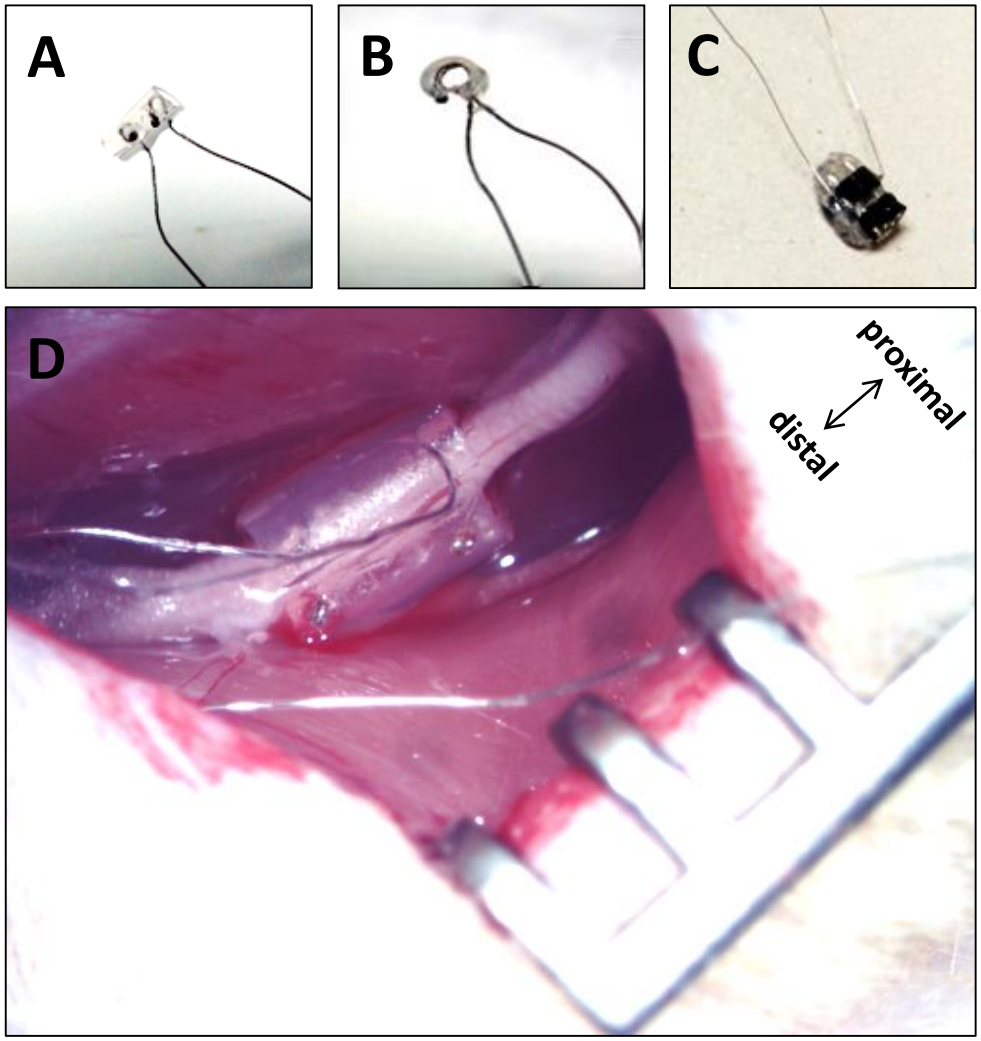

Fig.4.1. Electrodes and electrode implantation. (A) Medial and **(B)** lateral view of a silicone cuff and (**C**) connector. **(D)** Sciatic nerve with a cuff electrode placed around the nerve.

4.1.2. Cuff implants can potentially injure the nerve and create confounding results

As seen in **(Fig.4.2.B)** both CL and ES (20Hz, 2*MT, 0.2ms, 1h) show a tendency to enhance growth in these experimental conditions, however a sham animal also had extreme enhanced growth, was found to be a significant outlier and was excluded (Grubbs' test, ESD method (extreme studentized deviate), $p<0.05$). There were no other significant outliers. This indicates the possibility of conditioning from the surgery and/or chronic electrodes alone, however this tendency is isolated, and not a general tendency for all samples since after removal of the statistical outlier, the average growth from sham animals is comparable to growth of the naïve animals **(Fig.4.2.B)**, yet it calls for special attention to such surgical side effects. Thus to properly establish the ES effects alone before going into chronic implants, in the following experiments we only used acute

implants both for ES and sham surgeries, and extra care was taken to prevent any nerve injury.

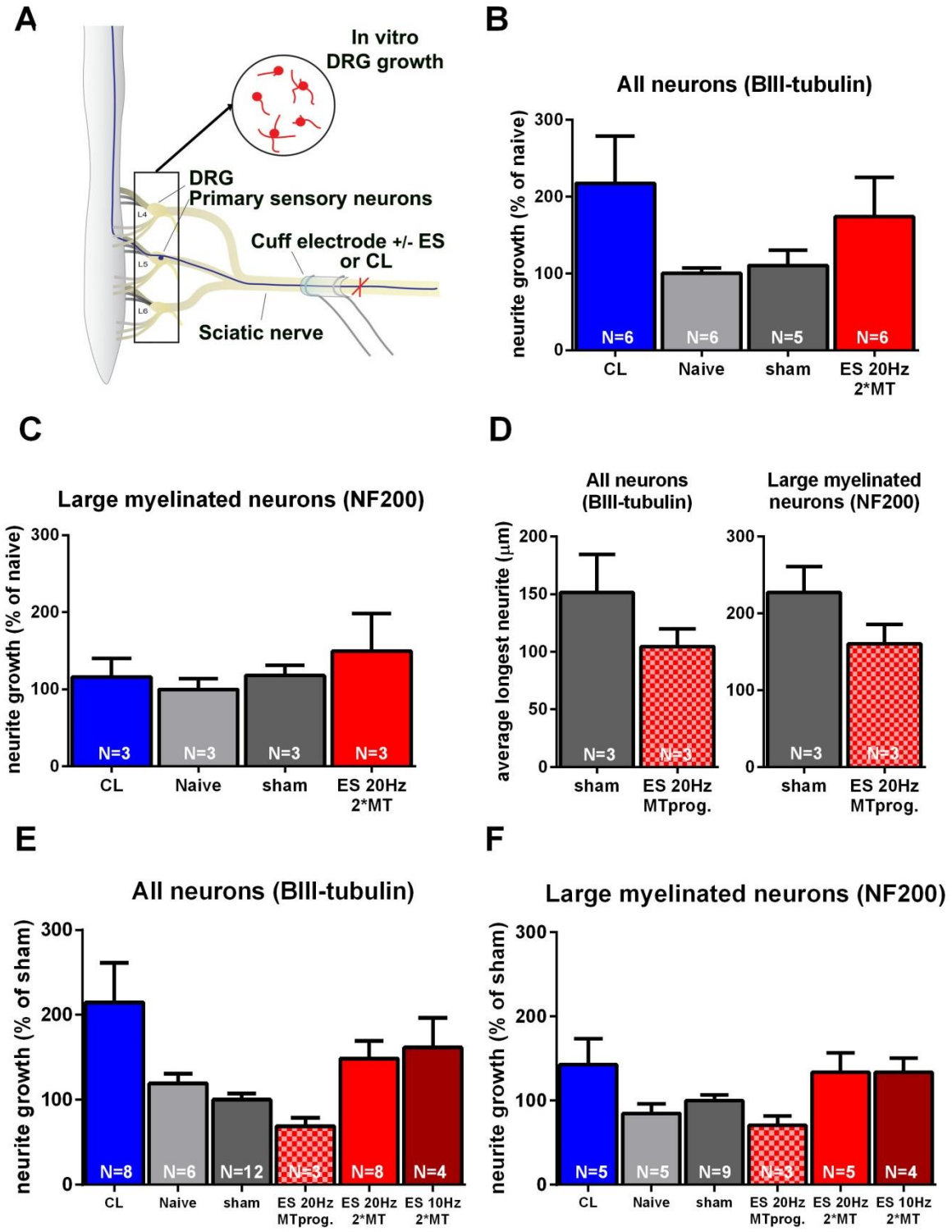

Fig.4.2. Screening of experimental parameters for assessment of neurite growth after ES in vivo. (A) DRGs (L4-L6) were isolated from naïve animals or at 7 days after CL, electrode cuff implantation (sham) or electrical stimulation (ES). **(B-F)** The neurons were grown on PDL/Laminin (0.5µg/µl) coated plates for 48 hours, fixed, labeled for βIII-tubulin and NF200, imaged and assessed in ImageJ. **(B, C)** Growth after ES (20Hz, 2*MT, 0.2ms, 1h) with chronically implanted electrodes, was assessed in ImageJ and was normalized to naïve, to test for any electrodes effects. One of the shams was significantly higher than the others, identified by an outlier test (Grubbs' test, ESD method (extreme studentized deviate), $p<0.05$), indicating potential CL from the surgery and chronic electrodes alone and was excluded. **(D)** Modifying the intensity of the ES to progressive starting from MT and 0.02ms pulse shows a tendency to inhibit growth. **(E, F)** Several experiments were normalized to their respective shams, to control for different experimental conditions. A different frequency ES protocol (10Hz, 2*MT, 0.2ms, 1h) was tested together with the standard ES (20Hz, 2*MT, 0.2ms, 1h). n=Independent samples quantified per condition. Bars represent mean±SEM.

4.1.3. Hind limb movement during the stimulation is not an indicator for ES induced effects on growth

During the stimulation, we noticed the disappearance of hind limb movements shortly after the beginning of the stimulation. To test if a protocol that results in constant hind limb movement, could further enhance neurite growth, ES (0.02ms pulse) with progressive intensity from MT (instead of 2*MT) was used. The intensity was increased in small steps to maintain constant hind limb movement. The overall increase of intensity needed across the duration of 1h, was 20.5±4.6% (mean ± SEM) relative to the starting value (MT) **(Fig.4.3)**. These parameters did not result in increased neurite growth but rather a tendency to inhibit growth **(Fig.4.2.D)**.

Such a protocol is more selective and stimulates less fibers, since motor fibers have the lowest threshold in the sciatic, while sensory fibers have a threshold between MT and 2*MT (Reilly and Antoni, 1992, Reilly et al., 1985) thus the effect, if direct, could be diluted. None the less, the lack of increased growth shows that actual movement is not an indicator of ES-induced growth. Additionally, the trend to induce opposite effects from previous stimulation protocol, suggests the effect of ES on growth is dependent on the parameters used, and thus specific.

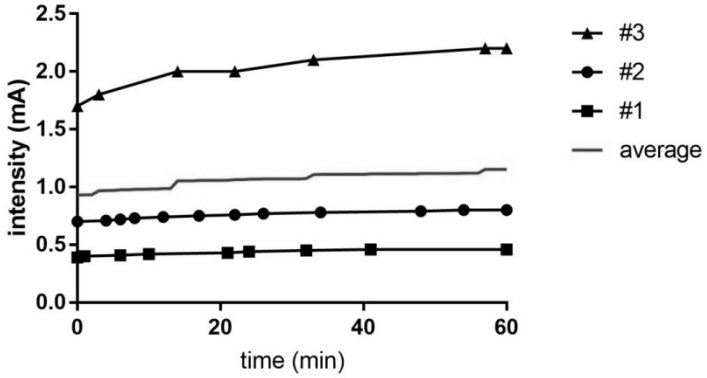

Fig.4.3. Intensity increase needed to maintain constant movement for in vivo ES of the sciatic. In a small number of animals, ES (0.02ms pulse) with progressive intensity starting from MT was used and the intensity was adjusted progressively in small steps to maintain constant hind limb movement.

4.1.4. 20Hz and 10Hz stimulation frequency have similar impact on growth

Stimulation with the original parameters (pulse 0.2ms, intensity of 2*MT, 1h) but at a frequency of 10Hz was also performed. ES10Hz shows the same tendency for growth as 20Hz stimulation and comparable to CL **(Fig.4.2.E, F)**. One significant outlier in ES10Hz with extreme growth was removed (Grubbs' test, ESD method (extreme studentized deviate), $p<0.05$), likely due to surgical related conditioning, and not from specific effects of the ES10Hz. Also 10Hz stimulation induces constant movement throughout the stimulation, compared to 20Hz, and it strengthens our conclusion that actual movement is not an indicator of ES-induced growth.

4.1.5. Large myelinated neurons vs. all neurons

In the first set of experiments, growth was quantified on fluorescence overlayed images of both βIII-tubulin and NF200 stainings in DRG cultures, measuring in ImageJ either large myelinated (double positive βIII-tubulin-NF200 neurons) or all neurons (βIII-tubulin). Both CL and EL showed a tendency to enhance growth in these experimental conditions, which is more pronounced when all neurons are assessed **(Fig.4.2.B,E)** compared to only large NF200 positive neurons **(Fig.4.2.C,F)**, thus for further evaluation, only quantification of βIII-tubulin positive fibers was used. Never the less, the lack of specificity is unexpected since the stimulation is done at 2*MT and non-myelinated fibers have been reported to have 10-15 times higher threshold than myelinated fibers (Reilly and Antoni, 1992, Reilly et al., 1985, Schlumm et al., 2013). Since the effects appear not to be restricted to large myelinated fibers, it suggests that other mechanisms are involved or the stimulation is not entirely restricted to large myelinated fibers.

4.1.6. Coating and growth duration modifications make assessment of growth changes more sensitive

The plating parameters used in the experiments described above (0.5µg/ml laminin) provide a permissive substrate, however a more permissive substrate such as 5µg/ml laminin coated plates with shorter incubation time (24h) might be more suitable to exhibit any growth effects after CL and ES. Thus to establish the modified assay sensitivity for growth changes, I compared control (naïve) DRGs cultures and DRGs 7 days after a CL, seeded on 5µg/ml laminin coated plates for 24h **(Fig.4.4)**. Another aspect that may influence sensibility is the assessment method that can be influenced by experimental conditions and several user dependent parameters. Thus besides the already used longest neurite assessment in NeuronJ, I also quantified with an additional method, CellP **(Fig.4.4)** and compared the two for magnitude of effect and correlation of growth **(Fig.4.5)**. When CL is evaluated with the new plating conditions (PDL/Laminin (5µg/ml laminin), 24h growth) both methods show a marked and robust effect both for total neurite length (difference between means ±SE= 441±70 %) and longest neurite length (365±54.1%) **(Fig.4.5)**, showing they are sensitive and overall equivalent. The values also correlate very well, in a linear fashion, R^2=0,96, p<0.0001 **(Fig.4.5.C)**. The two methods showing comparable results, ImageJ was chosen for standard assessment, because it allows for classification of neurite length into intervals and conclusions about the type of growth, such as influences on neurite elongation or initiation rather than branching can be drawn. This is not possible in CellP, as tracings are not associated with a single cell **(Fig.4.4.B,D)**. Thus, the longest neurite growth with ImageJ was used as main outcome measure for in vitro DRG neurite growth, while total neurite growth assessment was occasionally used as confirmation.

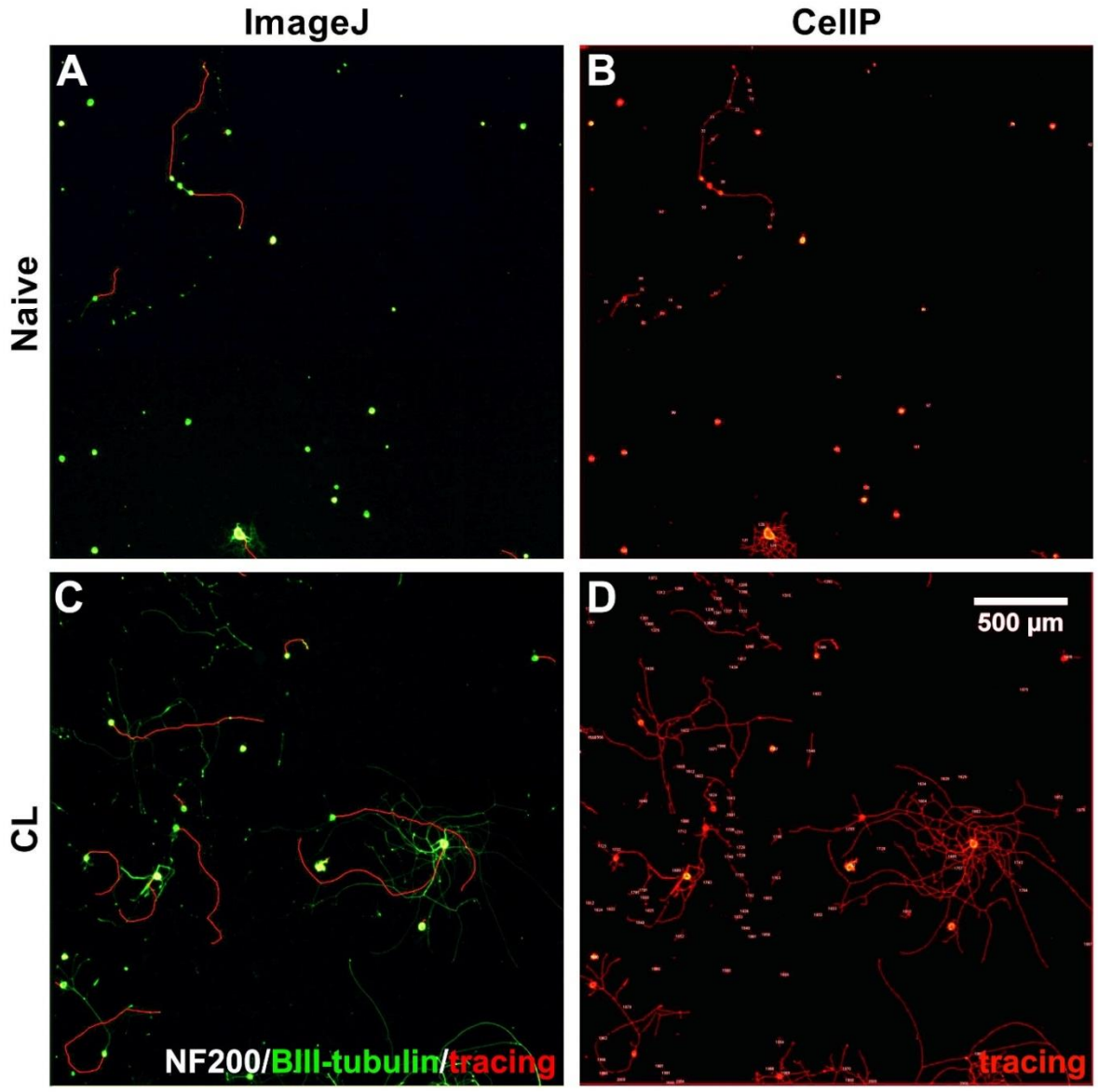

Fig.4.4. Neurite growth in vitro – longest neurite tracing with ImageJ and total neurites tracing with CellP. (A) and **(B)** show DRGs growth from a naïve animal while **(C)** and **(D)** after conditioning lesion. In ImageJ (NeuronJ) **(A, C)** the longest neurite is traced by a user, independently for each neuron. Total neurite length measurement with CellP **(B, D)** is done automatically by the software, with minimal user involvement. The resulting tracings units are not associated with a particular cell, but are frequently either connected from several cells or fragmented by small undetected neurite segments. While that does not influence the average total neurite length, it is not possible to classify cells in growth categories with CellP.

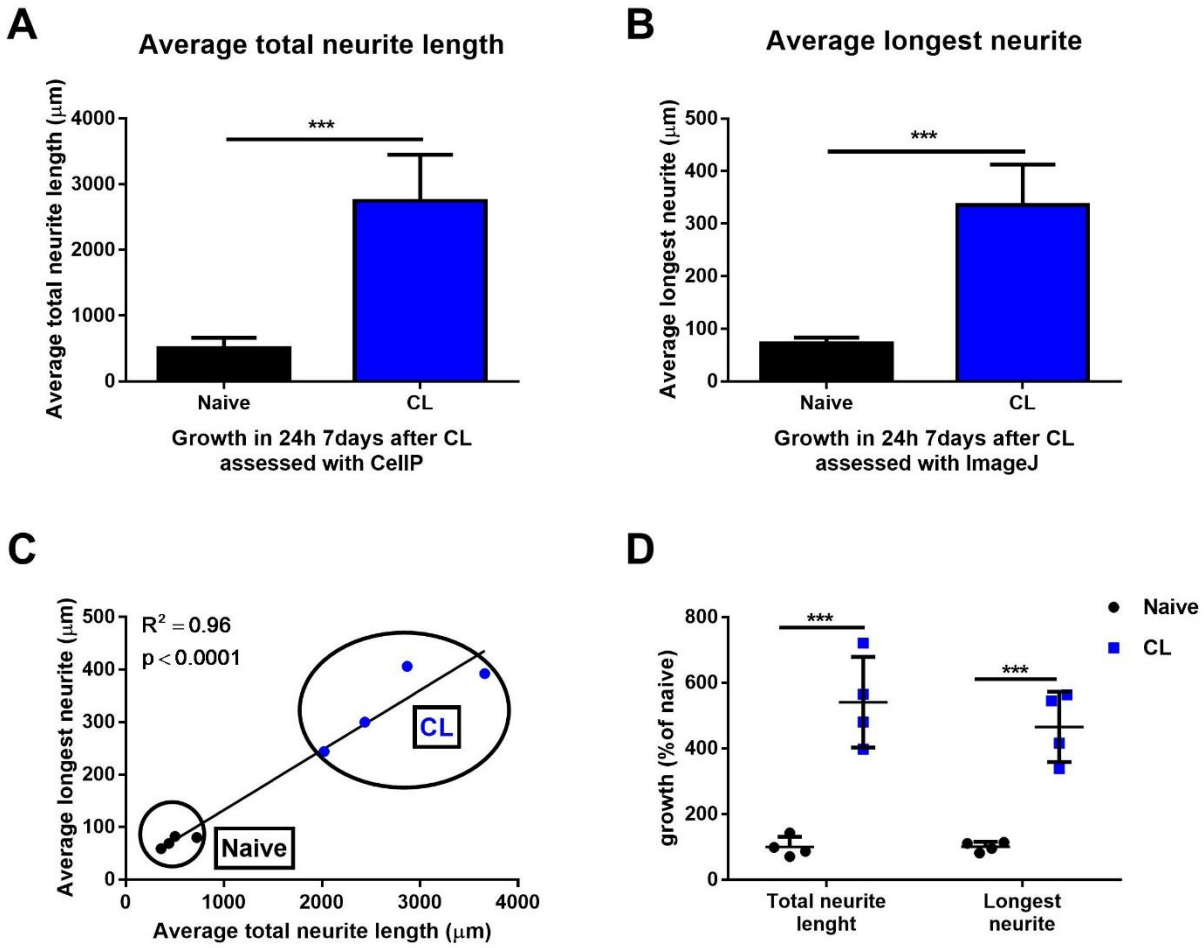

Fig.4.5. Validation of assessment methods for DRGs growth capacity changes in vitro. DRGs cultures from naïve and conditioned animals, 24h growth on 5ug/ml laminin coated plates, were assessed with NeuronJ and CellP. **(A)** and **(B)** Both methods show very clearly the conditioning lesion effect on growth, with high significance (*** $p<0.001$), **(D)** with similar effect magnitude (Difference between means=+441±70.58% for total neurite length) and (+365±54.1% for longest neurite length), and **(C)** correlation between the methods (R^2=0,96, $p<0.0001$).

Overall in the preliminary experiments, in vivo electrically stimulated sensory neurons were shown to have a tendency towards longer neurite extension in vitro than naïve, unstimulated DRG neurons, however surgical procedure and/or chronic cuffs were shown to potentially injure and thus condition the sciatic nerve in some isolated cases, making normalization to sham and an equal number of controls essential for all experiments. ES did not have a different trend of growth on myelinated versus non-myelinated fibers as shown by quantification of NF200 positive and ß3-tubulin positive cells, suggesting that some mechanisms to spread the effect are involved or the stimulation is not restricted to large myelinated fibers as would be expected, and ß3-tubulin quantification is sufficient.

Cultivation for 24h on PDL/Laminin (5µg/ml) was found to much better discriminate growth changes after CL, either using longest neurite assessment or total neurite growth. This called for reevaluation of ES effects with the new cultivation protocol, never the less the trends observed in the preliminary experiments are relevant to exclude retesting parameters which did not show any positive or relevant trends as well as for experimental design.

4.2. Ex-vivo effects of single stimulation – elongation and initiation

4.2.1. Electrical stimulation enhances ex-vivo growth of DRG neurons

We evaluated the effects of ES, in the new cultivation conditions, using the same stimulation protocol as previously described (20Hz, 2*MT, 0.2ms, 1h). Briefly, lumbar dorsal root ganglions (DRGs; L4-L6) were isolated from naïve animals and animals 7 days after the ES, CL or sham, then plated in 6-well plates coated with PDL (16.6µg/ml) and laminin (5µg/ml), fixed after 24h and labeled for ßIII-tubulin. Because surgical procedure and/or chronic cuffs were shown to potentially injure the nerve and thus condition neurons in some isolated cases, an equal number of control were added to all experimental days and all data was normalized to the sham values of the respective experiment.

In these experiments, I observed a significant increase in neurite growth after ES, confirming that ES has a consistent growth promoting effect **(Fig.4.6)**. CL increases growth relative to naïve more than 4-fold, while ES increases growth about 2-fold compared to sham and naïve animals**(Fig.4.6.E)**. When considering only neurite bearing cells, CL increases neurite length compared to naive by 374±44µm and ES compared to sham by 137±44µm **(Fig.4.6.F)**.

All neurons were classified by the length of their longest neurite in 4 categories (<20, 20-40, 40-100 and >100µm), revealing that CL increases the percentage of neurite bearing cells as well as the percentage of cells with long neurites, while ES does not influence the neurite initiation **(Fig.4.6.G)**. Like in conditioned neurons, growth is characterized by long, sparsely branched neurons and ES increased the percentage of neurons with neurites longer than 100µm after 24h in culture **(Fig.4.6.G)**. Thus ES seems to promote growth primarily through enhanced neurite extension.

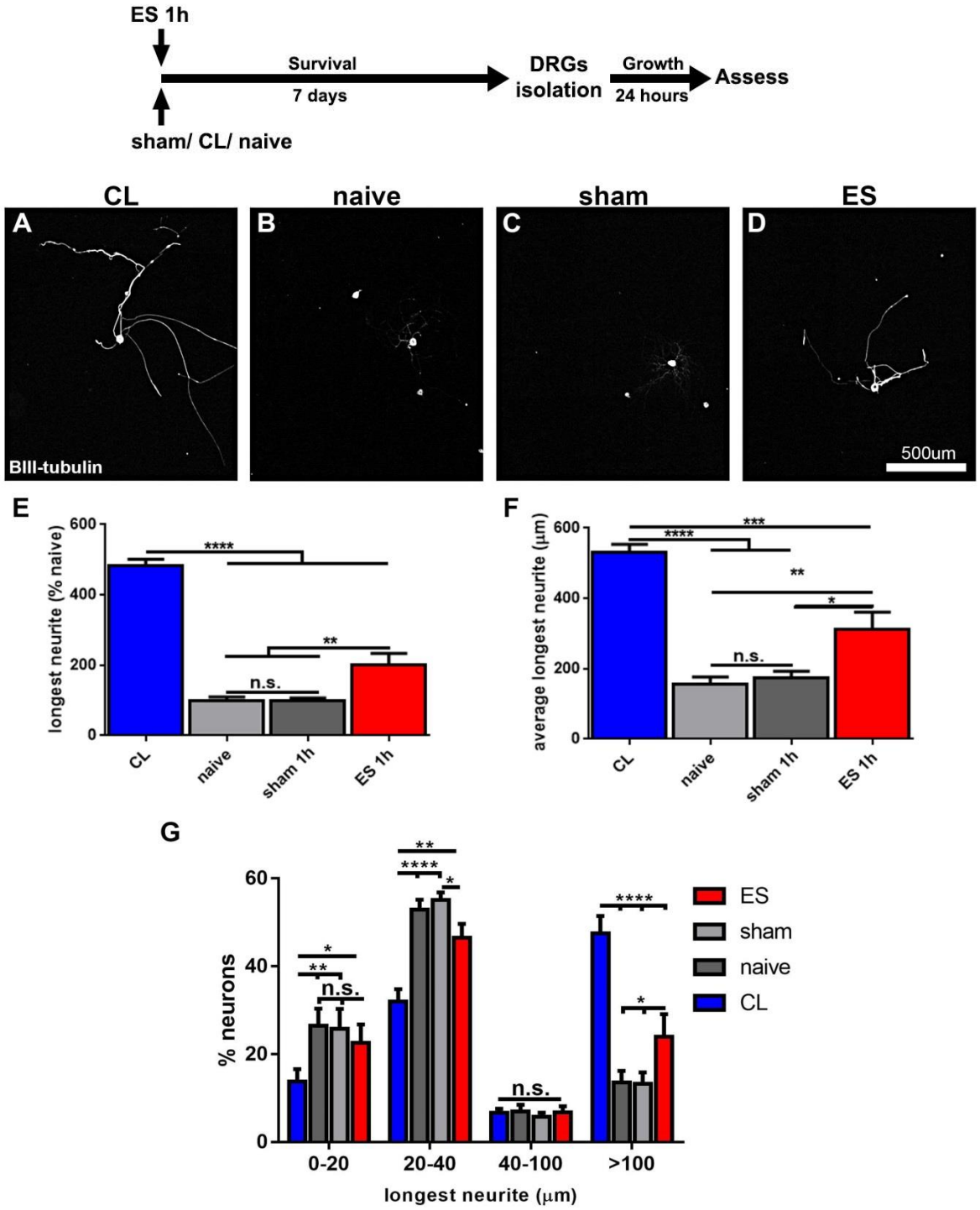
ES 1h
Survival
7 days
sham/ CL/ naive
DRGs isolation
Growth
24 hours
Assess
CL
naive
sham
ES
A
B
C
D
BIII-tubulin
500um
E
longest neurite (% naive)
600
400
200
0
****
**
n.s.
CL
naive
sham 1h
ES 1h
F
average longest neurite (µm)
600
400
200
0
***
****
**
*
n.s.
CL
naive
sham 1h
ES 1h
G
% neurons
60
40
20
0
**
****
*
*
**
n.s.
****
*
n.s.
0-20
20-40
40-100
>100
longest neurite (µm)
ES
sham
naive
CL

Fig.4.6. Neurite growth after ES of the sciatic nerve in vivo. DRGs (L4-L6) were isolated from **(A)** animals 7 days after CL, **(B)** naïve animals, **(C)** 7 days after sham or **(D)** electrical stimulation. Cells were grown on PDL-laminin(5µg/ml) coated plates for 24 hours, fixed, labeled for βIII-tubulin, imaged and assessed in ImageJ. **(E)** Quantification of neurite growth demonstrates a strong CL effect, but 1h ES 7d prior to isolation is also growth-promoting (n=8, ANOVA $p<0.0001$, Tukey´s multi comparison test). **(F)** Longest neurite growth for neurite bearing cells (n=8, ANOVA $p<0.0001$, Tukey´s multi comparison test). **(G)** Neurons classified by their longest neurites reveal that Conditioning lesions enhance neurite initiation and extension, whereas electrical stimulation primarily enhances neurite extension (n=8, ANOVA $p<0.0001$, Tukey´s multi comparison test). All data are presented as mean±SEM. $*p<0.05$, $**p<0.01$, $***p<0.001$, $****p<0.0001$.

This is the first time such an effect is reported in an inclusive set of experiments allowing for the comparison of the effects from ES and conditioning lesions while eliminating the possibility of a surgery-related conditioning by using appropriate sham controls.

In the context of the previous experiments where the growth after CL and ES on PDL-laminin (0.5µg/ml) coated plates showed the same trend, but was less robust, we can also conclude that the growth-promoting effect is influenced by substrate and growth duration, in a similar way to conditioning lesion effects, and can be better observed on a more permissive substrate.

4.2.2. A delay is required to observe positive effects on growth after ES

To determine whether a delay between the ES and the DRGs isolation, is necessary for growth enhancing effects to be observed, neurons were isolated 1 day after ES or sham electrode implantation. No difference in growth was observed 1 day after ES **(Fig.4.7)**. As effects of CL also require time between injury and enhanced growth effects, these similarities suggest that effects of ES like CL effects are due to modifications of the intrinsic growth potential via similar mechanisms, such as changes in gene expression and a delay is needed in both cases to reach significant levels.

However, unlike CL, ES has a weaker overall effect on neurite growth, and appears to promote growth primarily through enhanced neurite extension and not on initiation, suggesting that mechanistic overlap is only partial.

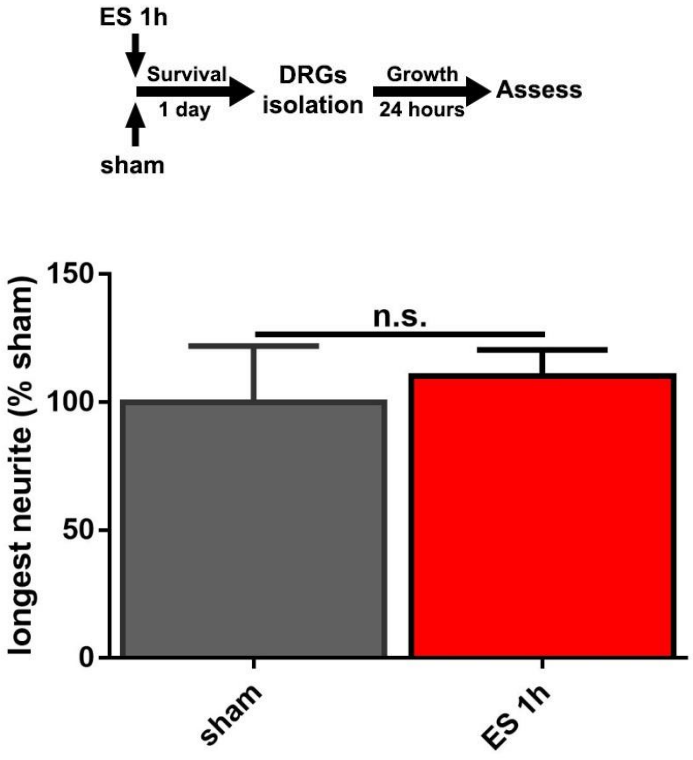

Fig.4.7. A delay longer than 1 day is needed to observe ES-mediated neurite growth stimulation. Neurite growth of DRGs (L4-L6) isolated 1 day after ES is not enhanced (n=6, t-test p=0.68, mean±SEM). Similar to conditioning lesions, a longer delay between stimulation and isolation is needed to initiate a growth program.

4.2.3. Absolute stimulation intensity does not influence neurite growth

In order to investigate what other parameters might influence the results on in vivo growth, we verified if the motor thresholds of the stimulated sciatic nerve correlates with the observed relative increase in growth. Linear regression analysis did not indicate a correlation between stimulus intensity and neurite growth **(Fig.4.8)**.

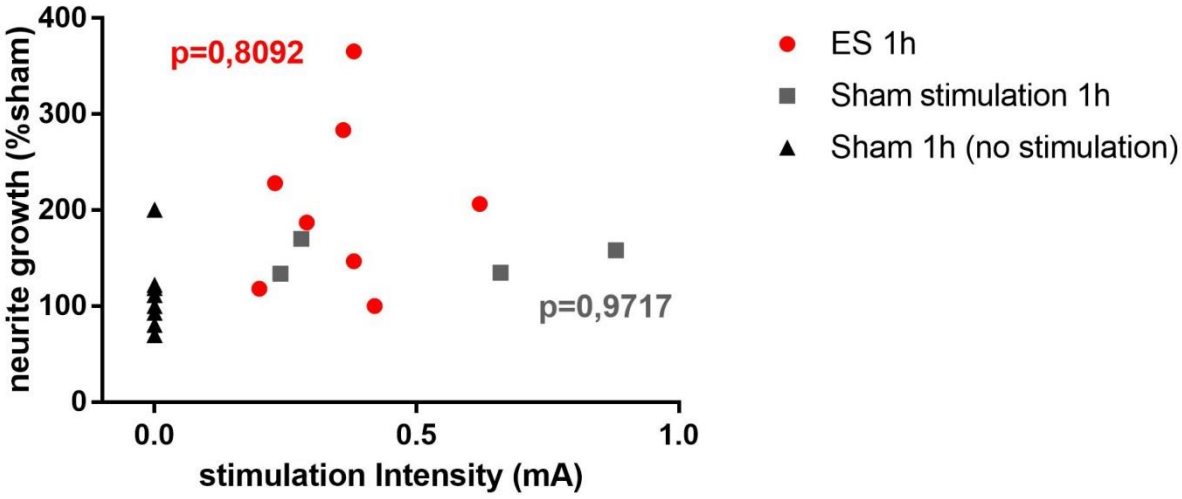

Fig.4.8. Stimulation intensity does not correlate with neurite growth. Stimulation intensity and neurite growth values of individual animals after ES (20Hz, 0.2ms, constant current stimulation, 1h). Neurite growth is indicated as % relative to sham 1h (no stimulation) animals set at 100%. Animals stimulated with constant voltage (sham stimulation 1h), do not show a significant increase in neurite growth compared to sham 1h (no stimulation). Linear regression analysis indicated no significant correlation between intensity and neurite growth in any of the groups ($p>0.05$).

4.3. Ex-vivo evaluation of increased duration of stimulation

A single 1h in vivo ES induced a significant enhancement of neurite growth when isolated after 7 days **(Fig.4.6)**. However, compared to CL, ES has a weaker overall effect. As CL results in long-term deafferentiation compared to a single 1h manipulation, and because repeated conditioning after a CL, can further increase peripheral lesion-induced neurite growth (Neumann et al., 2005), I determined whether repeated stimulation for 1h per day for 7 days had more profound neurite growth promoting effects. As an alternative approach, a single continuous stimulation for 7 hours was chosen to keep the timing between stimulation and cell isolation constant.

4.3.1. Increasing the duration of stimulation or repeated stimulation has no additional growth-promoting effect

Repeated stimulation **(Fig.4.9.A)** or increased duration for 7h in one stimulation session **(Fig.4.9.B)** both increased growth compared to sham by 56% (ES 1h Rx7) and 67% (ES 7h), respectively, and did not have any additional beneficial effect compared to 1h stimulation (compare to **Fig.4.6**). Rather, there was an apparent reduction in relative neurite growth compared to 1h stimulation. However, this is likely due to higher variability in chronic/7h cuff electrode implants.

The lack of additional effects from repeated and prolonged stimulation, suggests that the initial part of the stimulation is essential and sufficient. This is consistent with the short-term depolarization pattern observed after an axotomy, which is brief, and suggests that indeed the initial phase of the stimulation induces a growth response similar to a subset of the CL effects, but further stimulation in the same fashion is not additive. The lack of additional effects from the 7h stimulation also confirms that there are no unspecific effects from local tissue chemical reactions, because any unbalanced electrolysis from a constant protocol, should be directly proportional to the stimulation time according to Faraday's Law: $\mathrm{n} = \frac{Q}{Fz} = \frac{\int_0^t I(t)dt}{Fz}$ (where n=amount of substance in moles liberated, Q=charge, F=Faraday constant and z=valency number of ions of the substance) (Ehl and Ihde, 1954).

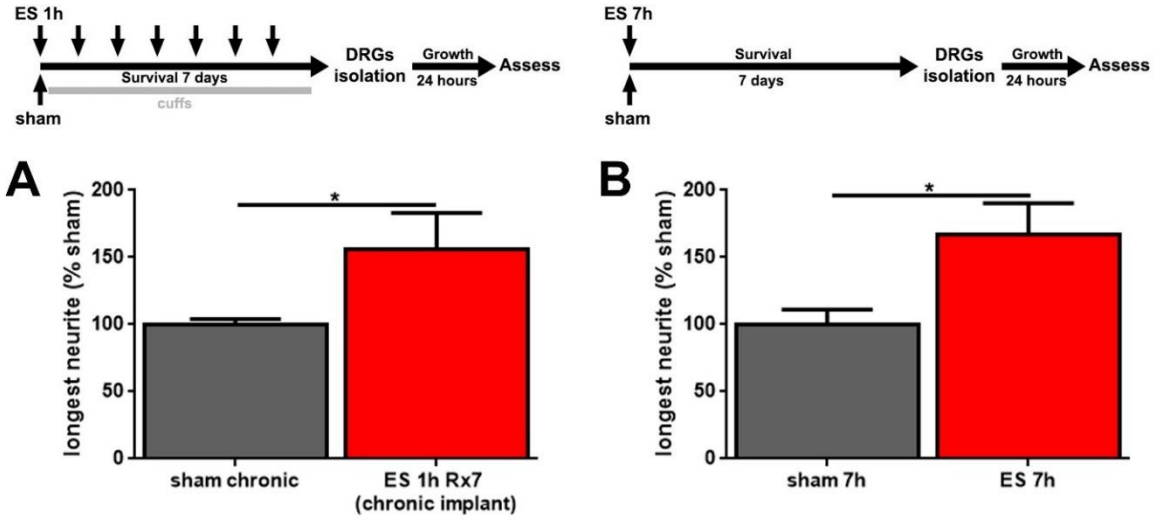

Fig.4.9. Increasing the duration of stimulation or repeated stimulation has no additional growth-promoting effect. DRGs (L4-L6) were isolated **(A)** 7 days after a single 7h stimulation or **(B)** after daily 1h stimulation for 7 days (n=5-8, t-test $p<0.05$; mean±SEM). The effect size is similar to single 1h stimulation (compare to **Fig.4.6**).

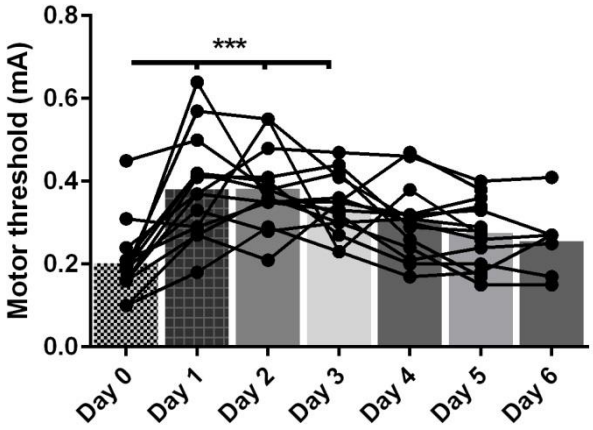

Fig.4.10. Motor threshold variation for repeated stimulation with chronic electrodes. In animals with chronic implants and repeated stimulation, the motor threshold was independently determined and recorded for every stimulated sciatic at every stimulation time-point. N=16, 2 outliers were excluded by ROUT (Robust regression and Outlier removal) method. 2-way ANOVA, $p<0.0001$, N=14. Dunnett's multiple comparisons test, compared to day 0. All data is presented as mean per day and individual repeated measures, *** $p<0.001$.

4.3.1. Motor threshold variation for repeated stimulation with chronic electrodes

Motor threshold was also recorded for repeated stimulation and analyzed. The intensity required to achieve a motor response was significantly increased in the first days after

electrode implantation, coinciding with post-operative analgesia, but then returned to baseline values, showing that the electrodes are stable and functional for at least 1 week **(Fig.4.10)**.

4.4. In vivo growth after DCL and MSCs injection into the lesion and electrical stimulation

4.4.1. Axon regeneration in vivo after 1h ES - axon sprouting into the graft

To test the effects of ES on central regeneration in vivo, animals underwent a C4 dorsal funiculus wire-knife lesion interrupting all dorsal column sensory fibers **(Fig.4.11)**. All groups received autologous GFP+ bone marrow stromal cells into the lesion to provide a cellular bridge. This strategy also allows evaluation of the efficiency of ES in combination with other therapeutic strategies for SCI such as cell transplantation, though BMSCs injection into a lesion does not have benefit by itself.

The border between the lesion filled with GFP+ BMSC and the caudal intact spinal cord tissue was visually delimited under epifluorescent illumination, and all axonal profiles crossing the border, or 50, 100, 250 or 500µm into the lesion, were quantified.

Compared to animals that only underwent a spinal cord lesion and cell transplantation, animals with a CL showed a higher number of axons extending beyond the lesion border into the graft as expected **(Fig.4.12.A-F)**. Naïve animals and animals with sham electrodes exhibited a similar small number of CTB labeled axons in the lesion **(Fig. 4.12.D-I)**. Importantly, ES increased the number of injured axons sprouting into the lesion **(Fig. 4.12.J-L).**

Quantification indicated a significantly higher number of fibers in CL animals at 0um, 50um and 100um compared to all other conditions **(Fig.4.12.M)**. ES was also associated with an increased number of fibers at 0um, 50um and 100um within the lesion, compared to sham animals **(Fig.4.12.N)** and the lesion only group. Thus, ES increases axonal growth, but to a lower magnitude than CL **(Fig.4.12.O, P).** In vivo effects are comparable to in vitro findings, including the effect size of ES in relation to CL. In addition, these data suggest that ES could be used in vivo in combination with other therapeutic strategies such as cell transplantation.

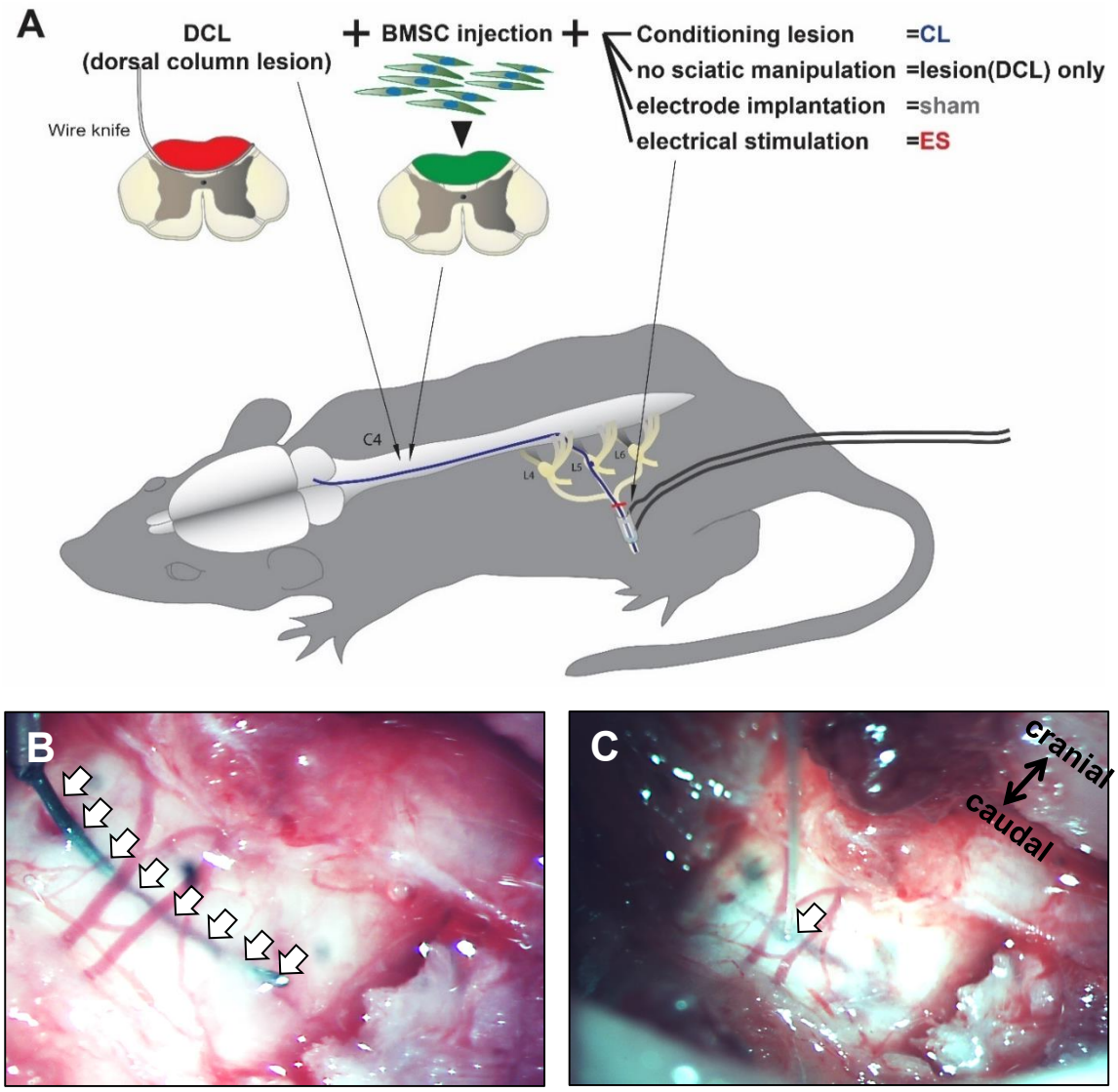

Fig.4.11. Schematic experimental design for in vivo regeneration after ES. (A) Animals received dorsal column wire-knife lesion and BMSCs injection in the lesion, followed by CL, no sciatic manipulation, sham or ES. **(B)** Spinal cord with the wire knife in place at the site of the lesion indicated by arrows, **(C)** lesion after wire knife removal with the glass pipette tip (indicated by arrow) located medially for cell injection.

Table 4.1: Axon growth into the cell graft at 4 weeks after DCL and 1h ES

Distance	CL (n=6)		lesion only (n=6)		sham 1h (n=6)		ES 1h (n=7)	
	Mean	SEM	Mean	SEM	Mean	SEM	Mean	SEM
0um	48,83	8,57	11,83	2,64	13,17	2,81	28,00	2,65
50um	37,50	8,91	10,50	2,32	9,83	1,74	19,14	2,05
100um	27,33	7,25	7,50	2,60	6,83	1,74	16,71	2,09
250um	10,00	2,97	1,67	0,61	2,50	0,62	7,00	1,35
500um	1,67	0,99	1,00	0,52	0,00	0,00	2,57	0,75

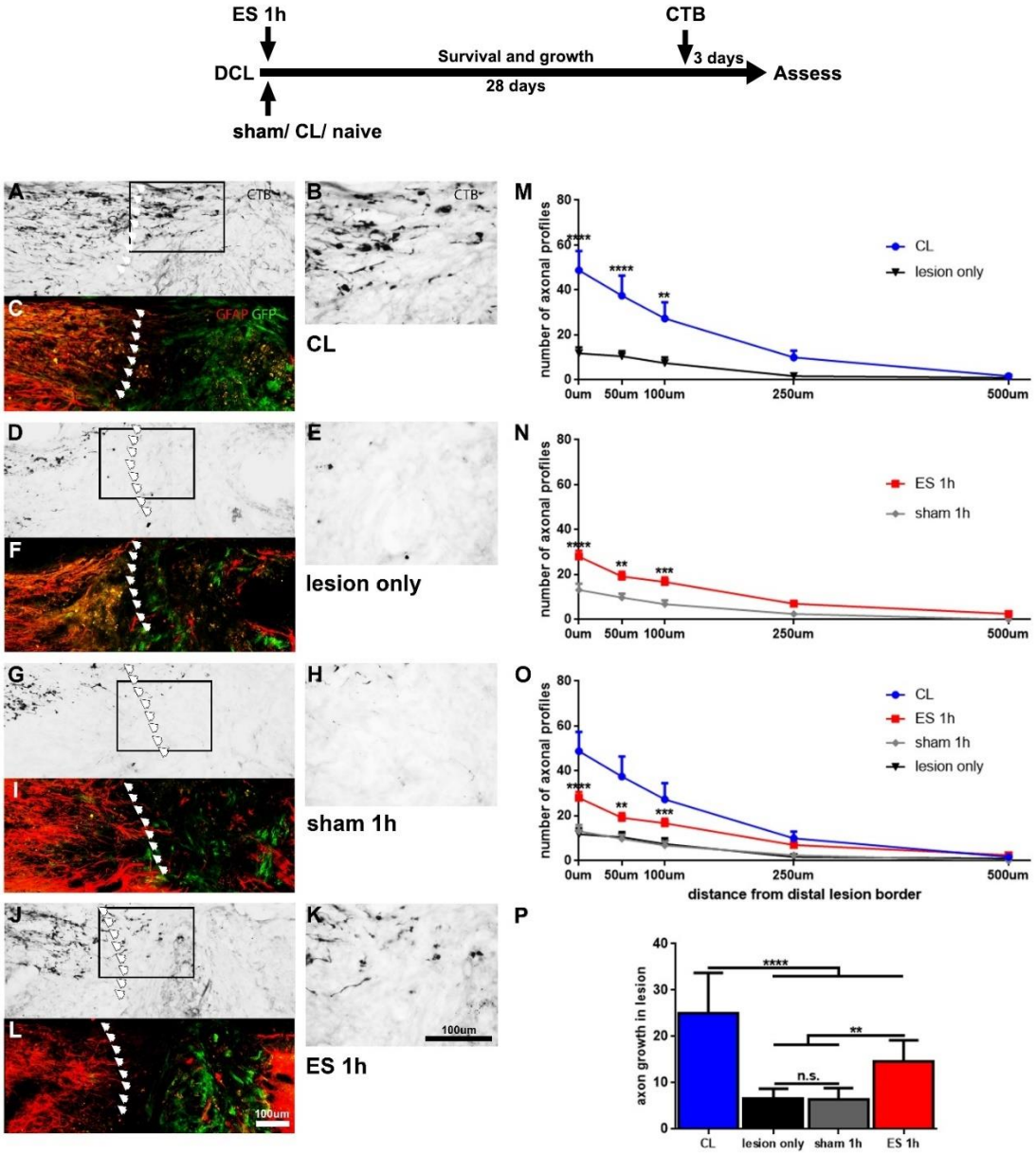

Fig.4.12. Axonal growth 4 weeks after dorsal column lesions (DCL) and single 1h ES. Following transection of ascending sensory axons at C4 and injection of GFP+ BMSCs into the lesion, animals received **(A-C)** bilaterally conditioning lesions, **(D-F)** no other manipulation, **(G-I)** electrodes with no stimulation or **(J-L)** electrical stimulation. (**C, F, I, L)** CTB-labeled axons were quantified at the caudal GFAP border (red) and within the lesion site filled with GFP^+ BMSCs (green). Arrows mark the caudal lesion border. **(B, E, H, K)** Higher magnifications of boxed areas shown in (A, D, G, J). **(M, N, O, P)** Number of axonal profiles at different distances from the lesion site were quantified in 1 out of 7 serial sagittal sections. For clarity, comparisons are shown separately for **(M)** CL vs naïve and **(N)** ES compared to sham and **(O)** all conditions. 2-way ANOVA, Tukey´s multi comparison test. **(P)** Quantification of overall axon growth in the graft. n=6-7/group, 2-way ANOVA, Tukey´s multi comparison test. Points/bars represent mean± SEM.

4.4.2. Axon regeneration in vivo after chronic implants and repeated stimulation

Though repeated/ stimulation in the pattern assessed by in vitro growth assays did not result in increased neurite length, other studies have indicated that repeated CL at 7 days after an initial CL has a greater effect than a single stimulation (Neumann et al., 2005). Such a more delayed pattern may also be more effective for ES, but cannot be assessed by ex vivo growth assays.

I therefore tested the hypothesis that repeated ES at 7 days after the initial ES could further increase growth compared to a single stimulation. All animals received spinal cord lesions and cell grafts as previously described, and one group received chronic cuff electrodes (n=6) and stimulation on the day of the DCL and 7 days later, while the corresponding control group received chronic sham electrodes (n=6).

The border between the lesion filled with GFP+ BMSC and the caudal host spinal cord tissue was identified and axonal profiles crossing the lesion border, or 50, 100, 250 or 500µm into the lesion were counted. ES 1hx2 was also associated with an increased number of fibers at 0um (**) and 50um (*) within the lesion, compared to lesion only animals, however no difference was detected compared to chronic sham animals at any distance **(Fig.4.13.A)**. Chronic sham animals were highly variable and showed significantly more fibers extending into the lesion (0um*) compared to the lesion only group masking the effects of ES 1hx2. The quantification of overall axon growth in the graft **(Fig.4.13.B)** demonstrates the same phenomenon.

These results are in line with the in vitro findings regarding chronic cuff electrodes and suggest that for repeated application in vivo, non-invasive stimulation would be desirable.

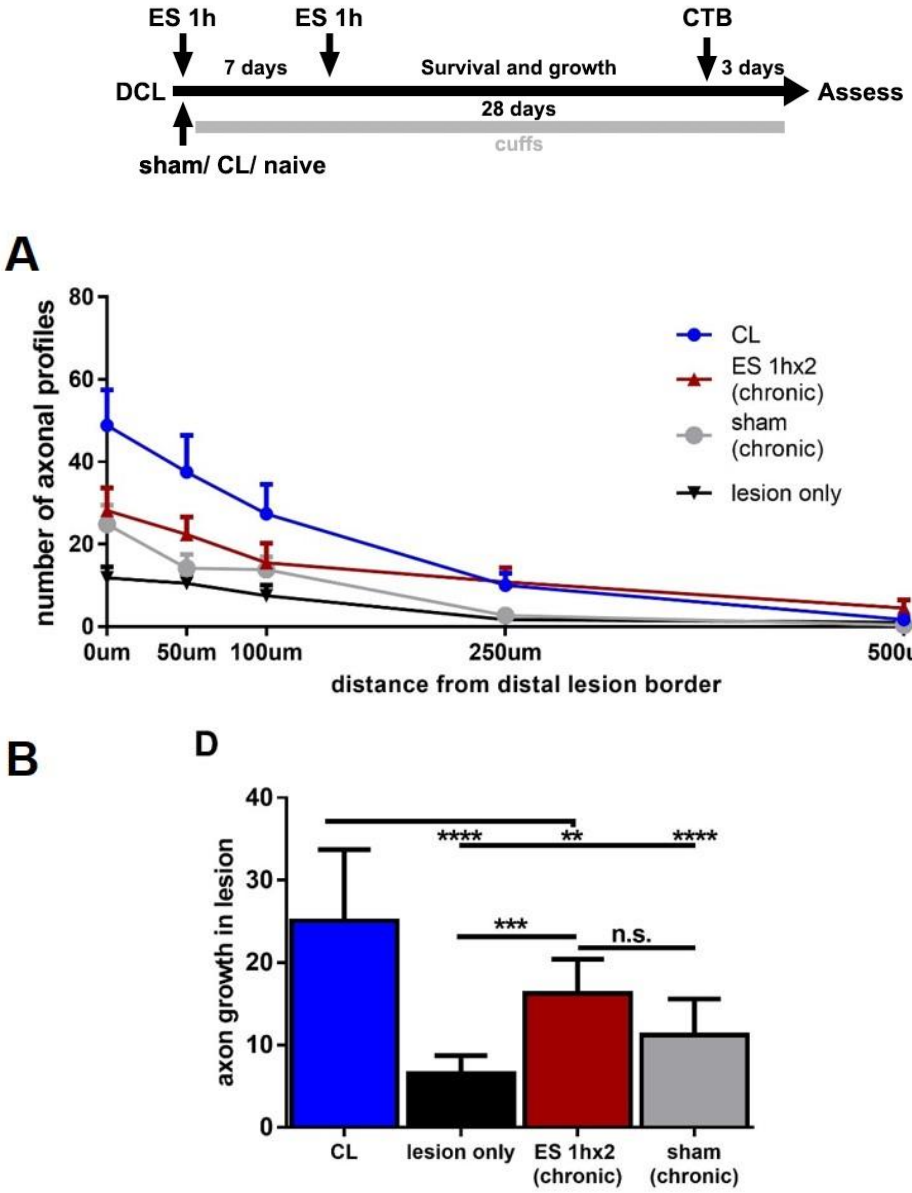

Fig.4.13. Axonal growth 4 weeks after dorsal column transection (DCL) and repeated stimulation with chronic electrodes. After C4 wire-knife lesions and GFP+ BMSCs injection into the lesion, animals received bilateral conditioning lesions, no other manipulation, chronic electrodes with no stimulation or electrical stimulation, once after the DCL and once 7 days later for 1h each. CTB-labeled axons were quantified at the caudal GFAP border and within the lesion site filled with GFP$^+$ BMSCs. **(A)** Number of axonal profiles at different distances from the lesion site were quantified from 1 out of 7 serial sagittal sections. Experiments were done in parallel to data shown in Fig. 4.12. There is no significant difference between ES and sham animals at any distance. **(B)** Quantification of overall axon growth in the graft. Compared to naïve animals, there is increased growth in the sham animals indicating a conditioning by chronic cuff implantation. n=6/group, 2-way ANOVA, Tukey´s multi comparison test. Points/bars represent mean± SEM.

Chronic cuff implants were evaluated macroscopically 24 days post-lesion, during CTB injection. **(Fig.4.14)**. All electrodes were in place around the nerve, with no apparent damage. Frequently, connective tissue covered the cuff fixing it in place, suggesting

removal of the electrode after a repeated stimulation, could not be done without additional damage to the nerve. The electrodes were not tested functionally, but appeared to be intact. I also observed neovascularization on the nerves with chronic cuff electrodes, including within the cuff electrode **(Fig.4.14.B)**. However, there didn't seem to be any compression of the nerve, due to the extra space in the inner diameter of the cuff electrode, which was selected especially for this purpose. Nerves which had undergone conditioning lesions were macroscopically similar to unlesioned nerves 24 days after the CL, showing a normal number of blood vessels and less connective tissue around the nerve compared to nerves with electrodes **(Fig.4.14.A)**. The intensity necessary to evoke a motor response increased slightly from day 0 to day 7 by 0.08±0.02mA ($p<0.05$) **(Fig.4.15)**, and all electrodes remained functional within this first week post-implantation.

Table 4.2: Axon growth into the cell graft at 4 weeks after DCL and 2x ES for 1h each.

Distance	**CL (N=6)**		**lesion only (N=6)**		**sham (chronic) (N=6)**		**ES 1hx2 (chronic implant) (N=6)**	
	Mean	SEM	Mean	SEM	Mean	SEM	Mean	SEM
0um	48,83	8,57	11,83	2,64	24,83	4,67	28,17	5,44
50um	37,50	8,91	10,50	2,32	14,17	3,30	22,33	4,28
100um	27,33	7,25	7,50	2,60	13,83	3,05	15,50	4,77
250um	10,00	2,97	1,67	0,61	2,67	0,92	10,83	3,46
500um	1,67	0,99	1,00	0,52	0,33	0,21	4,50	2,00

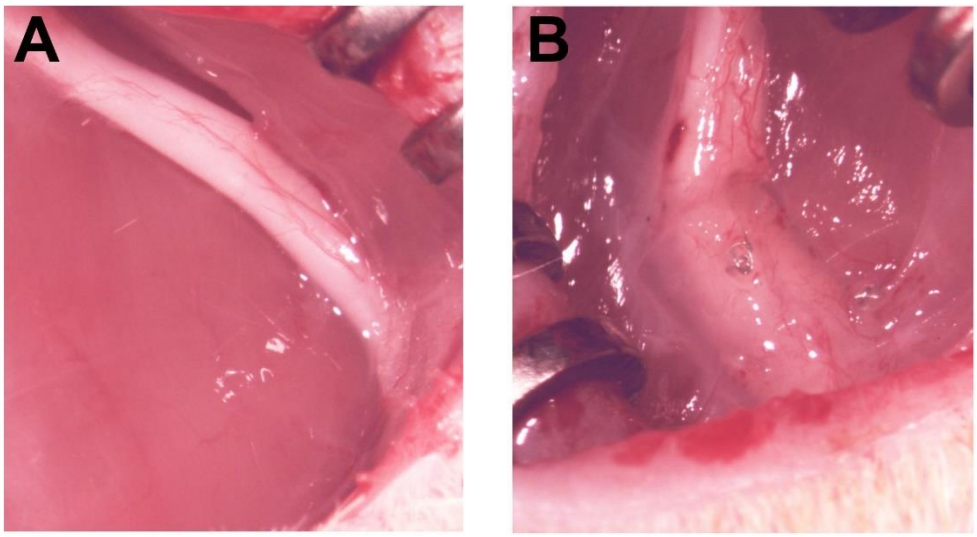

Fig.4.14. Chronic cuff electrodes 24 days after implantation. A) Nerves which received conditioning lesion or no manipulation were macroscopically identical at 24 days after the CL. B) Nerves that received cuff electrodes showed connective tissue covering the cuff and neovascularization on the nerves including within the cuff electrode.

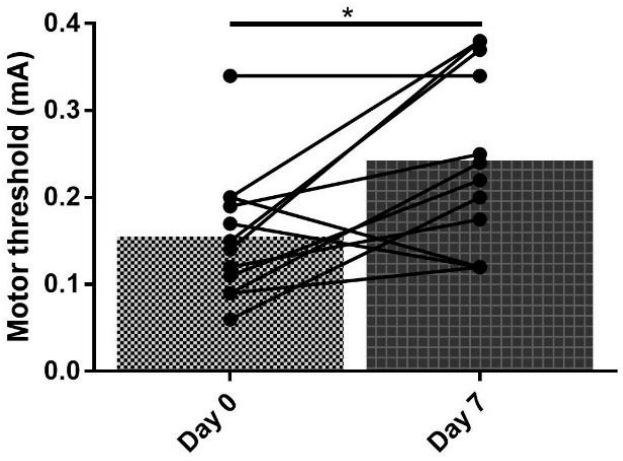

Fig.4.15. Motor threshold of animals with chronic electrodes in animals. In animals with chronic implants and repeated stimulation, the motor threshold (MT) was recorded for every stimulated sciatic at the 2 stimulation time points: day 0 and day 7 after spinal cord lesions. The MT for the second stimulation was significantly higher. Paired t-test. All data is presented as mean and individual repeated measures. * $p<0.05$.

4.4.3. Motor threshold is not influenced by anesthesia or DCL

Stimulated sciatic nerves showed some variability of the absolute intensity needed to evoke movement (motor threshold (MT)), across subjects and experiments which may have influenced effects of ES. Factors such as the contact with the nerve and the electrode, are eliminated by independently determining the MT and setting the stimulation intensity for every stimulated nerve. However, the acute phase of a DCL or anesthesia (Nowicki et al., 2014) could influence the excitability of nervous structures, thus I wanted to compare, if the MT across several experiments is similar.

All MT for sciatics stimulated with ES 20Hz, 0.2ms, constant current stimulation, from various experiments were included. In case of repeated stimulation, only the MT from the first stimulation session was included. We observe a very similar intensity for MT across all subjects and minimal influences from anesthesia or DCL **(Fig.4.16)**. A few outliers have been identified, which are likely due to defective cuffs (ROUT test, $p<0.05$), however as long as the stimulation was efficiently delivered animals were not excluded even if the motor threshold was higher than usual.

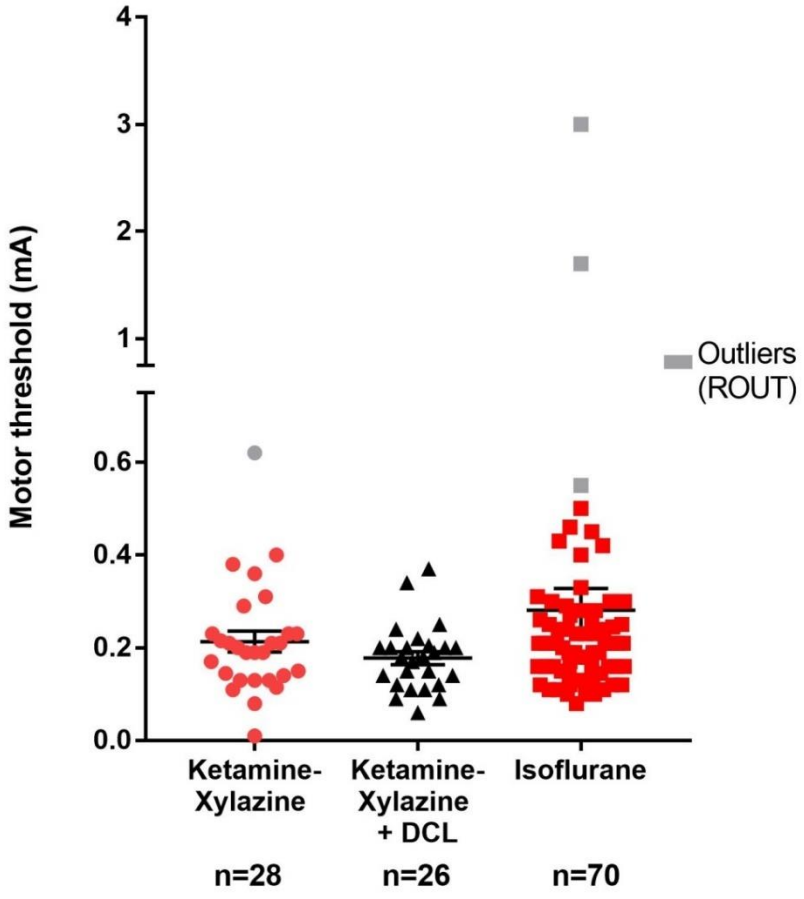

Fig.4.16. Motor threshold for sciatic nerve stimulation is similar across subjects from different experiments, independent of anesthesia and presence of DCL. MT for sciatics stimulated with ES 20Hz, 0.2ms, constant current stimulation, from various experiments were compared. 1-way ANOVA.

4.4.4. ES can stimulate axonal growth, but has no influence on dieback after DCL

It is known that after a lesion, axons can have different reactions to injury, some degenerating and retreating further towards the cell body while others are capable of recovery (Tuszynski et al., 1999, Kwon et al., 2002, Luo and O'Leary, 2005).

To determine whether ES influences axonal dieback, I also quantified the distance of CTB-labeled retraction bulbs from the caudal GFAP/GFP border. The border between spinal cord tissue and cell graft was defined in double fluorescence for GFAP and GFP, and the distance to any retraction bulb was measured. In all conditions there is axon retraction from the caudal lesion border (**Fig.4.17)**, on average 250µm. An influence of CL or ES (single or repeated) on dieback was not detected.

To further validate my findings shown in **Fig.4.12** and **Fig.4.13** using the eye-grid method, I also quantified the distance of axon tips (growth cones or retraction bulbs) relative to the tissue/graft border. Because axons and an observable ending may not be present in the same section, this method samples differently. When data is expressed in a similar way as in the previous assessment, (cumulative % at different lengths within the graft), a very similar trend was observed **(Fig.4.18)**. Electrically stimulated fibers, either ES 1h **(Fig.4.18)** as well as ES 1hx2 **(Fig.4.19)**, achieve on average a longer distance within the graft compared to their respective sham controls and lesion only.

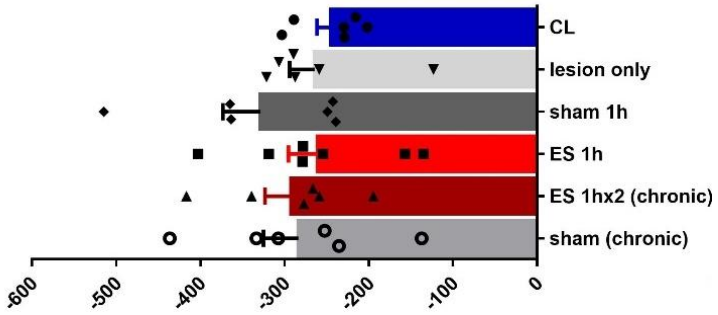

Fig.4.17. Quantification of retraction bulbs within the uninjured spinal cord. The distance of CTB-labeled retraction bulbs from the caudal GFAP/GFP border within the caudal spinal cord was measured with ImageJ. The average distance from the caudal lesion border into the host spinal cord is not influenced by CL or ES (single or repeated). n=6-7, 1-way ANOVA, Tukey´s multi comparison test. Mean ± SEM.

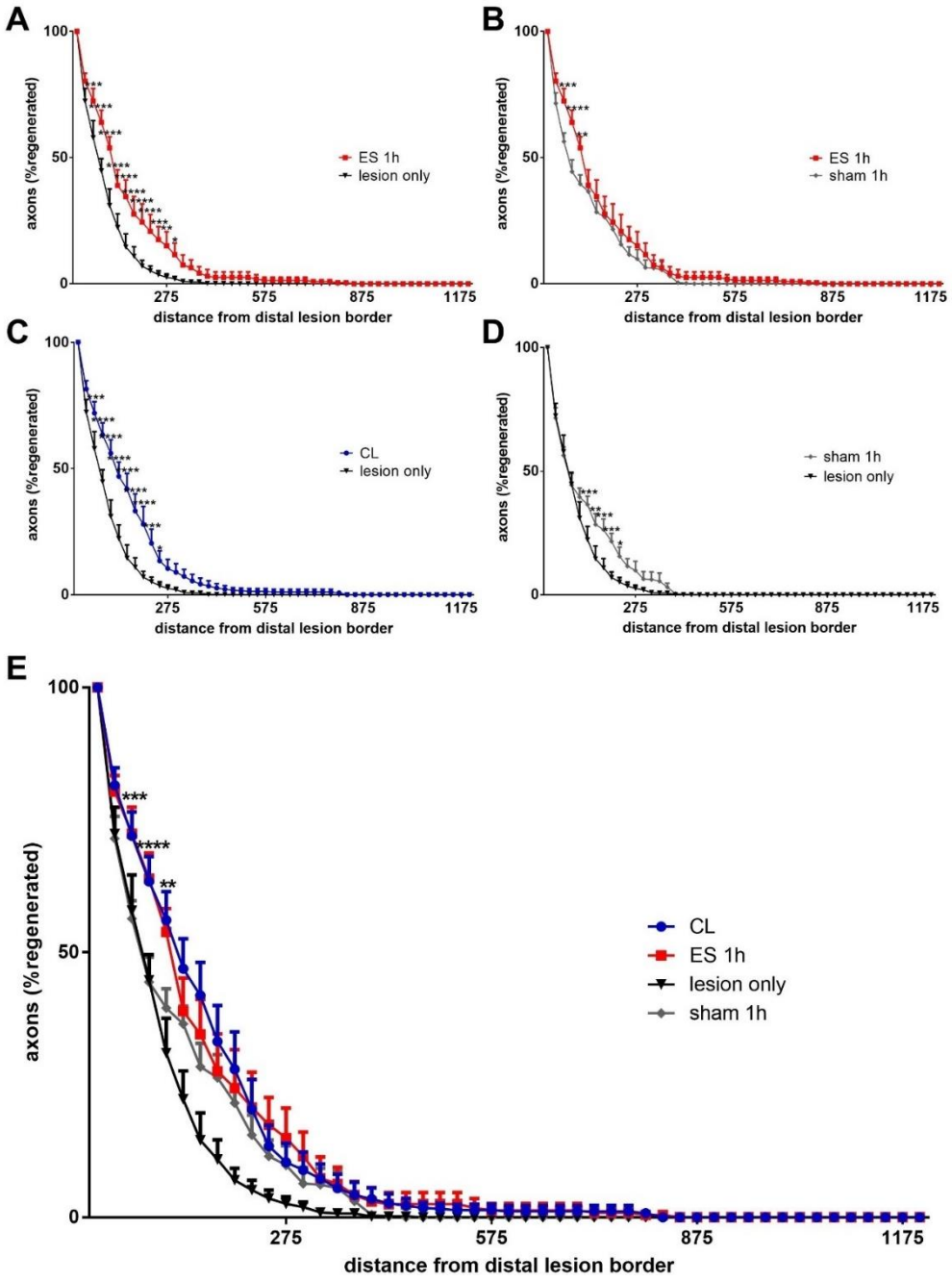

Fig.4.18. Growth cones/axon tips within the graft after ES 1h. The distance of CTB-labeled growth cones/axon tips within the graft was quantified from the caudal GFAP/GFP border with ImageJ, on sections from animals that received DCL and BMSCs injection and either CL, ES 1h or sham 1h. **(A)** The percentage of axons which achieve a longer distance into the graft is significantly increased in ES compared to lesion only and **(B)** compared to sham animals. **(C)** The percentage of axons which achieve longer distance growth into the graft is significantly increased in CL compared to lesion only. **(D)** Sham 1h also shows an effect compared to lesion only. (**E**) All conditions combined into a single graph. Significance shown only for ES 1h versus sham 1h. n=6-7, 2-way ANOVA, Tukey´s multi comparison test. Mean ± SEM.

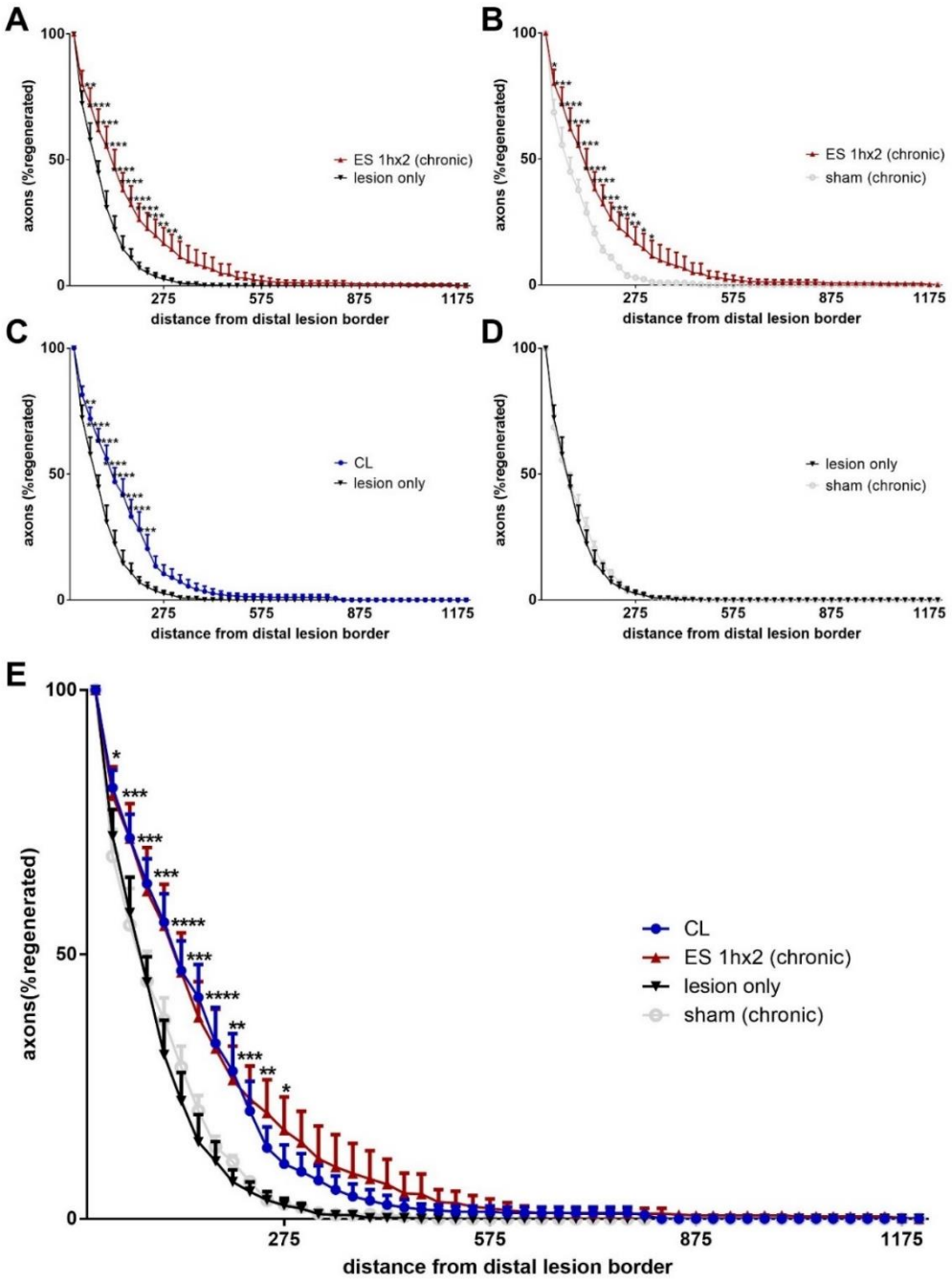

Fig.4.19. Growth cones/axon tips within the graft after ES 1hx2. The distance of CTB-labeled growth cones/axon tips within the graft was quantified from the caudal GFAP/GFP border with ImageJ, on sections from animals that received DCL and BMSCs injection and either CL, ES 1hx2 with a chronic cuff electrode or sham cuff chronic. **(A)** The percentage of axons which achieve a longer distance into the graft is significantly increased in ES 1hx2 compared to lesion only and **(B)** compared to sham chronic. **(C)** The percentage of axons which achieve a longer distance into the graft is significantly increased in CL compared to lesion only. **(D)** Sham chronic did not shows an effect compared to lesion only in this quantification. **(E)** All conditions. Significance shown only for ES 1hx2 versus sham chronic. N=6, 2-way ANOVA, Tukey´s multi comparison test. Mean ± SEM.

4.5. Evaluation of potential adverse effects with relevance for clinical translation

Chronic constriction of the sciatic nerve (Bennett and Xie, 1988), which could be induced by the chronic cuff electrodes, as well as development of pain from sprouting of the spared sural nerve into the plantar area (Decosterd and Woolf, 2000) can be causes for neuropathic pain. Additionally, sprouting induced by ES could also induce pain if it happens aberrantly in the lumbar spinal cord. Thus in animals that survived for 4 weeks, I chose to focus on 2 systems, fine touch and thermal sensitivity because they are typically associated with different tracts in the spinal cord, dorsal column, and anterior column respectively. Our lesion model specifically injures the dorsal column. Thus these tests could emphasize global changes in pain perception as well as any differential effects on injured/non-injured sensory tracts in our experimental setup.

4.5.1. Mechanical threshold testing using von Frey filaments

The fine-touch/mechanical sensibility was recorded as percentage withdrawal to von Frey filaments for all rats at day -1 before surgery, and at 4, 7, 15 and 24 days after. Behaviors such as turning of the head and vocalization, were recorded besides the withdrawal response at 7 and 15 days after surgery, but they were overall sporadic. Typical response was withdrawal alone, across all groups. The groups could not be matched based on baseline values for mechanical sensitivity due to experimental design, but there were no baseline differences in % response for any of the groups or filaments **(Fig.4.20.A-E)**.

Fine touch is abolished by the dorsal column lesion in all experimental groups **(Fig.4.20.F-H)**. In all groups the mechanical sensitivity shows mild, but no systematic tendencies to recover across time **(Fig.4.20.G-H)**.

There are no differences across groups, except in the CL, where at 24 days, the response is significantly higher than the lesion only group for 8g and 10g **(Fig.4.20.D,E)**, showing also a similar tendency in smaller filaments **(Fig.4.20.A-C)**. The fine touch is not affected by single or repeated ES compared to any other group **(Fig.4.20.A-E)**. The only group showing an indication of allodynia was the CL group, where the fine touch for 2g and 4g is significantly increased compared to the baseline at 24-days post-lesion **(Fig.4.20.F, G)**.

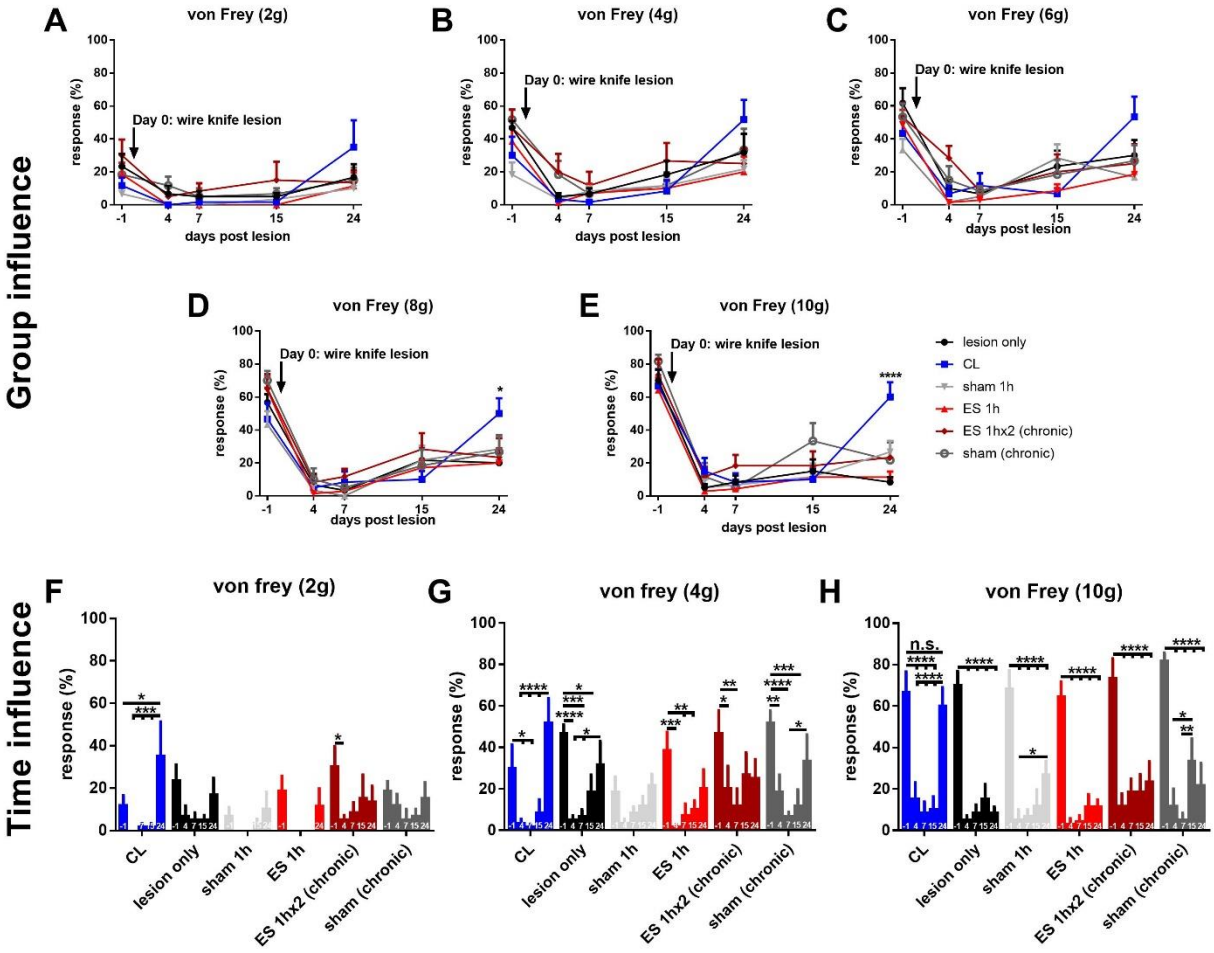

Fig.4.20. Analysis of fine touch in animals with dorsal column lesions does not indicate ES-mediated adverse effects. (A-E) There is no global difference between groups for any of the filaments tested (2, 4, 6, 8 10g). **(D-E)** Animals with CL seem to regain sensitivity to thicker filaments (8, 10 g) at 24 days after surgery compared to lesion only. **(F-H)** The time factor plays a similar role across groups. Responses after von Frey stimulation (2, 4, 10g) indicate a similar loss of sensitivity in all groups after the DCL, with some recovery, possible allodynia only in CL group (at 24 days the % response is significantly higher than baseline for 2g and 4g). Other modifications are non-systematic, indicate a tendency for recovery across all groups, but no adverse effects. N=6-7, 2-way ANOVA interaction and time $p<0.0001$, Tukey´s multi comparison test, mean ± SEM.

4.5.2. Hargreaves thermal sensitivity assay

The fine-touch/mechanical sensibility was recorded as latency to withdrawal after targeting of the hind paws with radiant heat source, in the behavioral test days, after the von Frey testing (day -1 before surgery, and at 4, 7, 15 and 24 days after). We observe an average delay to withdrawal of 15s, which is maintained, across time and experimental groups **(Fig.4.21)**. As expected, thermal sensitivity was not affected by the dorsal column lesion. Neither single or repeated ES showed a trend for increased thermal sensitivity (lowering of threshold) **(Fig.4.21)**.

In the CL group there was a tendency for increased latency at 4 and 7 days after the lesion, is most likely due to the peripheral injury. The pattern is consistent with variability of innervation of the paw, while the recovery can be due to regeneration of the sciatic or compensatory sprouting from the saphenous nerve at the level of the paw (Cobianchi et al., 2014). Additionally, it recovered early (between 7 and 15 days), while the recovery for the mechanical sensitivity in the same group appeared later, at 24 days, suggesting that the mechanisms are unrelated.

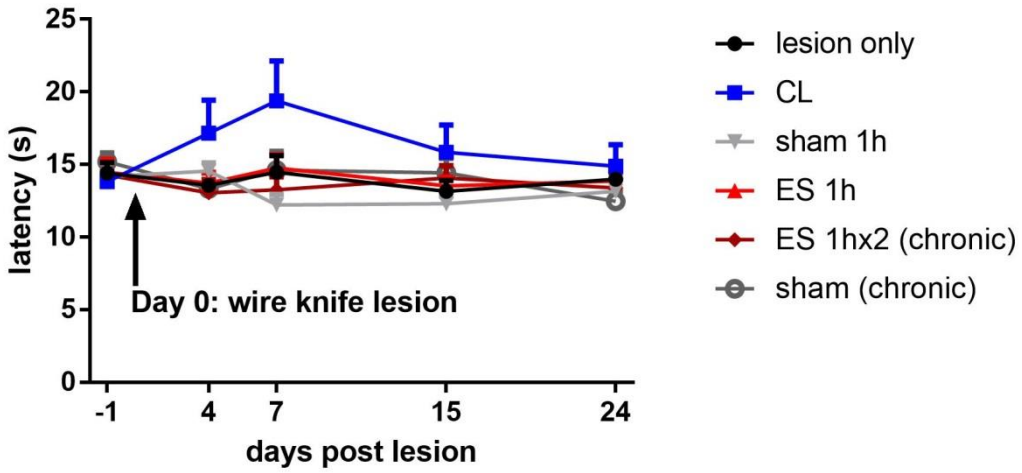

Fig.4.21. Analysis of thermal sensitivity in animals with dorsal column lesions does not indicate ES-mediated adverse effects. Hargreaves plantar heat test does not show differences across time or groups (2-way ANOVA $p>0.05$, mean ± SEM).

4.6. In vitro models of activity – effects of depolarization on neurite growth

Depolarization has been frequently used as an in vitro model of activity and has been shown in various cell types and experimental setups to have effects on neurite growth, survival, neurotransmitter release and other processes (Arcaro and Lnenicka, 1997, Ramakers et al., 1998, Reber et al., 1990, Vaillant et al., 1999, Enes et al., 2010). A high concentration of KCl in the media depolarizes neurons chronically, creating a state comparable to intense electrical activity, which I used as a positive signal to mimic neuronal activity.

4.6.1. KCl depolarization can inhibit or enhance growth in DRG neurons depending on the experimental conditions

Chronic depolarization with KCl for a long period of time has been reported to inhibit growth in adult neurons including in DRGs (Enes et al., 2010). Indeed, I confirmed this inhibition (66%) when DRG are incubated with KCl for 24h **(Fig.4.22.A-D)**.

However, a shorter, physiologically relevant, depolarization exposure would better reflect short-term in vivo stimulation and might not inhibit growth on the long term. To test this hypothesis, I incubated DRG with KCl for shorter intervals compared to the total growth duration.

Exposure of DRG neurons for 1h to KCl, followed by growth in regular media for up to 48h induced a mild stimulation of growth (11%), compared to control media or DGRs incubated with NaCl as osmolarity control **(Fig.4.22.E-H)**. While the effect of 1h KCl was limited, it showed that there is no inhibition from short, biologically relevant depolarization periods, but can rather result in neurite growth stimulation.

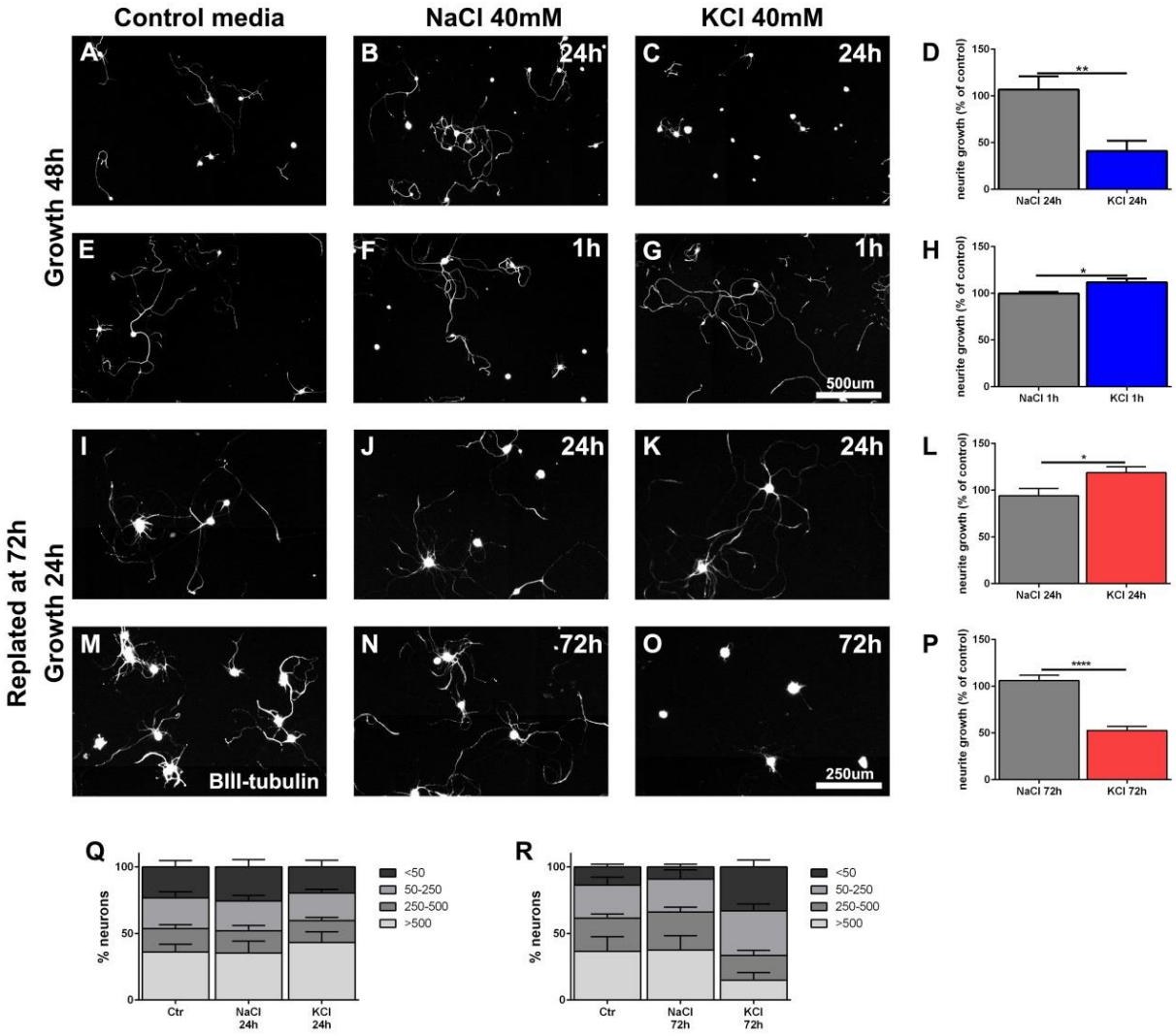

Fig.4.22. KCl depolarization can inhibit or enhance DRG neurite growth. Naïve DRGs were isolated and cultured on PDL/Laminin(0.5µg/µl) for either **(A-H)** 48h, or **(I-R)** were replated at 72h and regrown for 24h. KCl was added to the culture medium, at the beginning of incubation, for **(C)** 1h or **(G)** 24h, and **(K)** 24h and then was washed out and replaced with normal medium, or **(O)** DRGs were kept in media with KCl untill replating at 72h. As controls, some wells were incubated in **(A, E, I, M)** media only or **(B**, **F**, **J**, **N)** received NaCl (40mM) for osmolarity control for the same time as the KCl-treated DRGs. The longest ßIII-tubulin-labeled neurite was quantified. Average neurite length is expressed as % of control (176±80 neurons/well). **(A-D)** Growth is inhibited when DRGs are incubated in KCl for 24h (n=5-6 wells, 2 independent experiments). However, if **(E-H)** incubation is shorter (1h), total growth is enhanced (n=9-10 wells, from 3 independent experiments). **(I-L)** If DRGs are exposed to KCl for 24h then changed to normal media and replated at 72h in normal media, growth is enhanced (4 independent experiments). **(M-P)** If DRGs are exposed to KCl for 72h then replated in normal media, growth is inhibited (3 independent experiments). **(Q, R)** Neurons were classified by their longest neurite length (<50µm, 50-250µm, 250-500µm and >500µm) and expressed as % of the total number of neurons per condition. Bars represent means+SEM, One-way Anova, Sidak´s multiple comparison test, ∗p<0.05, ∗∗p<0.01, ∗∗∗p<0.001.

Furthermore, I tested if a 24h KCl exposure has long-term inhibitory consequences or only for the duration of the incubation with KCl. I incubated DRGs in KCl for 24h, changed them

to normal media and replated at 72h to reinitiate growth in normal media. After 24h of growth, the DRGs were fixed, stained and quantified. Under these experimental conditions, a mild growth stimulating effect of depolarization was observed (25%) compared to NaCl treated DRGs **(Fig.4.22.I-L)**.

However, if the depolarization is maintained for the full 72h before replating in standard media, I observed inhibition (53%) after replating **(Fig.4.22.M-P)**. This suggests that activity can have subsequent detrimental effects, if the duration exceeds a certain limit. None the less, limited periods of depolarization are certainly not long term inhibitory and could potentially positively influence growth in certain conditions.

To investigate the type of growth or inhibition observed after KCl exposure and replating, the neurons from all experiments were classified by their longest neurite length (<50µm, 50-250µm, 250-500µm and >500µm) and expressed as percentage of the total number of cells in each well **(Fig.4.22.Q, R).** The increase in neurite growth after 24h KCl **(Fig.4.22.L)** can be attributed to more DRG neurons with long neurites (>500µm) **(Fig.4.22.Q).** In case of the persistent inhibition induced by 72h KCl after replating in normal media **(Fig.4.22.P)**, an increase of DRGs with short or no neurites (<50µm) and a reduction of percentage of cells with long neurites (>500µm) was observed **(Fig.4.22.R)**, suggesting reduced initiation as well as reduced overall growth.

4.6.2. The inhibitory effects of depolarization on growth are present early after exposure, but disappear after a delay

The previous experiments show that 24h incubation with KCl can be either inhibitory during depolarization or mildly stimulating after a delayed replating, while 72h incubation appears to be inhibitory also after the re-initiation of growth. This raises the question whether the actual duration or the delay from KCl washout until the re-initiation of growth is the deciding factor. I therefore screened several conditions for depolarization duration, replating timeline and growth time. As seen in **Fig.4.23**, 24h exposure to KCl reduces relative neurite growth if the culture is replated directly, while 72h KCl does not have an inhibitory effect anymore replated at a delayed time point of 7 days.

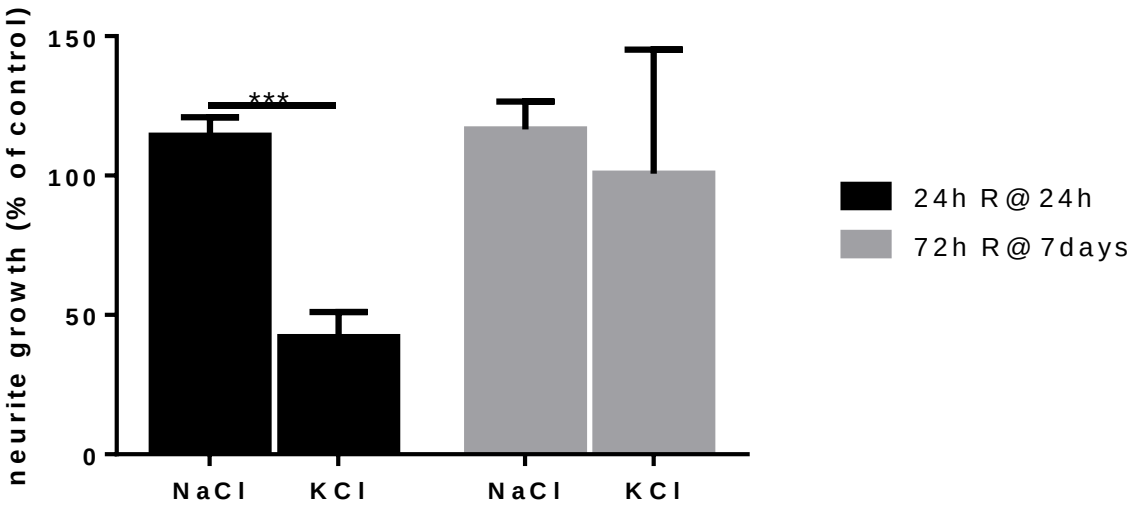

Fig.4.23. The delay to replating is the main factor that influences the effects of depolarization. Naïve DRGs were isolated and cultured on PDL/Laminin (0.5µg/µl) with KCl 40mM for either 24h or 72h, and the first were replated immediately at 24h, or at 7 days for a final growth time of 24h. Normal media or NaCl 40mM were used as control, for equal durations. The longest ßIII-tubulin-labeled neurite was quantified and average neurite length is expressed as % of control. 24h R@24h shows inhibition of growth (N=3, 108±24neurons/well, 1-way ANOVA) (compare to Fig.4.22.F), while 72h R@7days no longer shows inhibitory effects when replated at 7 days (N=3, 159±35neurons/well) (compare to Fig.4.22.P). Bars represent means+SEM. ***p<0.001.

4.7. Calcium signaling and neurite growth in DRGs cultures

Depolarization by KCl is known to induce calcium influx into neurons, including DRG neuron cultures **(Fig.4.24)**. Calcium influx upon peripheral injury is essential for the initiation of regenerative programs, via nuclear export of HDAC5 and PKCµ activation with nuclear translocation (Cho et al., 2013). Thus nuclear calcium signaling could be involved in the effects of depolarization and activity on neurite growth.

4.7.1. Blocking nuclear calcium signaling reduces neurite growth in DRGs culture

To determine whether Ca^{2+}/CaM signaling contributes to neurite growth in DRG neurons, I blocked nuclear calcium signaling via electroporation with a plasmid expressing CaMBP4 with a nuclear localization sequence (NLS). CaMBP4 is a peptide derived from skeletal muscle myosin light chain CaM-binding sequence, which eliminates the cellular function of CaM, by competing with endogenous target proteins (Wang et al., 1995). When restricted to the nucleus, it functionally neutralizes CaM mediated Ca^{2+}/CaM dependent signaling in the nucleus, including gene expression (Zhang et al., 2009).

To check the location of the expressed constructs, a HA-Tag antibody was used, confirming the cellular localization to the nucleus in about 90% of the positive cells, with remaining cells showing both nuclear and cytoplasmic labeling **(Fig.4.25).**

Freshly isolated DRG neurons were electroporated with plasmids expressing either CaMBP4 (pAAV_CMV_eGFP-T2A-CaMBP4-NLS-HA) or MutCaMBP4 (inactive) (pAAV_CMV_eGFP-T2A-mutCaMBP4(S2)-NLS_HA) and GFP, and grown in vitro for 48h or 72h, on PDL/Laminin (0.5µg/µl). Quantification of the longest ßIII-tubulin-labeled neurite of GFP+ neurons showed a progressive reduction in neurite length compared to the mutant construct (21% for 48h; 50% for 72h) **(Fig.4.26).**

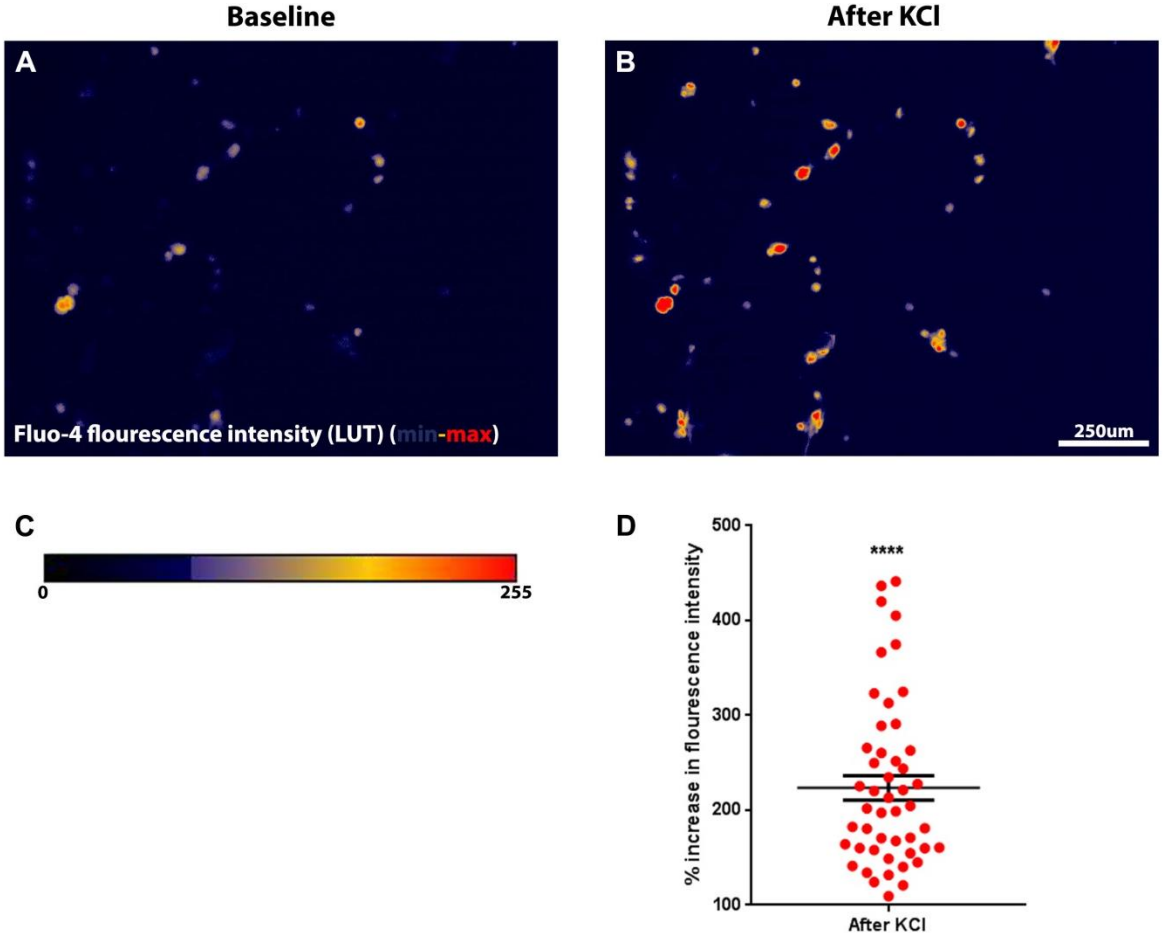

Fig.4.24. KCl induces calcium influx in DRG culture. (**A, B)** Naïve DRGs were isolated and cultured on PDL/Laminin (0.5µg/µl) for 72h. Plates were loaded with Fluo-4 calcium indicator, and time lapse images were recorded, starting before and continuing after the addition of KCl (50mM). **(A, B, C)** For visualization purposes intensity of the fluorescence (black and white 0-255) **(A)** before and **(B)** after KCl in is depicted using a **(C)** color scale (Lookup Table (LUT)). **(D)** For each imaged cell, the increase in fluorescence relative (%) to the initial values was quantified in ImageJ, in order to normalize for dye intake and baseline fluorescence. Typical response is relative increase in Fluo-4 fluorescence, indicating calcium entry into the cells. n=49 neurons from 4 independent wells, 2 experiments, paired t-test, ****p<0.0001.

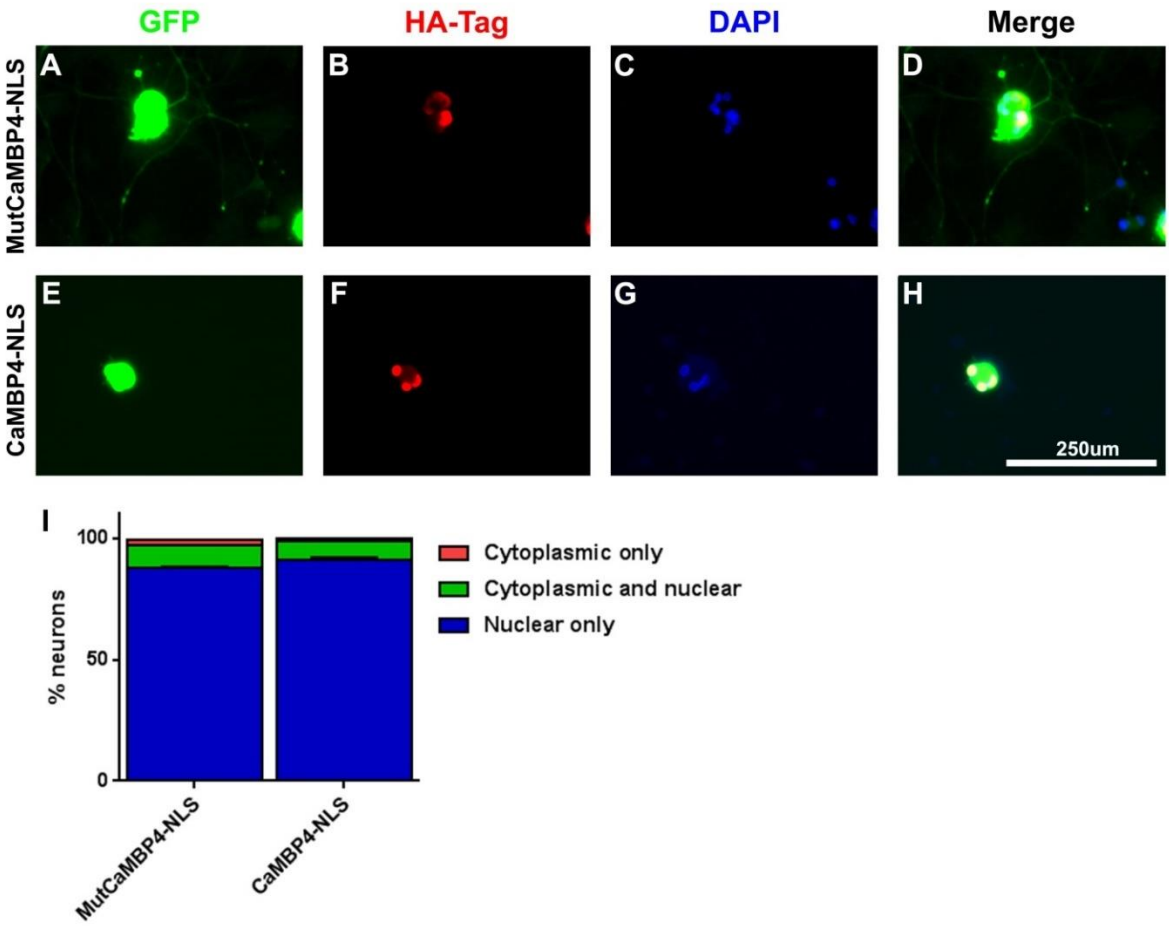

Fig.4.25. Localization of CMV_Mut/CaMBP4-NLS. Naïve DRGs were isolated and electroporated with plasmids expressing GFP and either **(A-D)** MutCaMBP4 or **(E-H**) CaMBP4-NLS with a HA-Tag. The DRGs were cultured on PDL/Laminin (0.5µg/µl) for 72h. Plates were labeled for **(A, E)** GFP, **(B, F)** HA-Tag and **(C, G)** stained with DAPI and imaged. **(D, H)** Triple fluorescence shows the cellular localization. **(I)** Positive neurons were classified as nuclear, nuclear and cytoplasmic, cytoplasmic only showing predominant nuclear localization and no significant difference between MutCaMBP4 and CaMBP4-NLS location. n=4. Bars represent mean±SEM. Two-way Anova.

In order to emphasize effects on neurite initiation, I used the culture-and-replate protocol as described by (Saijilafu et al., 2013), because growth is initiated anew, and the 2 axotomies (isolation and replating) recapitulate the peripheral axotomy-induced upregulation of several proteins involved in growth. In addition, gene expression of electroporated plasmids is up before neurite growth is newly initiated. Indeed, CaMBP4 reduced the growth of DRGs neurons after replating compared to the inactive construct **(Fig.4.26.F.)** by 46±7% and 32± 2% after 24h and 40h growth after replating, respectively.

To determine if the overall reduction observed is due to reduced growth or less neurite initiation, neurons were classified by the length of their longest neurite (<50µm, 50-250µm,

250-500µm and >500µm). CaMBP4 expressing neurons showed an increase in the percentage of cells with no or very short neurites (<50µm) and a reduction in the percentage of neurons with neurites longer than >500µm **(Fig.4.26.G, I).** There appear to be more neurons with long neurites (>500µm) at 40h growth suggesting the growth is only delayed compared to the control, while the changes between 24h and 40h growth in the percentage of neurons with no or very short neurites (<50µm) seem to be minimal **(Fig.4.26.C, E).** This pattern indicates that most likely, there is a delayed overall growth, but it also suggests impaired initiation at least in a subpopulation of DRG neurons.

Because the group (<50µm) contains both neurons with no or very short neurites, I further analyzed specifically the percentage of cells with no neurites (<15µm) **(Fig.4.26.I)**. This cutoff was based on the smallest DRGs cell body size. The percentage of CaMBP4+ neurons without neurites, remained constant between 24h and 40h growth post-replating, compared to mutCaMBP4, in which more than 50% of them acquire neurites in that time period **(Fig.4.26.I).** This further supports the idea that at least in some cells, neurite initiation after replating is completely inhibited by CaMBP4. This effect is not necessarily cell population specific, but may result from stronger or earlier expression of CaMBP4.

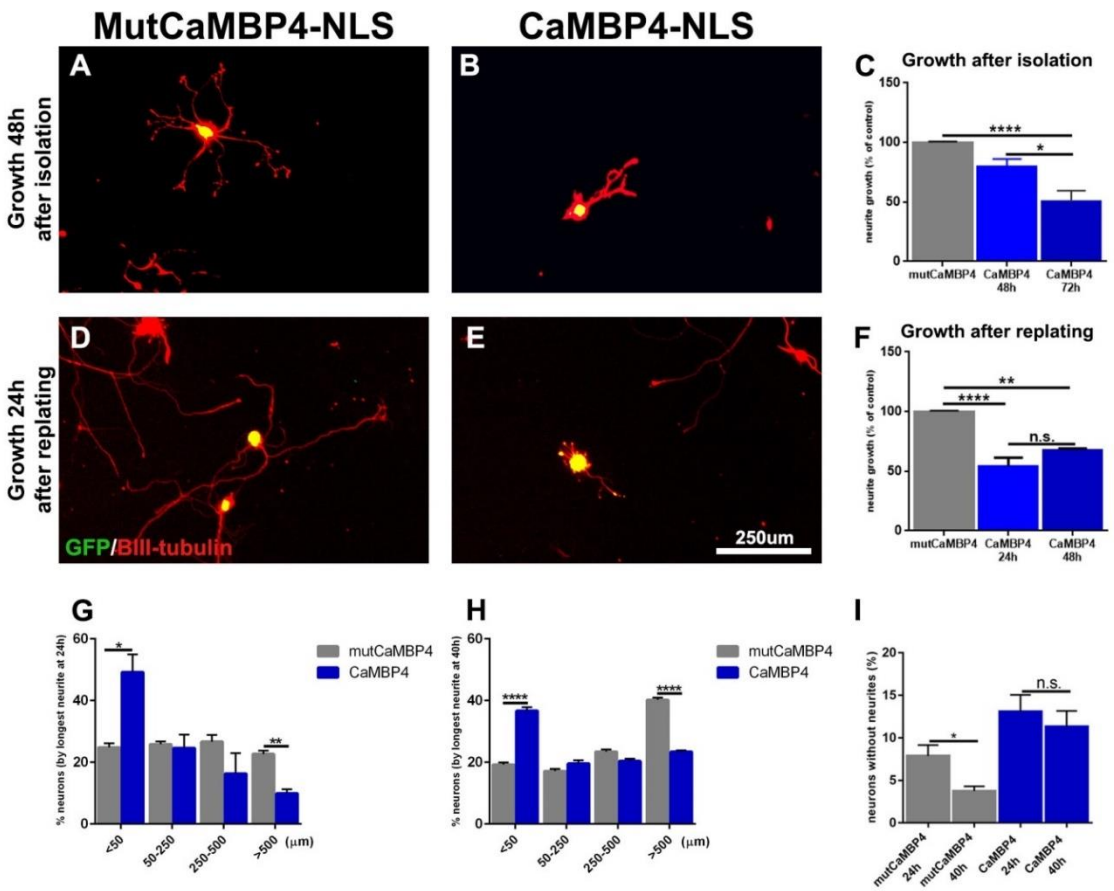

Fig.4.26. Blocking nuclear calcium signaling reduces neurite growth in culture. Naïve DRGs were isolated and electroporated with plasmids expressing either CaMBP4-NLS or MutCaMBP4-NLS (inactive control) and GFP under a CMV promoter. DRGs were cultured on PDL/Laminin (0.5µg/µl) for either **(A, B)** 48h or 72h, or replated at 72h and regrown for **(D, E)** 24h or 40h. **(C, F)** The longest neurite for double-labeled GFP-ßIII-tubulin neurons was quantified (80-250 neurons/well). Each experiment and time point had its independent controls for normalization and statistical analysis. MutCaMBP4 is depicted as one bar in **(C)** and **(F)** for visualization purposes only. **(C)** Average neurite length expressed as % of control (mutCaMBP4) shows reduction of growth (n=5-6 wells from 4 experiments, 2 independent experiments for each time point). **(F)** Average longest neurite is reduced after replating at 72h (n=3, 2 independent experiments). **(G, H)** Neurons were classified by their longest neurite length (<50µm, 50-250µm, 250-500µm and >500µm) at **(G)** 24h or **(H)** 40h after replating and expressed as % of the total number of neurons per condition (n=3, one-way Anova, Sidak's multiple comparisons test). **(I)** Neurons without neurites (<15µm) show reduction from 24h to 48h in MutCaMBP4, but not in CaMBP4 neurons (n=3, multiple ttest, FDR<0.05). Bars represent mean+SEM, $*p<0.05$, $**p<0.01$ $***p<0.001$ $****p<0.0001$.

4.7.2. Blocking cytoplasmic calcium signaling enhances neurite growth in DRGs culture after replating

Because cytoplasmic calcium signaling may have different effects, we also expressed CaMBP4 without the NLS sequence. For this we used a hSyn promoter construct, which has been shown to have a more than 96% specificity for neuronal expression in many brain tissues (Hioki et al. 2007). This minimizes possible influences from expression in glia, which could have an impact on the results. I also tested the cellular localization of this construct with an HA-Tag antibody and classified cells according to the location. As seen in **Fig.4.27,** the localization was mostly cytoplasmic and different from a MutCaMBP4 construct with an NLS sequence. While CaMBP4 was not entirely cytoplasmic, this is likely due to the weak signal from the HA tag and low expression levels, making the cytoplasmic localization difficult to differentiate from GFP (green channel) bleed through, possibly creating a negative bias.

In contrast to a nuclear calcium block, when expressing CaMBP4 in the cytoplasm, I did not see a reduction of neurite growth 48h or 72h after isolation **(Fig.4.28.C)**. To exclude that the expression level given by the Syn promoter is insufficient to block calcium signaling at early time points after the initial plating, I also tested the growth capacity at a later time point by replating neurons 72h after electroporation allowing neurite growth for an additional 48h. Surprisingly, when DRG neurons were replated, cytoplasmic CaMBP4 expression even enhanced growth compared to control neurons, by 35±11% **(Fig.4.28.F)**. Thus, the lack effect in the first set of experiments, was not due to lower level of

expression, but an actually differential contribution of calcium signaling to neurite growth in the cytoplasm compared to the nucleus.

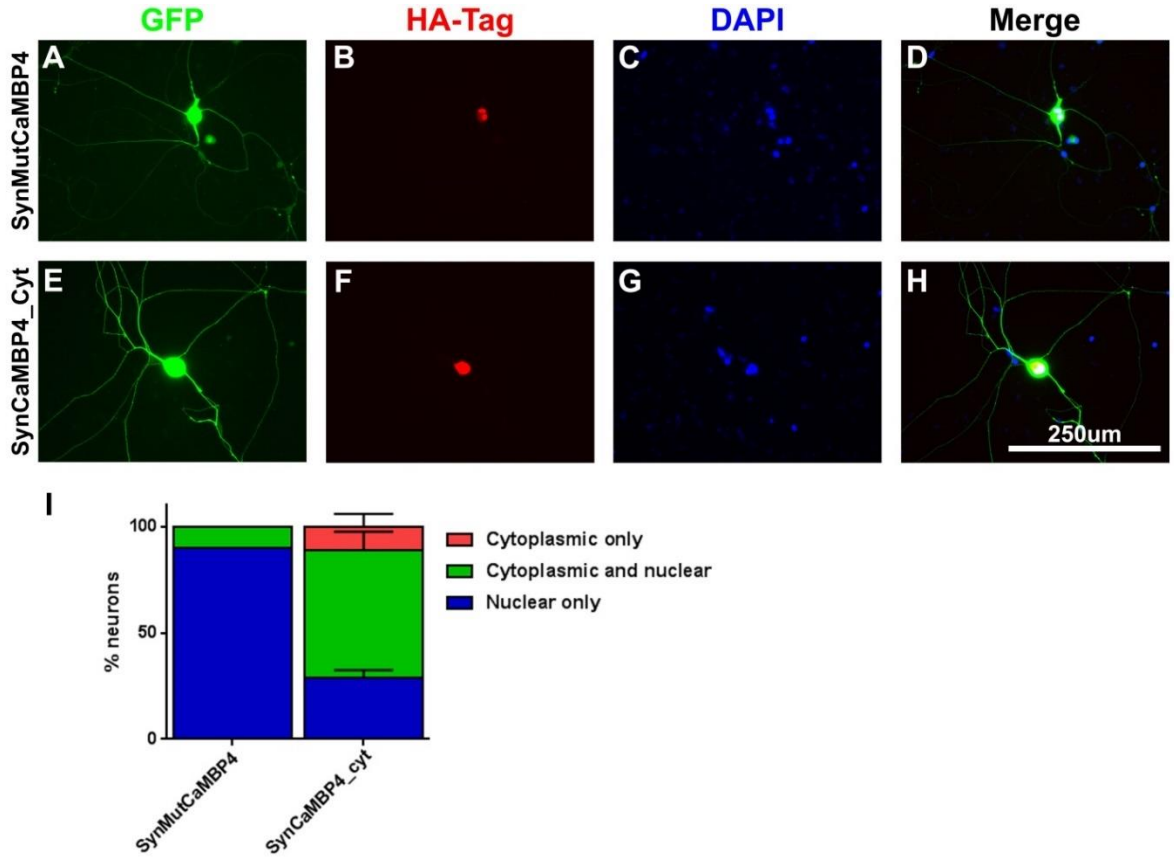

Fig.4.27. Localization of Syn_MutCaMBP4 and Syn_MutCaMBP4_cyt. Naïve DRGs were isolated and electroporated with plasmids expressing GFP and either **(A-D)** MutCaMBP4 or **(E-H**) CaMBP4-NLS with a HA-Tag. The DRGs were cultured on PDL/Laminin (0.5µg/µl) for 72h. Plates were stained for **(A, E)** GFP, **(B, F)** HA-Tag and **(C, G)** DAPI and were imaged at 20x. **(D, H)** Merged fluorescence images demonstrate the cellular localization. **(I)** Positive neurons were classified as nuclear, nuclear and cytoplasmic, or cytoplasmic only and expressed as percentage of all neurons showing predominant cytoplasmic location in the construct missing the NLS sequence. N=3. Bars represent mean±SEM.

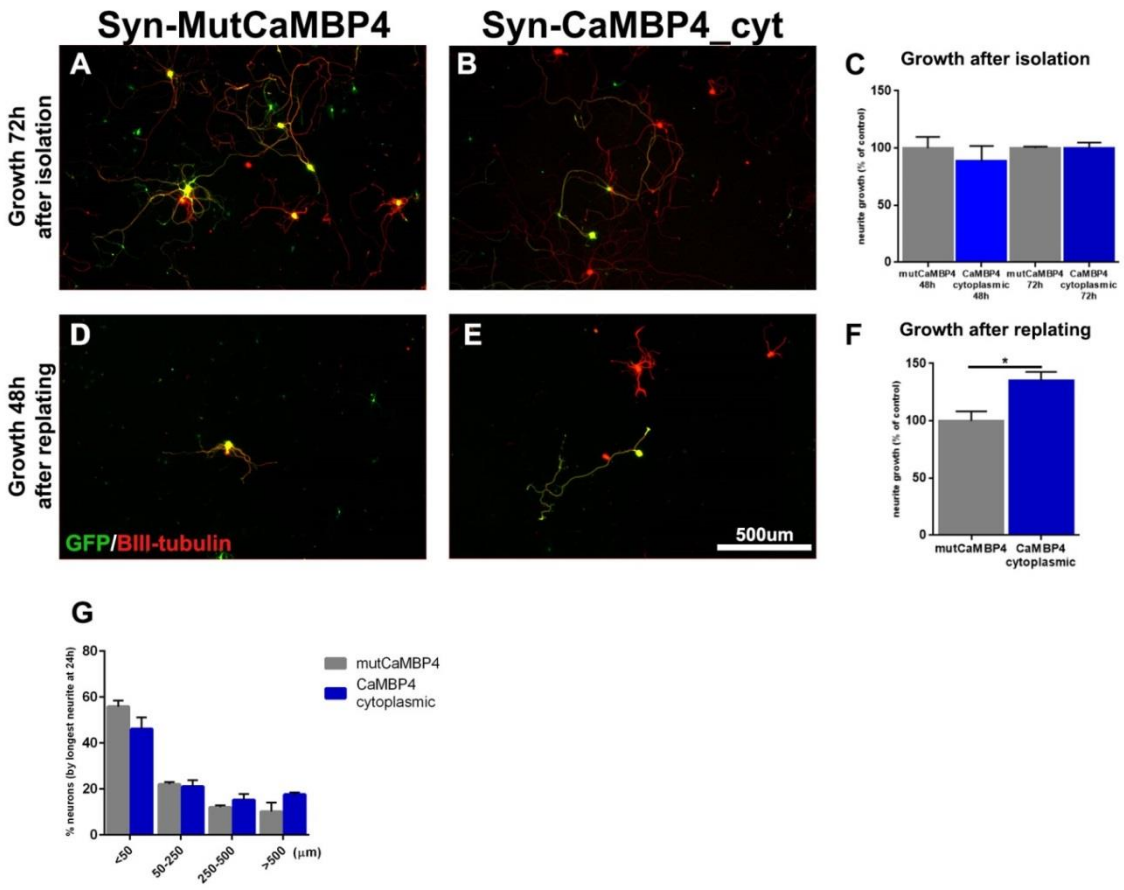

Fig.4.28. Blocking cytoplasmic Ca^{2+}/CaM signaling can stimulate neurite growth in DRG culture. Naïve DRGs were isolated and electroporated with plasmids expressing either CaMBP4 (cytoplasmic) or mutCaMBP4 and GFP under a Syn promoter. The DRGs were cultured on PDL/Laminin(0.5µg/µl) for either **(A)** 48h or 72h, or **(B)** were replated at 72h and regrown for 48h. **(C, F)** Plates were labeled for ßIII-tubulin and GFP, the longest neurite of each double-labeled neuron was quantified, and the average neurite length expressed as % of control (Syn-mutCaMBP4). **(C)** Average neurite length after isolation does not change when CaMBP4 is cytoplasmic (n=2-3 wells, independent experiments for each time point), however **(F)** it is enhanced after replating at 72h (n=6 wells, from 2 independent experiments). **(G)** Neurons were classified by their longest neurite length (<50µm, 50-250µm, 250-500µm and >500µm) and expressed as % of the total number of neurons per condition (n=3 wells). Bars represent mean+ SEM, ∗p<0.05.

Taken together, blocking nuclear calcium signaling inhibits growth, while cytoplasmic block can enhance growth after replating of DRGs. Thus, activity could stimulate growth in primary sensory neurons through nuclear calcium signaling-induced gene expression, while in the same time activity could have direct inhibitory effects at the level of the axon or growth cone, also via Ca^{2+}/CaM dependent processes.

4.8. Depolarization induces HDAC5 export in DRGs culture

In hippocampal neurons, export of HDAC5 and other class IIa HDACs is induced by activity and nuclear calcium signaling dependent (Schlumm et al., 2013). In order to determine whether the calcium influx induced by KCl is functionally relevant and that it indeed induces effective nuclear calcium signaling, I analyzed the cellular localization of HDAC5 after KCl exposure. Freshly isolated DRG neurons were electroporated with a HDAC5-FLAG construct and gene expression was allowed to ramp up for 72h. DRGs were then incubated for an additional hour with KCl (40mM), media alone or with NaCl for osmolarity control and then fixed. As seen in **Fig.4.29**, in basal conditions HDAC5 is predominantly nuclear (mean±SD = 92±5 %) and NaCl has no effects on the cellular distribution (89±5%), while KCl causes a significant HDAC5 export from the nucleus (14±1%) to the cytoplasm (57±3%).

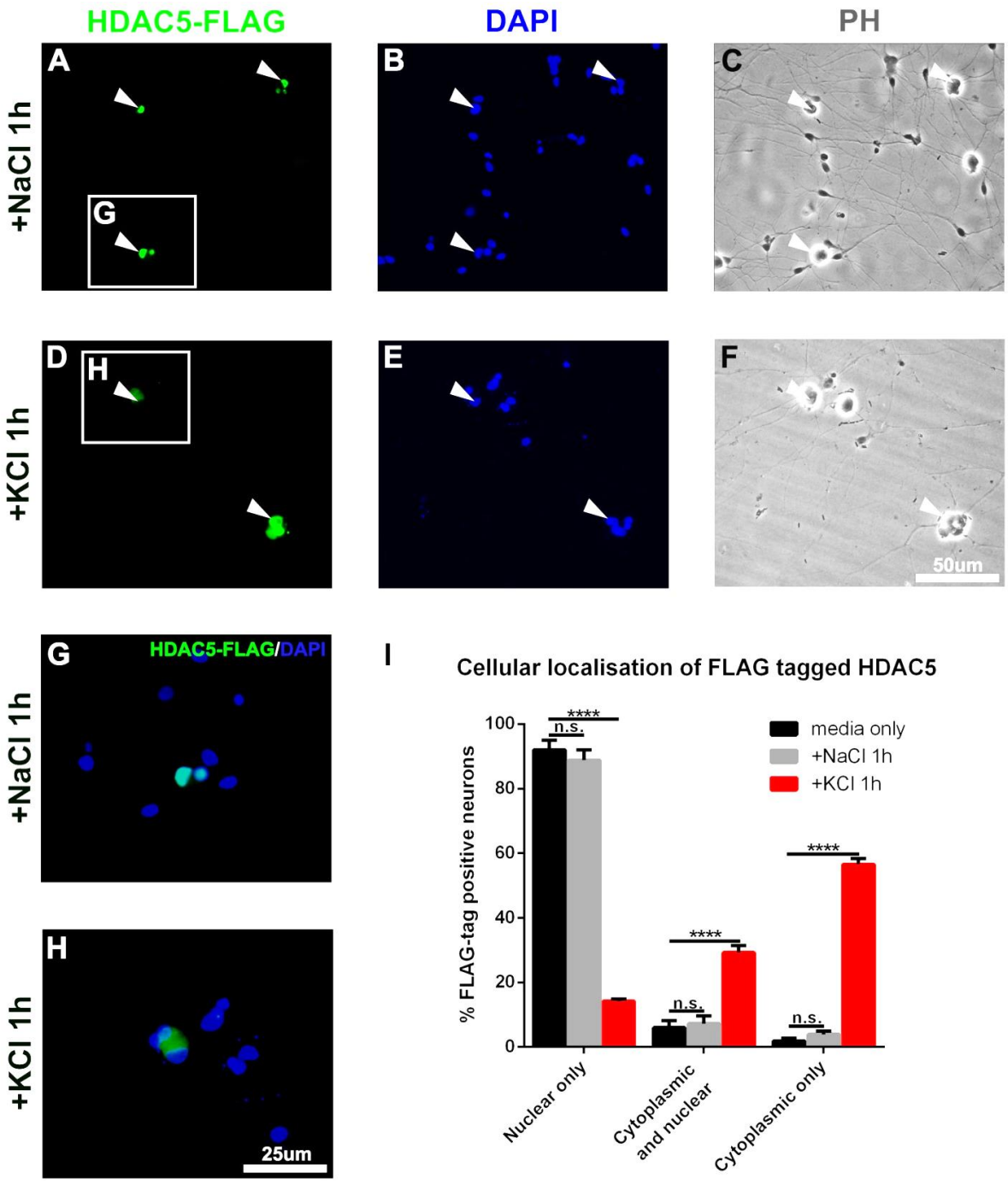
HDAC5-FLAG
DAPI
PH
+NaCl 1h
+KCl 1h
A
B
C
D
E
F
G
H
50um
HDAC5-FLAG/DAPI
25um
I
Cellular localisation of FLAG tagged HDAC5
% FLAG-tag positive neurons
media only
+NaCl 1h
+KCl 1h
n.s.
****
Nuclear only
Cytoplasmic and nuclear
Cytoplasmic only

Fig.4.29. Depolarization by KCl in vitro induces HDAC5 export from the nucleus. Naïve DRGs were electroporated with an HDAC5-FLAG expression construct. DRGs were cultured on PDL/Laminin (0.5µg/µl) for 72h and exposed to **(A, B, C, G)** NaCl (40mM) for 1h as control for osmolarity, or **(D, E, F, H)** KCl (40mM) for 1h. Additional control wells were incubated in media only. Plates were labeled for FLAG-Tag and DAPI, and **(I)** neurons were classified by the cellular localization of HDAC5-FLAG (nuclear only, nuclear and cytoplasmic or cytoplasmic only) and expressed as % of the total number of neurons per condition. **(D, E, H)** HDAC5-FLAG construct is mainly cytoplasmic after KCl, compared to **(A, B, G)** NaCl incubation (n=3 independent experiments). Bars represent mean+SEM, One-way ANOVA, Tukey's multi comparisons test, ∗∗∗∗p<0.0001.

To test if the CaMBP4 efficiently blocks the HDAC5 export induced by KCl in DRGs, I performed experiments using double electroporation of the CaMBP4 expressing plasmids and the HDAC5-FLAG plasmid, then the DRGs were grown for 72h on PDL/Laminin (0.5µg/µl). Subsequently, wells received KCl for 1h, while control wells remained in normal media for baseline assessment and the plates were fixed immediately thereafter. The DRGs were labeled for GFP, and FLAG and DAPI and based on the location of FLAG signal, neurons were classified by the cellular localization of HDAC5-FLAG (nuclear only, nuclear and cytoplasmic, cytoplasmic only) and expressed as % of the total number of neurons per condition. The experiment was repeated 3 times, however due to low rates of co-transfection, 2 could not be properly assessed, but showed a similar trend. The results suggest that HDAC5-FLAG is not exported to the cytoplasm after KCL when CaMBP4 is expressed in the nucleus **(Fig.4.30)**.

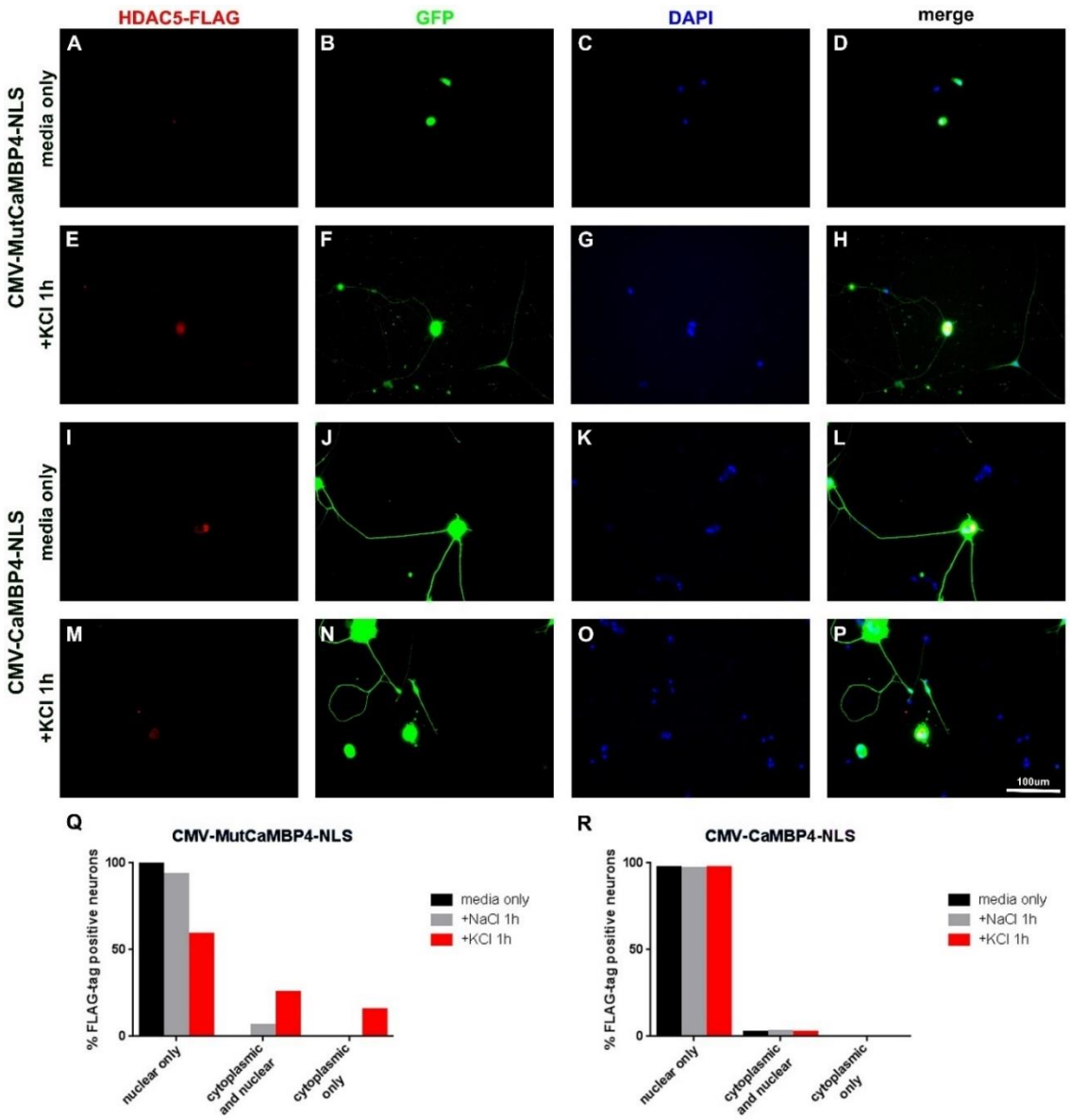

Fig.4.30. Localization of HDAC5-Flag in CMV-MutCaMBP4/CaMBP4-NLS expressing DRGs after depolarization with KCl for 1h. (A-P) Naïve DRGs were isolated and electroporated with HDAC5-FLAG plasmid and either **(A-H)** CMV-MutCaMBP4 or **(I-P)** CMV-CaMBP4-NLS. The DRGs were cultured on PDL/Laminin (0.5µg/µl) for 72h. After 72h wells received either **(E-H, M-P)** KCl 40mM or NaCl, for osmolarity control, or **(A-D, I-L)** fresh normal media as baseline control, and after 1h were fixed. Plates were stained for GFP, FLAG and DAPI and were imaged in triple fluorescence in order to see the cellular localization. **(Q, R)** Double positive FLAG-GFP neurons were classified as nuclear only, cytoplasmic and nuclear, and cytoplasmic only and expressed as % of total. n=1.

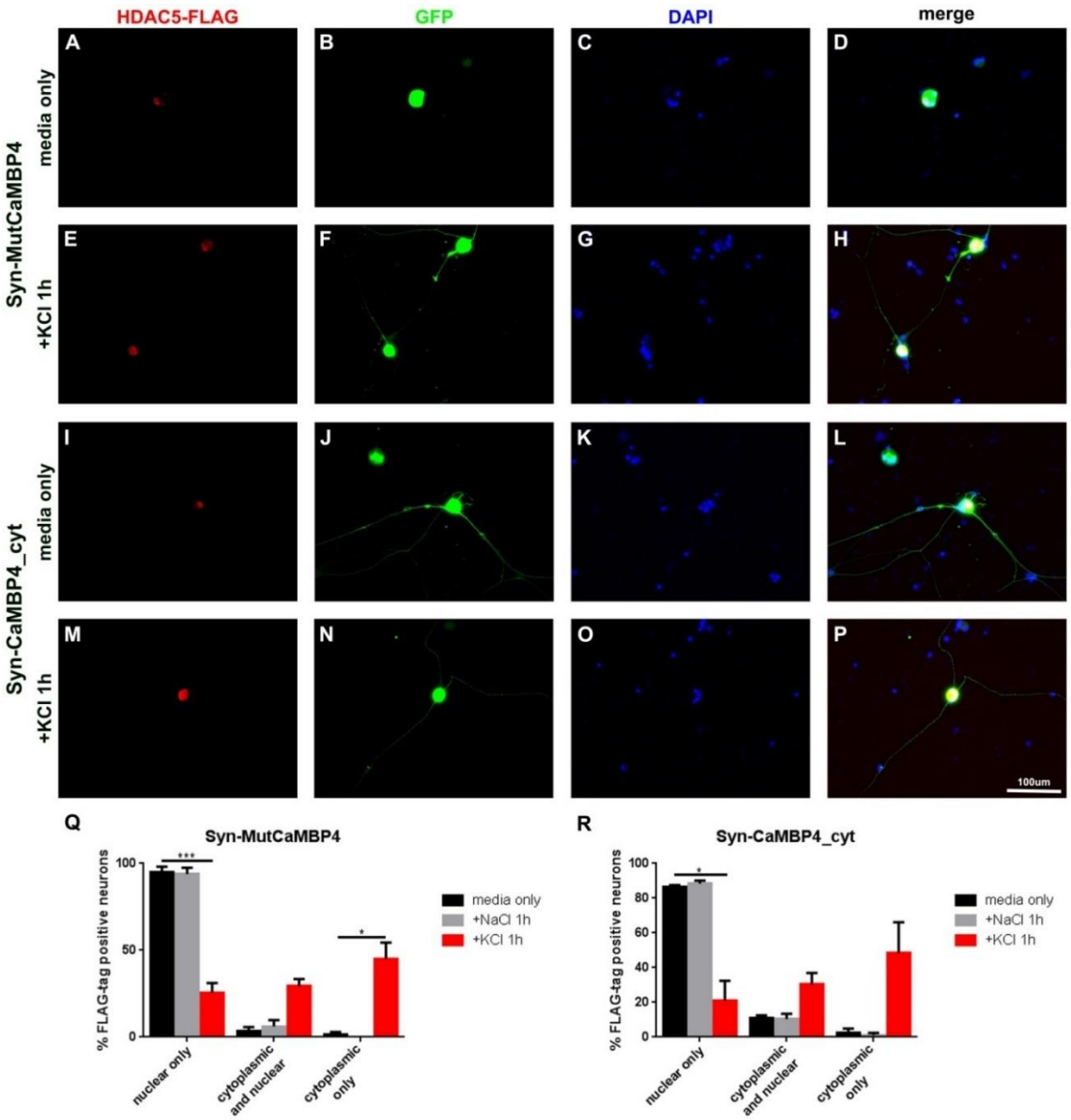

Fig.4.31. Localization of HDAC5-Flag in Syn-MutCaMBP4/CaMBP4_cyt expressing DRGs after depolarization with KCl for 1h. (A-P) Naïve DRGs were isolated and electroporated with HDAC5-FLAG plasmid and either **(A-H)** Syn-MutCaMBP4 or **(I-P)** Syn-CaMBP4_cyt. The DRGs were cultured on PDL/Laminin (0.5µg/µl) for 72h. After 72h wells received either **(E-H, M-P)** KCl 40mM or NaCl, for osmolarity control, or **(A-D, I-L)** fresh normal media as baseline control, and after 1h were fixed. Plates were stained for GFP, FLAG and DAPI and were imaged in triple fluorescence in order to see the cellular localization. **(Q, R)** Double positive FLAG-GFP neurons were classified as nuclear only, cytoplasmic and nuclear, and cytoplasmic only and expressed as % of total. N=3. Bars represent mean+SEM, 2-way ANOVA, Sidak's multi comparisons test, ∗p<0.05, ∗∗p<0.01, ∗∗∗p<0.001.

Similarly, because HDAC5 has also cytoplasmic roles in growth and there are several mechanisms that contribute to the re-localization in the nucleus after export, we wanted to

see if the cytoplasmic calcium block with Syn-CaMBP4 could influence HDAC5 cellular localization.

To test this, I electroporated DRGs both with HDAC5-FLAG and Syn-CaMBP4 or Mut-CaMBP4, and grew the DRGs in culture for 72h. The results suggest that HDAC5-FLAG is exported to the cytoplasm stronger after KCL when Syn-CaMBP4_cyt is expressed **(Fig.4.31)**. There also appears to be slightly more cytoplasmic HDAC5-FLAG in Syn-CaMBP4 positive neurons, already in baseline conditions **(Fig.4.31)**.

4.9. AAV blocking of cytoplasmic Ca^{2+}/CaM signaling in vivo

4.9.1. Neurite growth ex-vivo after blocking of cytoplasmic Ca2+/CaM signaling in vivo

As cytoplasmic calcium signaling blockage enhanced growth in DRGs culture after replating, we also wanted to test if it enhances growth in vivo after a CL.

To approach this question, we injected AAV1/2 expressing cytoplasmic CaMBP4 under the control of a Syn promoter into the L4 and L5 DRGs, in order to block the calcium signaling. As control, we used a virus producing MutCaMBP4. After injection of virus expressing either Syn-CaMBP4 or Syn-MutCaMBP4 and GFP, animals were allowed to recover for 4 weeks, to minimize the potential impact of the surgery and to allow for sufficient gene expression. After 4 weeks, some animals underwent CL and 7 days later the DRGs were isolated and cultivated in vitro for 24h. Due to limited amount of virus and animals, we could not perform all possible combinations, and instead focused on comparing neurite growth after CL in Syn-CaMBP4 injected animals (n=8) with Syn-MutCaMBP4 animals (n=10).

Infected neurons showed GFP labeling throughout the cell soma and neurites, making them easy to identify. Non-transfected neurons were intended to be used as internal control. However, this was not possible, due to very high infection rate of up to 100%, making the growth of non-infected neurons impossible to assess. One animal did not receive CL to see if there are hints of baseline modifications on growth from the DRGs injection alone (n=2) or from other factors. A limited number of additional controls (naïve (n=4) and naïve with CL (n=2)) were included as a reference but insufficient for statistical analysis. Instead we focused on comparing our main experimental groups: Syn-CaMBP4 and Syn-MutCaMBP4 animals.

We observed extensive growth both for longest neurite and for the total neurite length **(Fig.4.32.E, F)**, with a tendency towards more growth in Syn-CaMBP4 injected animals without CL compared to naïve animals, and in Syn-CaMBP4 injected animals with CL compared to Syn-MutCaMBP4, suggesting stimulation of growth, a trend consistent with the in vitro data. Comparing Syn-MutCaMBP4+CL with Syn-CaMBP4+CL, the tendency for increased growth was not statistically significant (t-test; $p>0.05$).

Though inconclusive, the data shows a similar trend as my in vitro electroporation data with a similar construct, suggesting that with an increased number of samples and/or reduced experimental variability, an effect would be detectable.

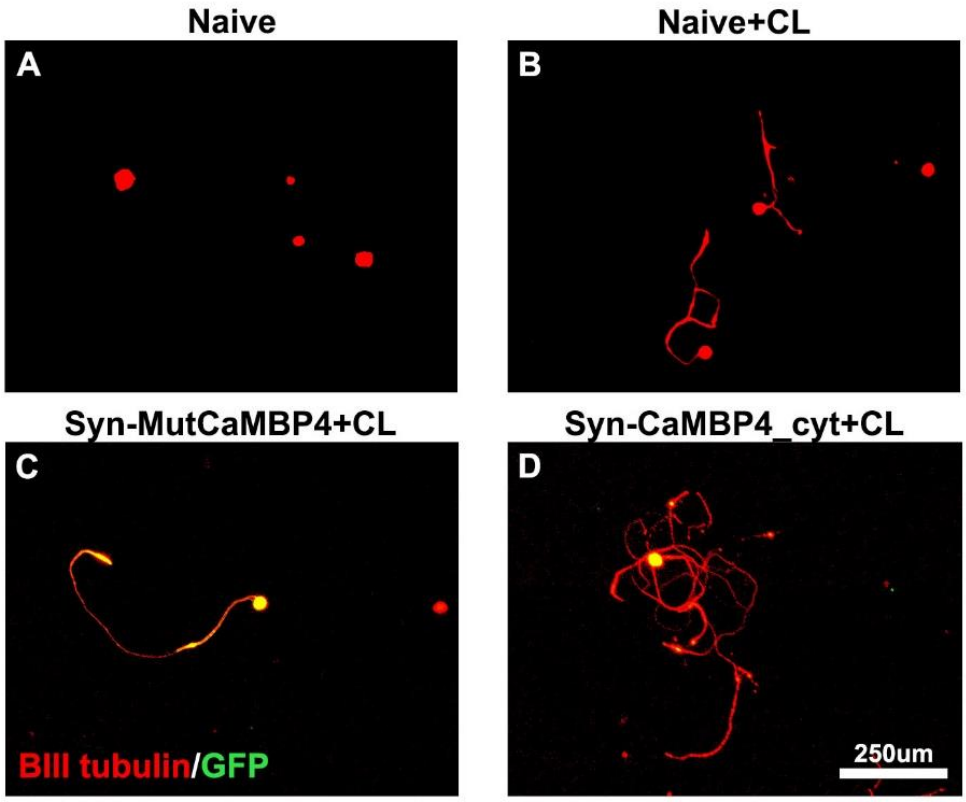
Naive
A
Naive+CL
B
Syn-MutCaMBP4+CL
C
Syn-CaMBP4_cyt+CL
D
BIII tubulin/GFP
250um

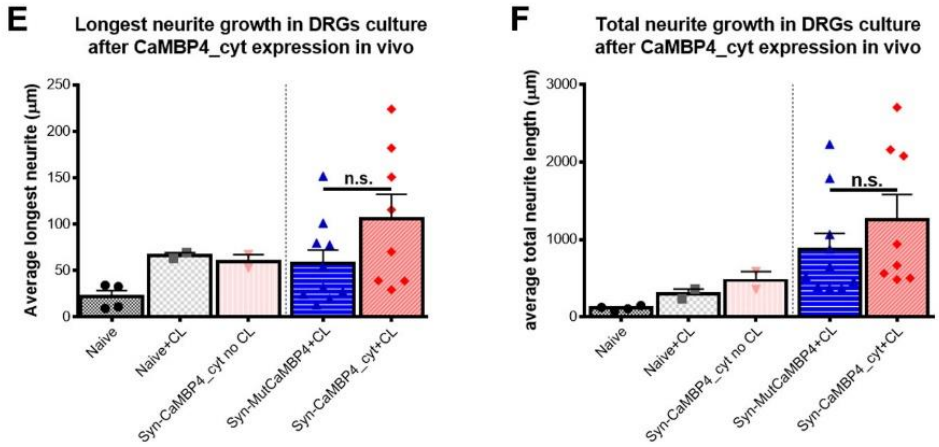
E
Longest neurite growth in DRGs culture after CaMBP4_cyt expression in vivo
Average longest neurite (µm)
250
200
150
100
50
0
n.s.
Naive
Naive+CL
Syn-CaMBP4_cyt no CL
Syn-MutCaMBP4+CL
Syn-CaMBP4_cyt+CL
F
Total neurite growth in DRGs culture after CaMBP4_cyt expression in vivo
average total neurite length (µm)
3000
2000
1000
0
n.s.
Naive
Naive+CL
Syn-CaMBP4_cyt no CL
Syn-MutCaMBP4+CL
Syn-CaMBP4_cyt+CL

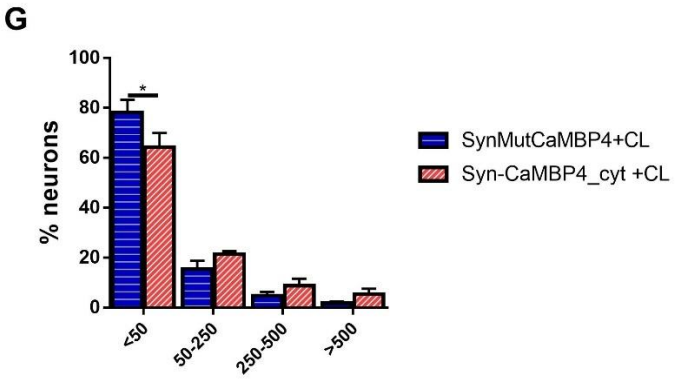
G
% neurons
100
80
60
40
20
0
*
<50
50-250
250-500
>500
SynMutCaMBP4+CL
Syn-CaMBP4_cyt +CL

Fig.4.32. Neurite growth after in vivo expression of an inhibitor of Ca^{2+}/CaM-dependent processes, CaMBP4, in the cytoplasm, followed by a conditioning lesion. L4 and L5 DRGs were injected with AAV1/2 expressing Syn-CaMBP4_cyt and GFP or as control, AAV1/2 expressing inactive Syn-mutCaMBP4 and GFP. After 28 days, animals received conditioning lesions (CL) and after an additional 7 days, DRGs were isolated and plated in vitro on PDL/Laminin (5µg/µl) for 24h. (A-D) Representative neurite growth aspect for **(A)** naïve, **(B)** naïve+CL, **(C)** Syn-CaMBP4_cyt+CL and **(D)** Syn-MutCaMBP4+CL. Each side of an animal received the same treatment, both virus and CL and were handled as separate samples. **(E)** Average longest neurite length and **(F)** average total neurite length after 24h growth of DRG cultures following expression of Syn-CaMBP4_cyt (n=8) or inactive control (n=10) and CL. A trend towards enhanced growth after Syn-CaMBP4_cyt expression is observed. As additional controls for growth, a limited number of naïve (n=4), naïve+CL (n=2) and Syn-CaMBP4_cyt with no CL (n=2), were plated and the growth is depicted only for visualization purposes. **(E, F)** t-test=n.s., p>0.05. Statistical power for the Syn-MutCaMBP4+CL, Syn-CaMBP4_cyt+CL comparison in **(E)** was post-hoc calculated with G-power. Power: (1-β error prob) =0.4794. **(G)** Neuronal distribution by longest neurite length (<50µm, 50-250µm, 250-500µm and >500µm) shows a small reduction of number of cells with short or no neurites in Syn-CaMBP4_cyt. Two-way Anova, Sidak's multiple comparisons test, *p<0.05. (E) was assessed by I.G. and (F) by an independent blinded observer.

4.9.2. Peripheral regeneration

During isolation of the DRGs in the experiments described above, the sciatic nerves were also dissected and post-fixed for 24h in 4%PFA, allowing us to look into the in vivo growth after the peripheral nerve lesion. Infected neurons express GFP throughout the cell body, including in the sciatic nerve making them easy to identify (See Methods. **Fig.3.4**). The sciatic nerves were cut 1 cm distal from the CL, in transversal 16µm sections and directly mounted and labeled for GFP, ßIII-tubulin and DAPI. The distance from the lesion was chosen based on reported regeneration rates in peripheral nerves of 1-3mm/day following an initial delay of 2-3 days, such that 1 cm distally from the crush would likely contain some regenerating sensory axons 7 days after the injury without reaching a plateau (Fugleholm et al., 1994, Holmquist et al., 1993, Oblinger and Lasek, 1984). Indeed, in animals that received a conditioning lesion we observe less fibers overall than in an intact animal, as well as an irregularly shaped nerve. For quantification, we counted GFP+ axon profiles per area in transversal sciatic nerve sections, expressing the values relative to the section area in mm^2. We observed a considerable regeneration of both Syn-MutCaMBP4 and Syn-CaMBP4 animals at 7 days after CL, indicating that Syn-CaMBP4 does not influence peripheral regeneration in this experimental design **(Fig.4.33)**.

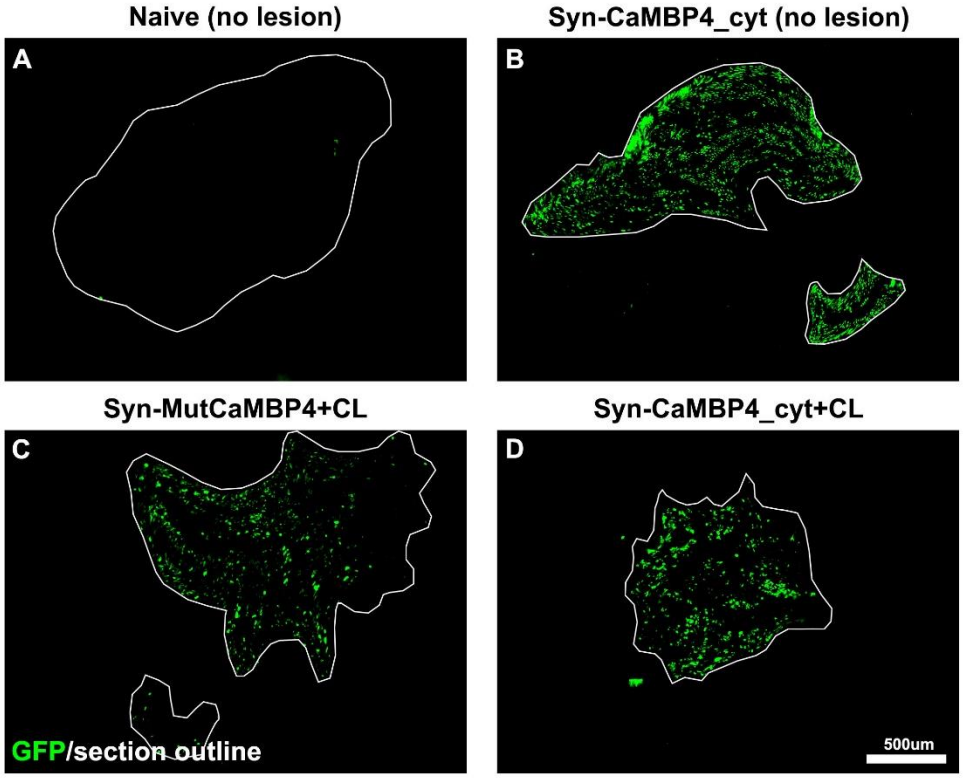
Naive (no lesion)
Syn-CaMBP4_cyt (no lesion)
A
B
Syn-MutCaMBP4+CL
Syn-CaMBP4_cyt+CL
C
D
GFP/section outline
500um

E

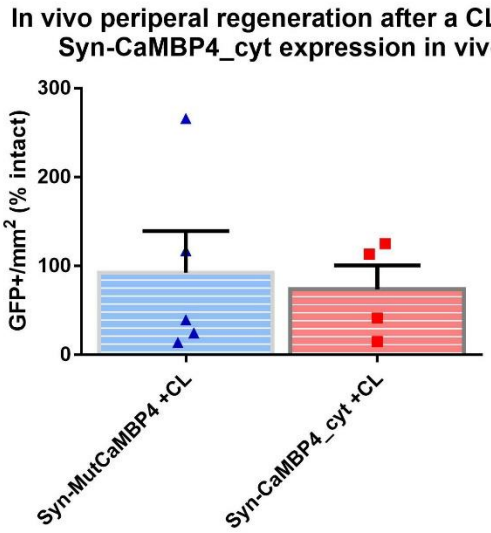
In vivo peripheral regeneration after a CL and Syn-CaMBP4_cyt expression in vivo
GFP+/mm2 (% intact)
300
200
100
0
Syn-MutCaMBP4 +CL
Syn-CaMBP4_cyt +CL

Fig.4.33. Sciatic nerve regeneration in vivo after in vivo expression of Syn-CaMBP4_cyt. L4 and L5 DRGs were injected with AAV1/2 expressing Syn-CaMBP4_cyt and GFP or as control inactive Syn-mutCaMBP4 and GFP. After 28 days, animals received CL and after an additional 7 days, animals were dissected and the sciatic nerves were post-fixed in 4%PFA. One sciatic per animal was sectioned 1 cm distal from the CL in 16µm thick sections and slides were labeled for ßIII-tubulin, GFP and DAPI. **(A, B, C, D)** The outline of the nerves was traced based on the ßIII-tubulin labeling to determine the nerve area (depicted in white) and GFP+ axonal profiles were counted on the sections. **(A)** Outlines of an intact nerve from an animal without virus injection. **(B)** Outline of an intact animal that received AAV1/2 expressing Syn-CaMBP4_cyt. Representative sciatic from **(C)** Syn-mutCaMBP4 and **(D)** Syn-CaMBP4_cyt animals after CL. The outlines are irregular due to post lesion nerve degeneration and regeneration, but both show GFP+ profiles from regenerating fibers. n=4-5. Bars represent means+SEM, t-test. **(E)** was assessed by an independent blinded observer.

4.10. Differential gene expression after ES

4.10.1. RNA Sequencing and differential gene expression

Animals received bilaterally either ES (20Hz, 2*MT, 0.2ms, 1h), sham cuffs, CL or just opening of the skin (naïve) and L4-L6 DRGs, were harvested and pooled for each animal at 1 day and 7 days to capture both early as well as sustained gene expression changes (n=4/group and time point). Reads were aligned with Tophat2 (Kim et al., 2013, Trapnell et al., 2009) to Rnor_5.0 (Ensembl release 79). All annotated genes with greater than one read per million mappable reads in at least four samples were included for differential gene expression with EdgeR (Bioconductor) (Robinson et al., 2010). In a first step a principal component analysis (PCA) was performed **(Fig.4.34.).**

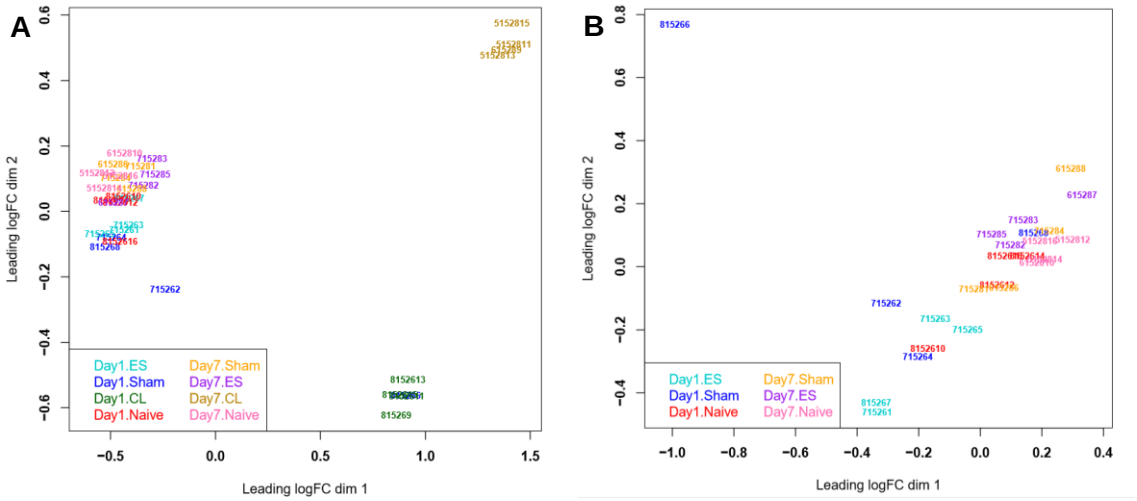

Fig.4.34. Principal component analysis (PCA) of RNA Sequencing differential gene expression. (A) PCA for ES (20Hz, 2*MT, 0.2ms, 1h), sham cuffs, CL or just opening of the skin (naïve) and DRGs at 1 day or 7 days. **(B)** PCA not including CL 1 or 7 days.

As seen in **(Fig.4.34)**, the initial clustering of biological replicat based on PCA, is not entirely clear. This can be due to various factors, such as technical noise (RNA isolation, sequencing or library preparation) or biological variation (Conesa et al., 2016). Variability appears to affect particularly 2 samples of the day 1 sham group, which cluster with or towards the CL. In such cases, unless an explanation can account for the variability, the standard recommendation is to remove and add more samples (ENCODE_Consortium, 2011). The variability in this case is likely due to surgery related conditioning, which justifies the exclusion. Comparisons of gene expression could also be performed with 2 biological replicates, however this decreases considerably the statistical power for differential gene expression (Conesa et al., 2016). Thus I have performed additional surgeries for new samples and for the current exploratory analysis I focused only on

differential gene expression at 7 days after ES, sham, CL and naïve setting the cutoff p value at p<0.01 **(Fig.4.35)**. Filtering of genes as previously mentions was minimal, and all genes with greater than one read per million mappable reads in at least four samples were taken into account. All conditions and samples were included in the analysis, totaling 32 samples divided in 8 groups and comparisons were made for 11963 distinct genes, with focus on ES vs sham and CL vs naïve as the most important pairs to emphasize relevant differential gene expression. Full list of upregulated and downregulated genes according to these criteria, annotated with DAVID Bioinformatics Resources 6.7, are available in **Annex 2** and **Annex 3** respectively.

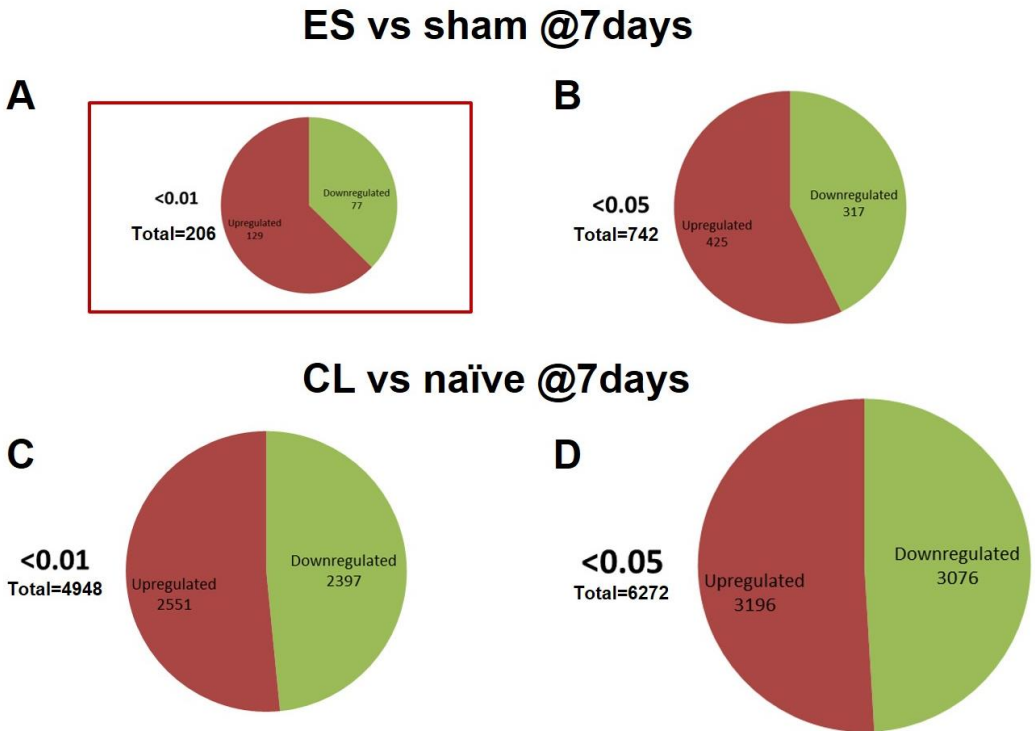

Fig.4.35. Number of differentially expressed genes at 7days time-point. (A, B) Differential gene expression at 7 days after ES vs. sham. **(C, D)** Differential gene expression at 7 days after CL vs. naïve. **(A,C)** p<0.01, **(B,D)** p<0.05, analysis by EdgeR, comparison of 11963 distinct genes, 8 conditions. N=4. See **Annex 2** and **3** for complete list.

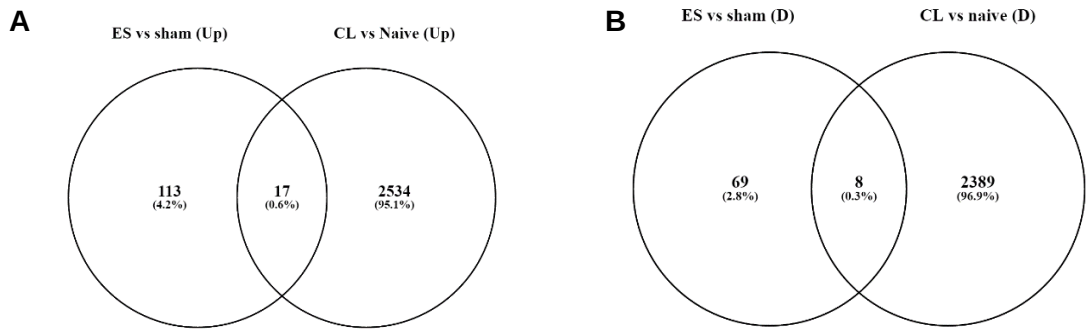

Fig.4.36. Overlap of differentially expressed genes at 7days time-point between ES vs sham and CL vs naive. (A) Upregulated genes at 7 days in ES vs. sham compared to CL vs. naïve. **(B)** Downregulated genes at 7 days in ES vs. sham compared to CL vs. naïve. p<0.01. Analysis by EdgeR, comparison of 11963 distinct genes, 8 conditions. n=4/group. **(A)** Upregulated overlap (Ankrd50, Faxc, Supt6h, Rab3gap2, Dysf, Lrrc58, Kalrn, Akap6, Pcdh18, Scand1, Macf1, Gpr88, Ace, Terc, Mcoln3, Ucn, Hpd) 13,1%. **(B)** Downregulated overlap (Itgb3bp, Oasl, Cox17, Ift22, Cstb, Sssca1, Cox6a1, Cox5b) 10,3%.

4.10.2. Functional clusters

A first analysis of the upregulated and downregulated genes was performed by gene functional classification clustering on DAVID Bioinformatics Resources 6.7 (Huang et al., 2009, Huang et al., 2008) **(Table 4.3,** respectively **4.4)**. For this, the following parameters were used: similarity term overlap (4), similarity (Kappa) threshold (0.35), initial group membership (2), final group membership (2) and linkage threshold (50%).

The main gene clusters for upregulated genes found were: myosins, voltage-gated potassium channels, voltage-gated potassium channels, DNA binding factors, ubiquitin peptidases, dyneins, G-coupled receptors and others as detailed in **Table 4.3.** Downregulated gene clusters are detailed in **Table 4.4.**

Table 4.3. Functional clusters - upregulated genes at 7 days after ES (vs sham). Functional classification clustering on DAVID Bioinformatics Resources 6.7. 83 genes from the 129 list are not in the output. Similarity (Kappa) score: Very High (0.75-1); High (0.5-0.75); Moderate (0.25-05). Threshold: 0.35.

Gene Group 1		**Enrichment Score: 4.6**	**Kappa score**
1	Myo1e	myosin IE(Myo1e)	0.77
2	Myo5b	myosin Vb(Myo5b)	0.55
3	Myo9a	myosin IXA(Myo9a)	0.52
4	Myo5a	myosin VA(Myo5a)	0.45
5	Myh10	myosin, heavy chain 10, non-muscle(Myh10)	0.41
Gene Group 2		**Enrichment Score: 3.3**	

1	Kcnb2	potassium voltage-gated channel subfamily B member 2(Kcnb2)	0.76
2	Hcn1	hyperpolarization-activated cyclic nucleotide-gated potassium channel 1(Hcn1)	0.66
3	Kcnh7	potassium voltage-gated channel subfamily H member 7(Kcnh7)	0.63
4	Kcnh5	potassium voltage-gated channel subfamily H member 5(Kcnh5)	0.47
5	Kcna2	potassium voltage-gated channel subfamily A member 2(Kcna2)	0.45
Gene Group 3		**Enrichment Score: 3.05**	
1	Scn8a	sodium voltage-gated channel alpha subunit 8(Scn8a)	0.84
2	Scn9a	sodium voltage-gated channel alpha subunit 9(Scn9a)	0.84
3	Scn1a	sodium voltage-gated channel alpha subunit 1(Scn1a)	0.81
Gene Group 4		**Enrichment Score: 2.41**	
1	Chd6	chromodomain helicase DNA binding protein 6(Chd6)	0.63
2	Snrnp200	small nuclear ribonucleoprotein 200 (U5) (Snrnp200)	0.57
3	Ddx6	DEAD-box helicase 6(Ddx6)	0.52
Gene Group 5		**Enrichment Score: 1.99**	
1	Usp9x	ubiquitin specific peptidase 9, X-linked(Usp9x)	0.89
2	Usp24	ubiquitin specific peptidase 24(Usp24)	0.50
3	Usp32	ubiquitin specific peptidase 32(Usp32)	0.48
Gene Group 6		**Enrichment Score: 1.61**	
1	Dync1h1	dynein cytoplasmic 1 heavy chain 1(Dync1h1)	0.90
2	Dync2h1	dynein cytoplasmic 2 heavy chain 1(Dync2h1)	0.79
Gene Group 7		**Enrichment Score: 1.59**	
1	Slc7a1	solute carrier family 7 member 1(Slc7a1)	0.74
2	Gpr158	G protein-coupled receptor 158(Gpr158)	0.70
3	Gpr88	G-protein coupled receptor 88(Gpr88)	0.54
Gene Group 8		**Enrichment Score: 1.58**	
1	Arfgef1	ADP ribosylation factor guanine nucleotide exchange factor 1(Arfgef1)	0.87
2	Arfgef2	ADP ribosylation factor guanine nucleotide exchange factor 2(Arfgef2)	0.78
Gene Group 9		**Enrichment Score: 1.16**	
1	Hipk3	homeodomain interacting protein kinase 3(Hipk3)	0.83
2	Dstyk	dual serine/threonine and tyrosine protein kinase(Dstyk)	0.71
Gene Group 10		**Enrichment Score: 1.11**	
1	Ubr1	ubiquitin protein ligase E3 component n-recognin 1(Ubr1)	0.96
2	Ubr2	ubiquitin protein ligase E3 component n-recognin 2(Ubr2)	0.65
Gene Group 11		**Enrichment Score: 1.04**	

1	Pcdh17	protocadherin 17(Pcdh17)	0.67
2	Golga3	golgin A3(Golga3)	0.67
3	Pcdh19	protocadherin 19(Pcdh19)	0.53
4	Faxc	failed axon connections homolog (Drosophila)(Faxc)	0.50
5	Golgb1	golgin B1(Golgb1)	0.48
6	Mcoln3	mucolipin 3(Mcoln3)	0.48
7	Pcdh18	protocadherin 18(Pcdh18)	0.47
8	Slc7a14	solute carrier family 7, member 14(Slc7a14)	0.42
9	Pcdh7	protocadherin 7(Pcdh7)	0.40
Gene Group 12		**Enrichment Score: 1.01**	
1	Nrcam	neuronal cell adhesion molecule(Nrcam)	0.90
2	Nfasc	neurofascin(Nfasc)	0.85
Gene Group 13		**Enrichment Score: 0.99**	
1	Peg3	paternally expressed 3(Peg3)	0.76
2	Zfx	zinc finger protein X-linked(Zfx)	0.47
3	Zc3h13	zinc finger CCCH type containing 13(Zc3h13)	0.41
Gene Group 14		**Enrichment Score: 0.99**	
1	Ttbk2	tau tubulin kinase 2(Ttbk2)	0.81
2	Map3k2	mitogen activated protein kinase kinase kinase 2(Map3k2)	0.70

Table 4.4. Functional clusters - downregulated genes at 7 days after ES (vs sham). Functional classification clustering on DAVID Bioinformatics Resources 6.7. 53 genes from the 77 list are not in the output. Similarity (Kappa) score: Very High (0.75-1); High (0.5-0.75); Moderate (0.25-05). Threshold: 0.35.

Gene Group 1		**Enrichment Score: 5.03**	**Kappa score**
1	Tnni1	troponin I1, slow skeletal type(Tnni1)	0.65
2	Tnnt1	troponin T1, slow skeletal type(Tnnt1)	0.75
3	Tnnt3	troponin T3, fast skeletal type(Tnnt3)	0.69
Gene Group 2		**Enrichment Score: 3.09**	
1	Atp5e	ATP synthase, H+ transporting, mitochondrial F1 complex, epsilon subunit(Atp5e)	0.54
2	Atp5i	ATP synthase, H+ transporting, mitochondrial Fo complex, subunit E(Atp5i)	0.39
3	Cox6c	cytochrome c oxidase subunit 6C(Cox6c)	0.74
4	Cox6a1	cytochrome c oxidase subunit 6A1(Cox6a1)	0.72
5	Cox7c	cytochrome c oxidase subunit 7C(Cox7c)	0.86
6	Slc25a37	solute carrier family 25 member 37(Slc25a37)	
7	Cox5b	cytochrome c oxidase subunit 5B(Cox5b)	0.71

Gene Group 3		Enrichment Score: 2.52	
1	Rpl19	ribosomal protein L19(Rpl19)	0.57
2	Rps4x	ribosomal protein S4, X-linked(Rps4x)	0.65
3	Rps11	ribosomal protein S11(Rps11)	0.76
4	Rpl27	ribosomal protein L27(Rpl27)	0.62
Gene Group 4		**Enrichment Score: 2.27**	
1	Tnnc1	troponin C1, slow skeletal and cardiac type(Tnnc1)	0.97
2	Tnnc2	troponin C2, fast skeletal type(Tnnc2)	0.49
Gene Group 5		**Enrichment Score: 2.05**	
1	Hist3h2a	histone cluster 3, H2a(Hist3h2a)	0.78
2	Hist1h1b	histone cluster 1, H1b(Hist1h1b)	0.49
3	Hist1h2bk	histone cluster 1, H2bk(Hist1h2bk)	0.64
4	Hist1h2ail1	histone cluster 1, H2ai-like1(Hist1h2ail1)	0.74
Gene Group 6		**Enrichment Score: 1.57**	
1	Myh4	myosin, heavy chain 4, skeletal muscle(Myh4)	0.73
2	Myh7	myosin, heavy chain 7, cardiac muscle, beta(Myh7)	0.95
Gene Group 7		**Enrichment Score: 0.64**	
1	Alpk3	alpha-kinase 3(Alpk3)	0.89
2	Mybpc2	myosin binding protein C, fast-type(Mybpc2)	0.71

4.10.3. Gene ontology classifications

Overrepresentation analysis with different parameters were performed on ConsensusPathDB (http://cpdb.molgen.mpg.de/) (Kamburov et al., 2013, Kamburov et al., 2009), presented in **Tables 4.5**, and **4.6**, **4,7** with the corresponding interaction network-graphics **Fig.4.37** and **Fig.4.38** respectively.

Table 4.5. Enriched gene ontology-based sets by molecular function for upregulated genes in ES compared to sham at 7 days. Overrepresentation analysis on ConsensusPathDB.

gene ontology term	category, level	set size	candidates contained	p-value	q-value
GO:0005515 protein binding	MF 2	10524	95 (0.9%)	9.99e-06	0.00024
GO:0097367 carbohydrate derivative binding	MF 2	2222	31 (1.4%)	6.04e-05	0.000725
GO:0036094 small molecule binding	MF 2	2612	34 (1.3%)	9.8e-05	0.000784
GO:0043167 ion binding	MF 2	6117	61 (1.0%)	0.000219	0.00131
GO:0022857 transmembrane transporter activity	MF 2	975	16 (1.6%)	0.000931	0.00447
GO:0032947 protein complex scaffold	MF 2	67	4 (6.0%)	0.00112	0.00449
GO:0005085 guanyl-nucleotide exchange factor activity	MF 2	193	6 (3.1%)	0.00207	0.00711
GO:0016874 ligase activity	MF 2	428	9 (2.1%)	0.00263	0.0079
GO:0022892 substrate-specific transporter activity	MF 2	1055	15 (1.4%)	0.00527	0.0141
GO:0016740 transferase activity	MF 2	2218	25 (1.1%)	0.00683	0.0164

Table 4.6. Enriched gene ontology-based sets by biological processes for upregulated genes in ES compared to sham at 7 days. Overrepresentation analysis on ConsensusPathDB.

gene ontology term	category, level	set size	candidates contained	p-value	q-value
GO:0051234 establishment of localization	BP 2	4636	58 (1.3%)	2.2e-07	9.96e-06
GO:1902578 single-organism localization	BP 2	4068	53 (1.3%)	3.02e-07	9.96e-06
GO:0016043 cellular component organization	BP 2	5857	66 (1.1%)	9.81e-07	2.16e-05
GO:0044700 single organism signaling	BP 2	6125	67 (1.1%)	2.21e-06	3.64e-05
GO:0044707 single-multicellular organism process	BP 2	6658	69 (1.0%)	1.12e-05	0.000124
GO:0033036 macromolecule localization	BP 2	2684	37 (1.4%)	1.25e-05	0.000124
GO:0044767 single-organism developmental process	BP 2	5607	61 (1.1%)	1.31e-05	0.000124
GO:0048856 anatomical structure development	BP 2	5056	56 (1.1%)	2.43e-05	0.0002
GO:0051641 cellular localization	BP 2	2921	38 (1.3%)	3.4e-05	0.000231
GO:0065009 regulation of molecular function	BP 2	2699	36 (1.3%)	3.5e-05	0.000231
GO:0065008 regulation of biological quality	BP 2	3431	42 (1.2%)	4.82e-05	0.000289
GO:0007626 locomotory behavior	BP 2	201	8 (4.0%)	6.8e-05	0.000374
GO:0044708 single-organism behavior	BP 2	409	11 (2.7%)	0.000109	0.000554
GO:0044763 single-organism cellular process	BP 2	12248	102 (0.8%)	0.00016	0.000755
GO:0051705 multi-organism behavior	BP 2	83	5 (6.0%)	0.000256	0.00105
GO:0051703 intraspecies interaction between organisms	BP 2	46	4 (8.7%)	0.000267	0.00105
GO:0016049 cell growth	BP 2	454	11 (2.4%)	0.00027	0.00105
GO:0044085 cellular component biogenesis	BP 2	2489	31 (1.2%)	0.000496	0.00182
GO:0050789 regulation of biological process	BP 2	10723	91 (0.9%)	0.000538	0.00187
GO:0009653 anatomical structure morphogenesis	BP 2	2616	30 (1.1%)	0.00238	0.00784
GO:0051716 cellular response to stimulus	BP 2	6944	61 (0.9%)	0.00726	0.0222
GO:0007155 cell adhesion	BP 2	1421	18 (1.3%)	0.0074	0.0222
GO:0009719 response to endogenous stimulus	BP 2	1573	19 (1.2%)	0.00984	0.0282

From 129 upregulated genes, grouped in non-exclusive categories, the most common molecular functions are protein binding (95 genes, 73.6%), ion binding (61 genes, 47.2%) and small molecule binding (34 genes, 23.6%), suggesting many of the candidates have multiple interactions and functions. A full description of molecular functions of the candidate dataset is given in **Table 4.5.**

A similar analysis was performed for biological processes **(Table 4.6)**. While some of the conveyed processes, such as single organism functions do not appear to be related to the experimental conditions, other processes may be relevant, such as regulation of biological processes (91 genes, 70.5%), establishment of localization (58 genes, 44.9%), cellular component organization (66 genes, 51.1%) and cellular response to stimulus (61 genes, 47.2%). As expected there is considerable overlap between these categories, genes being associated with several functions, as seen in **Fig.4.37**.

Fig.4.37. Interaction network-graph of enriched gene ontology-based sets by biological processes for upregulated genes in ES compared to sham at 7 days. Overrepresentation analysis on ConsensusPathDB.

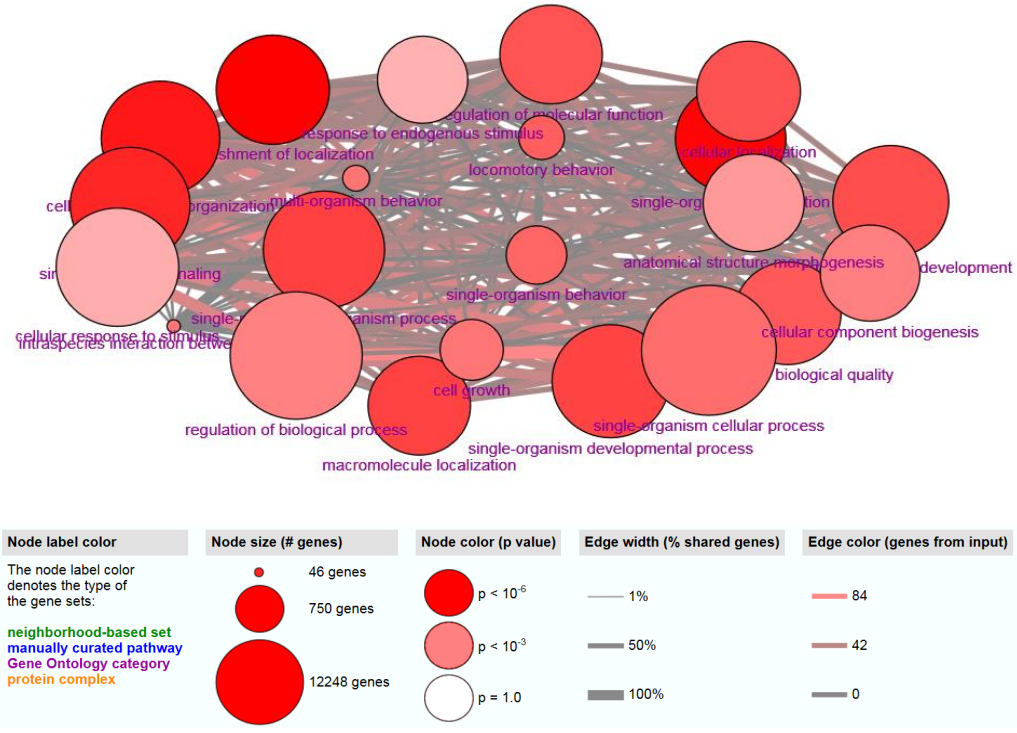

4.10.4. Enriched pathways and protein complexes

When analyzing the gene set according to previously described pathways using the ConsensusPathDB, the data indicates enrichment of L1-ankyrins interaction set, potassium channels, voltage-gated potassium channels, L1CAM, axon guidance, neurofascin interactions, developmental biology and others **(Table 4.7).** This is to some extent similar to the functional clusters in **Table 4.3**, however differs in methodology, since functional clusters on DAVID are defined more based on molecular similarity, while the pathway identification is based more on interactions.

Table 4.7. Enriched pathway-based sets for upregulated genes in ES compared to sham at 7 days. Overrepresentation analysis on ConsensusPathDB.

pathway name	set size	candidates contained	p-value	q-value	pathway source
Interaction between L1 and Ankyrins	29	5 (17.2%)	3.6e-06	0.000979	Reactome
Potassium Channels	100	6 (6.0%)	0.000178	0.0242	Reactome
Voltage gated Potassium channels	44	4 (9.1%)	0.00047	0.0426	Reactome
L1CAM interactions	100	5 (5.1%)	0.00137	0.0632	Reactome
Axon guidance	459	11 (2.4%)	0.00138	0.0632	Reactome
Neurofascin interactions	7	2 (28.6%)	0.0014	0.0632	Reactome
Translocation of GLUT4 to the plasma membrane	34	3 (8.8%)	0.00276	0.107	Reactome
Developmental Biology	586	12 (2.1%)	0.00315	0.107	Reactome
EPHB forward signaling	39	3 (7.7%)	0.00408	0.123	PID
actions of nitric oxide in the heart	42	3 (7.1%)	0.00504	0.133	BioCarta
LKB1 signaling events	43	3 (7.0%)	0.00539	0.133	PID
Polycystic Kidney Disease Pathway	17	2 (11.8%)	0.00856	0.194	Wikipathways

Fig. 4.38. Interaction network-graph of enriched pathway-based sets for upregulated genes in ES compared to sham at 7 days. Overrepresentation analysis on ConsensusPathDB.

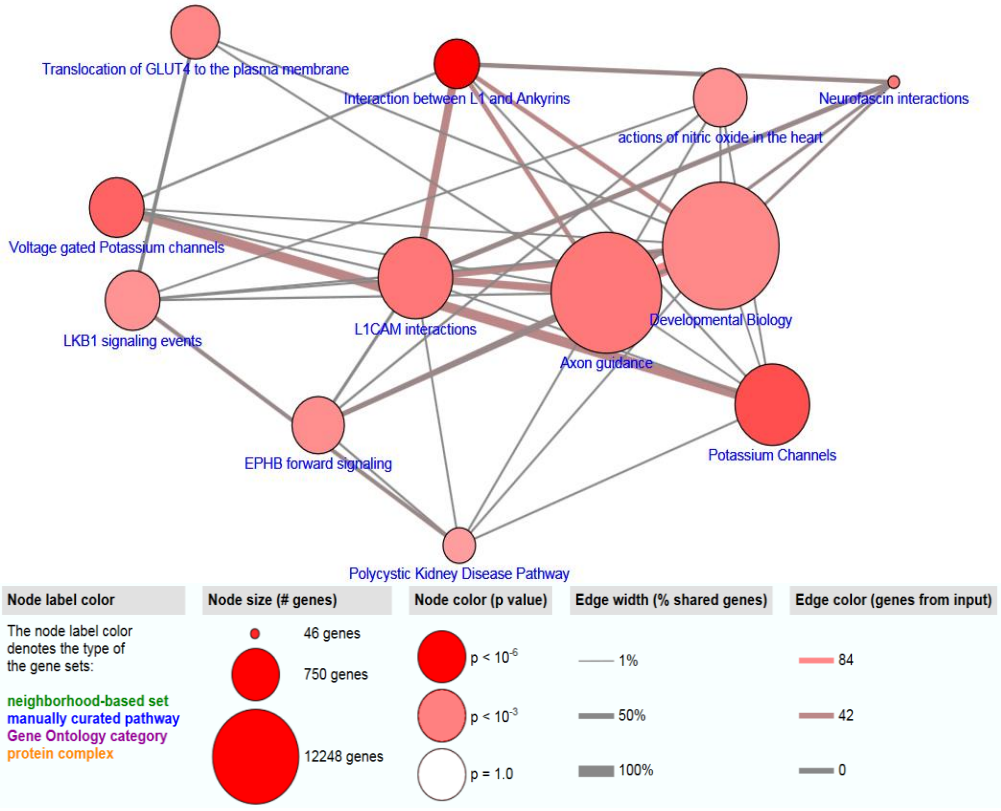

From the 95 genes found to be protein binding, some were found to be particularly involved in protein complexes **(Table 4.8.).** Most important findings are mTOR signaling complex and NFASC/NRCAM for which both components are upregulated in each of them (100% of set contained in the upregulated candidate set), while MAP1B/Lis1/Dynein heavy chains or has two out of three members of the data sets upregulated (66% of set). The upregulation is particularly significant for small sets of protein complexes as can be visualized in **Fig. 4.39**.

Table 4.8. Enriched protein-complex based sets for upregulated genes in ES compared to sham at 7 days. Overrepresentation analysis on ConsensusPathDB.

complex name	set size	candidates contained	p-value	q-value	complex source
mTOR-signaling complex (mTOR/FRAP1, RAPTOR)	2	2 (100.0%)	7.74e-05	0.00143	CORUM
NFASC:NRCAM	2	2 (100.0%)	7.74e-05	0.00143	Reactome
MAP1B/LIS1/Dynein heavy chain	3	2 (66.7%)	0.000231	0.00214	PID
mTORC1	3	2 (66.7%)	0.000231	0.00214	Reactome
mTORC1:FKBP38	4	2 (50.0%)	0.000459	0.00243	INOH
mTORC1 dimer	4	2 (50.0%)	0.000459	0.00243	Reactome
NSC	4	2 (50.0%)	0.000459	0.00243	PINdb
mTORC1/PGC1A/YY1	5	2 (40.0%)	0.000761	0.00313	PID
mTORC1/PRAS40/DEPTOR	5	2 (40.0%)	0.000761	0.00313	PID
mTORC1/PRAS40/DEPTOR/PML	6	2 (33.3%)	0.00114	0.0042	PID
U4 ATAC:U5:U6 ATAC Complex	16	2 (12.5%)	0.00858	0.0288	Reactome
U4:U5:U6 trisnRNP complex	17	2 (11.8%)	0.00966	0.0298	Reactome

Fig. 4.39. Interaction protein-complex based sets for upregulated genes in ES compared to sham at 7 days. Overrepresentation analysis on ConsensusPathDB.

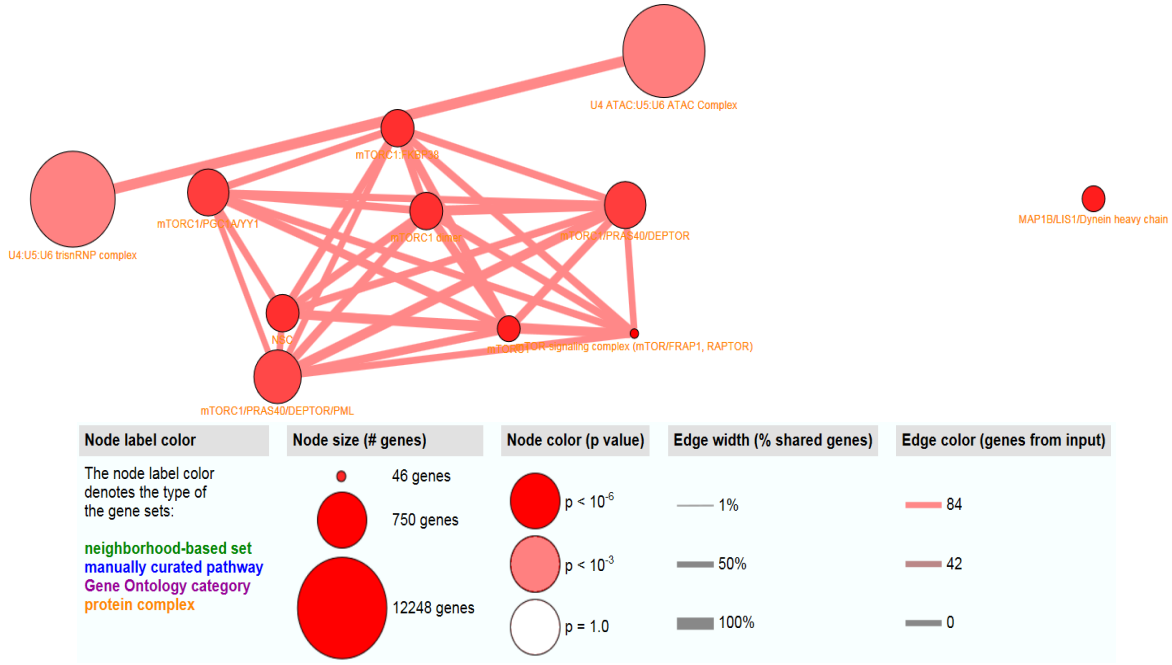

References

1. Arcaro, K. F. & Lnenicka, G. A. 1997. Differential effects of depolarization on the growth of crayfish tonic and phasic motor axons in culture. *J Neurobiol,* 33**,** 85-97.
2. Cho, Y., Sloutsky, R., Naegle, K. M. & Cavalli, V. 2013. Injury-induced HDAC5 nuclear export is essential for axon regeneration. *Cell,* 155**,** 894-908.
3. Cobianchi, S., De Cruz, J. & Navarro, X. 2014. Assessment of sensory thresholds and nociceptive fiber growth after sciatic nerve injury reveals the differential contribution of collateral reinnervation and nerve regeneration to neuropathic pain. *Exp Neurol,* 255**,** 1-11.
4. Conesa, A., Madrigal, P., Tarazona, S., Gomez-Cabrero, D., Cervera, A., Mcpherson, A., Szczesniak, M. W., Gaffney, D. J., Elo, L. L., Zhang, X. & Mortazavi, A. 2016. A survey of best practices for RNA-seq data analysis. *Genome Biol,* 17**,** 13.
5. Ehl, R. G. & Ihde, A. J. 1954. Faraday's electrochemical laws and the determination of equivalent weights. *Journal of Chemical Education,* 31**,** 226.
6. Encode_Consortium 2011. Standards, Guidelines and Best practices for RNA-Seq.
7. Enes, J., Langwieser, N., Ruschel, J., Carballosa-Gonzalez, M. M., Klug, A., Traut, M. H., Ylera, B., Tahirovic, S., Hofmann, F., Stein, V., Moosmang, S., Hentall, I. D. & Bradke, F. 2010. Electrical activity suppresses axon growth through Ca(v)1.2 channels in adult primary sensory neurons. *Curr Biol,* 20**,** 1154-64.
8. Fugleholm, K., Schmalbruch, H. & Krarup, C. 1994. Early peripheral nerve regeneration after crushing, sectioning, and freeze studied by implanted electrodes in the cat. *J Neurosci,* 14**,** 2659-73.
9. Holmquist, B., Kanje, M., Kerns, J. M. & Danielsen, N. 1993. A mathematical model for regeneration rate and initial delay following surgical repair of peripheral nerves. *J Neurosci Methods,* 48**,** 27-33.
10. Huang, D. W., Sherman, B. T. & Lempicki, R. A. 2008. Systematic and integrative analysis of large gene lists using DAVID bioinformatics resources. *Nat. Protocols,* 4**,** 44-57.
11. Huang, D. W., Sherman, B. T. & Lempicki, R. A. 2009. Bioinformatics enrichment tools: paths toward the comprehensive functional analysis of large gene lists. *Nucleic Acids Research,* 37**,** 1-13.
12. Kamburov, A., Stelzl, U., Lehrach, H. & Herwig, R. 2013. The ConsensusPathDB interaction database: 2013 update. *Nucleic Acids Research,* 41**,** D793-D800.
13. Kamburov, A., Wierling, C., Lehrach, H. & Herwig, R. 2009. ConsensusPathDB—a database for integrating human functional interaction networks. *Nucleic Acids Research,* 37**,** D623-D628.
14. Kim, D., Pertea, G., Trapnell, C., Pimentel, H., Kelley, R. & Salzberg, S. L. 2013. TopHat2: accurate alignment of transcriptomes in the presence of insertions, deletions and gene fusions. *Genome Biol,* 14**,** R36.
15. Kwon, B. K., Liu, J., Messerer, C., Kobayashi, N. R., Mcgraw, J., Oschipok, L. & Tetzlaff, W. 2002. Survival and regeneration of rubrospinal neurons 1 year after spinal cord injury. *Proc Natl Acad Sci U S A,* 99**,** 3246-51.
16. Luo, L. & O'leary, D. D. 2005. Axon retraction and degeneration in development and disease. *Annu Rev Neurosci,* 28**,** 127-56.
17. Neumann, S., Skinner, K. & Basbaum, A. I. 2005. Sustaining intrinsic growth capacity of adult neurons promotes spinal cord regeneration. *Proc Natl Acad Sci U S A,* 102**,** 16848-52.
18. Nowicki, M., Baum, P., Kosacka, J., Stockinger, M., Kloting, N., Bluher, M., Bechmann, I. & Toyka, K. V. 2014. Effects of isoflurane anesthesia on F-waves in the sciatic nerve of the adult rat. *Muscle Nerve,* 50**,** 257-61.
19. Oblinger, M. M. & Lasek, R. J. 1984. A conditioning lesion of the peripheral axons of dorsal root ganglion cells accelerates regeneration of only their peripheral axons. *J Neurosci,* 4**,** 1736-44.

20. Ramakers, G. J., Winter, J., Hoogland, T. M., Lequin, M. B., Van Hulten, P., Van Pelt, J. & Pool, C. W. 1998. Depolarization stimulates lamellipodia formation and axonal but not dendritic branching in cultured rat cerebral cortex neurons. *Brain Res Dev Brain Res,* 108**,** 205-16.
21. Reber, B. F., Porzig, H., Becker, C. & Reuter, H. 1990. Depolarization-induced changes of free intracellular Ca(2+) concentration and of [(3)H]dopamine release in undifferentiated and differentiated PC12 cells. *Neurochem Int,* 17**,** 197-203.
22. Reilly, J. P. & Antoni, H. 1992. *Electrical stimulation and electropathology,* Cambridge [England]; New York, Cambridge University Press.
23. Reilly, J. P., Freeman, V. T. & Larkin, W. D. 1985. Sensory effects of transient electrical stimulation--evaluation with a neuroelectric model. *IEEE Trans Biomed Eng,* 32**,** 1001-11.
24. Robinson, M. D., Mccarthy, D. J. & Smyth, G. K. 2010. edgeR: a Bioconductor package for differential expression analysis of digital gene expression data. *Bioinformatics,* 26**,** 139-40.
25. Saijilafu, Hur, E. M., Liu, C. M., Jiao, Z., Xu, W. L. & Zhou, F. Q. 2013. PI3K-GSK3 signalling regulates mammalian axon regeneration by inducing the expression of Smad1. *Nat Commun,* 4**,** 2690.
26. Schlumm, F., Mauceri, D., Freitag, H. E. & Bading, H. 2013. Nuclear calcium signaling regulates nuclear export of a subset of class IIa histone deacetylases following synaptic activity. *J Biol Chem,* 288**,** 8074-84.
27. Trapnell, C., Pachter, L. & Salzberg, S. L. 2009. TopHat: discovering splice junctions with RNA-Seq. *Bioinformatics,* 25**,** 1105-11.
28. Tuszynski, M. H., Gabriel, K., Gerhardt, K. & Szollar, S. 1999. Human spinal cord retains substantial structural mass in chronic stages after injury. *J Neurotrauma,* 16**,** 523-31.
29. Udina, E., Furey, M., Busch, S., Silver, J., Gordon, T. & Fouad, K. 2008. Electrical stimulation of intact peripheral sensory axons in rats promotes outgrowth of their central projections. *Exp Neurol,* 210**,** 238-47.
30. Vaillant, A. R., Mazzoni, I., Tudan, C., Boudreau, M., Kaplan, D. R. & Miller, F. D. 1999. Depolarization and neurotrophins converge on the phosphatidylinositol 3-kinase-Akt pathway to synergistically regulate neuronal survival. *J Cell Biol,* 146**,** 955-66.
31. Wang, J., Campos, B., Jamieson, G. A., Jr., Kaetzel, M. A. & Dedman, J. R. 1995. Functional elimination of calmodulin within the nucleus by targeted expression of an inhibitor peptide. *J Biol Chem,* 270**,** 30245-8.
32. Zhang, Z., Majava, V., Greffier, A., Hayes, R. L., Kursula, P. & Wang, K. K. 2009. Collapsin response mediator protein-2 is a calmodulin-binding protein. *Cell Mol Life Sci,* 66**,** 526-36.

5. Discussions

5.1. ES enhances growth capacity and regeneration after DCL into a cell graft

My findings indicate that DRG neurons respond to ES by increasing their growth capacity, as shown by increased neurite extension in vitro when isolated 7 days after ES **(Fig.4.6)**, as well as by in vivo growth 28 days after a DCL and cell transplantation, with ES applied acutely after the DCL **(Fig.4.12)**.

The ex-vivo DRG growth reported here is partially in line with previous findings, as ES has shown to increase ex vivo growth by 4-fold (Udina et al., 2008), however my data shows only 2-fold increase of neurite growth. The difference in effect size can be due to several factors, such as the culturing conditions or the way the stimulation was done. I show here also that the coating of the plates and culture duration influences the sensibility of the neurite growth assay for changes in growth potential **(Fig.4.4, 4.5)**, nevertheless, the differences for culturing between this study and (Udina et al., 2008) are minimal, thus it is more likely that other factors are involved.

One possibility is that surgery related events from sciatic manipulation can condition the DRGs and influence the reliability of the ex-vivo growth. In this study I also cultivated DRGs from animals that received identical manipulation, including electrode implantation, but no ES (sham) to account for surgery related conditioning, ensuring control for surgery related effects. DRGs from animals that received CL served as positive control. DRG growth from CL animals, allowed to compare the magnitude of effect to the high CL-induced activation of intrinsic growth potential, showing that ES-induced growth is intermediary between naïve and CL **(Fig.4.6)**. While a majority of sham implanted animals showed neurite extension comparable to naïve animals, in a few isolated cases, shams showed growth comparable to a CL, revealing the model to be indeed sensitive to surgical technique. To overcome this caveat, I always performed an equal number of shams and ES animals within a surgery and normalized the growth to the sham values. This is the first time growth effects of in vivo ES are explored in a comprehensive set of experiments allowing for the comparison of ES effects with CL effects and eliminating the possibility of a surgery-related conditioning by using appropriate sham controls.

Since the stimulation protocol, should preferentially stimulate large myelinated fibers, I measured separately the neurite growth for NF200-βIII-tubulin double labeled neurons as well as only βIII-tubulin **(Fig.4.2)**. Surprisingly there was no tendency for an effect

restricted to the large myelinated neurons, raising the question of mechanisms that could explain the lack of specificity of the ES induced growth. The selectivity of frequencies and pulse durations for activating certain fibers, has mostly been described in short duration electrophysiological studies, compared to which 1h is relatively long, thus for a long stimulation it may no longer be valid. In a long, intense stimulation several other factors may be involved such as cross-excitation of small unmyelinated fibers (Amir and Devor, 2000), release of diffusible mediators in response to ES (Amir and Devor, 1996) and neurotrophic factors (Al-Majed et al., 2000a). Depolarization can also play a role, since transmission of action potentials at the level of the DRGs can cause release of KCl, proportional to the frequency of the stimulus, and duration of stimulation (Forstl et al., 1982), possibly having an effect also on the unstimulated fibers.

While previous studies have generally used a 2-3mm wire loop as cathode around the sciatic with the anode placed just immediately distally either to the nerve suture, or on the intact nerve (Udina et al., 2008, Al-Majed et al., 2000a, Geremia et al., 2007), in this study, I stimulated the sciatic nerve using self-made cuff electrodes **(Fig.4.1).** These electrodes have several advantages such as good fixation around the nerve without tight contact, standardized geometry and better isolation from other tissues, however they may also influence the effects on growth. It has been reported that electrode impedance for cuff electrodes can vary considerably immediately after implantation, due to trapped air bubbles which are slowly removed and replaced by extracellular fluid (Loeb and Peck, 1996), thus the MT determination and the stimulation was started 5-10 min after the implantation itself, to let the tissue to accommodate. Additionally, stimulation was done in a constant current regime, thus the stimulation should be effective irrespective of impedance changes (Clark, 2006). In contrast, a stimulation at constant voltage is more influenced by changes in impedance and results in less effective stimulation (Dymond, 1976). Indeed, a constant voltage stimulation did not have effects on ex-vivo neurite growth, showing that compensating impedance changes to ensure efficiency of charge delivery, is essential for inducing effects on growth **(Fig.4.8)**.

Compared to looped wires, the active part of the wires is not in contact with the surrounding tissue but exclusively in contact with the nerve, as they are contained within an electrically isolating silicone tube. Since the cuff-nerve interface in the context of ES can be approximated to a “leaky capacitor” (a faradic impedance resistance (R_f) and a capacitator (C) in a parallel circuit, serried with electrode (R_e) and medium resistances (R_m)) (Dymond, 1976), the silicone cuff could influence the relation between intensity of stimulation and effects. However, we independently determined stimulation intensity for each nerve based

on observable motor effects and report that the absolute intensity of the stimulation, did not have an influence on neurite growth as long as relative intensity was 2*MT **(Fig.4.8)**. Additionally, circumferential contacts with a longitudinal separation may recruit nerve fibers more homogenously (Loeb and Peck, 1996) providing another advantage for using such cuff electrodes.

ES did not have any effects on growth when DRGs were isolated 1 day after ES **(Fig.4.7)**, but similar to CL, a delay was necessary for the effects to develop, suggesting transcriptional mechanisms are involved in a similar way to CL. The effect of ES was however smaller, about 2-fold increase, compared to 4-fold increase in CL **(Fig.4.6.E)**. Concomitantly there are other differences to CL, besides the magnitude of the effect. Unlike CL lesion which increased both elongation and initiation, ES increased only the percentage of neurons with neurites >100um, without influencing the percentage of neurite bearing neurons **(Fig.4.6.G)**. This emphasizes that average longest neurite measurement is increased due to enhanced elongation and not initiation. Moreover, when only neurite bearing neurons are considered, ES appears to have approximatively half of the impact of CL on growth **(Fig.4.6.F)**. Additionally, both ES and CL effects appear to be dependent on the substrate, because in the initial set of experiments neither effects could be clearly defined due to in vitro culture and plating procedures. Thus there are several similarities between ES effects and CL, both regarding pattern of growth and the timeline, supporting an overlap in mechanism, however the differences in magnitude of effect and qualitative growth such as initiation, suggest that the overlap is only partial.

In order to potentially enhance the effect, repeated stimulation 1h/day for 7 days or increased duration (7h) were applied, surprisingly with no additional effects over 1h stimulation **(Fig.4.9)**. This is consistent with previous findings in peripheral regeneration where ES applied continuously for up to 2 weeks did not have additional effects on motor axons recovery (Al-Majed et al., 2000b). Similarly, for sensory fibers, ES applied for longer than 1h, such as 3h, 7h, 1day or 14 days did not induce significant differences from the no-stimulation control in the femoral nerve (Geremia et al., 2007), and 1h ES daily for 4 weeks, had similarly no additional effects on sciatic regeneration (Asensio-Pinilla et al., 2009). These studies as well as my results, support the idea that initial activity immediately after injury is the important factor in “priming” the neurons, and a short application of a similar pattern of activity is sufficient to trigger the underlying mechanisms, while more stimulation does not induce additive effects and could even be detrimental.

Due to the electrodes used, local tissue reactions should be minimum, since stainless steel electrodes have good corrosion resistance and are recommended for such stimulation

(Riistama and Lekkala, 2006), however previous studies applying electrical stimulation, have also shown negative phenomena from long term ES, such as edema appearing as early as 2 days after ES and early axonal degeneration of large myelinated fibers appearing at 7 days (Agnew et al., 1989, McCreery et al., 1992). 50Hz stimulation to the peroneal nerve for 8-16h is sufficient to induce such degeneration at 7 days post stimulation even with a charge balanced impulse, while 20Hz 18h of stimulation with a similar pulse does not induce degeneration or edema (Agnew et al., 1989). However, in this study I used monophasic square pulses thus an impact of electrochemical reactions on growth or degeneration could not be immediately excluded. Unbalanced electrolysis from a constant pulsed protocol, should be directly proportional to the stimulation time according to Faraday's Law: $\mathrm{n} = \frac{Q}{Fz} = \frac{\int_0^t I(t)dt}{Fz}$ (where n=amount of substance in moles liberated, Q=charge, F=Faraday constant and z=valency number of ions of the substance) (Ehl and Ihde, 1954). The lack of larger effects on growth following a continuous 7h stimulation, indicates that there are no unspecific effects from local chemical tissue reactions, at least as far as growth is concerned. Additionally, short charge balanced pulses stimulating primarily large axons, have been found in an 8-hour ES protocol, to have a threshold for damage about 2.2-2.6 times higher than the intensity for full A-fibers recruitment (McCreery et al., 1992). Thus the intensity used here, 2*MT, ensuring full A-fibers recruitment, is considerably below the threshold for damage for 1h stimulation, and likely also for the 7h stimulation.

Several experiments also focused on additional parameters for in vivo electrical stimulation followed by in vitro assessment of growth in primary cultures. Stimulating the sciatic nerve for 1h with 10Hz instead of 20Hz, showed a similar trend on growth, though only half of the total number of pulses was delivered **(Fig.4.2.E)**. This is surprising, however it is known from in vitro studies that stimulation with 10Hz up to 30Hz, though inducing a different temporal dynamic, results in the same cumulative Ca^{2+} entry (Eshete and Fields, 2001), which could explain a similar magnitude, if the effect is mediated by calcium signaling. Another factor which was investigated was the presence or absence of hind limb movement throughout the stimulation. Active visible movement disappears shortly after the onset of the usual 20Hz stimulation protocol and is followed by static contraction for the rest of the stimulation. A protocol that induced constant movement of the hind-limb, showed however a tendency to inhibit growth, while 10 Hz stimulation, also inducing movement throughout the stimulation, did not display a different trend on growth compared to 20Hz, showing that hind-limb movement is not an indicator of ES-induced growth.

Growth effects of 1h ES were also assessed in vivo in a model of spinal cord injury, together with cell transplantation of BMSCs (bone marrow stromal cells) at 4 weeks post-injury. Axonal regeneration into the spinal cell graft was assessed, showing significantly enhanced growth in animals with ES for 1h within the lesion compared to sham animals, while the injected cells efficiently filled the lesion and served as substrate for growth **(Fig.4.11)**. This further supports the ex-vivo results, showing enhanced growth compared to naïve and sham, but less than CL-induced growth. In contrast to the ex-vivo experiments, the ES was applied after the DCL and cell transplantation, confirming the validity for translational purposes.

I evaluated the growth with two methods, quantifying axonal profiles crossing the tissue-lesion border, or 50, 100, 250 or 500µm into the lesion **(Fig.4.12)**, and measuring the distance from the border to growth cones/axon tips within the graft **(Fig.4.19)**. Both methods show similar results: increase number of fibers extending into the graft after ES, however they also show slight differences, likely due to different sampling. Measuring the distance of retraction bulbs within the distal spinal cord, showed that dieback of axons was not modified in any of the conditions **(Fig.4.18)**.

Though ES for 1h/day for 7 days, did not result in increased neurite length in my ex-vivo studies, repeated CL at 7 days after an initial CL has been shown to have a greater effect than the initial lesion alone (Neumann et al., 2005). Thus I tested a repeated stimulation with a similar timeline, using chronic electrodes: first stimulation immediately after the DCL and cell injection, followed by a second stimulation 7 days later. Such a stimulation did not have additional effects **(Fig.4.13)**, but the respective sham group revealed in that chronically implanted electrodes can cause a slight increase of growth.

It has previously been shown that the presence of a cuff on the nerve is sufficient to induce changes such as thickened epineurium and ingrowth of endometrial connective tissue within the cuff, while in chronic implantation virtually every surface gets covered by connective tissue (Agnew et al., 1989, Loeb and Peck, 1996). Thus, the cuffs used in this study were designed to be loose around the nerve, to avoid compression, taking into account sufficient space for connective tissue. As seen in chronically implanted cuffs, they indeed get enclosed in connective tissue **(Fig.4.14)**, and the presence of the cuffs over a long period of time such as 4 weeks, can influence growth, acting as a confounding factor **(Fig.4.13)**. Thus, transcutaneous stimulation would be desirable in future studies.

5.2. Depolarization and calcium signaling

A first approach to mimic activity in culture was to depolarize DRGs by KCl added to the normal medium, using NaCl as separate control for osmolarity. One previous study has shown that chronic depolarization as well as electrical stimulation inhibit neurite growth in adult rat DRGs (Enes et al., 2010). I report a similar finding when exposing DRGs for a long duration to KCl **(Fig.4.22)**, however this inhibitory effect of long exposure to KCl is likely influenced by several factors. First of all, it is questionable whether such a prolonged intense activity is biologically relevant, since neurons do not continuously fire for 24h-72h in vivo, but the activity is modulated by multiple cellular and network mechanism. Activity in primary sensory neurons in normal conditions is mostly stimulus evoked and phasic (Enes et al., 2010), thus shorter depolarization times would better reflect the in vivo situation, even in the context of an intense activity such as the one associated with injury potentials. Indeed, when inducing a short depolarization such as 1h, there are no detrimental effects on growth, but actually a slight stimulation of growth **(Fig.4.22)**. Additionally, though 24h exposure to KCl can inhibit neurite growth, if the DRGs are washed and replated at 72h, they have normal or even enhanced growth compared to control **(Fig.4.22)**.

Inhibition of growth by KCl has been shown in a similar way to produce retraction of growth cones from phasic motor axons, while growth cones of tonic axon continue to advance (Arcaro and Lnenicka, 1997). This suggests taht differences in Ca^{2+} regulation and/or sensitivity to intracellular Ca^{2+} involved in the normal physiologic pattern of activity influence the response to activity. In the same time, it would be theoretically possible for a neuron to adapt to a new activity regime, including changing their growth response to depolarization. In Helisoma neuron cultures, neurite growth is inhibited by KCl, but the effect is transient and after a certain period in culture (90min), the growth recovers to control levels even when still depolarized (Cohan, 1992), suggesting such an adaptive response. A similar effect has been reported in fetal mouse primary sensory neurons in culture, which are initially inhibited by a phasic stimulation or a tonic stimulation with 10Hz, but accommodate after a chronic 24h stimulation or longer and grow at a constant rate regardless of the presence of the normally inhibitory culturing conditions (Fields et al., 1990). Short depolarization has also been shown to have long lasting effects on other functions such as priming neurons to respond to neurotrophic factors, even after cessation of the depolarizing pulse (Schmidt et al., 1996). These studies suggest modifications of gene expression after an initial exposure activity/depolarization which prevents inhibitions to a second exposure. Such changes could influence the growth of adult DRG neurons upon KCl washout or replating.

Similarly, it has been reported that after a CL, ex vivo adult DRGs are no longer inhibited by KCl due to downregulation of L-type calcium channels (Enes et al., 2010). This has been accounted as a proof of calcium regulation or silencing contributing to growth, nevertheless the original trigger, may actually be the injury related spiking activity and back propagating calcium influx, shown to influence gene expression (Cho et al., 2013). Another possible explanation for the different impact of depolarization depending on the duration and timing of replating is that, depolarization induces direct inhibition of growth acting through cytoplasmic calcium signals, but at the same time acts in the nucleus to activate growth related programs, that can only manifest at a delayed time-point upon replating in normal media.

Calcium signaling is one of the main signaling pathways which has been reported to be involved in activity related effects on growth, both in developing and adult neurons, thus I wanted to test the impact of blocking Ca^{2+}/CaM signaling on DRG neurons growth. I have shown here that blocking nuclear calcium signaling in DRGs cultures reduces neurite growth in culture by 50 ± 10% at 72h in culture and by a similar percentage, 46±7%, after replating **(Fig.4.27)**. This suggests that nuclear calcium signaling is necessary in baseline conditions for gene expression involved in DRG neurite growth. It has been shown that after approximatively 24h in culture, naive DRGs increase their growth capacity in vitro by upregulating several genes and converting to an elongating phenotype (Smith and Skene, 1997), by recapitulating the CL in vitro (Saijilafu et al., 2013). The increase in growth capacity is emphasized when replating at different timepoints as seen in **(Fig.3.5)**. Blockage of nuclear calcium signaling could influence growth by inhibiting or delaying this “in-vitro conditioning effect”. In the same time, the second axotomy during the replating, is possibly associated with injury potentials and calcium influx. Unlike other approaches to inhibit nuclear signaling, blockage with CaMBP4 cannot be overcome by increased activity (Schlumm et al., 2013), thus we would expect a consistent effect with or without replating, which was indeed the case in my experiments.

Blocking cytoplasmic calcium signaling with a construct under a hSyn promoter had no major effects on growth when grown for up to 72h after electroporation **(Fig.4.28.C)**. This suggests that calcium signaling in the cytoplasm does not play a role in growth on growth capacity. None the less, the lack of effect in this experimental setup, could also be due to different levels of expression between the 2 sets of plasmids. The CMV promoter induces high initial neural expression that diminishes over time, while the more delayed, persistent hSyn promoted construct could take longer to express CaMBP4 at efficient levels. Additionally, the CMV promoted constructs are bicistronic with a T2A ribosome skip sequence, while the Syn plasmids have 2 separate hSyn promoters, which can also

contribute to expression differences between the 2 sets of constructs. However, in following experiments, it was revealed that blocking cytoplasmic calcium signaling can enhance growth upon replating by 35 ± 11% **(Fig.4.28.F)**, and has similar effects in vivo after adeno-associated virus gene transfer into lumbar DRGs **(Fig.4.32)**, confirming a differential effect of calcium in the cytoplasm compared to the nucleus.

This differential effect of nuclear and cytoplasmic calcium signaling is in line with previous reports, which have shown stimulation or reduction of growth following different types of neuronal activity. Consistent with this data, a potential mechanism through which activity could stimulate growth in primary sensory neurons is nuclear calcium signaling induced gene expression, while in the same time activity could have direct effects at the level of the axon or growth cone, inhibiting growth also via Ca^{2+}/CaM dependent processes.

Nuclear calcium signaling in the context of peripheral lesion has indeed been associated with histone deacetylase 5 (HDAC5) nucleo-cytoplasmic shuttling and gene expression (Cho et al., 2013). In hippocampal neurons, class IIa HDACs, including HDAC5, are exported from the nucleus after synaptic activity or depolarization, dependent on nuclear Ca2+/calmodulin signaling (Schlumm et al., 2013).

I investigated HDAC5 shuttling in the context of high K+ exposure in DRGs showing export from the nucleus (92 ± 5% nuclear before and 14 ± 1% after depolarization) **(Fig.4.30)**, suggesting such effects could contribute to regulation of gene expression after depolarization or even in vivo after ES. Nuclear calcium block was shown to block depolarization-induced HDAC5 export **(Fig.4.31)**, while cytoplasmic CaMBP4 had no influence **(Fig.4.32)**, thus correlating the cellular localization both with differential effects on growth and on HDAC5 shuttling.

Histone acetylation has been reported in several models to influence axonal regeneration through epigenetic changes of gene expression (for review see (Tang, 2014)). Class II HDACs, especially HDAC5 have been linked with enhanced intrinsic potential, as well as cytoplasmic proregenerative functions after peripheral injury (Cho et al., 2013), it is possible that a similar mechanism is involved in ES induced effects on growth.

5.3. Differential gene expression after ES

Considering that my previous experiments showed enhanced growth after ES and suggested translational changes, RNA sequencing was performed to investigate differential gene expression. DRGs from animals that received either ES, sham electrode or CL, as well as from naïve animals were collected at 1 day and 7 days to capture both

early as well as sustained gene expression changes. For the current exploratory analysis, I focused only on differential gene expression at 7 days after ES, sham, CL and naïve for $p<0.01$, with the mention that it is likely necessary to further analyze the extensive amount of data produced by this method.

CL induces an extensive collection of genes compared to naïve animals, while ES induced comparably less relative to the sham animals, and at lower expression rates. This is predictable since CL had greater in vitro and in vivo effects, as well based on the fact that a PNL affects all fibers in the sciatic, while ES might stimulate only a subpopulation. If the genes are upregulated in only one population of DRG neurons, the levels would be diluted since RNA was isolated from whole DRGs. The overlap for differential gene expression between ES vs sham and CL vs naïve is relatively small (10%), however, there are several genes and pathways that stand out, known to be involved in regeneration.

The main gene clusters for upregulated genes found were: myosins, voltage-gated potassium channels, voltage-gated sodium channels, DNA binding factors, ubiquitin peptidases, dyneins, G-coupled receptors and others as detailed in **Table 4.3.** Though typically associated with muscle functions, myosins have been described to modulate the actin cytoskeleton and play function in process outgrowth and growth cone motility in developing and sensory neurons (reviewed in (Brown and Bridgman, 2004)). Voltage-gated potassium channels have an important role in repolarizing the cells after activity and have also been reported to be necessary for neurite outgrowth and pathfinding in retinal ganglia cells, likely by regulating membrane excitability at the growth cone (McFarlane and Pollock, 2000). Similarly, other clusters or genes from the upregulated gene list appear to have some role in neuronal growth such as dynein by supporting microtubule advancement in growth cone (Grabham et al., 2007), neuronal cell adhesion molecule (NRCAM), neurofascin or Map3K2. Interestingly there is a cluster of histones downregulated after ES, however the biological relevance is unclear.

The gene ontology classification either by molecular function or by biological processes reveal that many genes from the upregulated data set have multiple interactions and functions, such as regulation of biological processes (91 genes, 70.5% of candidate set), establishment of localization (58 genes, 44.9%), cellular component organization (66 genes, 51.1%) and cellular response to stimulus (61 genes, 47.2%) **(Table 4.6)**.

An analysis of the pathways significantly upregulated in data set, reveals additionally L1-ankyrins interaction set, L1CAM, axon guidance, pathways involved in developmental biology and others **(Table 4.7)**. In the same time protein complexes were identified such

as mTOR signaling complex (100% of set contained in the candidate set), NFASC/NRCAM (100%), MAP1B/Lis1/Dynein heavy chains (66%). The upregulation is particularly significant for small sets of protein complexes as can be visualized in **Fig. 4.39**.

Genetic activation of mTOR has been shown initially to promote successful axon regeneration in optical nerve regeneration (Park et al., 2008). Consecutively it has also been demonstrated to promote regeneration of the corticospinal tract, being effective at least if the intervention is prior to SCI (Liu et al., 2010), indicating that it can promote regeneration in several neuronal types. Another important complex identified is MAP1B/LIS1/DYHC1 (Microtubule-associated protein 1B/Platelet-activating factor acetylhydrolase IB subunit alpha/ dynein heavy chain) which has been shown to be significant developmentally for neurite extension and neuronal migration (Jimenez-Mateos et al., 2005).

Adhesion molecules such L1 cell adhesion molecule (L1CAM) and L1-Ankyrins seem to also play a role and their expression has been described to be modulated by different patterns of activity (Itoh et al., 1997) supporting the hypothesis of activity-induced changes after ES.

This exploratory analysis indeed suggests an effect on regeneration through modified gene expression. Although the fold-changes were found to be generally small, ES could act through summation of several activated pathways. Additionally, if epigenetic mechanisms are involved, other changes in gene expression may be added in electrically stimulated neurons in case of dorsal column lesion or axotomy as part of the isolation process for in vitro culturing, adding a second layer of modified gene expression that could amplify the impact on growth.

ES might activate a general mechanism that could be translated and applied clinically to spinal cord injury as well as other conditions that involve damage to neurons either through disease or trauma, alone or in combination with other treatments.

5.4. Translation to clinic and perspectives

Taken together, my experiments examining nuclear calcium signaling, depolarization and electrical stimulation reveal the capacity of DRG neurons to modulate their growth response depending on activity in vivo, while enhancement of axonal growth by electrical stimulation, provides a potential therapeutic strategy to increase sensory axon regeneration in the injured spinal cord. Nevertheless, side effects need to be taken into consideration, as well as practical means to employ such a strategy in patients.

A first concern is that the neurite growth induced by ES could translate into aberrant spouting and induce allodynia or neuropathic pain. Chronic cuff electrodes could potentially also induce similar adverse effects. To exclude this possibility, I used the von Frey filaments test as a measure of mechanical sensitivity in animals with ES and DCL throughout the recovery showing no difference in sensory perception among the groups, with the exception of the CL at 24 days post injury **(Fig.4.20)**. CL indeed appeared to recover sensitivity and even induce a higher response to 2g and 4g filaments than in baseline conditions, however, increased withdrawal response does not necessarily mean allodynia since the sensation may or may not translate into pain perception (Saade et al., 2002). Withdrawal alone is a measure of mechanical sensitivity/fine touch, and is processed mainly through the dorsal column, since the response was dramatically affected by the DCL. In contrast, thermal sensitivity was not affected by DCL and there was no indication of thermal hyperalgesia in any of the groups **(Fig.4.21)**.

We chose to focus on fine touch and thermal sensitivity because they are typically associated with different tracts in the spinal cord, dorsal column, and anterior column respectively and our lesion model specifically injures the dorsal column, while everything else is left intact. Thus these tests could emphasize global changes in pain perception as well as any differential effects on injured/non-injured sensory tracts in our experimental setup.

The cuffs electrodes used in these experiments have been designed to minimize any side effects, however I also recorded isolated cases in which electrode implantation alone possibly injured the nerve. While for research, the potential bias is more of a concern, an even more important goal for translation is avoiding invasiveness. Thus for future studies and translational purposes, transcutaneous stimulation would be desirable. Whether the parameters and efficiency would be maintained it is not clear.

It is generally accepted that either one therapeutic strategy is unlikely to overcome the plethora of inhibiting factors for growth in the CNS and combining several strategies such as cell grafts, scar digestion, enhanced intrinsic growth potential and guidance of regenerating neurons are needed to foster sufficient axonal regeneration SCI in order to promote functional recovery (Fouad et al., 2005, Houle et al., 2006, Tom et al., 2009, Taylor et al., 2006). In this study I also show ES is effective in combination with cell transplantation, which is likely necessary for potential long distance regeneration, further supporting the translational potential of ES for SCI treatment.

References

1. Agnew, W. F., Mccreery, D. B., Yuen, T. G. & Bullara, L. A. 1989. Histologic and physiologic evaluation of electrically stimulated peripheral nerve: considerations for the selection of parameters. *Ann Biomed Eng,* 17**,** 39-60.
2. Al-Majed, A. A., Brushart, T. M. & Gordon, T. 2000a. Electrical stimulation accelerates and increases expression of BDNF and trkB mRNA in regenerating rat femoral motoneurons. *Eur J Neurosci,* 12**,** 4381-90.
3. Al-Majed, A. A., Neumann, C. M., Brushart, T. M. & Gordon, T. 2000b. Brief electrical stimulation promotes the speed and accuracy of motor axonal regeneration. *J Neurosci,* 20**,** 2602-8.
4. Amir, R. & Devor, M. 1996. Chemically mediated cross-excitation in rat dorsal root ganglia. *J Neurosci,* 16**,** 4733-41.
5. Amir, R. & Devor, M. 2000. Functional cross-excitation between afferent A- and C-neurons in dorsal root ganglia. *Neuroscience,* 95**,** 189-95.
6. Arcaro, K. F. & Lnenicka, G. A. 1997. Differential effects of depolarization on the growth of crayfish tonic and phasic motor axons in culture. *J Neurobiol,* 33**,** 85-97.
7. Asensio-Pinilla, E., Udina, E., Jaramillo, J. & Navarro, X. 2009. Electrical stimulation combined with exercise increase axonal regeneration after peripheral nerve injury. *Exp Neurol,* 219**,** 258-65.
8. Brown, M. E. & Bridgman, P. C. 2004. Myosin function in nervous and sensory systems. *J Neurobiol,* 58**,** 118-30.
9. Cho, Y., Sloutsky, R., Naegle, K. M. & Cavalli, V. 2013. Injury-induced HDAC5 nuclear export is essential for axon regeneration. *Cell,* 155**,** 894-908.
10. Clark, G. 2006. *Cochlear Implants: Fundamentals and Applications*, Springer New York.
11. Cohan, C. S. 1992. Depolarization-induced changes in neurite elongation and intracellular Ca2+ in isolated Helisoma neurons. *J Neurobiol,* 23**,** 983-96.
12. Dymond, A. M. 1976. Characteristics of the metal-tissue interface of stimulation electrodes. *IEEE Trans Biomed Eng,* 23**,** 274-80.
13. Ehl, R. G. & Ihde, A. J. 1954. Faraday's electrochemical laws and the determination of equivalent weights. *Journal of Chemical Education,* 31**,** 226.
14. Enes, J., Langwieser, N., Ruschel, J., Carballosa-Gonzalez, M. M., Klug, A., Traut, M. H., Ylera, B., Tahirovic, S., Hofmann, F., Stein, V., Moosmang, S., Hentall, I. D. & Bradke, F. 2010. Electrical activity suppresses axon growth through Ca(v)1.2 channels in adult primary sensory neurons. *Curr Biol,* 20**,** 1154-64.
15. Eshete, F. & Fields, R. D. 2001. Spike frequency decoding and autonomous activation of Ca2+-calmodulin-dependent protein kinase II in dorsal root ganglion neurons. *J Neurosci,* 21**,** 6694-705.
16. Fields, R. D., Neale, E. A. & Nelson, P. G. 1990. Effects of patterned electrical activity on neurite outgrowth from mouse sensory neurons. *J Neurosci,* 10**,** 2950-64.
17. Forstl, J., Galvan, M. & Ten Bruggencate, G. 1982. Extracellular K+ concentration during electrical stimulation of rat isolated sympathetic ganglia, vagus and optic nerves. *Neuroscience,* 7**,** 3221-9.
18. Fouad, K., Schnell, L., Bunge, M. B., Schwab, M. E., Liebscher, T. & Pearse, D. D. 2005. Combining Schwann cell bridges and olfactory-ensheathing glia grafts with chondroitinase promotes locomotor recovery after complete transection of the spinal cord. *J Neurosci,* 25**,** 1169-78.
19. Geremia, N. M., Gordon, T., Brushart, T. M., Al-Majed, A. A. & Verge, V. M. 2007. Electrical stimulation promotes sensory neuron regeneration and growth-associated gene expression. *Exp Neurol,* 205**,** 347-59.
20. Grabham, P. W., Seale, G. E., Bennecib, M., Goldberg, D. J. & Vallee, R. B. 2007. Cytoplasmic dynein and LIS1 are required for microtubule advance during growth cone remodeling and fast axonal outgrowth. *J Neurosci,* 27**,** 5823-34.

21. Houle, J. D., Tom, V. J., Mayes, D., Wagoner, G., Phillips, N. & Silver, J. 2006. Combining an autologous peripheral nervous system "bridge" and matrix modification by chondroitinase allows robust, functional regeneration beyond a hemisection lesion of the adult rat spinal cord. *J Neurosci,* 26**,** 7405-15.
22. Itoh, K., Ozaki, M., Stevens, B. & Fields, R. D. 1997. Activity-dependent regulation of N-cadherin in DRG neurons: differential regulation of N-cadherin, NCAM, and L1 by distinct patterns of action potentials. *J Neurobiol,* 33**,** 735-48.
23. Jimenez-Mateos, E. M., Wandosell, F., Reiner, O., Avila, J. & Gonzalez-Billault, C. 2005. Binding of microtubule-associated protein 1B to LIS1 affects the interaction between dynein and LIS1. *Biochem J,* 389**,** 333-41.
24. Liu, K., Lu, Y., Lee, J. K., Samara, R., Willenberg, R., Sears-Kraxberger, I., Tedeschi, A., Park, K. K., Jin, D., Cai, B., Xu, B., Connolly, L., Steward, O., Zheng, B. & He, Z. 2010. PTEN deletion enhances the regenerative ability of adult corticospinal neurons. *Nat Neurosci,* 13**,** 1075-81.
25. Loeb, G. E. & Peck, R. A. 1996. Cuff electrodes for chronic stimulation and recording of peripheral nerve activity. *J Neurosci Methods,* 64**,** 95-103.
26. Mccreery, D. B., Agnew, W. F., Yuen, T. G. & Bullara, L. A. 1992. Damage in peripheral nerve from continuous electrical stimulation: comparison of two stimulus waveforms. *Med Biol Eng Comput,* 30**,** 109-14.
27. Mcfarlane, S. & Pollock, N. S. 2000. A role for voltage-gated potassium channels in the outgrowth of retinal axons in the developing visual system. *J Neurosci,* 20**,** 1020-9.
28. Neumann, S., Skinner, K. & Basbaum, A. I. 2005. Sustaining intrinsic growth capacity of adult neurons promotes spinal cord regeneration. *Proc Natl Acad Sci U S A,* 102**,** 16848-52.
29. Park, K. K., Liu, K., Hu, Y., Smith, P. D., Wang, C., Cai, B., Xu, B., Connolly, L., Kramvis, I., Sahin, M. & He, Z. 2008. Promoting axon regeneration in the adult CNS by modulation of the PTEN/mTOR pathway. *Science,* 322**,** 963-6.
30. Riistama, J. & Lekkala, J. 2006. Electrode-electrolyte interface properties in implantation conditions. *Conf Proc IEEE Eng Med Biol Soc,* 1**,** 6021-4.
31. Saade, N. E., Baliki, M., El-Khoury, C., Hawwa, N., Atweh, S. F., Apkarian, A. V. & Jabbur, S. J. 2002. The role of the dorsal columns in neuropathic behavior: evidence for plasticity and non-specificity. *Neuroscience,* 115**,** 403-13.
32. Saijilafu, Hur, E. M., Liu, C. M., Jiao, Z., Xu, W. L. & Zhou, F. Q. 2013. PI3K-GSK3 signalling regulates mammalian axon regeneration by inducing the expression of Smad1. *Nat Commun,* 4**,** 2690.
33. Schlumm, F., Mauceri, D., Freitag, H. E. & Bading, H. 2013. Nuclear calcium signaling regulates nuclear export of a subset of class IIa histone deacetylases following synaptic activity. *J Biol Chem,* 288**,** 8074-84.
34. Schmidt, M. F., Atkinson, P. B. & Kater, S. B. 1996. Transient elevations in intracellular calcium are sufficient to induce sustained responsiveness to the neurotrophic factor bFGF. *J Neurobiol,* 31**,** 333-44.
35. Smith, D. S. & Skene, J. H. 1997. A transcription-dependent switch controls competence of adult neurons for distinct modes of axon growth. *J Neurosci,* 17**,** 646-58.
36. Tang, B. L. 2014. Class II HDACs and neuronal regeneration. *J Cell Biochem,* 115**,** 1225-33.
37. Taylor, L., Jones, L., Tuszynski, M. H. & Blesch, A. 2006. Neurotrophin-3 gradients established by lentiviral gene delivery promote short-distance axonal bridging beyond cellular grafts in the injured spinal cord. *J Neurosci,* 26**,** 9713-21.
38. Tom, V. J., Sandrow-Feinberg, H. R., Miller, K., Santi, L., Connors, T., Lemay, M. A. & Houle, J. D. 2009. Combining peripheral nerve grafts and chondroitinase promotes functional axonal regeneration in the chronically injured spinal cord. *J Neurosci,* 29**,** 14881-90.
39. Udina, E., Furey, M., Busch, S., Silver, J., Gordon, T. & Fouad, K. 2008. Electrical

stimulation of intact peripheral sensory axons in rats promotes outgrowth of their central projections. *Exp Neurol,* 210**,** 238-47.

Supplementary data:

Annex 1: Experimental groups

Experiment no.	Group no.	Name	Surgery	Electrical stimulation (ES)	Repeated ES (chronic implant)	Survival	Outcome measure	N total	Excluded
1)[c]	1	**ES1h**	Cuff electrode placement	**1h**, 20Hz, 0.2ms pulse, 2xMT	Not repeated	7 days	DRG growth 48h	N=3	-
	2	**sham**	Cuff electrode placement	-	but chronic		(Laminin 0.5µg/ml)	N=3	-
	3	**CL**	Conditioning lesion*	-	Implant (test)		IF: β3tub, NF200	N=3	-
	4	**naive**	-	-				N=3	-
2)[c]	5	**ES1h**	Cuff electrode placement	**1h**, 20Hz, 0.2ms pulse, 2xMT	Not repeated	7 days	DRG growth 48h	N=3	-
	6	**sham**	Cuff electrode placement	-	but chronic		(Laminin 0.5µg/ml)	N=3	1**
	7	**CL**	Conditioning lesion*	-	Implant (test)		IF: β3tub	N=3	-
	8	**naive**	-	-				N=3	-
3)	9	**ES1h**	Cuff electrode placement	**1h**, 20Hz, 0.2ms pulse, 2xMT	no	none	EMG recordings	N=1	
4)[c]	10	**ES1hprog**	Cuff electrode placement	**1h**, 20Hz, 0.02ms pulse, start at MT, progressively increase I to maintain constant movement	no	7 days	DRG growth 48h (Laminin 0.5µg/ml) IF: β3tub, NF200	N=3	-
	11	**sham**	Cuff electrode placement	-				N=3	-
5)[c]	12	**ES1h**	Cuff electrode placement	**1h**, 20Hz, 0.2ms pulse, 2xMT	no	7 days	DRG growth 48h	N=4	-
	13	**ES1h10Hz**	Cuff electrode placement	**1h**, 10Hz, 0.2ms pulse, 2xMT			IF: β3tub, NF200	N=8	1**
	14	**sham**	Cuff electrode placement	-				N=3	-
	15	**CL**	Conditioning lesion*	-				N=3	-
	16	**naive**	-	-				N=2	-
6)a[b]	17	**ES1h**	Cuff electrode placement	**1h**, 20Hz, 0.2ms pulse, 2xMT	no	7 days	DRG growth 24h	N=4	-
	18	**sham**	Cuff electrode placement	-			(Laminin 5µg/ml)	N=4	-
	19	**CL**	Conditioning lesion*	-			IF: β3tub	N=4	-
	20	**naive**	-	-				N=4	-
6)b[b]	17	**ES1h**	Cuff electrode placement	**1h**, 20Hz, 0.2ms pulse, 2xMT	no	7 days	DRG growth 24h	N=4	-

	18	**sham**	Cuff electrode placement	-			IF: β3tub	N=4	-
	19	**CL**	Conditioning lesion*	-				N=4	-
	20	**naive**	-	-				N=4	-
7)[b]	21	**ES6h**	Cuff electrode placement	**6h**, 20Hz, 0.2ms pulse, 2xMT	no	7 days	DRG growth 24h	N=6	1**
	22	**sham**	Cuff electrode placement	-			IF: β3tub	N=6	-
8)[b]	23	**ES1hR**	Cuff electrode placement	**6x1h**, 20Hz, 0.2ms pulse, 2xMT	1h/day, 6 days yes	7 days	DRG growth 24h IF: β3tub	N=6	-
	24	**sham chronic**	Cuff electrode placement	**-**					
9)[b]	25	**ES1h**	Cuff electrode placement	**1h**, 20Hz, 0.2ms pulse, 2xMT	no	1 day	DRG growth 24h	N=6	-
	26	**sham**	Cuff electrode placement	-			IF: β3tub	N=6	-
10)[b]	27	**ES1hR**	Cuff electrode placement	**7x1h**, 20Hz, 0.2ms pulse, 2xMT	1h/day, 7 days	7 days	DRG growth 24h IF: β3tub	N=8	2(died)
	28	**sham chronic**	Cuff electrode placement	-	yes			N=8	-
11)[b]	29	**ES7h**	Cuff electrode placement	**7h**, 20Hz, 0.2ms pulse, 2xMT	no	7 days	DRG growth 24h	N=6	1
	30	**sham**	Cuff electrode placement	-			IF: β3tub	N=6	-
12)[b]	31	**ES1h**	Cuff electrode placement	**1h**, 20Hz, 0.2ms pulse, 2xMT	no	7 days	DRG sections IHC: GAP43, ATF3, c-Jun	N=4	-
	32	**ES7h**	Cuff electrode placement	**7h**, 20Hz, 0.2ms pulse, 2xMT				N=4	-
	33	**sham**	Cuff electrode placement	-				N=4	-
	34	**CL**	Conditioning lesion*	-				N=4	-
13)	35	**ES1h**	DCL (C4) + BMSCs injection (Passage 2-4) 2µl (60.000 cells/ul) +Cuff electrode placement	**1h**, 20Hz, 0.2ms pulse, 2xMT	no	28 days	Perfusion, sagittal sections spinal cord	-	
	36	**sham**	+Cuff electrode placement	-			IHC: CTB, GFAP, GFP, DAPI	-	
	37	**CL**	+Conditioning lesion*	-				-	
	38	**lesion only**	-	-				-	
14)	39	**ES1hx2**	DCL (C4) + BMSCs injection +Cuff electrode placement	**1h**, 20Hz, 0.2ms pulse, 2xMT	At 7 days	28 days	Perfusion, sagittal sections spinal cord	-	

	40	**sham chronic**	(Passage 2-4) 2µl (60.000 cells/ul)	+Cuff electrode placement	-	yes		IHC: CTB, GFAP, GFP, DAPI	-	
	41	**CL**		+Conditioning lesion*	-				-	
	42	**lesion only**		-	-				-	
15)	43	**ES1h**	Cuff electrode placement		**1h**, 20Hz, 0.2ms pulse, 2xMT	no	1 day	DRGs RNA	N=1	-
	44	**sham**	Cuff electrode placement		-				N=1	-
	45	**CL**	Conditioning lesion*						N=2	-
	46	**naive**	-						N=2	-
16)	45	**ES1h**	Cuff electrode placement		**1h**, 20Hz, 0.2ms pulse, 2xMT	no	1 day	DRGs RNA	N=6	-
	46	**sham**	Cuff electrode placement		-				N=6	- (2***)
	47	**CL**	Conditioning lesion*		-				N=4	-
	48	**naive**	-		-				N=4	-
17)	45	**ES1h**	Cuff electrode placement		**1h**, 20Hz, 0.2ms pulse, 2xMT	no	7 days	DRGs RNA	N=4	-
	46	**sham**	Cuff electrode placement		-				N=4	-
	47	**CL**	Conditioning lesion*		-				N=4	-
	48	**naive**	-		-				N=4	-

*jeweler's forceps, 20sec; **exclusion criteria: Grubbs' test (ESD method - extreme studentized deviate, $p<0.05$); values excluded were extremely high suggesting surgical related CL. *** not excluded from this analysis, but in principal component analysis (PCA) of gene expression, values clustered towards CL, suggesting surgical related CL.

[b]=bilateral: sides were treated identically and assessed independently; [c]=combined conditions: the two sides of animals were differently treated and assessed independently.

Annex 2: Differentially expressed upregulated genes at 7 days - ES vs sham.
Differential gene expression at 7 days by RNA sequencing, p<0.01. Full list. Genes marked with "*" are also upregulated at the same time point in CL vs naïve. Annotated using DAVID Bioinformatics Resources 6.7.

OFFICIAL_GENE_SYMBOL	Gene Name
Abca5	ATP-binding cassette, sub-family A (ABC1), member 5
Ace*	angiotensin I converting enzyme (peptidyl-dipeptidase A) 1
Adamts3	ADAM metallopeptidase with thrombospondin type 1, motif 3
Ahnak	AHNAK nucleoprotein
Akap11	A kinase (PRKA) anchor protein 11
Akap6*	A kinase (PRKA) anchor protein 6
Akap9	A kinase (PRKA) anchor protein (yotiao) 9
Ankrd17	ankyrin repeat domain 17
Ankrd50*	ankyrin repeat domain 50
Ankrd52	ankyrin repeat domain 52
Arfgef1	ADP-ribosylation factor guanine nucleotide-exchange factor 1(brefeldin A-inhibited)
Arfgef2	ADP-ribosylation factor guanine nucleotide-exchange factor 2 (brefeldin A-inhibited)
Atp2b3	ATPase, Ca++ transporting, plasma membrane 3
Birc6	tetratricopeptide repeat domain 27; baculoviral IAP repeat-containing 6
Bmpr2	bone morphogenetic protein receptor, type II (serine/threonine kinase)
Cand1	cullin-associated and neddylation-dissociated 1
Casc5	cancer susceptibility candidate 5
Cgnl1	cingulin-like 1
Chd6	chromodomain helicase DNA binding protein 6
Crim1	cysteine rich transmembrane BMP regulator 1 (chordin like)
Dync1h1	dynein cytoplasmic 1 heavy chain 1
Dync2h1	dynein cytoplasmic 2 heavy chain 1
Dysf*	dysferlin
Fry	similar to hypothetical protein CG003
Golga3	golgi autoantigen, golgin subfamily a, 3
Golgb1	golgi autoantigen, golgin subfamily b, macrogolgin 1
Gpr158	similar to G protein-coupled receptor 158 isoform a; G protein-coupled receptor 158
Gpr88*	G-protein coupled receptor 88 *(orphan receptor)*
Gucy1a2	guanylate cyclase 1, soluble, alpha 2
Hcn1	hyperpolarization-activated cyclic nucleotide-gated potassium channel 1
Herc2	hect domain and RLD 2
Hipk3	homeodomain interacting protein kinase 3
Hpd*	4-hydroxyphenylpyruvate dioxygenase
Htt	huntingtin
Il6st	interleukin 6 signal transducer
Kalrn*	kalirin, RhoGEF kinase
Kcna2	potassium voltage-gated channel, shaker-related subfamily, member 2

Kcnb2	potassium voltage gated channel, Shab-related subfamily, member 2
Kcnh5	potassium voltage-gated channel, subfamily H (eag-related), member 5
Kcnh7	potassium voltage-gated channel, subfamily H (eag-related), member 7
Kcnma1	potassium large conductance calcium-activated channel, subfamily M, alpha member 1
Kif1b	cortistatin; kinesin family member 1B
Lemd3	LEM domain containing 3; methionine sulfoxide reductase B3
Lnpep	leucyl/cystinyl aminopeptidase
Lrp1b	low density lipoprotein-related protein 1B (deleted in tumors)
Lrrc58*	leucine rich repeat containing 58
Macf1*	microtubule-actin crosslinking factor 1
Map1b	microtubule-associated protein 1B
Map2	microtubule-associated protein 2
Map3k2	mitogen activated protein kinase kinase kinase 2
Mcoln3*	mucolipin 3
Megf10	multiple EGF-like domains 10
Mib1	mindbomb homolog 1 (Drosophila)
Mllt4	myeloid/lymphoid or mixed-lineage leukemia (trithorax homolog, Drosophila); translocated to, 4
Mpdz	multiple PDZ domain protein
Mtor	mechanistic target of rapamycin (serine/threonine kinase)
Mycbp2	MYC binding protein 2
Myh10	myosin, heavy chain 10, non-muscle
Myo1e	myosin IE
Myo5a	myosin Va
Myo5b	myosin Vb
Myo9a	myosin IXA
Ncoa1	nuclear receptor coactivator 1
Nf1	neurofibromin 1
Nfasc	neurofascin
Nrcam	neuronal cell adhesion molecule
Nrxn1	neurexin 1
Ntrk3	neurotrophic tyrosine kinase, receptor, type 3
Pcdh17	protocadherin 17
Pcdh18*	protocadherin 18
Pcdh19	protocadherin 19
Pcdh7	protocadherin 7
Peg3	paternally expressed 3
Pgm2l1	phosphoglucomutase 2-like 1
Pi4ka	phosphatidylinositol 4-kinase, catalytic, alpha
Pkd1	polycystic kidney disease 1 homolog (human)
Plec	plectin 1
Plxna2	plexin A2
Polr3b	polymerase (RNA) III (DNA directed) polypeptide B
Prpf8	PRP8 pre-mRNA processing factor 8 homolog (S. cerevisiae)

Rab3gap2*	RAB3 GTPase activating protein subunit 2
Ranbp2	RAN binding protein 2
Rapgef6	Rap guanine nucleotide exchange factor (GEF) 6
Rasa1	RAS p21 protein activator (GTPase activating protein) 1
Rptor	regulatory associated protein of MTOR, complex 1
Ryr2	ryanodine receptor 2, cardiac
Scand1*	SCAN domain-containing 1
Scn1a	sodium channel, voltage-gated, type I, alpha
Scn8a	sodium channel, voltage gated, type VIII, alpha subunit
Scn9a	sodium channel, voltage-gated, type IX, alpha
Slc24a2	solute carrier family 24 (sodium/potassium/calcium exchanger), member 2
Slc7a1	solute carrier family 7 (cationic amino acid transporter, y+ system), member 1
Stxbp5	syntaxin binding protein 5 (tomosyn)
Supt6h*	suppressor of Ty 6 homolog (S. cerevisiae)
Synj1	synaptojanin 1
Taf1	TAF1 RNA polymerase II, TATA box binding protein (TBP)-associated factor
Terc*	telomerase RNA component
Thsd7a	thrombospondin, type I, domain containing 7A
Tnrc6b	trinucleotide repeat containing 6B
Trim2	tripartite motif-containing 2
Trrap	transformation/transcription domain-associated protein
Ttbk2	tau tubulin kinase 2
Ucn*	urocortin
Usp24	ubiquitin specific protease 24
Usp32	ubiquitin specific protease 32
Usp9x	ubiquitin specific peptidase 9, X-linked
Utrn	utrophin
Vps13a	vacuolar protein sorting 13 homolog A (S. cerevisiae)
Vps13d	vacuolar protein sorting 13D (yeast)
Wfs1	Wolfram syndrome 1 homolog (human)
Zc3h13	similar to KIAA0853 protein; zinc finger CCCH type containing 13
Zfx	zinc finger protein X-linked
40973	
Faxc*	Failed Axon Connections Homolog
Prrc2c	**Proline Rich Coiled-Coil 2C**

Annex 3: Differentially expressed downregulated genes at 7 days - ES vs sham.
Differential gene expression at 7 days**,** RNA sequencing, p<0.01. Full list. Genes marked with "*" are also downregulated at the same timepoint in CL vs naïve. Annotated using DAVID Bioinformatics Resources 6.7.

OFFICIAL_GENE_SYMBOL	Gene Name
Acta1	actin, alpha 1, skeletal muscle
Actn3	actinin alpha 3
Alpk3	alpha-kinase 3
Anxa8	annexin A8
Atp2a1	ATPase, Ca++ transporting, cardiac muscle, fast twitch 1
Atp5e	ATP synthase, H+ transporting, mitochondrial F1 complex, epsilon subunit
Atp5i	ATP synthase, H+ transporting, mitochondrial F0 complex, subunit E
Cacna1s	calcium channel, voltage-dependent, L type, alpha 1S subunit
Car3	carbonic anhydrase 3
Ckm	creatine kinase, muscle
Cks2	CDC28 protein kinase regulatory subunit 2
Cnpy2	similar to MIR-interacting saposin-like protein precursor (Transmembrane protein 4) (Putative secreted protein ZSIG9); canopy 2 homolog (zebrafish)
Coro1a	coronin, actin binding protein 1A
Cox17*	cytochrome c oxidase, subunit XVII assembly protein homolog (S. cerevisiae)
Cox5b*	cytochrome c oxidase subunit Vb
Cox6a1*	cytochrome c oxidase, subunit VIa, polypeptide 1
Cox6c	cytochrome c oxidase, subunit VIc
Cox7c	cytochrome c oxidase, subunit VIIc
Cstb*	cystatin B (stefin B)
Des	desmin
Dnajc17	DnaJ (Hsp40) homolog, subfamily C, member 17; similar to RIKEN cDNA 1700025B16; similar to DnaJ (Hsp40) homolog, subfamily C, member 17
Dynll1	dynein light chain LC8-type 1
Eno3	enolase 3, beta, muscle
Fignl1	fidgetin-like 1
Gmnn	geminin
Hist1h1b	histone cluster 1, H1b
Hist3h2a	histone cluster 1, H2ai; similar to histone 2a; histone cluster 1, H2an; histone cluster 3, H2a; similar to histone 1, H2af
Hmgb2	similar to High mobility group protein 2 (HMG-2); high mobility group box 2
Hnrnpf	heterogeneous nuclear ribonucleoprotein F
Ifit3	interferon-induced protein with tetratricopeptide repeats 3
Itgb3bp*	integrin beta 3 binding protein (beta3-endonexin)
Kifc1	kinesin family member C1
Leng1	leukocyte receptor cluster (LRC) member 1
Mki67	antigen identified by monoclonal antibody Ki-67
Mybpc2	myosin binding protein C, fast-type
Myh4	myosin, heavy chain 4, skeletal muscle

Myh7	myosin, heavy chain 7, cardiac muscle, beta
Myl1	myosin, light polypeptide 1
N6amt1	N-6 adenine-specific DNA methyltransferase 1 (putative)
Nppb	natriuretic peptide precursor B
Nusap1	nucleolar and spindle associated protein 1
Oasl*	2'-5'-oligoadenylate synthetase-like
Pdia2	Rho GDP dissociation inhibitor (GDI) gamma; protein disulfide isomerase family A, member 2
Pdpn	podoplanin
Pgam2	phosphoglycerate mutase 2 (muscle)
Polr2j	polymerase (RNA) II (DNA directed) polypeptide J, 13.3kDa
Pygm	phosphorylase, glycogen, muscle
Rpl19	similar to ribosomal protein L19; ribosomal protein L19
Rpl27	similar to ribosomal protein L27; ribosomal protein L27
Rpl37	ribosomal protein L37; similar to ribosomal protein L37
Rpl39	ribosomal protein L39
Rps11	ribosomal protein S11
Rps4x	ribosomal protein S4, X-linked
Slc25a37	solute carrier family 25, member 37
Sssca1*	Sjogren's syndrome/scleroderma autoantigen 1 homolog (human)
Stx8	similar to syntaxin 8; syntaxin 8; hypothetical gene supported by NM_031656
Sypl2	synaptophysin-like 2
Tnnc1	troponin C type 1 (slow)
Tnnc2	troponin C type 2 (fast)
Tnni1	troponin I type 1 (skeletal, slow)
Tnnt1	troponin T type 1 (skeletal, slow)
Tnnt3	troponin T type 3 (skeletal, fast)
Tomm7	translocase of outer mitochondrial membrane 7 homolog (yeast)
Trim13	tripartite motif-containing 13
Ttc22	tetratricopeptide repeat domain 22
Uba52	ubiquitin A-52 residue ribosomal protein fusion product 1
Uhrf1	ubiquitin-like with PHD and ring finger domains 1
Vps25	WNK lysine deficient protein kinase 4; similar to Vacuolar protein sorting protein 25 (ELL-associated protein of 20 kDa); vacuolar protein sorting 25 homolog (S. cerevisiae); cyclin N-terminal domain containing 1
Xirp2	xin actin-binding repeat containing 2
Zgpat	zinc finger, CCCH-type with G patch domain; Lck interacting transmembrane adaptor 1
Hist1h2ail1	
Ift22*	Intraflagellar Transport 22
Mien1	Migration And Invasion Enhancer 1